

y5972441

1330592

A THESIS

entitled

ON THE FALSE-DIFFUSION PROBLEM IN THE NUMERICAL  
MODELLING OF CONVECTION-DIFFUSION PROCESSES

Submitted in partial fulfilment of the  
requirements for the award of the

DEGREE OF DOCTOR OF PHILOSOPHY

of the

COUNCIL FOR NATIONAL ACADEMIC AWARDS

by

MAYUR K. PATEL

Faculty of Technology  
School of Mathematics, Statistics and Computing  
Thames Polytechnic  
LONDON

December 1986

Thesis  
532  
05/10  
2/85  
PAT

## ABSTRACT

This thesis is concerned firstly with the classification and evaluation of various numerical schemes that are available for computing solutions for fluid-flow problems, and secondly, with the development of an improved numerical discretisation scheme of the finite-volume type for solving steady-state differential equations for recirculating flows with and without sources.

In an effort to evaluate the performance of the various numerical schemes available, some standard test cases were used. The relative merits of the schemes were assessed by means of one-dimensional laminar flows and two-dimensional laminar and turbulent flows, with and without sources. Furthermore, Taylor series expansion analysis was also utilised to examine the limitations that were present.

The outcome of this first part of the work was a set of conclusions, concerning the accuracy of the numerous schemes tested, *vis-a-vis* their stability, ease of implementation, and computational costs. It is hoped that these conclusions can be used by 'computational fluid-dynamics' practitioners in deciding on an optimum choice of scheme for their particular problem.

From the understanding gained during the first part of the study, and in an effort to combine the attributes of a successful discretisation scheme, eg positive coefficients, conservation and the elimination of 'false-diffusion', a new flow-oriented finite-volume numerical scheme was

devised and applied to several test cases in order to evaluate its performance.

The novel approach in formulating the new CUPID<sup>#</sup> scheme (for Corner UPwInDing) underlines the idea of focussing attention at the control-volume corners rather than at the control-volume cell-faces. In two-dimensions, this leads to an eight neighbour influence for the central grid point value, depending on the flow-directions at the corners of the control-volume. In the formulation of the new scheme, false-diffusion is considered from a pragmatic perspective, with emphasis on physics rather than on strict mathematical considerations such as the order of discretisation, etc.

The accuracy of the UPSTREAM scheme (for UPwind in STREAMlines) indicates that although it is formally only first-order accurate, it considerably reduces 'false-diffusion'. Scalar transport calculations (without sources) show that the UPSTREAM scheme predicts bounded solutions which are more accurate than the upwind-difference scheme and the unbounded skew-upstream-difference scheme. Furthermore, for laminar and turbulent flow calculations, improved results are obtained when compared with the performances of the other schemes.

---

# The up-to-date name of the scheme is CUPID; however, in what follows the old name, UPSTREAM [Patel, Markatos & Cross (1985b)], will be used throughout.

The advantage of the UPSTREAM-difference scheme is that all the influence coefficients are always positive and thus the coefficient matrices are suitable for iterative solution procedures. Finally, the stability and convergence characteristics are similar to those of the upwind-difference scheme, eg converged solutions are guaranteed. What cannot be guaranteed, however, is the conservatism of the scheme and it is recommended that future work should be directed towards improving that disadvantage.

## ACKNOWLEDGEMENTS

I sincerely wish to acknowledge my supervisors, Drs N C Markatos and M Cross for their guidance throughout my research, encouragement when my spirits were flagging and to whom I am also indebted for their careful checking of this manuscript.

I would like to express my gratitude for the useful discussions which I have had with various colleagues, in particular, Drs C W Richards, V Voller, and the Research Staff at the school of Mathematics, Statistics and Computing of Thames Polytechnic, and Dr D G Tatchell of CHAM Limited, Wimbledon. I would also like to thank the Thames Polytechnic Computer Centre Staff, in particular, Mr John Payne, Mr Robert Paynter and Mrs Sandra Castle, for providing me with advice and adequate computer resources.

I am also grateful to Aiana Imrie for her excellent typing of this thesis.

Finally, I would like to extend my gratitude to my parents for their constant support throughout my studies, and to my wife for her encouragement and help.

<u>TABLE OF CONTENTS</u>	<u>PAGE NO.</u>
ABSTRACT	(i)
ACKNOWLEDGEMENTS	(iv)
TABLE OF CONTENTS	(v)
<u>CHAPTER 1</u>	
1. INTRODUCTION	1
1.1 Background	1
1.2 Literature Survey	4
1.21 Classification	5
1.21.1 Finite-difference methods	5
1.21.2 Control-volume methods	5
1.21.3 Finite-element methods	6
1.21.4 Other methods	6
1.22 Finite-difference and control-volume methods - a survey	7
1.23 Finite-element methods - a survey	17
1.3 Closure	20
<u>CHAPTER 2</u>	
2. DIFFERENTIAL EQUATIONS AND FINITE- VOLUME EQUATIONS	21
2.1 Introduction	21
2.2 Conservation Equations	21
2.21 The partial-differential equations	21
2.22 The time-averaged form of the equations	23
2.23 The general equations to be solved	23

TABLE OF CONTENTSPAGE NO.

2.3	Discretisation Procedure	24
2.31	Finite-domain equations	25
2.32	Finite-volume grid and variable locations	25
2.33	General- and boundary-control-volume	26
2.4	Derivation of Finite-Volume Equations	27
2.41	The diffusion term	27
2.42	The source term	28
2.43	The convection term	29
2.44	The overall finite-volume equations	29
2.5	Convergence Criteria and Physical Constraints	30
2.51	Information in analytical solutions	30
2.52	Information in discretised equations	31
2.53	Grid-to-flow skewness	34
2.6	Closure	34

CHAPTER 3

3.	SOLUTION PROCEDURE FOR THE FINITE-VOLUME EQUATIONS	36
3.1	Introduction	36
3.11	The SIMPLE algorithm	37
3.12	The NEAT algorithm	39
3.2	Sources of Inaccuracy in Solution Procedures	49
3.21	Numerical approximation errors	40
3.22	Convergence	41

TABLE OF CONTENTS

PAGE NO.

3.23	Relaxation practice	42
3.3	Closure	42

CHAPTER 4

4.	NUMERICAL SCHEMES	44
4.1	Introduction	44
4.11	Diffusion terms	44
4.11.1	Central-differencing scheme	45
4.12	Convection term	45
4.12.1	Central-differencing scheme	46
4.12.2	Upwind-difference scheme	47
4.12.3	Hybrid-difference scheme	48
4.12.4	Locally-exact-difference scheme	49
4.12.5	Power-difference scheme	50
4.12.6	Leonard-difference scheme	51
4.12.7	Leonard-upwind-difference scheme	52
4.12.8	Leonard-superupwind-difference scheme	53
4.12.9	Quadratic upstream-difference scheme	54
4.12.10	Quadratic upstream-difference scheme extended	56
4.12.11	Quadratic-upstream-difference scheme extended-revised	57
4.12.12	Residual-difference scheme	58
4.12.13	The skew-difference scheme	60

TABLE OF CONTENTS

PAGE NO.

4.2	Overview and Discussion of Influence	
	Coefficients	62
4.3	Closure	65

CHAPTER 5

5.	TRUNCATION ERROR AND FALSE-DIFFUSION	66
5.1	Introduction	66
5.2	Truncation Error	67
5.3	False-Diffusion	70
5.4	Closure	73

CHAPTER 6

6.	APPLICATION TO TEST PROBLEMS	74
6.1	One-Dimensional Study	74
6.11	Introduction	74
6.12	Objectives	74
6.13	The test problem	75
6.14	The schemes investigated	75
6.15	The test cases	76
6.16	Presentation of results	77
6.17	Discussion of results	78
6.18	Conclusions	82
6.2	Two-Dimensional Laminar Study	86
6.21	Introduction	86
6.22	Objectives	87
6.23	The schemes investigated	87

TABLE OF CONTENTSPAGE NO.

6.24	The laminar test cases	87
6.24.1	Flow through a sudden enlargement	88
6.24.2	Flow in a cavity with a moving lid	89
6.25	Presentation of results	89
6.25.1	Flow through a sudden enlargement	90
6.25.2	Flow in a cavity with a moving lid	93
6.26	Discussion of results	94
6.26.1	Flow through a sudden enlargement	94
6.26.2	Flow in a cavity with a moving lid	96
6.27	Conclusions	97
6.3	Two-Dimensional Turbulent Study	99
6.31	Introduction	99
6.32	Objectives	100
6.33	The test problem	100
6.34	Presentation of results	102
6.35	Discussion of results	103
6.36	Conclusions	104
6.4	Flow at an Angle to the Grid Lines	106
6.41	Introduction	106
6.42	Objectives	106
6.43	The schemes investigated	107
6.44	The test problem	107
6.45	Presentation of results	108
6.46	Discussion of results	109
6.47	Conclusions	110

TABLE OF CONTENTS

PAGE NO.

6.5	Overall Conclusions	111
6.6	Closure	115

CHAPTER 7

7.	NOVEL APPROACH	116
7.1	Introduction	116
7.11	Objectives	117
7.12	Differencing schemes for reducing 'false-diffusion'	118
7.13	The novel approach: UPSTREAM scheme	119
7.2	Closure	121

CHAPTER 8

8.	APPLICATIONS OF THE NOVEL APPROACH: UPSTREAM SCHEME	122
8.1	Introduction	122
8.11	Objectives	122
8.12	The schemes investigated	122
8.2	The Test Problems	123
8.3	Presentation of Results	123
8.31	Transport of a scalar in a uniform velocity-field	124
8.32	Discussion of results	124
8.33	Flow through a sudden enlargement	126

<u>TABLE OF CONTENTS</u>		<u>PAGE NO.</u>
8.34	Discussion of results	126
8.35	Flow in a cavity with a moving lid	125
8.36	Discussion of results	128
8.37	Flow of heat/smoke in a rectangular enclosure	129
8.38	Discussion of results	129
8.4	Conclusions	132
8.5	Closure	133
 <u>CHAPTER 9</u>		
9.	CONCLUSIONS	134
9.1	One-Dimensional Study – Conclusions	134
9.2	Two-Dimensional Study – Conclusions	135
9.3	Summary of Overall Conclusions and Findings	137
9.4	Closure	140
 <u>CHAPTER 10</u>		
10.	FURTHER RECOMMENDATIONS	142
	REFERENCES	144
	TABLES	163
	FIGURES	169
	APPENDICES	229

## CHAPTER 1

### 1. INTRODUCTION

#### 1.1 Background

The numerical modelling of fluid-flow problems involves phenomena such as convection and diffusion of momentum, heat and mass which are of major importance in various engineering fields.

Examples of some of these fields are:

##### The Aerospace field:

- # modelling aircraft wings with respect to drag and lift; and
- # modelling missiles with respect to their overall design, etc.

##### The Medical field:

- # modelling of airflow through the human body; and
- # modelling of the temperature in the human torso, etc.

##### The Power field:

- # modelling of nuclear reactor cores in critical regions (ie nuclear burnout); and
- # modelling of various engines (eg rocket, car), etc.

## The General field

- # Modelling of any situation involving flows created due to various types of gradients and the presence of velocities (eg movement of smoke in enclosures due to a fire source, movement of ice in lakes, etc).

In recent years, a lot of interest and thought has been directed towards the understanding of transport phenomena and their numerical modelling, with regard to accuracy and overall representation.

In general, fluid-flow phenomena are approximated by simple interpolation formulae, based on the vast experience gathered from the past, either by intuition or experiments. However, when more complex phenomena are considered, these interpolation methods may deteriorate in terms of accurate representation of the problem.

Since the knowledge of fluid-flow phenomena is based on the conservation laws of physics, usually expressed in terms of partial-differential equations, classical methods only serve to provide practical solutions to limited problems of importance.

However, the introduction of the computer into the engineering practice, has resulted in the rapid growth of a completely new field, formally termed 'computational fluid dynamics', which has led to the development of new mathematical methods for solving the equations of fluid-flow (ie the Navier-Stokes equations). Nevertheless, there still exist a few deficiencies in these new mathematical methods which need to be

resolved carefully, before they become fully reliable, accurate and cost-effective.

The detailed study reported in this thesis, is mainly concerned with the overall improvement of accuracy and efficiency of the 'control-volume' type of numerical solution procedures, used for the partial-differential equations that govern fluid-flow phenomena. The control-volume method (CVM) is of practical interest to engineers of all fields.

In general, if the computational cost is of no objection, then the available methods can perform very well. However, since expensive numerical methods are of limited practical importance, the aim of any new or improved method should be to combine acceptable accuracy with cost. Hence, the aim of the present study is (a) to evaluate the cost-effective numerical methods, from the considerable number available today; and, (b) to suggest, if possible, new directions in devising such efficient methods.

The important negative aspect of most available methods of discretisation is 'false-diffusion', present because of non-aligned flows and grids. The 'false-diffusion' problem usually occurs because simplifying assumptions are made to approximate complex aspects.

The basic assumption leading to 'false-diffusion' is that the flow is treated as locally unidirectional, so as to apply easily the approximating methods in each of the coordinate directions. This approximation provides easy extension of one-dimensional considerations to multi-dimensional problems, but involves numerical errors for practical

grid sizes.

The alternative is to model the flow by tracing the local streamlines; that would reduce 'false-diffusion', but at the expense of introducing possible instabilities.

The ultimate theme of this thesis is to devise, in principle, a numerical scheme that reduces 'false-diffusion' without the expense of extensive grid refinement, and without any inherent instabilities. This proves a daunting task; however, if tackled in an orderly, step-by-step method, it would provide valuable information, assisting the practitioner to choose a scheme best suited to his particular problems.

## 1.2 Literature Survey

During the past decade or so, a vast amount of literature has appeared on solution techniques for incompressible flow problems, and it is not surprising that modern fluid-dynamics is greatly contributing to the current development of the finite-difference/control-volume methods, which are of importance to numerical analysts.

Attention is here focussed on the role of convection and diffusion on transport in flows of practical interest, which may be single- or multiphase, and multidimensional. Only steady-state problems are considered, so as to keep the nature of the survey within reasonable bounds. However, important contributions which rely on transient problems will also be referred to.

## 1.21 Classification

The relevant fluid-flow partial-differential equations can be discretised in many ways. In what follows, we shall outline the most common methods available and providing critical comments on their performance.

### 1.21.1 Finite-difference methods

The finite-difference method operates directly on the differential equation to obtain a set of algebraic equations. The relevant approximations are derived via truncated Taylor-series expansions, where the assumption is made that the expansion depends on a polynomial in only one of the coordinate directions, so that the higher derivatives are rendered unimportant. This method of approximation, ie Taylor-series expansion, is fairly simple and straightforward, but allows only little flexibility and provides less insight into the proper physical meaning of the terms involved.

### 1.21.2 Control-volume methods

The control-volume method operates on the integral of the partial-differential equation, over a control-volume enclosing each discrete grid-point. Algebraic equations are then obtained by representing the variation of the dependent variable between grid points via piecewise profiles. This method of approximation is easy to understand and lends itself directly to the importance of physical

interpretation; ie the conservation principle is enforced by the very nature of the method. Furthermore, there is complete freedom of choice in the assumption of profiles for different dependent variables. It is this method that was chosen for carrying out the present study.

### 1.21.3 Finite-Element Methods

The finite-element method approximates the distribution of the dependent variable within elements that are defined by mesh lines. The algebraic set of equations are then constructed by ensuring continuity of the dependent variable between elements, together with the satisfaction of some weighted residual or functional of the differential equation over each element.

### 1.21.4 Other methods

Other methods, which are not discussed here in any detail, include:

- # finite-analytic methods;
- # spline methods;
- # flux-correction methods; and
- # flux-corrected transport methods.

The above methods, although useful in some applications, have not reached as yet the level of sophistication of the ones described above, and they do not appear to lend themselves for easy generalisation.

Therefore, attention is now turned to surveying the two most developed methods at present, eg the finite-difference and control-volume methods.

## 1.22 Finite-Difference and Control-Volume Methods - A Survey

### Locally one-dimensional schemes

Over the years a vast amount of literature has appeared with regard to the formulation and application of numerical schemes. In general, the selection of a particular numerical scheme, from the great number available, depends on its accuracy, stability, consistency with physical laws (ie the conservation principles), computational cost (ie efficiency) and the level of programming (ie the actual coding of the procedure) required by the scheme.

The solution of the convection-diffusion equation, which forms a sub-set of the fluid-dynamics modelling problems, has posed serious difficulties to the numerical analyst. It is the main aim of the present section to classify some of the numerical schemes, with regard to their introduction, improvements and applications already reported by various authors.

The earliest numerical scheme used by numerical analysts was the standard central-difference scheme. It is the straightforward way to discretise the convection term, leading to a second-order scheme derived from the Taylor-series analysis. The earliest attempts to obtain a numerical solution of elliptic equations was that by Thom (1933), who

was interested in the prediction of the steady, laminar-flow of fluid over a circular cylinder. The resulting algebraic equations were solved by an iterative technique with successive-substitution. However, this approximation does not lead to diagonal dominant matrices for cell Peclet numbers greater than 2. This was reported by Thom (1933), together with quite accurate predictions for flow Reynolds numbers of the order of 50. For cell Peclet numbers greater than 2, the central-difference scheme formulation can, and often does, lead to oscillations (ie 'wiggles') in the numerical solution.

The appearance of wiggles is a sign of not conforming to the physical law being approximated. Since iterative solution procedures are preferred for cost effectiveness (ie to avoid the storage of large coefficient matrices), very inaccurate and sometimes no solution at all (ie divergence) are predicted. Thom and Apelt (1961) reported increasing difficulties, also reported by Kawaguti (1961) and Simuni (1964), for higher Reynolds numbers. To obtain accurate solutions by the use of central-difference schemes, one needs to use very fine grids so that the cell Peclet numbers are restricted to below 2; this is a very serious restriction due to the power of present day computers and the excessive cost it implies. The effect of very fine grids is that the importance of the convection term diminishes to a level where it is negligible, in other words, the flow is diffusion dominated. A way around the need for fine grids is to use under-relaxation to control the instability as reported by Thom and Apelt (1961). Nevertheless, many authors have persevered to obtain solutions to various problems using the central-difference scheme and its variants (ie the higher-order central-difference scheme).

Burgraff (1966) made use of the under-relaxation technique of Thom and Apelt (1961) to predict the flow-field in a square cavity, obtaining solutions for Reynolds numbers as high as 400. However, Burgraff's (1966) work revealed the serious shortcoming of the technique, since higher computing times were required to compensate for the instability at higher Reynolds numbers.

Among other authors to use and/or report about the central-difference scheme, are the following: Blowers (1971), Spalding (1972) de Vahl Davis and Mallinson (1976), Raithby (1976a), Chien (1977), Leschziner (1977, 1980), Lillington and Shepard (1978), Atkins, Maskell and Patrick (1980), Stabley, Raithby and Strong (1980), and Barrett (1982).

However, it is the author's opinion that there is a basic weakness in the central-difference formulation, in that convection is by its very nature a non-symmetrical phenomenon, while central-differencing implies otherwise.

It is clear that the aim of the numerical practitioner is to formulate an unconditionally stable numerical scheme for the solution of higher Reynolds number flows. The development of numerical schemes to improve the above mentioned instabilities, can be credited to Courant, Isaacson and Rees (1952) for their efforts to develop a solution procedure for hyperbolic equations (ie for supersonic flows), where links with characteristic methods are demonstrated, together with the use of the term 'upstream'. It was shown that when the convection term was replaced by an approximation which took into account the local direction of the flow (eg the above mentioned asymmetry of convection), this

greatly improved the stability of the iterative solution procedure. The consequences of the 'upstream'-direction influence generate diagonal dominant matrices, leading to the stability of the iterative solution procedure. Such numerical schemes, which take into account the local direction of the flow are termed 'upwind-differencing' schemes.

The upwind-difference scheme also suggested by Spalding (1966), was incorporated into a solution procedure for solving laminar flow problems by Runchal and Wolfshtein (1966). The laminar flow problems being considered were the impingement of a jet, and the flow in a square cavity. The application of the upwind-difference scheme were later reported by Wolfshtein (1967), Pun and Spalding (1967) and Runchal, Spalding and Wolfshtein (1967). These efforts were also collectively reported in detail by Gosman, Pun, Runchal and Spalding (1969). A similar numerical scheme was, independently, reported by Greenspan (1967).

Numerous applications of the upwind-difference scheme have been reported and some of these are listed below for completeness: Wolfshtein (1968), Dennis and Chang (1969), Blowers (1971), Runchal (1972), Markatos (1974), de Vahl Davis and Mallinson (1976), Raithby (1976a), Griffiths (1977), Atias, Wolfshtein and Israell (1977), Chow and Tien (1978), Atkins, Maskell and Patrick (1980), Kellogg, Shubin and Stephens (1980), Markatos and Pericleous (1984), and many more.

However, the accuracy of the first-order accurate upwind-difference scheme has caused a major controversy among the members of the computational fluid dynamics community. Although the expected

superiority of the upwind-difference scheme over the second-order central-difference scheme has been demonstrated and confirmed in numerous publications, see for example: Runchal (1972), Raithby and Torrance (1974), Castro (1978), Patel, Markatos and Cross (1985a), Patel and Markatos (1986a) and many others, there still exists room to improve the upwind-difference scheme for flows where there is a grid-to-flow angle present. These inaccuracies arise in the presence of non-aligned grids to the flow direction as reported by Raithby (1976a), de Vahl Davis and Mallinson (1976), Leschziner (1980) and Patel and Markatos (1986a). Indeed, the well known smearing effect of the upwind-difference scheme is clearly illustrated by Raithby (1976b) among others, where the transport of a scalar in a uniform flow-field is considered at various angles to the grid lines. The smearing effect, when present in multi-dimensional problems, is termed 'false-diffusion' [Patankar (1980)]. The conditions which give rise to false-diffusion were first determined by Wolfshtein (1968), who obtained an expression with the aid of numerical calculations of uniform flow over a square mesh at infinite Peclet number. Later, de Vahl Davis and Mallinson (1976), and Leschziner (1980), reported similar expressions via analytic means.

The false-diffusion expression, a function of the flow-to-grid skewness angle is only applicable to locally one-dimensional differential schemes. The actual cause of false-diffusion and the form of the expression is not difficult to perceive, since from the physical point of view it is clear that, in circumstances where the grids do not follow the flow, the upwinding technique should follow the streamlines/characteristics, and not the grid lines. However, mathematically, it can be argued that the error is one of trying to construct a solution procedure of complex multi-dimensional

transport phenomena by super-positioning of solutions, which are in essence of the one-dimensional transport equation.

Nevertheless, although the upwind-difference scheme has taken a lot of criticism, it still provides realistic and plausible solutions for most practical problems of importance, if sufficient care is taken to ensure the grid-independence of its predictions. The latter, however, can lead to high costs and, therefore, there still exists room to improve this scheme. This has already been recognised by many practitioners of numerical analysis, and indeed, modified versions of the scheme have been reported by, for example, Spalding (1972), Raithby and Torrance (1974) and Patankar (1980). These modified, but still locally one-dimensional, versions of the upwind-difference scheme respond to the cell Peclet numbers and not to the local skewness of the flow to the grid lines.

A step forward to improving the upwind-difference scheme was proposed by Spalding (1972). The proposed scheme termed the 'hybrid-difference' scheme is a combination of both the central- and upwind-difference schemes. The term 'hybrid' arises from the blending of the advantages of the two numerical scheme to achieve an improved scheme. The hybrid-difference schemes utilises the central-difference scheme for mesh Peclet numbers less than  $|2|$  and the upwind-difference scheme otherwise. However, this scheme still poses a restriction on the Peclet number over which the false-diffusion error will be present. Therefore, care must be taken to distribute the grids so as to utilise the central-difference scheme. This would again prove expensive and does little to alleviate the problem of false-diffusion.

Thus, the hybrid-difference scheme will only produce accurate results for the entire range of cell Peclet numbers when the grid is aligned to the flow.

The hybrid-difference scheme has been utilised by many authors and reported by the following: Markatos (1974,1978), Leschziner (1980), Leschziner and Rodi (1981), Han, Humphrey and Launder (1981) and others. The paper by Leschziner (1980) is an excellent comparative study, using five different flow configurations, and showed that the hybrid-difference scheme was the least accurate of the other schemes compared.

The locally-exact-difference scheme, first formulated by Allen and Southwell (1955) and later reintroduced by Il'in (1969), Spalding (1972) and Raithby and Torrance (1974), utilises the analytic solution of the one-dimensional convection-diffusion equation. The influence coefficients for the scheme involve the evaluation of exponential functions, which is expensive. Of course, for one-dimensional problems, the scheme is guaranteed to produce the exact solution for all Peclet numbers without any false-diffusion. However, the scheme suffers from false diffusion in multi-dimensional flow calculations since it still neglects the grid-to-flow skewness (see for example: Patel and Markatos (1986a)). Modifications of the locally-exact-difference scheme have been reported by Dennis (1960,1973), Allan (1962), Briggs (1975) and Chien (1977), among others.

Only one of the modified versions of the locally-exact-difference scheme is considered here, this being the power-difference scheme of Patankar

(1980). The power-difference scheme is aimed at reducing the computational cost of evaluating the above mentioned exponential functions. In the scheme proposed by Patankar (1980), the exponential function is replaced by a fifth-order power law. (Various ranges of mesh Peclet numbers exist within which a different approximation is used). This greatly reduces the time required to evaluate the exponential function in the first instance. The scheme has not been extensively used since its results are very similar to the hybrid- and upwind-difference schemes, and since it does not cure the smearing when grid-to-flow skewness exists.

The idea of upwinding was further extended by Leonard (1977) who considered the contribution of an extra upstream grid node in approximating the convection term. The scheme combines the merits of upwind-differencing with those of higher-order quadratic interpolation, but still without explicit reference to the actual flow angle. The scheme, referred to here by the shorter name quadratic-upstream-difference scheme, is claimed to reduce false-diffusion, erroneously to the author's opinion. The scheme, as reported by many authors, see for example: Han, Humphrey and Launder (1981), Pollard and Siu (1982) and Patel and Markatos (1985a), suffers from oscillations since the influence coefficients may become negative, infringing the transportive criteria, thus making it unbounded.

Indeed, a lot of convergence problems have been encountered by users of the quadratic-upstream-difference scheme, for example: Leschziner (1980) and Pollard and Siu (1982), show that the scheme gives rise to unbounded solutions with the amplitude of the oscillations being small.

This is attributed to the central coefficient becoming infrequently zero for infinite mesh Peclet number. Han, Humphrey and Launder (1981), among others, concluded from their results of both laminar and turbulent flow calculations in a square cavity with a moving lid, that the extra computational cost per grid point required by the scheme over that for the upwind- and hybrid-difference schemes, for a converged solution, is more than compensated for by the greater accuracy, when the flow is aligned with the grid. However, when this is not possible, very fine grids are required to overcome the problems of convergence that may be encountered. Apart from these disadvantages, the scheme also requires special practices at boundaries together with some modification of the influence coefficients, for example: Han, Humphrey and Launder (1981) reported that modified influence coefficients were achieved by using pseudo sources to give a stable scheme. All these diminish the practicality and generality of the scheme.

Extensions of the quadratic-upstream-difference scheme are reported by Leonard, Leschziner and McQuirk (1978) and Pollard and Siu (1982). The latter authors reported two modified versions of the quadratic-upstream-difference scheme which were termed the extended and extended-revised versions. The scheme is first reformulated to ensure always positive influence coefficients, in the absence of sources, to conform to the boundedness property. This leads to the extended version of the quadratic-upstream-difference scheme. The scheme performs well, see Pollard and Siu (1982) and Patel and Markatos (1986a), in the absence of sources and when the flow is mainly along one of the coordinate directions. However, since sources cannot be neglected in real problems, its applicability is still limited.

The aforementioned deficiencies in the quadratic-upstream-difference scheme-extended are rectified by further linearisation of the sources according to the practice of Patankar (1980). This leads to the revised-extended version of the scheme as reported by Pollard and Siu (1982). Unfortunately, no other reported applications of the scheme have been traced to date, except that by Pollard and Siu (1982) and Patel and Markatos (1986a). The modified schemes although accurate, prove expensive, and do not explicitly take into account the flow angle, ie they do not address directly the problem of 'false diffusion'.

It is the author's opinion that the 'way-ahead' is to look towards flow oriented schemes, which directly take into account the grid-to-flow angle, ie to apply the approximation along the local streamlines.

The earliest reported flow-oriented schemes were those by Le Favre (1970) and Zuber (1972), who introduced schemes with explicit grid-to-flow angle dependence. However, the schemes were non-conservative and thus not fully suitable for general use. Later, Raithby (1976b) formulated what was termed the skew-upstream-difference scheme, which was non-conservative. The skew-upwind-difference scheme of Raithby (1976b), although formally only first-order accurate, yields a significant reduction in skewness errors by partially simulating an upwind discretisation coordinate system. In this case, skewness errors are entirely absent, that is, the scheme tends to simulate the locally multi-dimensionality of the flow. Applications of Raithby's (1976b) scheme have been reported by Militzer, Nicoll and Alpay (1977), Castro (1978), Leschziner (1980) and Lillington (1980, 1981), although the difficulty of the scheme to converge

always, for complex fluid-flow problems, and the possibility of 'wiggles' or 'oscillations' still exist. Furthermore, the scheme is complex in its implementation in generally available fluid-flow software.

Variations of the skew-upstream-difference scheme have been reported by Lillington (1981) termed as the 'vector-upstream-difference scheme' and Hassan, Rice and Kim (1983) reported the 'mass-flow-weighted skew-upwind difference scheme'. The former is modified by representing the source differently to the original scheme of Raithby (1976b) and the latter reformulated the coefficients to ensure always positive influence coefficients. Both the above modified schemes have been used for complex flow problems by the above authors, but no mention of the difficulties of programming matter were stressed upon.

### 1.23 Finite-Element Methods - A Survey

A great deal of effort has been devoted recently to the application of finite-element methods in fluid-dynamics. Along with this development has come the realisation that the normal Galerkin method, the finite-element counterpart of the central-difference scheme, is not always suitable. This is because convection operators are non-symmetric and Galerkin method application leads to occasional spurious oscillations in the results, for flows at high Peclet numbers (Gresho and Lee (1979)). A similar situation was encountered by the control-volume practitioners in the 1960s, and was then overcome by the introduction of the upwinding schemes. Indeed, some of the finite-element methods are also subject to the same criticisms as the conventional upwind finite-difference

methods.

Convection dominated phenomena have proven to be one of the most difficult types of problems to be successfully dealt with by numerical methods. Although the Galerkin method has proved satisfactory in applications to linear and non-linear symmetric operators, its applications to non-symmetric operators often gives rise to 'wiggles'. These 'wiggles' can be eliminated only by severe mesh refinement.

An excellent review of the applications of finite-element methods to fluid-flow problems is given by Gallaher et al (1978) and Glowinski (1982). Detailed background and general information on developments of the method is easily obtained from standard finite-element text books (eg Zienkiewicz (1977)). Therefore, the reader should refer to the above books for detailed information with regard to the background and applications of finite-element methods.

What follows is a summary of most of the earlier and later finite-element techniques that are now commonly used by fluid-dynamics practitioners.

To overcome the problems encountered by the Galerkin finite-element method for convection-diffusion problems, several upwind type finite-element methods have been reported (for example see: Hughes et al (1979) and Heinrich et al (1977)). The extended methods for two-dimensional flow problems were reported by Heinrich et al (1977).

In general, all such upwinded-finite-element methods suffer from numerical/'false diffusion' similar to that experienced by the conventional

upwind-difference finite-difference methods.

The flow-oriented schemes were the next step to improve the finite-element methods. This was reported by Hughes and Brooks (1979) where a 'streamline-upwind scheme' similar to the skew-upstream-difference scheme of Raithby (1976b) was proposed, although the solutions were not always bounded. This clearly shows that the finite-element methods also suffer from the same deficiencies as those of the finite-difference/volume methods.

Superficially, it is easy to conclude that the finite-element methods are advantageous over the finite-volume methods since the former can handle complex shapes of calculation domains due to the great flexibility in the element shapes that can be utilised. However, conservation is not usually satisfied over the whole calculation domain, which is a disadvantage on all situations where the overall balance of the fluxes are important.

A further disadvantage of the finite-element methods is that the coefficient matrix is not always regular; thus, computing requirements tend to become demanding and always greater than the finite-volume methods.

Recently, due to the advent of grid generation techniques, finite-volume methods have been utilised to calculate flow-fields for complex geometries using 'body-fitted grids' [Malin, Rosten, Spalding and Tatchell (1985)] and, in general, the computing costs are far less than those required by the finite-element methods.

### 1.3 Closure

This chapter has presented a classification of the numerical techniques used for solving fluid-flow problems, together with a literature survey for finite-difference/control-volume methods and finite-element methods.

## CHAPTER 2

### 2. DIFFERENTIAL EQUATIONS AND FINITE-VOLUME EQUATIONS

#### 2.1 Introduction

This chapter describes the general mathematical framework (ie the Navier-Stokes equations) employed in the calculations of the laminar and turbulent flows. The partial-differential equations presented here express the physical laws of conservation of mass, momentum, enthalpy and other conserved fluid properties. Both laminar and turbulent flows are modelled by the same set of equations, which is achieved by prescribing 'effective' exchange coefficients for the relevant variables. The equations are given in cartesian tensor notation form for the general time-dependent problem.

#### 2.2 Conservation Equations

##### 2.21 The partial-differential equations

The equations listed in this section are equally applicable to both laminar and turbulent flows.

For multi-dimensional flows, the time-dependent equations for the conservation of mass, momentum and any conserved scalar property can be expressed in cartesian tensor form as follows [(eg Bradshaw (1976))]:

$$\frac{\partial}{\partial t} (\rho) + \frac{\partial}{\partial x_j} (\rho u_j) = 0 \quad (2.21-1);$$

$$\frac{\partial}{\partial t} (\rho u_i) + \frac{\partial}{\partial x_j} (\rho u_j u_i - \tau_{i,j}) - S_{u_i} + \frac{\partial P}{\partial x_j} = 0 \quad (2.21-2a);$$

where:

$$\tau_{ij} = -\mu \left( \frac{\partial u_i}{\partial x_j} + \frac{\partial u_j}{\partial x_i} - \frac{2}{3} \frac{\partial u_k}{\partial x_k} \delta_{ij} \right) \quad (2.21-2b);$$

and

$$\begin{aligned} \delta_{ij} &= 0 & i \neq j \\ &= 1 & i = j \end{aligned} \quad (2.21-2c).$$

#### Conservation of scalar property $\phi$

$$\frac{\partial}{\partial t} (\rho \phi) + \frac{\partial}{\partial x_j} (\rho u_j \phi - J_{\phi,j}) - S_{\phi} = 0 \quad (2.21-3a);$$

where  $S_{\phi}$  is the source/sink term for  $\phi$ , and  $J_{\phi,j}$  stands for the diffusion fluxes, which are of the following form:

$$J_{\phi,j} \equiv \frac{\mu}{\sigma_{\phi}} \frac{\partial \phi}{\partial x_j} \quad (2.21-3b);$$

where  $\sigma_{\phi}$  is the Prandtl number.

## 2.22 The time-averaged form of the equations

The exact time-dependent equations apply to both laminar and turbulent flows. In theory, it should be possible to solve these equations for turbulent flows directly; however, in practice, their solution is not possible at present, or in the foreseeable future [(eg Launder and Spalding (1972))]. Simulation of turbulent flows is obtained from the equations presented above by means of the following substitution:

$$\phi = \bar{\phi} + \phi' \quad (2.22-1);$$

where  $\bar{\phi}$  is the time-averaged value and the prime, ( $\phi'$ ), denotes the fluctuating part of  $\phi$ . The introduction of equations (2.22-1) into the equations of Section 2.21 yields the relevant forms of the time-averaged equations. These are listed in Appendix A2.1.

## 2.23 The general equations to be solved

A review of the relevant partial-differential equations of interest, listed above, indicates that they are similar in their structure for all conserved properties and can be represented by a single general equation, which for steady-state phenomena is as follows:

Polar

$$\rho \left( \frac{1}{r} \frac{\partial}{\partial r} (rv\phi) + \frac{\partial}{\partial x} (u\phi) \right) = \frac{1}{r} \frac{\partial}{\partial r} \left( r\Gamma_{\text{eff},\phi} \frac{\partial \phi}{\partial r} \right)$$

$$+ \frac{\partial}{\partial x} (\Gamma_{\text{eff},\phi} \frac{\partial \phi}{\partial x}) = S_{\phi} \quad (2.23-1a).$$

### Cartesian

$$\frac{\partial}{\partial x} (\rho u \phi) + \frac{\partial}{\partial y} (\rho v \phi) = \frac{\partial}{\partial x} (\tau \frac{\partial \phi}{\partial x}) + \frac{\partial}{\partial y} (\tau \frac{\partial \phi}{\partial y}) + S_{\phi} \quad (2.23-1b);$$

where  $\Gamma_{\text{eff},\phi}$ ,  $\tau$  and  $S_{\phi}$  are deduced from the parent equations (see Appendix A2.1).

The terms on the left-hand side of equation (2.23-1) represent the transport of  $\phi$  by convection and the terms on the right-hand side, except  $S_{\phi}$ , represent the diffusion of  $\phi$ ;  $S_{\phi}$  is the source expression which includes real sources/sinks and terms that do not neatly fit into the convection or the diffusion terms.

### 2.3 Discretisation Procedure

In Section 2.2 above, the partial-differential equations which govern steady-state flow were presented. The task of this sub-section is to present briefly the numerical procedure which has been used to solve the relevant equations.

The aim is to employ numerical methods, of the finite-volume type. The domain of interest is subdivided into a finite-number of control-volumes, by using a finite-volume grid. The grid points are surrounded by non-overlapping 'control-volumes' which when taken together completely fill the domain of interest.

The finite-volume algebraic equations, at each grid point, are obtained by integrating the differential equations over each control-volume. Integration enables interpolation assumptions for the variables of values and gradients between grid nodes.

The above discretisation method provides a set of algebraic equations which are non-linear (by means of their coefficients being functions of the dependent variables) and strongly coupled. This necessitates the use of iterative solution procedures (iteration as opposed to direct matrix inversion).

### 2.31 Finite-domain equations

In this section, the finite-volume algebraic representations for the general equations (2.23-1) are derived.

### 2.32 Finite-volume grid and variable locations

The domain of interest is sub-divided into finite-volumes by orthogonal intersecting grid-lines which are distributed parallel to the coordinate axes.

The points of intersection are called grid points or nodes, and represent the locations where every scalar is evaluated.

Figure 2.32-1 represents a typical grid arrangement, together with the

locations of storing and computing the dependent variables in the finite-volume grid. All scalar variables (eg.  $P$ ,  $k$ ,  $\epsilon$ ,  $T$ ,  $H$ , etc) are stored at the grid points whereas the velocity components (eg.  $u$ ,  $v$ ) are stored midway between two adjacent grid points. This approach [Harlow and Welch (1965)] is conventional and termed as the 'staggered-grid' arrangement is adopted here. Its advantages are:

- \* the velocities are available directly for flux evaluations at the control-volume faces; and,
- \* the pressures are stored on either side of velocities, which enables pressure gradients (which drive the velocities) to be evaluated easily. The 'L' shapes, in Figure 2.32-1 depict the manner in which the dependent variables are grouped; In other words, the triad of points inside the L's refer to the same storage location.

### 2.33 General- and boundary-control-volumes

Each dependent variables is defined within a control-volume, over which the integration is performed. Since there are three different locations for the dependent variables in Figure 2.32-1 there exists three distinct types of control-volumes. These are depicted in Figure 2.33-1. The shaded areas A, B and C refer to the control-volumes for the  $u$ ,  $\phi$  and  $v$  variables, respectively.

Each dependent variable has a different representation for near-boundary

control-volumes. These are depicted in Figure 2.33-2. The shaded areas A', B' and C' refer to the near-boundary control-volumes for the u,  $\phi$  and v variables, respectively.

This arrangement is utilised so that at the near-boundary control-volume faces, the velocity components and the boundary grid points coincide with the boundary value.

#### 2.4 Derivation of Finite-Volume Equations

With reference to the general equation (2.23-1), attention is focussed here on the derivation of the finite-volume, algebraic equations relating  $\phi_p$  to its surrounding neighbours. The notation is depicted in Figure 2.4-1. The differential equation is integrated over the control-volume and each term will be discussed in turn.

##### 2.41 The diffusion term

Integration of the equation over a typical control-volume P, Figure 2.4-1, for the diffusion term yields the following expression:

$$\int_{x_w}^{x_e} \int_{r_s}^{r_n} - \left( \frac{1}{r} \frac{\partial}{\partial r} (r \Gamma_\phi \frac{\partial \phi}{\partial r}) + \frac{\partial}{\partial x} (\Gamma_\phi \frac{\partial \phi}{\partial x}) \right) = [D_e + D_w + D_n + D_s] \phi_p$$

$$- [D_e\phi_E + D_w\phi_W + D_n\phi_N + D_s\phi_S] \quad (2.41-1a);$$

where the D's stand for the diffusion expression, evaluated at various locations around the point P.

For example:

$$D_e = \Gamma_{\phi_e} \frac{A_e}{\delta x_e} = \left( \frac{\Gamma_{\phi_P} + \Gamma_{\phi_E}}{2} \right) \frac{A_e}{\delta x_e} \quad (2.41-1b);$$

which is the total flux due to diffusion across the east face of the P control-volume.

## 2.42 The source term

Integration of the source term,  $S_\phi$ , over a typical control-volume P, together with the linearisation procedure of Patankar (1980) yields the following expression:

$$\int_{x_w}^{x_e} \int_{r_s}^{r_n} r S_\phi dx dr = S_\phi r_p \Delta x \Delta r \quad (2.42-1a);$$

$$= S_a^\phi + S_b^\phi \phi_P \quad (2.42-1b).$$

The restriction on  $S_b$ , one of the linearisation coefficients is that it must be negative so as to ensure numerical stability [see Patankar (1980)].

## 2.43 The convection term

It is the intention of the present study to evaluate a number of possible approximate representations for the convective fluxes across a control-volume face, since numerous numerical schemes have been reported for this purpose, and none appears entirely satisfactory.

The integration of the convection term of equation (2.23-1a) over a typical control-volume, leads to the following expression:

$$\int_{x_w}^{x_e} \int_{r_s}^{r_n} \left( \frac{1}{r} \frac{\partial}{\partial r} (\rho v r \phi) + \frac{\partial}{\partial x} (\rho u \phi) \right) = C_p \phi_p - \sum C_{nb} \phi_{nb} \quad (2.43-1a);$$

where the C's denote mass fluxes and nb, the neighbouring values involved in the calculation. The expression of  $C_e$ , say, is:

$$C_e = \rho_e u_e A_e \equiv \frac{(\rho_E + \rho_P)}{2} u_e A_e \quad (2.43-1b).$$

In general the expression utilised for the approximation at the control-volume faces of the dependent variable of interest is important. This is the subject of a later chapter.

## 2.44 The overall finite-volume equations

Finally, the overall finite-volume representation can be obtained by substituting expressions (2.41-1), (2.42-1) and (2.43-1) into equation (2.23-1).

This representation is given below in a compact form:

$$A_p \phi_p = \sum A_{nb} \phi_{nb} + S \quad (2.44-1);$$

where  $A_{nb}$  denotes the neighbouring grid-point value contributions to  $\phi_p$  due to the influences of convection and diffusion [Patankar (1980)].

## 2.5 Convergence Criteria and Physical Constraints

Since the differential equations are approximated by finite-volume equations (2.44-1), it is very important to retain within the discretisation procedure, the relevant information from the original partial-differential equations. It is on this basis that the finite-volume equations should be constructed.

### 2.51 Information in analytical solutions

#### (i) The conservation property

The volume integral (in vector notation) of the differential equation for a region (R) bounded by a surface ( $S_R$ ) is given by:

$$\oint_{S_R} (\rho \underline{u} \phi - \Gamma \text{grad}(\phi)) \underline{n} \, dS_R = \int_R S \, dR \quad (2.51.1-1);$$

where  $\underline{n}$  is the unit normal vector (positive outwards) to the surface.

The conservation requirement preserves the integral conservation relations of the continuity equation.

(ii) The boundedness property

Within a region (R), the maximum principle [Forsythe and Wasow (1960)] implies for  $S=0$ , that the solution of a differential equation cannot assume either a negative minimum or a positive maximum. This implies that the solution must be bounded in the region (R), by the values on the surface ( $S_R$ ).

That is:

$$\min (\phi_{S_R}) \leq \phi \leq \max (\phi_{S_R}) \quad (2.51.2-1).$$

(iii) The transportive property

The transportive property implies that the effect of a perturbation, in the absence of sources, does not interfere with the solution [Roach and Mueller (1970), Roach (1972)] in regions of strongly convective flows.

## 2.52 Information in discretised equations

(i) The conservation property

For the discretised procedure to satisfy the conservation property, the integral conservation expression (2.51.1-1) must be satisfied both within

each control-volume, locally, and over the whole region of interest, globally.

Therefore, to meet the requirements of global conservation, flux continuity at control-volume faces must be enforced. This is clear from expression (2.51.1-1), when written for each control-volume in turn, and summed over the domain of interest. To achieve this, the fluxes must be continuous at the control-volume faces (ie. reciprocity), thus ensuring appropriate cancellations within the domain of interest, leaving only the exterior surface integral.

(ii) Boundedness property

The boundedness property for the discretised equations is ensured when equation (2.44-1) in the absence of sources, satisfies the following expression:

$$A_p \geq \sum A_{nb} \quad ; \quad A_{nb} \geq 0 \quad (2.52.2-1);$$

thus ensuring mass conservation and system boundedness.

For example, consider one-dimensional flow, for which the following algebraic equation is valid:

$$A_p \phi_p = A_E \phi_E + A_W \phi_W \quad (2.52.2-2a).$$

The diagonal dominance of this system is ensured by requiring that:

$$|A_p| \geq |A_E| + |A_W| \quad (2.52.2-2b).$$

It follows that:

$$|A_E| + |A_W| \geq |A_{E+W}| = |A_p| \geq |A_E| + |A_W| \quad (2.52.2-2c);$$

and hence,

$$|A_E| + |A_W| = |A_{E+W}| \quad (2.52.2-2d);$$

which implies,

$$\min(\phi_E, \phi_W) \leq \frac{1}{A_p} (A_E \phi_E + A_W \phi_W) = \phi_p \leq \max(\phi_E, \phi_W) \quad (2.52.2-2e).$$

It is to be observed that  $\phi_p$  lies within the range of its neighbouring values, implying physically realistic solutions (ie. no over/under-shoots).

It follows that if the numerical scheme in matrix form is diagonally dominant, then all coefficients ( $A_{nb}$ ), have the same sign.

Effects of non-diagonally dominant systems can be illustrated by the following simple example:

$$A_p \phi_p = \{ (A_E + A_W)^- \phi_{LEFT} + (A_E + A_W)^+ \phi_{RIGHT} \} \quad (2.52.2-2f);$$

where the coefficient of  $\phi_{LEFT}$  is negative and that of  $\phi_{RIGHT}$  is positive.

This system has the potential for over/under-shoots.

(iii) Transportive property

For discretised equations, the links of a grid point with neighbours lying outside the domain of interest should not feature in the calculation of the value at that grid point. Failure to satisfy this rule, would lead to non-positive coefficients, thus violating the boundedness property.

2.53 Grid-to-flow skewness

In general, flows which are inclined to the grid (eg. recirculations) have to be treated by the differencing scheme so as to take into account the local direction of the flow. This idea is discussed in detail in a later chapter.

2.6 Closure

This chapter has presented, in brief, the mathematical formulation of flow and heat/mass transfer phenomena that are considered in this thesis.

The partial-differential equations for continuity, momentum and a general scalar property,  $\phi$ , have been introduced and discussed.

Furthermore, the finite-volume representation of the partial-differential equations has been derived, in a general context, together with the introduction of such properties of the original differential equations as

conservation, boundedness and transportive principles that have to be satisfied also by the finite-volume equations.

## CHAPTER 3

### 3. SOLUTION PROCEDURE FOR THE FINITE-VOLUME EQUATIONS

#### 3.1 Introduction

In the previous chapter the partial-differential equations, relevant to the present study, were set out together with the general form of the finite-volume equations. The task in this chapter is to present briefly, the solution procedure that is used to solve the set of finite-volume equations.

Patankar and Spalding (1972) described a three-dimensional calculation procedure for parabolic flows; for example, a flow in a duct is calculated by marching in the predominant direction of flow. This idea was incorporated into a three-dimensional computational structure [Caretto, Gosman, Patankar, Potter and Spalding (1972); Patankar (1975)].

The particular technique by which the velocity and pressure links are handled has been given the name SIMPLE (for Semi-Implicit Method for Pressure Linked Equations; although the method is actually fully-implicit; semi-implicit was used only for euphony).

Later the NEAT (Nearly Exact Addjustment of Terms) method of Spalding (1976) was also incorporated within the SIMPLE method. The method is, despite its name, a fully-implicit solution procedure for solving the relevant system of equations by cycles of guess-and-correct operations on a line-by-line basis, that utilises the tri-diagonal matrix algorithm

known as TDMA or Thomas algorithm [Smith (1969); Roach (1976); Conte and de Boor (1980)].

### 3.11 The SIMPLE algorithm

A brief description of the SIMPLE solution procedure is presented here for completeness, but the reader is referred to Patankar and Spalding (1972), and Patankar (1980) for full details.

#### The algorithm

The momentum equations are solved using a 'guessed' pressure field.

The continuity equation is not directly solved, but is manipulated instead to yield an equation for 'pressure-corrections' that are used to correct pressures and velocities.

#### Operations

The following are the formal steps of the solution algorithm [Pun and Spalding (1977)]:

1. Guess the pressure field.
2. Solve the momentum equations on the first line, for  $u^*$  and  $v^*$  using the TDMA procedure, where the 'starred' velocities denote the solution based on the guessed pressure field.

3. The 'starred' velocities do not, in general, satisfy continuity. Substitution of these velocities in the continuity equation yields therefore mass errors.
4. The pressure-correction equation is solved, having as its source term, the mass errors evaluated in Step 3.
5. The pressure-corrections are applied to correct the velocities and pressure, in such a way so as to eliminate the continuity errors.
6. Steps (2) to (5) are repeated until convergence to a preset tolerance has been obtained.
7. Advance to the next line and repeat Steps (2) to (6).
8. Continue until a domain sweep is completed. (a domain sweep consists of visiting every line in the domain).
9. Perform as many sweeps as required for convergence. This leads to a converged solution within a preset tolerance.

The above solution procedure is also applicable to three-dimensional problems, where 'line' is replaced by 'slab', eg. groups of cells having the same z-coordinate.

### 3.12 The NEAT algorithm

The NEAT algorithm, is a line-by-line technique which uses the TDMA as its basic unit of operation.

In two-dimensional problems, equation (2.44-1) is solved for all  $\phi$ -variables along a grid-line, where the neighbouring  $\phi$ -values used are the best estimates available. It is this assumption that enables the TDMA procedure to be used. NEAT performs an additional 'block correction' between lines, so as to accelerate convergence.

Rearranging equation (2.44-1) gives, for the TDMA procedure, the following set of equations (for a constant x-line):

$$A_P\phi_P = A_N\phi_N + A_S\phi_S + S_{LUMP} \quad (3.12-1a):$$

where  $S_{LUMP}$  is given by:

$$S_{LUMP} = S + A_E\phi_E + A_W\phi_W \quad (3.12-1b).$$

The TDMA procedure is then applied to equation (3.12-1a) as described in Appendix A3.1.

The above solution is embodied in the computer code 2/E/FIX (2-Dimensional Elliptic FIXed grid) used in the present study [Pun and Spalding (1977)].

### 3.2 Sources of Inaccuracy in Solution Procedures

There are two sources of error which, in general, influence the overall accuracy of the solutions obtained by numerical solution procedures, such as the one described above.

They are identified as:

- (a) errors and uncertainties in physical/mathematical modelling, eg. turbulence differential-equation models [Patel, Cross, Markatos & Mace (1986)], two-phase flow iterations, etc; and
- (b) errors due to numerical approximations, and computer round-off.

Only the first part of the second source of errors, eg. numerical-approximation errors, is of importance in this study and it is therefore the only one discussed below.

#### 3.21 Numerical approximation errors

These errors arise because the continuous nature of the equations is replaced by a discrete representation (ie. by interpolation formulae). These errors are mainly due to the fact that steep gradients which are, in general, present in the final solution may not be accurately approximated by the numerical formulae used. In case of unwise choice of numerical formulae, accurate representations can only be

achieved by the use of very fine grid distributions; this, however, leads to the increase of the computer round-off errors that may affect seriously the final outcome.

Furthermore, very fine-grid solutions are too expensive to use, in terms of computer resources. One way out of these difficulties is the use of better approximations that will improve the accuracy for coarser grids. Further discussion on numerical errors is provided in Chapter 5.

### 3.22 Convergence

The degree of accuracy of the final solution is also dependent on the convergence criterion imposed on a given solution procedure. Therefore, precise definition of 'converge' is required.

A 'converged' solution in the present study is deemed to be obtained by satisfying the following two specific requirements, concerning the error levels:

- (a) the sum of absolute residual errors in the solution of any variable must be low i.e.  $\leq 10^{-6}$ ; and
- (b) the absolute (volume) continuity errors must be less than 0.1% of a typical volume-flow rate.

In general, the latter requirement was satisfied before the former.

### 3.23 Relaxation practice

Due to the non-linear nature and the strong coupling between the differential equations, the iterative procedure may necessitate relaxation, in order to converge. When the iteration-to-iteration variation in values is large, there is a possibility of divergence and to combat this, it is advisable to employ some sort of under-relaxation.

The conventional practice was followed, eg:

$$\phi_{\text{present}} = \alpha\phi_{\text{new}} + (1-\alpha)\phi_{\text{old}} \quad (3.23-1);$$

where  $\phi_{\text{new}}$  is the  $\phi$ -value evaluated at the current iteration;  $\phi_{\text{old}}$  is the  $\phi$ -value from the previous iteration.  $\phi_{\text{present}}$  is the resulting  $\phi$ -value at the present iteration after being relaxed, and  $\alpha$  is the relaxation parameter.

### 3.3 Closure

This chapter has presented, briefly, the solution procedure by which the algebraic equations, derived in Chapter 2, can be solved. The procedure used is the SIMPLE algorithm together with the NEAT adjustment.

The solution procedure is flexible and general, and may be applied to calculate numerous flow situations of practical interest.

Finally, the accuracy of the numerical solution procedure and constraints of convergence were identified.

## CHAPTER 4

### 4. NUMERICAL SCHEMES

#### 4.1 Introduction

In this chapter, the numerical schemes for convection considered for this investigation are introduced. The diffusion term is approximated by the central-difference scheme, which is, in general, a good approximation, since it is third order [Leonard, Leschziner and McGuirk (1978)].

On the contrary, convection, which is by its nature a non-symmetrical phenomenon, may introduce considerable inaccuracy when approximated by numerical schemes.

In what follows, thirteen numerical schemes (ie. interpolation techniques) for the convection term are described [Patel, Markatos and Cross (1985a), Patel and Markatos (1986a)], with the aim of evaluating and comparing their accuracy and practicality of implementation.

#### 4.11 Diffusion terms

For a general grid, Figure (4.11-1), the integrated diffusion term, in two dimensions, is given by:

$$\left(\Gamma \frac{\partial \phi}{\partial x}\right)_e a_e - \left(\Gamma \frac{\partial \phi}{\partial x}\right)_w a_w + \left(\Gamma \frac{\partial \phi}{\partial y}\right)_n a_n - \left(\Gamma \frac{\partial \phi}{\partial y}\right)_s a_s \quad (4.11-1);$$

where approximations for the quantities in brackets are sought.

#### 4.11.1 Central-differencing scheme

The central-difference scheme, which is used for the diffusion term approximation, assumes in the present study a piecewise linear profile between two grid points, as it is usually used to approximate the  $\phi$ -gradient. Therefore the terms in expression (4.11-1) are replaced by:

$$\begin{aligned} & \frac{\Gamma_e}{\delta x_e} (\phi_E - \phi_P) a_e - \frac{\Gamma_w}{\delta x_w} (\phi_W - \phi_P) a_w \\ & + \frac{\Gamma_n}{\delta y_n} (\phi_N - \phi_P) a_n - \frac{\Gamma_s}{\delta y_s} (\phi_S - \phi_P) a_s \end{aligned} \quad (4.11.1-1).$$

#### 4.12 Convection term

Integration of the convection term, over a typical control-volume, Figure (4.11-1), yields:

$$(\rho u \phi)_e a_e - (\rho u \phi)_w a_w + (\rho v \phi)_n a_n - (\rho v \phi)_s a_s \quad (4.12-1).$$

The objective of the present study is to investigate various forms of approximating the  $\phi$ -value used at the control-volume faces (ie.  $\phi_e$ ,  $\phi_w$ ,  $\phi_n$ ,  $\phi_s$ ), and suggest new ones. The velocities at the faces do not need any averaging since when solving for any scalar  $\phi$  they are already located at the cell faces.

#### 4.12.1 Central-difference scheme

The central-difference scheme assumes a linear profile to evaluate the convected face values as follows:

$$\begin{aligned}\phi_e &= \frac{1}{2} (\phi_E + \phi_P) \\ \phi_w &= \frac{1}{2} (\phi_W + \phi_P) \\ \phi_n &= \frac{1}{2} (\phi_N + \phi_P) \\ \phi_s &= \frac{1}{2} (\phi_S + \phi_P)\end{aligned}\tag{4.12.1-1}.$$

#### The influence coefficients

The overall A coefficients of equation (2.44-1) which concern contributions of both convection and diffusion are, for the central-difference scheme, as follows:

$$\begin{aligned}A_E &= D_e - \text{mod} \left( \frac{C_e}{2} \right) + \mathbf{[-C_e, 0]} \\ A_W &= D_w - \text{mod} \left( \frac{C_w}{2} \right) + \mathbf{[C_w, 0]} \\ A_N &= D_n - \text{mod} \left( \frac{C_n}{2} \right) + \mathbf{[-C_n, 0]} \\ A_S &= D_s - \text{mod} \left( \frac{C_s}{2} \right) + \mathbf{[C_s, 0]}\end{aligned}\tag{4.12.1-2};$$

where the D terms are defined by equation (2.41-1b) and the C terms are defined by equation (2.43-1b), and

$$[A,B] \equiv \max (A \text{ and } B).$$

This is a convenient way of presenting the various schemes and will be used for all of them, in what follows.

#### 4.12.2 Upwind-difference scheme

The upwind-difference scheme, first suggested by Courant, Issacson and Rees (1952) assumes the upwind- $\phi$  value to be convected through the faces, instead of the average of two neighbours values of the convected property. This leads to the following approximation for the convected  $\phi$ -values at the faces:

$$\phi_e = \phi_P \quad u_e \geq 0$$

$$= \phi_E \quad u_e < 0$$

$$\phi_w = \phi_W \quad u_w \geq 0$$

$$= \phi_P \quad u_w < 0$$

(4.12.2-1).

$$\phi_n = \phi_P \quad v_n \geq 0$$

$$= \phi_N \quad v_n < 0$$

$$\phi_s = \phi_S \quad v_s \geq 0$$

$$= \phi_P \quad v_s < 0$$

#### The influence coefficients

The influence coefficients for the upwind-differencing scheme are:

$$A_E = [D_e, D_e - C_e]$$

$$A_W = [D_w, D_w + C_w]$$

$$A_N = [D_n, D_n - C_n]$$

$$A_S = [D_s, D_s + C_s]$$

(4.12.2-2).

#### 4.12.3 Hybrid-difference scheme

The hybrid-difference scheme, introduced by Spalding (1972) combines the advantages of both the central-difference scheme and upwind-difference scheme. It leads to the following expressions for the convected face values:

$$\begin{aligned} \phi_e &= \phi_P & \dot{m}_e > 2D_e \\ &= \frac{1}{2} (\phi_P + \phi_E) & \dot{m}_e \leq 2D_e \end{aligned}$$

$$\begin{aligned} \phi_w &= \phi_W & \dot{m}_w > 2D_w \\ &= \frac{1}{2} (\phi_P + \phi_W) & \dot{m}_w \leq 2D_w \end{aligned}$$

(4.12.3-1)

$$\begin{aligned} \phi_n &= \phi_P & \dot{m}_n > 2D_n \\ &= \frac{1}{2} (\phi_P + \phi_N) & \dot{m}_n \leq 2D_n \end{aligned}$$

$$\begin{aligned} \phi_s &= \phi_S & \dot{m}_s > 2D_s \\ &= \frac{1}{2} (\phi_P + \phi_S) & \dot{m}_s \leq 2D_s \end{aligned}$$

where  $m$ 's are the absolute values of the mass-flow rates through each face denoted by the lower-case subscripts.

### The influence coefficients

The influence coefficients for the hybrid-difference scheme are:

$$A_E = [0, D_E - C_E/2, -C_E]$$

$$A_W = [0, D_W + C_W/2, C_W]$$

$$A_N = [0, D_N - C_N/2, -C_N]$$

$$A_S = [0, D_S + C_S/2, C_S]$$

(4.12.3-2).

#### 4.12.4 Locally-exact-difference scheme

The locally-exact-difference scheme, traced back to the paper by Allen and Southwell (1955) and later rediscovered by Spalding (1972) and others, makes use of the one-dimensional analytical solution for the convection-diffusion equation (without sources) to approximate the convected values across the faces.

Since the analytical solution for the one-dimensional convection-diffusion equation is an exponential function, the face values according to this scheme are approximated as follows:

$$\phi_W = \phi_P + \frac{\exp(P_W) - 1}{\exp(P) - 1} (\phi_P - \phi_W)$$

$$\phi_E = \phi_P + \frac{\exp(P_E) - 1}{\exp(P) - 1} (\phi_E - \phi_P)$$

$$\phi_N = \phi_P + \frac{\exp(P_N) - 1}{\exp(P) - 1} (\phi_N - \phi_P)$$

$$\phi_S = \phi_P + \frac{\exp(P_S) - 1}{\exp(P) - 1} (\phi_P - \phi_S)$$

(4.12.4-1);

where  $P$  is the Peclet number and  $P_e$ ,  $P_w$  etc are the mesh Peclet numbers.

#### The influence coefficients

The influence coefficients for the locally-exact difference scheme are:

$$A_E = \frac{P_e}{\exp(P_e)-1} + [-C_e, 0]$$

$$A_W = \frac{P_w}{\exp(P_w)-1} + [C_w, 0]$$

$$A_N = \frac{P_n}{\exp(P_n)-1} + [-C_n, 0]$$

$$A_S = \frac{P_s}{\exp(P_s)-1} + [C_s, 0]$$

(4.12.4-2).

For details see Appendix A4.1.

#### 4.12.5 Power-difference scheme

The power-difference scheme, an extension of the locally-exact-difference scheme, makes use of a fifth order power law to approximate the exponential functions that occur in the locally-exact-difference scheme [Patankar (1980)]. The convected value at the faces is approximated as follows:

$$(1+\beta_e)\Phi_{\text{upstream}} - \beta_e\Phi_{\text{downstream}}$$

(4.12.5-1a);

where:

$$\beta_e = (1 - |P_e|/10)^5 / |P_e| \quad (4.12.5-1b).$$

The influence coefficients

$$A_E = D_e [0, \beta_e |P_e|] + [-C_e, 0]$$

$$A_W = D_w [0, \beta_w |P_w|] + [C_w, 0]$$

$$A_N = D_n [0, \beta_n |P_n|] + [-C_n, 0]$$

$$A_S = D_s [0, \beta_s |P_s|] + [C_s, 0]$$

(4.12.5-2).

4.12.6 Leonard-difference scheme

The Leonard-difference scheme [Barratt (1982)] uses two upstream grid-point values to approximate the first-derivative (convection term) by the following expressions:

$$\left(\frac{\partial \phi}{\partial x}\right)_P = \frac{\phi_E - \phi_W}{2\Delta x} - \frac{\phi_E - 3\phi_P + 3\phi_W - \phi_{WW}}{6\Delta x} \quad u > 0$$

$$\left(\frac{\partial \phi}{\partial x}\right)_P = \frac{\phi_E - \phi_W}{2\Delta x} - \frac{\phi_{EE} - 3\phi_E + 3\phi_W - \phi_W}{6\Delta x} \quad u < 0$$

(4.12.6-1).

The influence coefficients

The influence coefficients for the Leonard-difference scheme are:

$$A_E = 6D_e - [2C_e.0]$$

$$A_W = 6D_w + [-2C_w.0]$$

$$A_N = 6D_n - [2C_n.0]$$

$$A_S = 6D_s + [-2C_s.0]$$

(4.12.6-2).

$$A_{EE} = [C_{ee}.0]$$

$$A_{WW} = - [C_{ww}.0]$$

$$A_{NN} = [C_{nn}.0]$$

$$A_{SS} = - [C_{ss}.0]$$

#### 4.12.7 Leonard-upwind-difference scheme

The Leonard-upwind-difference scheme [Barratt (1982)] approximates the  $\phi$ -value at the faces by using three upstream values, and leads to the following expressions:

$$\left(\frac{\partial \phi}{\partial x}\right)_P = \frac{11\phi_P - 18\phi_W + 9\phi_{WW} - 2\phi_{WWW}}{6\Delta x} \quad u > 0$$

(4.12.7-1).

$$\left(\frac{\partial \phi}{\partial x}\right)_P = \frac{2\phi_{EEE} - 9\phi_{EE} + 18\phi_E - 11\phi_P}{6\Delta x} \quad u < 0$$

### The influence coefficients

The influence coefficients for the Leonard-upwind-difference scheme are:

$$A_E = 6D_e - [18C_e, 0] : A_{EE} = [-9C_{ee}, 0]$$

$$A_W = 6D_w + [-18C_w, 0] : A_{WW} = - [-9C_{ww}, 0]$$

$$A_N = 6D_n - [18C_n, 0] : A_{NN} = [-9C_{nn}, 0]$$

(4.12.7-2).

$$A_S = 6D_s + [-18C_s, 0] : A_{SS} = - [-9C_{ss}, 0]$$

$$A_{EEE} = - [-2C_{eee}, 0] : A_{WWW} = [2C_{www}, 0]$$

$$A_{NNN} = - [2C_{nnn}, 0] : A_{SSS} = [2C_{sss}, 0]$$

#### 4.12.8 Leonard-superupwind-difference scheme

The Leonard-superupwind-difference scheme [Barratt (1982)] is devised to reproduce the exact solution at the nodal points close to the boundaries. To achieve this, the Leonard-difference scheme and the Leonard-upwind-difference scheme are used in conjunction with a weighting parameter evaluated from the exact solution. According to this scheme, the first derivatives are approximated by:

$$\left(\frac{\partial\phi}{\partial x}\right)_P = \lambda \left(\frac{\partial\phi}{\partial x}\right)_P^{\text{LDS}} + (1-\lambda) \left(\frac{\partial\phi}{\partial x}\right)_P^{\text{LU DS}} \quad (4.12.8-1).$$

where  $\lambda$  is a weighting parameter. For details, see Appendix A4.2.

### The influence coefficients

The influence coefficients for the Leonard-superupwind-difference scheme are evaluated from those of equations (4.12.6-2) and (4.12.7-2). Their combination is of the form:

$$A_{nb} = \lambda A_{nb}^{\text{LDS}} + (1-\lambda) A_{nb}^{\text{LUDS}} \quad (4.12.8-2).$$

### 4.12.9 Quadratic upstream-difference scheme

The quadratic-upstream-difference scheme, proposed by Leonard (1979), is claimed to combine the accuracy of quadratic interpolation with the stability of upstream weighting. This scheme can be interpreted as a pure upwind scheme which is, however, augmented by gradient/curvature-type correction terms. This allows the  $\phi_w$  value, for example, to respond to the transport processes which occur only in directions normal to that considered. In other words, it allows the coupling of the component flows through one-dimensional approximations, which, however, include only corner nodes when the curvature-type corrections are made. According to this scheme, the  $\phi$ -values convected through the control-volume faces are expressed, (see Figure 4.12.9-1), as follows:

$$\begin{aligned}
\phi_e &= \frac{1}{2} (\phi_P + \phi_E) \\
&\quad - \frac{1}{8} \left\{ \frac{U_e + |U_e|}{2U_e} (\phi_E + \phi_W - 2\phi_P) \right. \\
&\quad \left. + \frac{U_e - |U_e|}{2U_e} (\phi_P + \phi_{EE} - 2\phi_E) \right\}
\end{aligned}
\tag{4.12.9-1}$$

$$\begin{aligned}
\phi_w &= \frac{1}{2} (\phi_P + \phi_W) \\
&\quad - \frac{1}{8} \left\{ \frac{U_w - |U_w|}{2U_w} (\phi_P + \phi_{WW} - 2\phi_W) \right. \\
&\quad \left. + \frac{U_w + |U_w|}{2U_w} (\phi_W + \phi_E - 2\phi_P) \right\}
\end{aligned}$$

The influence coefficients

$$\begin{aligned}
A_E &= M_e^+ (D_e - 3C_e/8) + M_e^- (D_e - 3C_e/4 - C_w/8) \\
A_W &= M_w^- (D_w + 3C_w/8) + M_w^+ (D_w + 3C_w/4 + C_e/8) \\
A_N &= M_n^+ (D_n - 3C_n/8) + M_n^- (D_n - 3C_n/4 - C_s/8) \\
A_S &= M_s^- (D_s + 3C_s/8) + M_s^+ (D_s + 3C_s/4 + C_n/8)
\end{aligned}
\tag{4.12.9-2}$$

$$S_a^{QUDS} = S_a^{UDS} - \frac{1}{8} (M_w^+ C_w \phi_{WW} + M_s^+ C_s \phi_{SS} - M_e^- C_e \phi_{EE} - M_n^- C_n \phi_{NN})$$

$$S_b^{QUDS} = S_b^{UDS} + \frac{1}{8} (M_e^+ C_e + M_n^+ C_n - M_w^- C_w - M_s^- C_s)$$

where:

$$M_j^{\pm} = (C_j \pm |C_j|) / (2C_j) \quad j=e,w,n,s$$

and

$$\overset{\text{UDS}}{S_a} \quad , \quad \overset{\text{UDS}}{S_b}$$

are the conventional upwind-difference scheme sources.

#### 4.12.10 Quadratic upstream-difference scheme extended

The quadratic upstream-difference scheme extended, reported by Pollard and Siu (1982), is an extension of the quadratic upstream-difference scheme, in that the influence coefficients are reformulated to ensure positive coefficients. For example, when the flow is from left to right, and bottom to top, then the quadratic upstream coefficients, neglecting diffusion, are:

$$\begin{aligned} A_E' &= \left(\frac{3}{8} C_e\right) & : & \quad A_N' = \left(\frac{3}{8} C_n\right) \\ A_W' &= -\left(\frac{1}{8} C_e + \frac{3}{4} C_w\right) & : & \quad A_S' = -\left(\frac{1}{8} C_n + \frac{3}{4} C_s\right) \quad (4.12.10-1a). \\ A_{WW} &= \left(\frac{1}{8} C_w\right) & : & \quad A_{SS} = \left(\frac{1}{8} C_s\right) \end{aligned}$$

These are replaced in the quadratic-upstream-difference scheme extended, by:

$$\begin{aligned} A_E' &= \left(\frac{3}{4} C_e\right) & : & \quad A_N' = \left(\frac{3}{4} C_n\right) \\ A_W' &= \left(\frac{3}{4} C_w + \frac{1}{8} C_e\right) & : & \quad A_S' = \left(\frac{3}{4} C_s + \frac{1}{8} C_n\right) \\ A_{WW} &= 0 & : & \quad A_{SS} = 0 \quad (4.12-10-1b); \\ S_a &= -\frac{1}{8} [C_w \phi_{WW} + C_s \phi_{SS}] - \frac{9}{8} (C_e \phi_E + C_n \phi_N) \end{aligned}$$

$$S_b = -\frac{1}{8} [C_e + C_n] - \frac{9}{8} (C_w + C_n)$$

where (') denotes without diffusion.

A similar approach for all combination of flows yields the complete set of influence coefficients.

#### The influence coefficients

The influence coefficients, as reported by Pollard and Siu (1982) are:

$$A_E = [(D_e + 3C_e/4), (D_e - 3C_e/4 - C_w/8), (D_e - 3C_e/4), (D_e + 3C_e/4 - C_w/8)]$$

$$A_W = [(D_w - 3C_w/4), (D_w + 3C_w/4 + C_e/4), (D_w + 3C_w/4), (D_w - 3C_w/4 + C_e/8)]$$

$$A_N = [(D_n + 3C_n/4), (D_n - 3C_n/4 - C_s/8), (D_n - 3C_n/4), (D_n + 3C_n/4 - C_s/8)]$$

(4.12.10-2).

$$A_S = [(D_s - 3C_s/4), (D_s + 3C_s/4 + C_n/8), (D_s + 3C_s/4), (D_s - 3C_s/4 + C_n/8)]$$

$$S_a^{QUDSE} = S_a^{QUDES} - \frac{9}{8} (M_e^+ C_e \phi_E + M_n^+ C_n \phi_n - M_w^- C_w \phi_w - M_s^- C_s \phi_s)$$

$$S_b^{QUDSE} = S_b^{QUDES} + \frac{9}{8} (M_s^+ C_s - M_w^+ C_w - M_e^- C_e - M_n^- C_n)$$

#### 4.12.11 Quadratic-upstream-difference scheme extended-revised

A further linearisation of the source terms in the quadratic-upstream-difference scheme extended, leads to the revised version of the scheme. The linearisation is as reported by Patankar (1980), ie:

$$S_a = S_a + S_b \phi_P \text{ and } S_b = 0$$

(4.12.11-1):

where the  $\phi$ -values for the linearisation step are obtained from the previous iteration cycle.

#### The influence coefficients

The influence coefficients are as given by equations (4.12.10-2), except for the source, which are evaluated as per equation (4.12.11-1).

#### 4.12.12 Residual-difference scheme

The residual-difference scheme [Bhattacharyya and Datta (1985)] is obtained by considering the residual of the equations for each coordinate direction. The complete equation is manipulated to yield approximations which depend on the mesh Peclet numbers and exponential functions. For illustration purposes, consider the one-dimensional equation (with sources) evaluated with guessed values of the  $\phi$ -variable, and therefore presenting a residual, Res:

$$\rho u \frac{d\phi}{dx} - \Gamma \frac{d^2\phi}{dx^2} - S_\phi = \text{Res} \quad (4.12.12-1a).$$

Substitution of an expression of the form:

$$\phi = A_0 + A_1 x - A_2 \exp(\rho u x / \Gamma) \quad (4.12.12-1b);$$

leads to:

$$\frac{\rho U}{2\Delta x} (\phi_E - \phi_W) - \frac{\Gamma}{\Delta x} Q[P_x] (\phi_E + \phi_W - 2\phi_P) - S_\phi = \text{Res} \quad (4.12.12-1c);$$

where

$$P_x = \frac{\rho U \Delta x}{\Gamma}, \quad Q[P_x] = 1 + P_x^2/16 \quad |P_x| < 4 \quad (4.12.12-1d);$$

$$= \frac{|P_x|}{2} \quad |P_x| \geq 4$$

and the finite-difference scheme is obtained by setting Res, the residual, to zero.

#### The influence coefficients

The influence coefficients for the residual-difference scheme are:

$$A_E = D_e Q[P_e] - \text{mod}\left(\frac{C_e}{2}\right) + [-C_e, 0]$$

$$A_W = D_w Q[P_w] - \text{mod}\left(\frac{C_w}{2}\right) + [C_w, 0]$$

(4.12.12-2);

$$A_N = D_n Q[P_n] - \text{mod}\left(\frac{C_n}{2}\right) + [-C_n, 0]$$

$$A_S = D_s Q[P_s] - \text{mod}\left(\frac{C_s}{2}\right) + [C_s, 0]$$

where  $Q[P]$  is given by equation (4.12.12-1d).

#### 4.12.13 The skew-difference scheme

The skew-difference scheme is a form of flow-oriented differencing and was reported by Raithby (1976b). It aims to reduce or eliminate 'false-diffusion', an inherent problem of locally one-dimensional schemes.

The earliest reported flow-oriented scheme was, to the author's best knowledge, the one reported by Le Feuvre (1970) and independently by Zeber (1972). However, these were non-conservative, and their use was rather limited.

The Raithby skew scheme uses four distinct interpolation regions (to account for all possibilities of flow-directions) to evaluate the convected  $\phi$ -value at the, or example, east face of the control-volume. These are represented by Figure 4.12.13-1. The approximation for  $\phi_e$  for the particular inclination of Figure 4.12.13-1 is:

$$(\rho u)_e \Delta y \phi_e = \left(\frac{1}{2} C_e - K_e\right) 2\phi_P + 2K_e \phi_S \quad (4.12.13-1a);$$

where

$$\begin{aligned} K_e &= \left|\frac{C_e}{2}\right| \min\left[1, \frac{1}{2} \left|\frac{U_e}{V_e}\right| \frac{\delta x}{\delta y}\right] \\ &= \frac{1}{2} C_e \min\left[1, \frac{1}{2} \tan \theta_e \frac{\delta x}{\delta y}\right] \end{aligned} \quad (4.12.13-1b).$$

The weighting factor used, for example:

$$F_{xe} = \frac{1}{2} \left| \frac{U_e}{V_e} \right| \delta x / \delta y \quad (4.12.13-1c);$$

has to be restricted to be less than unity to avoid extrapolation, ie: in Raithby's skew scheme it is restricted between zero and one. However, interpolation is used for weighting functions greater than unity [Lillington (1981)]. For  $F_{xe}$  equal to zero, there is no cross-stream velocity component and the skew-scheme reduces to the conventional upwind-difference scheme.

In essence, the skew-scheme accounts for grid-to-flow skewness (ie the main cause of false-diffusion), but at the expense of stability and conservatism.

Similar expressions can be obtained for all other possibilities.

#### The influence coefficients

The influence coefficients for the skew-difference scheme are:

$$\begin{aligned} A_E &= D_e - (C_e/2 - K_e) (1 - S_{ue}) \\ A_W &= D_w + (C_w/2 - K_w) (1 + S_{uw}) \\ A_N &= D_n - (C_n/2 - K_n) (1 - S_{vn}) \\ A_S &= D_s + (C_s/2 - K_s) (1 - S_{vs}) \end{aligned} \quad (4.12.13-2);$$

where the S's take the sign of the subscripted velocity components and the SE, SW, NE, NW contribution are included in the source term after

linearisation. For a full formulation see Patel (1985).

#### 4.2 Overview and Discussion of Influence Coefficients

The main-points that arise from a close inspection of the influence coefficients, equations (4.12.2) are:

- (1) The central-difference scheme influence coefficients become negative for  $C > 2D$ , thus leading to oscillatory and non-convergent solutions. The cause of the negative coefficients in this instance is because downstream values are used in the flux approximations at high Peclet numbers. This infringes the transportive property.
- (2) The upwind-difference scheme influence coefficients strictly obey the transportive property and thus lead to unconditionally positive coefficients. This, in turn, leads to physically plausible solutions at all Peclet numbers, but its accuracy is limited by its first-order discretisation error. However, for flows aligned with the grids, the scheme is accurate at high Peclet numbers. To reduce the discretisation errors, the need arises to use finer grids which may prove expensive.
- (3) The hybrid-difference scheme influence coefficients obey the transportive property since it is just a combination of the central/upwind scheme. This practice ensures stability and improves accuracy of pure upwinding.

- (4) The locally-exact-difference scheme influence coefficients are always positive and thus convergence and boundedness are assured. For one-dimensional, steady-state flow, the scheme is guaranteed to produce the exact solution for any Peclet number and with a fairly coarse grid.
- (5) The power-difference scheme influence coefficients are just a variation of the locally-exact-difference scheme, in that it uses an approximation for the exponential function in power form.
- (6) The Leonard-difference scheme contains two types of influence coefficients, but since the effect of the downstream coefficient diminished in highly convective cases, the restriction on the scheme is  $C > 3D$ , the violation of which will lead to oscillatory solutions. In general, however, since all contributions lying outside the immediate neighbours are 'dumped' in the source term, the scheme is computationally viable.
- (7) The Leonard upwind-difference scheme influence coefficients include a further-downstream contribution, thus needing modified representations close to the boundary.
- (8) The Leonard superupwind-difference scheme influence coefficients are just a weighted combination of the Leonard/Leonard-upwind difference scheme influence coefficients, where the weighting parameter is evaluated from a knowledge of the analytical solution. Thus, the influence coefficients can never become negative, but the need arises to

evaluate a series of exponential functions, which can be expensive.

- (9) The quadratic-upstream-difference scheme influence coefficients may suffer from instabilities, that is, the coefficients can become negative when convection effects are strong enough. Furthermore, negative coefficients appear when  $(A_p - S_p) < 0$ . A simple way to overcome this is to switch over to the upwind-difference scheme at certain Peclet numbers. However, this treatment destroys generality, which for practical implementation, is a strong desideration.
- (10) The extended version of the quadratic-upstream-difference scheme possesses positive influence coefficients, regardless of the magnitude of the convection term, but the source terms may still induce negative coefficients.
- (11) The revised version of the quadratic-upstream-difference scheme extended ensures always positive coefficients, by introducing a linear source which depends on the previous iteration field values.
- (12) The residual-difference scheme influence coefficients are always positive, this being achieved by the inclusion of exponential functions. The coefficients are similar to the central-difference scheme, except for the diffusion terms which are appropriately modified.

(13) The skew-difference scheme influence coefficients can be a mixture of both positive and negative. The main grid point coefficients (ie.  $A_E$ ,  $A_W$ ,  $A_N$ ,  $A_S$ ) can become negative because they include elements of outflows. However, the remaining coefficients (ie.  $A_{SW}$ ,  $A_{SE}$ ,  $A_{NW}$ ,  $A_{NE}$ .) are always positive and have some favourable stabilising consequences, ie. they can be included into the source term on the right hand side of the algebraic equation.

#### 4.3 Closure

In this chapter, the numerical schemes under investigation were introduced together with a discussion of their advantages and disadvantages with regards to convergence and computer implementation.

The causes of negative influence coefficients have been discussed and are summarised as follows:

- (a) infringement of transportive property;
- (b) use of higher-order approximations; and
- (c) approximations in terms of outflows.

## CHAPTER 5

### 5. TRUNCATION ERROR AND FALSE-DIFFUSION

#### 5.1 Introduction

The numerical solution of the convection-diffusion equation involves the use of interpolation assumptions, introduced in Chapter 4, for the variation of the fluid properties and their gradients between discrete points on a computational grid that covers the domain of interest.

The majority of common interpolation assumptions fail to consider obvious physical properties of the flow, as for example, the local direction of flow within a control-volume. It is this failure that constitutes a major weakpoint of convection-diffusion formulations. Hence, the commonly misinterpreted term known as 'false-diffusion' has caused considerable controversy, misunderstanding and confusion, as it is frequently thought of as just a truncation error type of inaccuracy, among the numerical analysis practitioners.

It must be mentioned that the interpolation assumptions, unless very unwisely done, will not affect the final solution, provided that sufficiently large numbers of grid-points are used. However, the use of a large number of grid-points is not always feasible, since the computational cost in obtaining iterative solutions to a large set of equations increases very rapidly and becomes prohibitive. Therefore, sufficiently accurate interpolation assumptions must be utilised to obtain accurate solutions with relatively coarse grids, particularly when strong convection processes

are present.

For multi-dimensional, multi-phase flow phenomena involving two or more space dimensions and several equations, the power of even present day computer capacity and speed generally proves to be the limiting factor in the use of very fine grids. Therefore, in reality, if solutions to complex problems are to be obtained efficiently, the interpolation schemes for the convective transport term are required to be sufficiently accurate. To achieve this, the interpolation assumptions should in some way reflect the behaviour of the original differential equation. To clarify the problems involved, it is important to identify the main sources of 'error' that are present within numerical schemes; these being the truncation errors, the round-off errors, and the errors due to false-diffusion. The round-off errors are a function of the machine used and the number of grid-nodes used and fall out of the scope of the present work. Attention therefore now turns to the two other types of errors.

## 5.2 Truncation Error

Taylor series expansions are often used to represent differentials in an approximate manner. The accuracy of these approximations are usually indicated by the highest term that is omitted from the series expansion. In general, truncation error is the only source of inaccuracy (apart from round-off error), when the finite-domain equations are solved accurately, for one-dimensional problems. For completeness, an example of central and upwind difference approximations are illustrated below:

Considering the one-dimensional transport equation:

$$\frac{d}{dx}(\rho u \phi) - \Gamma \frac{d^2 \phi}{dx^2} = 0 \quad (5.2-1);$$

and the Taylor series expansions for the east and west nodal points:

$$\phi_E = \phi_P + \frac{1}{1!} \Delta \phi|_P + \frac{1}{2!} \Delta^2 \phi''|_P + \frac{1}{3!} \Delta^3 \phi'''|_P + \text{HOT} \quad (5.2-2);$$

and,

$$\phi_W = \phi_P - \frac{1}{1!} \Delta \phi|_P + \frac{1}{2!} \Delta^2 \phi''|_P - \frac{1}{3!} \Delta^3 \phi'''|_P + \text{HOT} \quad (5.2-3);$$

where  $\Delta$  is the uniform mesh length, and the second and first derivatives can be approximated as follows:

$$\phi''|_P = \frac{1}{\Delta^2} (\phi_E - 2\phi_P + \phi_W) - O(\Delta^2 \phi''''|_P) \quad (5.2-4);$$

and

$$\phi'|_P = \frac{1}{2\Delta} (\phi_E - \phi_W) + O(\Delta^2 \phi'''|_P) \quad (5.2-5);$$

or

$$\phi'|_P = \frac{1}{\Delta} (\phi_P - \phi_W) + O(\Delta \phi''|_P) \quad (5.2-6).$$

Expressions (5.2-4, 5, 6) are the 2nd derivative central-difference

approximation. 1st derivative central difference and upwind-difference approximations of orders  $\Delta^2$ ,  $\Delta^2$  and  $\Delta$ , respectively.

Analysis of the truncation errors of expressions (5.2-4, 5.6) gives:

<u>EXPRESSION</u>	<u>TRUNCATION ERROR</u>	<u>APPROXIMATION TYPE</u>
5.2-4	$1/12 \Delta^2 \phi''''_p$	Central (diffusion)
5.2-5	$1/3 \Delta^2 \phi''''_p$	Central (convection)
5.2-6	$1/2 \Delta \phi'''_p$	Upwind (convection)

The controversy relates to the truncation error for expression (5.2-6) which is similar in nature to the 2nd derivative (ie diffusive). However, deriving finite-domain equations in this manner should be interpreted with reservations, since the truncation errors can easily mislead the numerical analyst. The argument for this is as follows:

# Taylor series expansions reveals errors of order  $\Delta^2$  for the central-difference approximation whereas for the upwind-difference scheme, it reveals errors of order  $\Delta$ . Therefore, the central-difference approximation should yield more accurate solutions. However, for large  $\Delta$ 's, the central-difference approximation in no way represents the true physical solution. This is not true for the upwind-difference approximation, since it yields reasonable and realistic solutions. The reason is that the central-difference approximation influence coefficients become negative for mesh Peclet numbers greater than 2.

# For one-dimensional problems, if the error of the central-difference approximation is to be achieved by using the upwind-difference approximation, the diffusion coefficient  $\Gamma$  in the latter should be replaced by  $\Gamma + \rho u \Delta / 2$ , a false-diffusion coefficient, according to some authors. This is not true, however, because if it were then even the locally exact approximation, which is the analytical solution itself, reveals a false-diffusion coefficient (which is certainly not true).

It is therefore asserted that 'false-diffusion' is not governed by the order of the scheme, since for steady-state, uniform flow in the coordinate direction, the first order upwind are locally-exact approximations have no false-diffusion but only high truncation errors.

### 5.3 False-Diffusion

Having just discussed truncation errors as a source of error commonly connected with false-diffusion, a view which is indeed misleading, it is now the intention to define false-diffusion in its true and more meaningful sense, according to the author's opinion, used in the present work.

The proper view of false-diffusion [Patankar (1980)] is firstly that it is a multi-dimensional phenomena; and secondly, that it only exists if the numerical scheme fails to account for the true local direction of the flow. This is easily understood and illustrated by the following example.

Consider a square region which has four parallel streams of equal

velocities, but unequal temperatures that come into contact, as depicted in Figure 5.3-1. When the diffusion coefficient is non-zero, mixing layers will appear, since there is a temperature gradient between  $T_{HOT}$  and  $T_{COLD}$ , and the width of the stream layer will increase in the downstream direction. However, if the diffusion coefficient is zero, then the temperature discontinuities will persist in the streamwise direction and no mixing layers will appear. A method of observing if any diffusion is present within a numerical scheme is to set the physical diffusion to zero, and observe that for a test problem like the one just described, there exists no mixing layers, or, if they do exist, that their spread indicates the influence of errors similar to the diffusion term.

As an illustration, the upwind and quadratic upstream-difference schemes were used to solve the test case. Results at the grid-points are represented in Figure 5.3-2, at a flow angle of  $45^\circ$  to the gridlines. Note that, if there was no false-diffusion, we should obtain a sharp discontinuity similar to the left boundary condition, moving downstream.

The reason for choosing the UDS and QUDS schemes is because the former is supposed to entail false-diffusion errors whereas the latter is not [Leonard (1979)]. However, the results seem to suggest that both these schemes suffer from false-diffusion. Figures 5.3-4 to 5.3-13 depict  $\phi$ -profiles at various downstream stations for the UDS/QUDS schemes, together with a nodal-interpolated analytical solution. It is easily seen that both the UDS and QUDS schemes smear the profile at the very first IX-line from the left hand boundary, although supposedly the QUDS does not suffer from false-diffusion [Leonard (1979)]. Therefore, in general, higher order interpolation in coordinate directions

does not eliminate or reduce false-diffusion; it simply reduces the truncation error.

The following are therefore the obvious conclusions:

- # False-diffusion occurs for flows which are oblique to grid-lines; and when there are dependent variable gradients present normal to the flow direction.
- # False-diffusion can be reduced for the locally one-dimensional type of numerical schemes only by grid refinement (ie. by diminishing the importance of local convection).
- # The cause of false-diffusion is the neglect of the effects of the local flow-direction, across each control-volume face, by the numerical scheme (ie. the multi-dimensional nature of the flow should be taken into account even on the control-volume scale).
- # Approximate expressions of the false-diffusion coefficients are given by for two-dimensional situations as follows:

# Wolfshtein (1968):

$$\Gamma_{\text{false}}^1 \cong 0.36\rho|V| \Delta \sin 2\theta \quad (5.3-1a);$$

# De Vahl Davis and Mallinson (1976):

$$\Gamma_{\text{false}}^2 \cong \frac{1}{4(\sin^3\theta + \cos^3\theta)} \rho |\underline{V}| \Delta \sin 2\theta \quad (5.3-1b);$$

# Leschziner (1980):

$$\Gamma_{\text{false}}^3 \cong \frac{\sqrt{2}}{4} \rho \sin\left(\frac{\pi}{4} + \theta\right) |\underline{V}| \Delta \sin 2\theta \quad (5.3-1c);$$

where all three relations yield  $\Gamma_{\text{false}}=0$  at  $\theta=0, \pi/2$  and a maximum value of  $0.36|\underline{V}|\Delta$  at  $\theta=\pi/4$ . This implies that at an angle of  $\theta=45^\circ$ , the upwind-difference scheme introduces an effective diffusion coefficient equivalent to  $|\text{Pe}|\approx 2.8$ , regardless of the magnitude of the real Peclet number. Profiles of expressions (5.3-1) are represented in Figure 5.3-3. Therefore, considering expressions such as (5.3-1a) it is necessary to incorporate the flow direction within the interpolation assumptions [Raithby (1976a)], to reduce or eliminate false-diffusion; Patel, Markatos and Cross (1985a).

#### 5.4 Closure

In this chapter, the topic of truncation error and false-diffusion which have caused considerable controversy, misunderstanding and confusion among numerical analysis practitioners has been presented.

Distinctions between truncation error and false-diffusion are presented, together with an example to illustrate the differences between the two.

## CHAPTER 6

### 6. APPLICATION TO TEST PROBLEMS

#### 6.1 One-Dimensional Study

##### 6.11 Introduction

A comparative study of seven of the numerical schemes presented in Chapter 4 was undertaken, to generally evaluate their accuracy, numerical stability and CPU requirements, for a series of test problems with and without sources.

The numerical schemes are tested for Peclet numbers between  $1-10^5$  and mesh Peclet numbers between  $0.2-10^3$ , for all test problems [Patel, Markatos and Cross (1985a)].

##### 6.12 Objectives

The objectives of the one-dimensional study are to evaluate the discretisation errors that are involved when the flow is in the direction of the grid-lines. It is stressed here, that although the upwind-difference scheme is used, the scheme suffers from no false-diffusion for one-dimensional flow, since there is no grid-to-flow skewness. It is true that the scheme overestimates the diffusion, however, this is true of all schemes.

### 6.13 The Test Problem

The test problem considered is the one-dimensional convection-diffusion equation with a source term of the form:

$$S(x) = ax^2 + bx + c \quad (6.13-1a);$$

where  $a$ ,  $b$  and  $c$  are constants.

The results obtained, numerically, were compared with the analytic solution, which is characterised by a viscous boundary layer of thickness  $1/P$ , and is:

$$\begin{aligned} \phi(x) &= Z[e^{Px}-1]/[e^P-1] + E \\ E &= a^1x^3 + b^1x^2 + c^1x \\ Z &= 1-a^1-b^1-c^1 \\ a^1 &= a/3P, \quad b^1=b/2P + a/P^2 \\ c^1 &= c/P + b/P^2 + 2a/P^3 \end{aligned} \quad (6.13-1b).$$

### 6.14 The Schemes Investigated

The schemes investigated for the one-dimensional study are:

1. the central-difference scheme;
2. the upwind-difference scheme;
3. the locally-exact-difference scheme;
4. the Leonard-difference scheme;

5. the Leonard-upwind-difference scheme;
6. the Leonard-superupwind-difference scheme; and
7. the quadratic-upstream-difference scheme.

The truncation errors for these schemes are tabulated in Table 6.14.1, for  $S(x)=0$ .

#### 6.15 The test cases

The finite-difference schemes were tested over a wide range of Peclet numbers for eight test cases with zero, linear and quadratic source terms. The number of nodes,  $N$ , ranged from 5-100 in steps of 5 for all test cases. Table 6.15.1 presents a summary of the cases considered.

The ranges of Peclet numbers,  $P$  and mesh Peclet numbers,  $P_\theta$  studied were from  $1-10^5$  and  $0.2-10^3$ , respectively, for all cases. The presented sample results for simplicity refer to Peclet numbers and mesh Peclet numbers from 1-100 and 1-50 respectively, since the behaviour for the higher Peclet number cases is the same. As seen in Table 6.15.1, the following one-dimensional convection-diffusion situations were considered. Test case 1, was the standard 'no source' situation, whereas Test case 2 was one with a constant source term. Test cases 3 and 4 had linear source terms with positive and negative gradients, respectively. Test cases 5-8 all had quadratic source terms, with different constants,  $a$ ,  $b$  and  $c$ .

## 6.16 Presentation of results

The main results are presented in Table 6.16.1 and Figures 6.16-1 to 6.16-13.

Table 6.16.1 summarises the results for each scheme under consideration, for  $P=20$ .

In all figures presented (Figures 6.16-1 to 6.16-13), the accompanying table summarises the important characteristics such as maximum error, evaluated as:

$$\max(|\phi_i - \phi_L|/\phi_N) \quad (6.16-1);$$

the error norm evaluated by:

$$(\sum(|\phi_i - \phi_L|)^2)^{1/2} \quad (6.16-2);$$

and finally, the predicted flux at the outflow boundary,  $\phi_N$ , evaluated by:

$$-(\phi_{N-2} - 4\phi_{N-1} + 3\phi_N)/2\Delta x \quad (6.16-3);$$

for the finite-difference schemes, and by:

$$-(ZPe^P/(e^P-1)) + 3a^1x^2 + b^1x + c^1 \quad (6.16-4);$$

for the analytic solution.

Figure 6.16-1 represents the analytic behaviour of  $\phi$  for several Peclet numbers for the cases with zero source.

Figure 6.16-2 compares the solutions obtained by the various schemes for the test case with zero source against the analytic solution.

Figures 6.16-3 and 6.16-4 compare the results of the various schemes for the cases with a linear source term with positive and negative gradients, respectively.

Figures 6.16-5 and 6.16-6 compare the results of the various schemes for the cases with a quadratic source term with positive and negative gradients, respectively.

Figures 6.16-7 and 6.16-8 compares the performance of the schemes for cases with large source terms, generated by the expressions for test case 5-8, in Table 6.15.1.

Figures 6.16-9 to 6.16-12 present typical maximum error profiles as functions of the number of nodal points used, for all scheme tested.

Figure 6.16-13 presents the computational requirements in terms of CPU seconds on the Prime series 750 computer.

## 6.17 Discussion of results

Figure 6.16-1 clearly depicts the viscous boundary layer, where the solution,  $\phi(x)$ , rapidly changes from  $\phi(0)$  to  $\phi(1)$ . The curves for large Peclet numbers do not vary considerably within the first  $(N-2)$  nodal points for  $P \gg 0$ .

Figure 6.16-2 depicts an oscillatory behaviour of the CDS solution and indicates that the UDS overpredicts the nodal  $\phi$ -values further downstream

of the 70% station. Inspection of the results reveal that the UDS is inaccurate even for moderate Peclet numbers, unless the grid is sufficiently fine; but that it does predict qualitatively realistic solutions, unlike the 'wiggles' of the CDS. The LDS and the LUDS solution are not much of an improvement, the former being also oscillatory. In contrast, the LSUDS and the LEDS are seen to be in excellent agreement with the analytical solution, throughout the domain.

Figures 6.16-3 and 6.16-4 correspond to the linear source cases, and indicate again that both the CDS and LDS solutions are oscillatory in nature. The other comments relating to the case with zero source (Figure 6.16-2) are also valid, the UDS overpredicting  $\phi$  downstream, and the LSUDS and the LEDS solutions being very accurate over the whole domain.

Figures 6.16-5 and 6.16-6 correspond to the quadratic source cases, and indicate that both the CDS and LDS are once again oscillatory.

Figures 6.16-7 and 6.16-8 correspond to the large source cases, and clearly depict the unboundedness in the oscillatory nature of the CDS, whereas they indicate that LEDS predicts very good results. The LDS appears to predict oscillatory results within the last few nodal points.

Inspection of Figures 6.16-2 to 6.16-8 reveals that, in general, all the test cases were well modelled by both the LEDS and the LSUDS with errors of  $\max(|\phi_j - \phi_j| / \phi_N)$  less than  $10^{-6}$ , for all Peclet numbers. However, considerable errors are indicated when using the LEDS for very large source terms. The CDS performed well for mesh Peclet numbers

less than 2, but was grossly in error for higher Peclet numbers, for both test case 1 (with zero source, Figure 6.16-2), and when the type of source,  $S(x)$ , did not affect the outcome to a great extent (ie. when the source and solution profiles are similar in shape (Figure 6.16-3)).

Inspection of Table 6.16.1 reveals that wiggles are predicted by the CDS, whereas the UDS, although always stable, is in considerable error at all flow rates and practical mesh sizes. The results indicate that the UDS always overestimated the solution by at least 15%, even for relatively fine grids, whereas the QUDS underpredicted the solution by only a few percent. The LEDS appeared to overestimate the solution for the problems with large source terms by around 5% at the extreme, whereas the LSUDS was within 0.01% for all test cases considered, including those with large source terms. This is expected since the exact solution is a combination of an exponential and a cubic, in which case the LSUDS is 'exact', except for inaccuracies arising near boundaries. Also indicated in Table 6.16.1 are the wiggles in the solutions obtained by the LDS and QUDS, owing to the ill-conditioned influence coefficients.

It is clear from Figures 6.16-2 to 6.16-8 and Table 6.16.1 that the LSUDS and the LEDS give by far the most accurate solutions, as expected. However, before any judgement can be formulated about the relative performance of the schemes, it is important to compare the profiles of the maximum errors both as functions of the mesh size and of the Peclet number, and with respect to the computational requirements for the schemes. After all, if a scheme is convergent, a more accurate solution may always be obtained by mesh refinement, until round-off error dominates truncation error. Therefore, it is the author's

opinion that accuracy should be compared on the basis of relative CPU and storage costs together with convenience of programming effort. This information is provided by Figures 6.16-9 to 6.16-13.

Figure 6.16-9 presents the behaviour of the maximum error with increasing Peclet number (from  $P=10^0$  to  $10^5$ ) for a constant grid size ( $\Delta x=0.1$ ). The profiles shapes for the UDS and LUDS are similar and those for the LDS and QUDS are also similar. The CDS error profile diverges as the Peclet number increases. The LEDS and LSUDS profiles are not depicted in Figure 6.16-9 as they lie close to the P-axis.

Figure 6.16-10 shows that there exists a critical region of the mesh size, over which the UDS error is maximum (being from  $N=15$  to  $N=40$  for this particular case). Outside this region the maximum error does not increase with decrease in mesh size. It is interesting to observe that for the UDS the error profile flattens out very slowly. The number of nodal points,  $N$ , required to obtain a given accuracy by the UDS is nearly three times that of the LDS (eg LDS requires  $N=30$  and UDS requires  $N=80$  for this particular case).

Figures 6.16-11 and 6.16-12 depict the maximum error profiles versus  $N/P^{1/2}$  for constant  $P$  and constant  $N$ , respectively, the range of  $N$  for the former being between 10 and 100 and the range of  $P$ , for the latter, being between  $10^0$  and  $5 \times 10^4$ . The error profiles for increasing  $P$  indicate that the maximum errors tend to zero for both UDS and LUDS, but that they tend towards a limiting value, considerably greater than zero, for the QUDS and LDS (for this particular case). The profiles for

the LEDS and LSUDS are not presented, as they lie close to the  $N/P^{1/2}$ -axis in Figure 6.16-12.

Figure 6.16-13 show crude computational requirements in CPU seconds, on a PRIME series 750 computer. It is seen that the time requirements for the LDS are about three times those for the UDS. This is true in general, so that for a given accuracy (up to a limit) the UDS is marginally cheaper than the LDS, considering that the former requires less than three times the number of nodes required by the latter for the same accuracy. The presented computer time requirements are for obtaining a given accuracy and should not be interpreted as machine accurate because of the limitations in the time printout. What is established however is that the upwind- and central-difference schemes are the least expensive, as expected, closely followed, as may not be expected, by the locally exact scheme. It should be mentioned in this context that the calculation of the exponentials involved in the latter was reprogrammed by the author and appeared to be more efficient than the standard PRIME-library calculations. In practice, and to avoid overflow, asymptotic formulae avoiding calculation of exponentials completely would be used for large exponents in all schemes. The LSUDS and the QUDS are both about 2.0 times more expensive than the above three schemes, for the same number of nodal points, and the LDS and LUDS are about 3.0 times more expensive.

## 6.18 Conclusions

A comparative study in terms of accuracy and computer requirements has

been presented for seven numerical schemes, which were applied to a series of simple one-dimensional convection-diffusion problems including linear and non-linear sources. One-dimensionality was imposed in order to eliminate the additional complexity of the multi-dimensional 'false-diffusion'.

The main findings may be summarised as follows:

1. The central-difference and Leonard's LD and LUD schemes proved the most unstable. The first two were also inaccurate although they are both second order. This indicates that it is not only the order of the scheme that dictates the accuracy of the solution in convection/diffusion problems, but also the particular formulation which must account for the asymmetric nature of convection.
2. The central- and upwind-difference schemes lead to inaccurate solutions for moderate and high Peclet numbers, and for moderate grids. The upwind-difference scheme presents a flat error profile versus number of nodes, for moderately fine grids. There is therefore a danger that moderate grid refinement may indicate as grid-independent a solution which is still in considerable error. Indeed, in order to obtain with the UDS the same accuracy as with the LSUDS the number of nodes had to be increased to 200. Therefore, for grid-independency studies with the UDS a many-fold increase in the number of nodes may be necessary.

3. For moderate grids, the higher order schemes were, in general, more accurate (when convergent!) than the first order upwind-difference scheme. An exception was the CDS for  $Pe > 2$  when it became highly inaccurate. However, all the schemes except the central- and locally-exact-difference schemes were 2.0 to 3.0 times more expensive than the UDS in computational terms.
4. The LSUDS was, as expected, the most accurate scheme, very closely followed by the LEDS and the QUDS. However, the latter was sometimes oscillatory. The LEDS was both accurate and economical. Furthermore, the influence coefficients (ie  $g_m$  and  $g_p$ ; see Appendix A4.1) of the LEDS can be calculated and tabulated to improve even further the computational requirements.
5. The schemes considered here fall into three categories, in order of increasing demand in terms of computational requirements, as follows:
  - (a) Central-difference scheme  
Upwind-difference scheme  
Locally-exact-difference scheme
  - (b) Leonard superupwind-difference scheme  
Quadratic upstream-difference scheme

(c) Leonard-upwind-difference scheme

Leonard-difference scheme

The CPU times required are compared with the UDS. For the one-dimensional cases considered, the LDS was found to be approximately three times as expensive as the UDS, whereas the accuracy was within 10%, unlike the UDS, which was at least 20% in error. The LSUDS required just about twice the computer time compared to the UDS, but the LSUDS was within 0.01% in error. Finally the LEDS required between 2 and 3% less CPU time for a maximum error of around 5% (because it required much fewer iterations for a given accuracy), which means that the LEDS could prove a very efficient scheme. The combination of the findings of this study on accuracy *vis-a-vis* computer requirements leads to the following general conclusions:

- (i) When a 5% average error of the numerical solution at the grid points is acceptable, one might as well use the UDS with fine grids because it is unconditionally stable and convenient in programming effort. The total CPU requirements will be the same as for the most accurate schemes with coarser grids.
- (ii) Should a very accurate solution be required then one should abandon the UDS because of its flat error response to further grid refinement, and choose either the QUDS or LSUDS or LEDS. Of those three the first may be unstable, the second is the most accurate and the third the cheapest. The above conclusions are based on the detailed study of a series of

linear one-dimensional problems with linear and non-linear sources, only. Therefore, the general applicability of these conclusions is by no means established as yet. It is suggested that the LEDS may have not received the attention it deserves from the computational fluid-dynamics community, and that further research in evaluating and developing it (particularly in two- and three-dimensional cases, where its application along streamlines would also eliminate multi-dimensional false diffusion) may prove fruitful. Work on two-dimensional problems is reported in the next sub-section.

## 6.2 Two Dimensional Laminar Study

### 6.21 Introduction

A comparative study of eight of the numerical schemes presented in Chapter 4 was undertaken, with the intention of getting an insight of the problems that occur with regards to convergence and the existence of 'false-diffusion', due to the multi-dimensional nature of the flow. Four standard, well-documented, laminar flows were chosen for the study and the schemes were tested for stability under normal, extreme, and even hypothetical flow conditions (eg. very high Reynolds number 'laminar' flows) [Patel and Markatos (1984, 1985a, 1985b, 1986a)].

However, since the first two cases were considered to check the programming, they are not considered here. For further details see Patel and Markatos (1985b).

## 6.22 Objectives

The objectives of the two-dimensional, laminar study are to evaluate the inherent problems of 'false-diffusion' for the locally, one-dimensional, coordinate schemes. Some light is shed upon the relative merits and performances of the schemes.

## 6.23 The schemes investigated

The schemes investigated for the two-dimensional laminar study are:

1. the central-difference scheme;
2. the upwind-difference scheme;
3. the hybrid-difference scheme;
4. the locally-exact-difference scheme;
5. the power-difference scheme;
6. the quadratic-upstream-difference scheme;
7. the quadratic-upstream-difference scheme extended; and
8. the quadratic-upstream-difference scheme extended revised.

## 6.24 The laminar test cases

The schemes were applied to a series of uniform property, two-dimensional laminar flows, two of which are presented here [Patel & Markatos (1986a)]:

- (a) flow through a sudden enlargement in a pipe; and
- (b) flow in a cavity with a moving lid.

Only two test cases are presented here, since they exhibit very strong effects of 'false-diffusion' but other simple test cases [Patel & Markatos (1985a)] were considered just as a means of gaining insight into the relative convection-interpolation performances of the various schemes. Indeed, the simple test cases (eg. flow in a pipe) provide a means by which the programming matters can be checked, ensuring, as far as possible, that the incorporation of the schemes in the program are error-free [Patel and Markatos (1985b)].

#### 6.24.1 Flow through a sudden enlargement

Fluid enters the half-open pipe, Figure 6.24.1-1, of length equal to 25 times the half-open diameter. There is a recirculation region formed behind the closed half of the pipe, within a length  $l_r$  from the entrance, and the velocity-vector directions within the eddy are inclined at various angles to the local grid. This makes the solution to this problem, and the next test case, a good test on 'false-diffusion'.

#### The boundary conditions

The boundary conditions are:

Inlet: specified parabolic velocity profile.

Outlet:  $\partial u/\partial x=0$  and  $v=0$ .

Wall boundaries:  $u=0$  and  $v=0$ .

Axis of symmetry:  $\partial u/\partial r=0$  and  $v=0$ .

#### 6.24.2 Flow in a cavity with a moving lid

Fluid is forced to rotate within the square cavity by a moving lid of specified velocity. Figure 6.24.2-1. This implies that there is no predominant flow direction which results in the differential equations becoming highly elliptic.

##### The boundary conditions

Top wall:  $u=u_{\text{top}}$  and  $v=0$ .

Other walls:  $u=0$  and  $v=0$ .

#### 6.25 Presentation of results

The schemes were tested over a wide range of Reynolds numbers, between 50 and 2000 and with different numbers of grid nodes; between 100 (10x10) and 1200 (30x40), for artificially high Reynolds numbers ( $10^4$ – $10^6$ ) 'laminar flows'.

### 6.25.1 Flow through a sudden enlargement

Fluid flowing in a pipe, containing an abrupt change in cross-sectional area, always results in fluid flow reversal in the immediate vicinity of the step change.\* In general, the flow reversal is characterised by points of flow detachment and re-attachment, and the location of the re-attachment point is a function of the following quantities [Pollard (1980)]:

- (i) the size of the enlargement;
- (ii) the inlet velocity profile; and
- (iii) the Inlet Reynolds number.

A study, in detail, for the sudden expansion was reported as early as 1967 [Macagno and Hung (1967)]. They used an expansion ratio of 0.5 together with a parabolic profile at the inlet. Their conclusion of the results reported were, that there existed a linear relationship of the re-attachment length with inlet Reynolds number. Later, Back and Roschke (1972) reported re-attachement length relationships with Reynolds number, for an expansion ratio of 0.3846 for both laminar and turbulent regions.

---

\* Examples of such flows are encountered in heat exchangers and also in biological systems such as prosthetic devices.

Their results compared with those of Macagno and Hung (1967) revealed that the results of Back and Roschke (1972) had a greater slope than those of Macagno and Hung (1967), this was explained due to the effects which are consistent with the mixing length theory. However, Pollard (1980) reported that the slope obtained using uniform inlet profiles must be lower than those obtained using a fully developed parabolic inlet profile.

Iribarne, Frantisak, Hummel & Smith (1972) also provided results of re-attachment lengths against Reynolds number for an expansion ratio of 0.505 and reported no change when compared with those of Macagno and Hung (1967). However, this is surprising, in that the inlet velocity profile were different.

Results were also compared with Back and Roschke (1972). A re-examination of their earlier results, Back and Roschke (1976) concluded that the inlet velocity profile is an important condition for obtaining re-attachment lengths.

Leschziner (1980), compared results predicted by three schemes [Spalding (1972), Ralby (1976b) and Leonard (1979)] and reported no difference in the predictions of the re-attachment length. Experimental results have been reported [Denham and Patrick (1974)] and calculations using the upwind-difference scheme have been reported [Atkins, Maskell and Patrick (1980)]. It was found that the upwind-difference scheme underestimates both the length and the intensity of the recirculation zone compared to the central-difference scheme.

Here attention is directed to the effects on the centreline velocity profiles, by varying the Reynolds number, grid size and re-attachment lengths predicted by various schemes for a fixed grid size.

Calculations were performed at  $Re=50$  to  $1000$ , although only results for  $Re=200$  are presented here. Predictions by using various schemes for centreline velocity profiles are shown in Figures 6.25.1-1 and 6.25.1-2, for a grid of  $16 \times 24$ . Results for the axial-velocity profiles using grids of  $10 \times 10$ ,  $20 \times 20$ , and  $30 \times 30$  are presented in Figure 6.25.1-3 for the central-difference scheme and Figure 6.25.1-4 for the quadratic-upstream-difference scheme.

Table 6.25.1.1 summarises details of computational requirements for each scheme, with reference to the upwind-difference scheme. In this table,  $N$  is the number of iterations required to obtain a given accuracy,  $T$  is the time in CPU seconds and  $N_u$ ,  $T_u$  are the respective  $N$  and  $T$  for the upwind-difference scheme.

Results for the re-attachment lengths  $l_r$  are depicted by Figures 6.25.1-5 and 6.25.1-6. Table 6.25.1.2 summarises the normalised re-attachment lengths obtained by a  $16 \times 24$  grid for various Reynolds numbers and Table 6.25.1.3, the values given by Pollard (1980) and Macagno and Hung (1967).

Results for the vortex-centre,  $L_v$ , are depicted by Figure 6.25.1-7 together with results of Macagno & Hung (1967).

### 6.25.2 Flow in a cavity with a moving lid

Steady-state flow in a cavity with a moving lid, due to its geometric simplicity and highly elliptic character, has become a popular example for testing and comparing numerical methods, for several years. However, most of the earlier work [Burggraf (1966); Bourcier and Francois (1969); Greenspan (1969); Fortin, Peyret and Temam (1971); Bosmann and Dalton (1973); Denham and Patrick (1974); Roache (1975); de Vahl Davis and Mallinson (1976); Rubin and Khosla (1977); Tuann and Olson (1978); Gupta and Manohar (1979a); and, Atkins, Maskell and Patrick (1980), dealt with the stream function ~ vorticity formulation.

Burggraf (1966), performed an excellent study of this test case for a range of successively finer grids, and various high Reynolds numbers, using the central-difference scheme, for the convective term.

Calculations were performed for  $Re=100$  and  $400$ , with a grid size of  $10 \times 10$ . Results for the centreline velocity profiles for  $Re=100$  are depicted by Figures 6.25.2-1 and 6.25.2-2. For grid independency purposes, solutions for grids of  $20 \times 20$  and  $30 \times 30$  were performed. Results for the centreline velocity profiles are depicted by Figures 6.25.2-3 and 6.25.2-4 for the central-difference scheme, Figures 6.25.2-5 and 6.25.2-6 for the upwind-difference scheme, and Figures 6.25.2-7 and 6.25.2-8 for the quadratic upstream-difference scheme, for  $Re=400$ . Finally, Figures 6.25.2-9 to 6.25.2-12 depicts the centreline  $u$ -velocity profile for the upwind-difference scheme and the quadratic upstream difference scheme extended revised for  $Re=1000$  and

2000 respectively.

Table 6.25.2.1, shows the details for the computational requirements for each of the schemes, with reference to the upwind-difference scheme.

Finally, Figure 6.25.2-13, depicts the upstream vortex height for a Reynolds number range of 50-500 for the central-, hybrid-, quadratic upstream-, quadratic upstream revised extended-difference schemes, together with results obtained from various references: [Nallasamy and Krishna Prasad (1977); Pan and Acrivos (1967); Bozeman and Dalton (1973); and, Burggraf (1966)].

## 6.26 Discussion of results

### 6.26.1 Flow through a sudden enlargement

The u-velocity profiles, Figure 6.25.1-1 fall into two groups (ie as predicted by first- and second-order methods) whereas the v-velocity profiles fall into three groups (ie. CDS/QUDS, QUDSE/R and UDS/HDS/LEDS/PDS).

The second-order methods (namely CDS/QUDS/E/R) predicted similar, and in some instances identical, velocity profiles which were always at lower values as compared with the first-order methods. This may be attributed to the larger discretisation error of the latter.

An examination of Table 6.25.1.1 reveals the following findings, relative to the UDS:

The CDS requires about 24% more computational time per node with an increase of 78% in the number of iterations, whereas the QUDS requires 40% more computational time per node with a decrease of 7% in the number of iterations. This shows an advantage in having a higher order interpolant (ie. decrease in iteration numbers), the disadvantage being that there is an increase in the unit computational time. The HDS/LEDS and PDS were all similar in their requirements, which suggests that the LEDS does perform well, given that exponential functions have to be evaluated. For the QUDSER the time per iteration was 40% more than for the UDS, with an increase of 52% in the number of iterations required. The QUDSE was similar to the QUDSER in unit time, but required less iterations by a factor of 1.7. Figures 6.25.1-3 and 6.25.1-4, for the CDS and QUDS at  $Re=200$ , clearly show that the CDS velocity profiles are still grid dependent for a grid size of  $30 \times 30$ , whereas the QUDS gives virtually grid-independent results for the  $20 \times 20$  grid.

It is worth noting that the  $10 \times 10$  velocity profiles predicted by the CDS and QUDS were identical. The re-attachment length, an important feature of this test case, is tabulated in Table 6.25.1.2, together with results obtained from other sources Table 6.25.1.3. Predictions have been obtained over a range of Reynolds numbers from 50-1000. The results for the re-attachment lengths of Table 6.25.1.2 were in good agreement with those in Table 6.25.1.3. The predicted re-attachment lengths are plotted in Figures 6.25.1-5 and 6.25.1-6, where Figure 6.25.1-5 shows  $l_r/h$  vs  $Re$  whereas Figure 6.25.1-6 shows  $l_r/d$  vs  $Re$ .

For low Reynolds number flows ( $\leq 300$ ), the re-attachment length data

indicate a linear relationship with respect to the Reynolds number. [Macagno and Hung (1967); Back and Roschke (1972); and Iribarne, Frantisak, Hummel and Smith (1972)] as demonstrated by Figures 6.25.1-5 and 6.25.1-6. The results confirm the findings of Leschziner (1980), and are in close agreement for all schemes.

An important feature of this problem is that the re-attachment length increases linearly until it reaches a maximum, then reduces to a constant value for turbulent flow.

#### 6.26.2 Flow in a cavity with a moving lid

The velocity profiles depicted in Figures 6.25.2-1 and 6.25.2-2 are all in close agreement except for the UDS profiles, which always underpredicts (ie. predicts a flatter profile).

An examination of Table 6.25.2.1 reveals the following findings, relative to the UDS for Reynolds numbers 100 and 400.

The first order schemes were all found to be similar in their computational requirements per iteration except for the LEDS which was slightly higher in its requirements.

The QUDS required about 30% more computational time per iteration with an increase of 15% in the number of iterations required.

The QUDSE required twice the computational time per node with a 2.5-fold increase in the number of iterations.

The QUDSER required 60% more computational time per node with a 2-fold increase in the number of iterations.

Grid independency studies show that the CDS and QUDS are virtually identical and are grid independent for grids of around 30x30, whereas, the UDS predicts a much flatter profile and the solution is still grid independent for grids of 30x30. For Reynolds numbers 1000 and 2000, the QUDSER predicted results much closer to the true solution whereas the UDS predicted highly diffused solutions. The QUDSER, 10x10 grid, predicted results similar to the UDS, 30x30 grid, which is clearly depicted by Figures 6.25.2-11 and 6.25.2-12 for the high Reynolds number flows.

Finally, the upstream vortex heights, Figure 6.25.2-13, all lie in a band-width of around  $\pm 0.05$  when compared with experimental results.

## 6.27 Conclusions

A comparative study in terms of accuracy and computer requirements has been presented for eight numerical schemes, which were applied to a series of two-dimensional convection-diffusion problems, two of which were presented.

The main findings of this study may be summarised as follows:

# The CDS/QUDS/E proved the most unstable schemes at high Reynolds numbers.

# The UDS/HDS/LEDS/PDS/QUDSER suffered from no instabilities for the test cases considered here.

# The performance of the QUDS/E/R were found to be accurate and identical for QUDSE/R. when they converged, for all Reynolds numbers considered.

# The QUDS/E were found to be unstable for high flow rates/coarse grids, unlike the QUDSER which was stable for those flows considered.

# The QUDSER was the most expensive scheme in terms of computational requirements; the reason being that the source terms are less implicit in nature than the QUDSE.

# In general the QUDSER required twice the number of iterations to secure the same level of accuracy as the QUDSE scheme. This is true, independently of the way the source is linearised.

# The QUDS/E/R required more iterations to secure convergence for flow situations with recirculating zones.

# In terms of accuracy and computational efficiency it appears that the QUDS/E/R may offer the best compromise at present, however, none of the above schemes is satisfactory from all

aspects and it is felt that new directions in research on this topic are urgently needed.

# The QUDSER predicted highly accurate solution for coarser grids, unlike the UDS which even for a three-fold increase in grids, predicted results slightly worse than the QUDSER.

# The UDS/HDS requires a many-fold increase in the grids to obtain accuracies close to the QUDS/E/R schemes.

### 6.3 Two-Dimensional Turbulent Study

#### 6.31 Introduction

A comparative study of eight discretisation schemes for the equations describing convection-diffusion transport phenomena is presented for predicting velocity and temperature distributions in enclosures containing a fire source. Other similar convective motions which results from buoyancy-induced effects arise, for example, in the insulation of buildings, in the space between the cover plates and the absorber of a solar collector and in the gas-filled cavity surrounding a nuclear reactor core.

To the author's best knowledge the numerical schemes have been tested to date only for simplified test cases which help to implement and evaluate ideas. However, real practical problems are much more complicated by virtue of such physical phenomena as turbulence. The

uncertainties in modelling turbulence and the relevant errors may be of a much higher magnitude than those introduced by the numerical schemes. Therefore, a study was undertaken to investigate the performance of the schemes for a real case, namely the smoke flow in enclosures. The practical flow application concerns of course fires and the design of reliable safety devices. The problem is physically very complicated as it involves turbulence and strong buoyancy forces that interact with both mean and fluctuating fields. To the authors' best knowledge, this is the first time that such a comparison exercise for practical problems is reported, based on the work of Markatos, Malin and Cox (1982); and, Kumar and Cox (1983).

#### 6.32 Objectives

The aim of the present work is two-fold:

Firstly, it is desired to predict the performance of the various scheme, for the smoke in enclosure problems.

Secondly, the present two-dimensional study forms a sound basis for extensions to three-dimensional studies, which could prove fruitful.

#### 6.33 The test problem

It is well known that the direction of the flow influences the magnitude of false diffusion. This means that the performance of numerical schemes

In this regard can be 'assessed only by test cases in two- and three-space dimensions.

The physical problem considered concerns a two-dimensional rectangular enclosure with a heat/smoke source, as depicted by Figure 6.33-1.

The flow domain is extended to the 'free boundary' region outside the doorway for computational purposes. In this test case, the flow is dominated by buoyancy and the turbulence serves to promote the rate of diffusion of mass, momentum and heat/smoke. The process involves the drawing of cold air from the bottom of the 'soffit' of height  $D$  and its spread throughout the enclosure of height  $H$ .

Near the left-hand side wall, a heat/smoke source on the floor, creates a rising plume. At the ceiling, heated gases exist which form a layer that exits from the upper part of the 'soffit'. The length of the enclosure is  $L$ , and the length outside the 'soffit' is  $H_1$ .

#### The schemes investigated

The schemes investigated for the two-dimensional turbulent study are as those for the two-dimensional laminar study (see sub-section 6.23).

The finite-difference schemes were tested for two inputs of heat/mass sources, for a grid size of  $44 \times 22$  in the  $x$ - and  $y$ -directions, respectively.

#### Test case 1:

A low source case was used to evaluate the performance of the schemes for low and moderate Peclet numbers. The source was 25.0kw.

#### Test case 2:

A high source case was used to evaluate the performance of the schemes for high Peclet numbers. The source used was 250.0kw.

#### Test case considered:

The domain considered was as follows (Markatos, Malin and Cox (1982)):  $L=9\text{m}$ ;  $H=3\text{m}$ ;  $H_1=3\text{m}$ ;  $D=1\text{m}$  and  $1.5\text{m}$ ; the source was 270Kw and spread over a  $0.45\text{m} \times 1.73\text{m}$  area,  $1.25\text{m}$  from the rear wall.

### 6.34 Presentation of results

The results are presented in the form of temperature and velocity profiles at various axial stations in the enclosure, as shown in Figure 6.33-1.

The temperature profiles are plotted at the  $x=6.77\text{m}$  plane, whereas the  $u$ -velocity profiles at the  $x=6.93\text{m}$  plane. The  $v$ -velocity is plotted at the  $y=2.438\text{m}$  plane.

Further plots of the  $u$ -velocity are also presented at the entrance or 'soffit' of the enclosure.

#### Test case 1:

Figure 6.34-1 depicts the temperature profile for the low source

problem.

Figure 6.34-2 depicts the u-velocity profile for the low source problem.

Figure 6.34-3 depicts the v-velocity profile for the low source problem.

Figure 6.34-4 depicts the u-velocity profile at the entrance of the enclosure.

#### Test case 2:

Figure 6.34-5 depicts the temperature profile for the high source problem.

Figure 6.34-6 depict the u-velocity profile for the high source problem.

Figure 6.34-7 depicts the u-velocity profile at the entrance of the enclosure, for the high source problem.

### 6.35 Discussion of results

#### Test case 1: low source

The temperature profiles, Figure 6.34-1, show that the HDS and PDS are similar in their accuracy within the enclosure, except at the boundaries. The UDS and LEDS are quite different in their predictions where the latter overpredicts the temperature by about 10% when compared with the former. The HDS and PDS underpredict the temperature by about 9%, when compared with the UDS.

The u-velocity profiles, Figure 6.34-2, were all in close agreement with the UDS, except for the PDS which predicted slightly higher velocities at the 20% station, whereas the HDS overpredicted velocities at the ceiling.

The v-velocity profiles, Figure 6.34-3, are virtually indistinguishable, except at the lower boundary.

The u-velocity profiles at the entrance to the enclosure, Figure 6.34-4, once again show that the velocity profiles are very similar except at the level of 20% of the height.

#### Test case 2: high source

Although the temperature profiles, Figure 6.34-5, were all similar in shape within the enclosure, it was noted that the HDS and LEDS were underpredicted by about 15%. The PDS temperature profile is not depicted since it was indistinguishable from the HDS temperature profile.

The u-velocity profiles, Figure 6.34-6, were largely in disagreement with each other.

The v-velocity profiles, Figure 6.34-7, are once again similar in shape except for the UDS, which lead to a flat profile. The profile shapes are similar to those for the low source case.

#### 6.36 Conclusions

A comparative study in terms of accuracy and computer requirements was performed for eight numerical schemes. Turbulence was imposed upon in order to evaluate the performances of the schemes when applied to complex practical problems that are encountered in the standard engineering environment.

An examination of the alternative schemes revealed the principal findings:

# The UDS, HDS, LEDS and PDS schemes predicted the expected trends of high temperature close to the ceiling.

# The UDS, HDS, LEDS and PDS schemes required between 10-11.5 seconds per sweep on the Prime 750 mini-computer.

# For low heat sources, there was an overall disagreement of about 10% among the temperature profiles predicted by the schemes. For high heat sources the disagreement was even higher.

# The highest degree of disagreement among the schemes was found at about 75% of the height of the room.

# For low heat sources the vertical velocity profiles predicted by the various schemes were in agreement to within 2%, whereas the horizontal velocity profiles displayed a maximum level of discrepancy of 5%. For higher heat sources large differences were observed in the velocity profiles.

# The QUDS, QUDSE and QUDSER schemes failed to converge for this test problem, despite the author's best efforts (see Appendix A6.1).

# Later the above schemes will be presented for cases for which

experimental data exists, to prove which of them is the most accurate.

## 6.4 Flow at an Angle to the Grid Lines

### 6.41 Introduction

A comparative study of five of the numerical schemes presented in Chapter 4 was undertaken, in general to evaluate, first the effects of false-diffusion for schemes which are applied locally one-dimensionally and secondly, the effects of the inclusion of the local flow-direction within the numerical scheme (ie flow-oriented scheme). The numerical schemes were tested for Peclet numbers ranging between  $10^0$ - $10^5$  and mesh Peclet numbers ranging between  $10^0/30$  -  $10^5/30$  (ie 30x30 grids). The flow angle ranged between  $0^\circ$  and  $45^\circ$ .

### 6.42 Objectives

The objectives of the study reported here were to develop a foundation for a new convective-term finite-difference scheme and to demonstrate the deficiencies of a number of schemes that are commonly used for approximating the transport equation. The test case chosen, is a standard case of flow at angles to the grid, with a prescribed uniform flow. Therefore, in the 2/E/FIX code [Pun and Spalding (1976)], the convective terms in the energy equation were refined using various schemes.

#### 6.43 The schemes investigated

The schemes investigated are:

1. the upwind-difference scheme;
2. the quadratic-upstream-difference scheme;
3. the quadratic-upstream-difference scheme extended revised;
4. the residual-difference scheme; and,
5. the skew-difference scheme.

The skew scheme reduces false-diffusion by approximating the convective-flux with a nine-point approximation, bringing within its calculation procedure the corner cells, SE, SW, NE and NW.

#### 6.44 The test problem

The transport of a scalar, in the form of a step change, in a uniform velocity-field, has received considerable attention [see for example, Raithby (1976b), Lillington (1981)], Figure 6.44-1.

The velocity-field is inclined at various angles to the grid-lines and the 2/E/FIX continuity and momentum calculations are bypassed. Two uniform inlet boundary conditions are set for the scalar, namely,  $T_{hot}=260^{\circ}$  and  $T_{cold}=10^{\circ}$ , for the west and south faces respectively. For the purpose of avoiding any mixing, the physical diffusion was set to  $10^{-10}$ , so that the discontinuity in the scalar would persist through the flow domain, and the Peclet number is  $10^{10}$ .

6.45 Presentation of results

The schemes were tested over a wide range of Peclet and mesh-Peclet numbers, together with the following grid-to-flow angles:

$\theta_1$	$0^\circ$	
$\theta_2$	$11.3^\circ$	
$\theta_3$	$21.8^\circ$	(6.45-1).
$\theta_4$	$31.0^\circ$	
$\theta_5$	$38.7^\circ$	
$\theta_6$	$45^\circ$	

The results are presented in the form of  $\phi$ -profiles at a constant  $x$ -value, and also in Table 6.45.1 for  $\theta=45^\circ$ , where the false-diffusion is at its maximum. The relative error in the diffusion coefficient, for  $\theta=\theta_i$ ,  $i=1,6$ , is tabulated below:

$\theta_1$	0	
$\theta_2$	$.1\Delta$	
$\theta_3$	$.2\Delta$	(6.45-2).
$\theta_4$	$.27\Delta$	
$\theta_5$	$.34\Delta$	
$\theta_6$	$.35\Delta$	

Figures 6.45-1 to 6.45-6 depict the  $\phi$ -profiles predicted by various schemes at a constant  $x$ -line ( $x=0.5$ ) for  $\theta=\theta_i$ ,  $i=1,2,\dots,6$ , together with the analytic solution depicted by the solid-line with no symbols.

## 6.46 Discussion of results

The scalar transport problem, illustrated in Figure 6.44-1, is extremely effective in identifying the ability of schemes to reduce the smearing effects caused by the presence of false-diffusion which depend on the angle  $\theta$  between the flow direction and the grid-lines. Table 6.45.1 reveals the false-diffusion errors for the schemes, and in particular, the root-mean square error for the two-nodal point convective-flux approximation scheme of the locally one-dimensional kind is around  $351^{\circ}$ . This value decreases as the number of nodal points used to approximate the convective-flux, for example the quadratic-upstream-difference scheme. However, when the locally one-dimensional upwind-difference scheme is applied along local streamlines, that is the skew scheme, a  $0^{\circ}$  root-mean square difference is obtained. For the problem under consideration, the false-diffusion effect for the skew scheme is zero for  $\theta=0^{\circ}$ ,  $45^{\circ}$  and  $90^{\circ}$ , however, for the rest of the schemes under investigation, the false-diffusion is at a maximum when  $\theta=45^{\circ}$ , as shown in Figures 6.45-1 and 6.45-6.

An assessment of Figures 6.45-1 to 6.45-6 reveals the following findings, for the schemes under investigation:

- # The higher-order interpolation and skew schemes predict oscillations for high Peclet numbers and large grid-to-flow angles.
- # The skew scheme predicts very accurate results for flow angles of  $45^{\circ}$ , where the false-diffusion is at its maximum for the

other schemes.

- # The skew scheme, for this particular problem, poses no convergence problems. However, since in general it may lead to negative coefficients, its application to general multi-dimensional problems is severely restricted.
- # Although the skew scheme is only first-order accurate, it yields a significant reduction or virtual elimination of false-diffusion for certain grid-to-flow angles (ie  $45^\circ$ ).
- # Although the upwind scheme always converges, it predicts a lot of smearing for angles greater than about  $10^\circ$  to either the vertical or horizontal.
- # For the locally one-dimensional schemes, false-diffusion increases continuously from  $\theta=0^\circ$  to  $\theta=45^\circ$ , however for the skew scheme, maximum false-diffusion occurs at around  $\theta=22.5^\circ$ .

#### 6.47 Conclusions

The skew scheme of Raithby (1976b) is compared with various locally one-dimensional schemes (see Section 6.43). On the basis of the test problem, the skew scheme is shown to be more accurate than the rest for certain grid-to-flow angles. The false-diffusion content of the skew scheme is much less than the others and in certain cases it is

eliminated. The skew scheme is not easy to implement and is expensive in the computational sense.

The study leaves no doubt that the locally one-dimensional schemes or their variants should not be used in approximating convection processes unless the mesh can be either closely aligned with the flow or a very fine mesh is used which reduces the importance of convection.

It now appears that to attack the problem of false-diffusion, there exists two approaches:

# One, is to use higher-order approximations with fine meshes. However this is not sensitive to grid-to-flow angles.

# Second, is to use local velocity vectors within the approximation (eg skew scheme). However, it is important to impose certain restrictions and constraints within such schemes to allow physical laws of conservation to be fulfilled.

Finally, the present contribution is related to the second of these improvements and the next chapter presents a novel approach of improving the basic framework of the skew scheme.

## 6.5 Overall Conclusions

From the studies of one- and two-dimensional test problems just discussed, it is important to extract all relevant information and try and

conclude what the next step would be in improving some of the numerical schemes. In general, the numerical analyst has a number of possible choices of schemes which can be used for a problem. However, it is not clear which particular scheme would be suited to a particular class of problems (eg recirculations). From the numerous schemes available, a majority of them (if not all!) suffer from false-diffusion, and to combat this, it is important to inject some basic rules within a new and robust numerical scheme. The basis of a new scheme stems from the studies just discussed with regards to the treatment of, for example, sources, gradients and flow-directions.

# The heat flux that leaves a cell through a particular face must be identical to the heat flux that enters the next cell through a common face. If this is violated, then the overall balance would not, in general, be satisfied, thus heat fluxes at cell faces must be carefully treated.

# The conservation of a species must be ensured for any numerical scheme that is going to be a 'good' representation of a differential equation.

# In all situations of interest, the value of the dependent variable at a given grid-point is always influenced by the neighbouring grid-points. It is therefore clear that an increase at one grid-point should in general induce an increase in the neighbouring grid-points and not a decrease. This leads to coefficients of the finite-domain representations to be always of the same sign.

# The sources must be treated in a special manner so as to reduce the occurrence of unbounded solutions which are source dominated. In general, the source should be linearisation with a negative-slope. However, depending on the strength of the source, it may be possible to violate this rule.

# To be consistent with the differential equation, the finite-domain equation for a given cell must obey the relation:

$$a_p = \sum a_{nb}$$

In the absence of sources and boundary conditions. Indeed, in the absence of sources, and uniform  $\phi$ -field, the centre-cell should take the value of its neighbours. It is only poor discretisation schemes which fail to achieve this.

# Since all iterative schemes are prone to divergence, the finite-domain equations must obey certain criteria to ensure convergence. The Scarborough criterion is one such rule. A sufficient condition for convergence is that:

$$\frac{\sum |a_{nb}|}{|a_p|} < 1 \quad \text{for all equations}$$

$$< 1 \quad \text{for at least one equation}$$

which is a sufficient condition and not a necessary one.

# A numerical scheme which induces a dissipative nature is of no use to the numerical analyst, since to reduce the dissipative nature of a scheme, one needs to employ very fine grids to

eliminate the importance of convection. Therefore, a successful numerical scheme must be non-dissipative in nature.

- # All schemes tested in this chapter (except the SKEW scheme) are of the locally one-dimensional type, that is, no true flow direction is physically accounted for by the numerical scheme. It is therefore stressed that a new numerical scheme which could prove successful, must incorporate the local flow direction within the numerical approximation profile.

Finally, to summarise, the basic rules that a 'good' scheme should satisfy are:

(a) Convergence criteria

- # Positive coefficients

(ie  $a_{nb} \geq 0$ ).

- #  $a_p = \sum a_{nb}$  (in the absence of sources and boundary conditions).

- # Negative - slope linearisation

( $s = s_a + s_p \phi_p : s_p \leq 0$ ).

- # Scarborough criterion

$$\left\{ \begin{array}{l} \frac{\sum |a_{nb}|}{|a_p|} \leq 1 \text{ for all equations} \\ < 1 \text{ at least one equation} \end{array} \right\}$$

(b) Physical criteria

- # Consistency of fluxes at cell-faces.
- # Conservation.
- # Non-dissipative nature.
- # Take into account the flow direction.

6.6 Closure

In this chapter, both one- and two-dimensional test problems were used to evaluate the advantages and disadvantages of numerical schemes so as to develop basic criteria for developing a new numerical scheme.

Embodying all the ingredients of the differential equation and the outcome of the study, would ensure physically realistic behaviour of the formulation which could be a key to the success of the new scheme.

## CHAPTER 7

### 7. NOVEL APPROACH

#### 7.1 Introduction

False-diffusion errors in numerical solutions of convection-diffusion problems, in two- and three-dimensions arise from the numerical approximations of the convection term in the conservation equations. For finite-difference based methods, one way to overcome these errors is to use upwind approximations which follow the streamlines. An approach such as this, originally derived by Raithby (1976b) and refined by a number of others [eg. Lillington (1981) and Castro, Cliffe and Norgett (1982)], is formally called the skew-upwind-difference scheme.

The novel method outlined here, a modified form to that reported earlier [Patel, Markatos & Cross (1985b)] retains the general objectives of the Raithby approach, but uses an entirely different formulation that eliminates the shortcomings of the original scheme of Raithby.

The underlying idea is to focus attention at the corners of the cells in the mesh, Markatos (1984), rather than at the cell-faces. Thus, in a two-dimensional grid, flow into the control-volume may occur from any of the eight neighbouring cells, depending on the flow direction.

The objectives are to describe the formulation of the modified novel method in this chapter.

## 7.11 Objectives

In this formulation of a numerical scheme, false-diffusion is considered from a pragmatic perspective and is performed in the context of a control-volume, primitive-variable discretisation of the convection-diffusion equation. Previous contributions by the author [Patel, Markatos and Cross (1985a); Patel and Markatos (1985b); Patel and Markatos (1986a); and, Markatos and Patel (1986b)] focussed upon assessing how interactions between false-diffusion, numerical stability and/or oscillations and the source formulation affects the accuracy and convergence of the existing published schemes, see Chapter 4. The objectives were to clarify the influence of each factor and therefore help the practitioner in choosing an appropriate scheme for his particular problem. Furthermore, the understanding acquired has led to a new robust and reliable, modified, scheme.

The flow oriented scheme of Raithby (1976b) was evaluated separately. Improvements to this family of schemes were identified and then implemented, tested and assessed especially with respect to their generality and practicability. Although these schemes appeared promising, they did suffer certain serious shortcomings, which for the Raithby scheme (1976b) may be summarised as follows:

- (i) the influence coefficients in the finite-volume equations are not constrained to be non-negative. Consequently, there are occasions when the scheme will produce non-physical oscillatory solutions or fail to converge at all;

- (ii) even though the formulation was carried out in the context of the control-volume framework (which normally guarantees conservation) the scheme may actually be non-conservative; and.
- (iii) the scheme is complex to implement; also it is slow to converge when it does so, and thus, expensive in computer time.

The novel method outlined in this paper retains the general objectives of the Raithby (1976b) scheme, yet formulates the scheme in such a way so as to ensure:

- (i) that the influence coefficients are always positive so that non-physical oscillations are avoided and convergence is enhanced;
- (ii) conservation is retained; and,
- (iii) the scheme is easy to implement and efficient in computer time.

#### 7.12 Differencing schemes for reducing 'false-diffusion'

Over the last decade or so a wide variety of schemes have been proposed to reduce the problems arising from 'false-diffusion'. A wide variety of schemes have been suggested and recently many have been

assessed against suites of test problems which aim to reveal the essential limitations of the proposed schemes [Patel, Markatos & Cross (1985a); Hung, Launder and Leschziner (1985); and, Patel and Markatos (1985a)]. Whilst it is not appropriate to go into detail here, it is worth pointing out that all the schemes, which essentially involve discretisation improvements on the simple upwind representation of the convection term, have severe restrictions on their utility. Most higher-order schemes fail to converge at high grid Peclet numbers, unless something special is done [Patel, Markatos & Cross (1985b)]. Furthermore, for flows inclined to the grids, they do not perform substantially better than the rest, because although they reduce the truncation/discretisation errors of the variable,  $\phi$ , in the cell, they are not dealing with the multi-dimensional, 'false-diffusion' problem at all.

Raithby (1976b) has described a class of schemes which allow for grid-flow direction inclination. These schemes tend to involve (in two dimensions) the diagonal neighbouring cells as well as those opposite to each face. As highlighted in the introduction, the skew schemes based upon Raithby suffer from a number of shortcomings, which have been recently illustrated [Hung, Launder and Leschziner (1985)].

#### 7.13 The novel approach: UPSTREAM scheme

A new scheme is proposed and formulated by adopting new ideas, to account for the flow-angles at the corners whilst preserving desired properties such as unconditional convergence and conservation. The central idea is to concentrate attention at the corners of the finite volume

cells rather than the cell faces as Raithby (1976b) does.

A description of the 'novel-scheme' and results obtained are presented here to demonstrate its potential.

The key to the possible success of the scheme lies in considering the control-volume corners and not the four cells-faces. For simplicity, referring to the configuration of the flow in Figure 7.13-1 the idea is to distribute the mass flow rates and transported properties according to the angle that the bold arrows at the corners make with the positive x-direction.

Considering the SW corner of the P control-volume, the inflow contribution is either from W and SW or SW and S, depending on the angle  $\theta_1$ . Similarly, considering the NE corner of the P control-volume, the outflow contribution is either to N and NE or NE and E depending on the angle  $\theta_3$ ; a similar process also being applied at the NW and SE corners. The contributions of the 8-points around the P control-volume are approximated by linear profiles.

Considering the SW corner inflow, the west face flux is evaluated as follows:

if  $\theta_1 < 45$

$$\rho u_w \Delta y \phi_w = c_w \left( \max \left[ \frac{45 - \theta_1}{45}, 0 \right] \phi_w + \min \left[ \frac{\theta_1}{45}, \frac{90 - \theta_1}{45} \right] \phi_{SW} \right)$$

$$\rho v_s \Delta x \phi_s = c_s \phi_s :$$

if  $\theta_1 > 45$

$$\rho u_w \Delta y \phi_w = c_w \phi_w$$

$$\rho v_s \Delta x \phi_s = c_s \left( \max \left[ \frac{\theta_1, 0 - 45}{45} \right] \phi_s + \min \left[ \frac{\theta_1}{45}, \frac{90 - \theta_1}{45} \right] \phi_{SW} \right) \quad ;$$

If  $\theta_1 = 45$

$$\rho u_w \Delta y \phi_w = c_w \phi_{SW}$$

$$\rho v_s \Delta x \phi_s = c_s \phi_{SW}$$

(7.13-1).

It is worth emphasising that the above formulation leads to unconditionally positive coefficients; and that its implementation in existing codes is relatively simple. A similar approach at the remaining corners leads to the formulation of the 'novel-scheme'.

Finally, using the constraint:

$$\sum \text{inflows} = \sum \text{outflows} \quad (7.13-2):$$

conservation is ensured. When applying the scheme to the momentum equations, satisfaction of equation (7.13-2) requires an adjustment stage, which is applied equally to both relevant convections,  $C_w$ ,  $C_s$  (see Figure 7.13-1).

## 7.2 Closure

In this chapter, the novel approach namely the UPSTREAM scheme was introduced. The scheme is formulated with the knowledge of the previous chapters to minimise the errors that arise due to 'false-diffusion'.

## CHAPTER 8

### 8. APPLICATIONS OF THE NOVEL APPROACH: UPSTREAM SCHEME

#### 8.1 Introduction

In this chapter, the new numerical scheme, described in the previous chapter is evaluated by applying it to various two-dimensional laminar/turbulent flows. The results are compared with some of the most used scheme presently available, at various Peclet and Reynolds numbers.

#### 8.11 Objectives

The objectives of the present study are to evaluate the relative performances of the UPSTREAM scheme with respect to some standard and most used schemes.

#### 8.12 The schemes investigated

The schemes investigated for the present applications are a combination of the following:

1. the upwind-difference scheme;
2. the quadratic-upstream-difference scheme;
3. the skew-difference scheme; and.

4. the upstream-difference scheme.

## 8.2 The Test Problems

The test problems for the present investigation are:

1. transport of a scalar in a uniform velocity-field (see Section 6.44, Figure 6.44-1);
2. flow through a sudden enlargement (see Section 6.24.1, Figure 6.24.1-1);
3. flow in a cavity with a moving lid (see Section 6.24.2, Figure 6.24.2-1); and
4. flow of heat/smoke in a rectangular enclosure (see Section 6.33, Figure 8.2-1).

## 8.3 Presentation of Results

The results obtained are in the form of  $\phi$ -profiles, contour-plots and vector-plots. The  $\phi$ -profiles are depicted at various stations in the region of interest, for each of the four test problems.

### 8.31 Transport of a scalar in a uniform velocity-field

Figures 8.31-1 to 8.31-6 depict  $\phi$ -profiles at a constant x-line ( $x=0.5$ ) for all four schemes (see sub-Section 8.12) and angles of  $0^\circ$ ,  $11.3^\circ$ ,  $21.8^\circ$ ,  $31^\circ$ ,  $38.7^\circ$  and  $45^\circ$ , respectively, for an  $11 \times 11$  uniform grid.

Figures 8.31-7 to 8.31-9 depict  $\phi$ -profiles at a constant y-line ( $y=0.4$ ) for four schemes and an angle of  $67.5^\circ$ , for uniform grids of  $11 \times 11$ ,  $21 \times 21$  and  $31 \times 31$ , respectively, for grid refinement purposes.

### 8.32 Discussion of Results

The transport of a scalar in a given uniform velocity-field has provided an excellent test problem to evaluate the presence of false-diffusion within various schemes. Figures 8.31-6 show consistent differences between upwind and quadratic-upstream-difference schemes on one hand, and skew and upstream-difference schemes on the other, particularly in respect of the position of the step and the presence of over-undershoots predicted by the quadratic-upstream and skew schemes.

The skew and quadratic-upstream difference scheme performances are similar for grid-to-flow angles of below  $15^\circ$ , whereas the upwind and upstream scheme performances are similar for the range of  $0^\circ$ - $15^\circ$ . For angles greater than  $15^\circ$ , the quadratic upstream scheme predicts overshoots and indeed at  $45^\circ$ , manages to smear the step. However, the quadratic upstream scheme smears the step far less than the upwind

difference scheme for the same grid. The skew scheme predicts highly oscillatory solutions for angles greater than  $11^\circ$  and less than  $45^\circ$ . The upstream scheme performs better than the other schemes, particularly for grid-to-flow angles greater than  $11^\circ$  to either the vertical or horizontal and with the absence of any over/undershoots.

Figures 8.31-7 to 8.31-9, serve the purpose of grid-refinement studies. For flow-to-grid angle of  $67.5^\circ$ , it is clear that the upwind-difference scheme although grid independent, is far from reproducing the step change accurately. The skew scheme on the other hand reduces the maximum undershoot value with grid-refinement, however, this is rather slow and thus a very fine grid is required to obtain wiggle free solutions. The quadratic-upstream-difference scheme predicts both over/undershoots, which persist with grid refinement, although these can again only be eliminated by the use of very fine grids or selective grid refinement. The upstream-difference scheme performs very well with grid refinement, and predicts no over-undershoots. The general tendency of all schemes, is to approach zero degrees, that is, when the velocity vector is orthogonal to the grid.

The excessive spread of  $\phi$ , normal to the velocity-vector is easily quantified with the aid of:

$$\Gamma_{\text{false}} = \frac{\rho u \Delta x \Delta y \sin^2 \theta}{4(\Delta y \sin^3 + \Delta x \cos^3 \theta)}$$

which shows that for  $\theta=67.5^\circ$ ,  $\Gamma_{\text{false}}$  assumes the value of  $0.255\Delta|u|$ , which in turn implies an 'artificial' effective Peclet number of 3.92. Therefore, if a high velocity region is at significantly large flow-to-grid

angles, and the mesh Peclet number in both x- and y-directions are greater than 2, than the upwind scheme produces solutions which are unrepresentative of the physical solution, even with a very fine grid.

### 8.33 Flow through a sudden enlargement

Figures 8.33-1 to 8.33-8 depict the  $\phi$ -profiles at a constant x-line ( $x=0.5$ ) for the upwind-difference scheme with grids of 20x20 and 25x25 and the upstream-difference scheme with a grid of 20x20. The range of Reynolds numbers considered varies between 50-3000.

### 8.34 Discussion of results

The schemes show a large discrepancy for  $Re=50$  for the same number of nodes, with a maximum difference of about 8% close to the axis of symmetry. The finer-grid upwind (25x25) and the coarser upstream (20x20) difference scheme predict results to within 2% at the symmetry plane.

For moderate Reynolds numbers (250-1000), Figures 8.33-2 and 8.33-3, the upwind (20x20 and 25x25) and the upstream (20x20) difference schemes predicted the  $\phi$ -profiles with less discrepancy between them. The upwind (20x20) and upwind (25x25) predictions were quite identical except at the top wall where the recirculation region exists.

For high Reynolds numbers ( $>1000$ ), Figures 8.33-4 to 8.33-8, the

existence of the recirculation is quite evident at the centre x-line ( $x=0.5$ ). In general, the upwind-difference scheme smears the profile around a height of 0.06 (see Figures 8.33-4 to 8.33-8). The upstream-difference scheme with a 20x20 grid predicts the influence of the recirculation and shows quite a large difference from the upwind  $\phi$ -values, at around  $\phi=0.2$ .

For  $Re=3000$ , the sharp dip at  $\phi=0.2$  for the upwind (25x25) and upstream (20x20) shows a discrepancy of around 20%. This is mainly due to the effect of upwinding in the coordinate directions as opposed to the streamline directions.

It is clearly shown that where the flow is aligned with the coordinate direction, the upwind and upstream-difference scheme predictions are quite close, as expected.

### 8.35 Flow in a cavity with a moving lid

Figures 8.35-1 and 8.35-2 depict the  $\phi$ -profiles at a constant x-line ( $x=0.5$ ) for the upwind-difference scheme (20x20 and 25x25) and the upstream-difference scheme (20x20), together with experimental results obtained from Nallaswamy & Prasad (1977) for  $Re=100$  and 1000, respectively.

Figure 8.35-3 and 8.35-4 depict the  $\phi$ -profiles at a constant y-line ( $y=0.5$ ) for the upwind-difference scheme (20x20 and 25x25) and the upstream-difference scheme (20x20), together with experimental results

obtained from Nallaswamy & Prasad (1977) for  $Re=100$  and  $1000$ , respectively.

### 8.36 Discussion of Results

The upwind-difference scheme  $\phi$ -profiles ( $x=0.5$ ), although similar in shape, show quite a departure from the experimental results at around a height of  $0.7$  for  $Re=100$ , see Figure 8.35-1. In contrast, the upstream-difference scheme predicts the experimental values quite accurately, taking into account the coarse grid and the sharp gradient present near the top of the cavity.

For  $Re=1000$  the discrepancies at the  $x$ -centreline, Figure 8.35-2, between the upwind ( $20 \times 20$  and  $25 \times 25$ ) and the upstream is larger, as expected; and there is still a large difference in the minimum value of  $\phi$  at the centre of the cavity as predicted by the upwind ( $25 \times 25$ ) when compared with the experimental value. On the other hand, the upstream ( $20 \times 20$ ) scheme appears quite accurate within the bulk of the cavity, except close to the moving lid, where the sharp kink in the profile was not predicted.

The comparison of the profiles at the  $y$ -midplane ( $y=0.5$ ), see Figures 8.35-3 and 8.35-4, show quite a difference between the experimental, upwind- and upstream-difference schemes; the upwind-difference scheme overpredicting by about 25% at a width of about  $0.5$ . The upstream-difference scheme predicted results to within 10% of the experiments, with the  $20 \times 20$  grid. In general, the numerically predicted

profile shapes were similar to those observed experimentally, but the upwind-difference scheme predictions were flatter within the centre of the cavity.

### 8.37 Flow of heat/smoke in a rectangular enclosure

The u-velocity profiles are depicted at the  $x=2.63\text{m}$ ,  $5.81\text{m}$  and  $8.87\text{m}$  planes in Figures 8.37-1 to 8.37-3, respectively; and the temperature profiles at  $x=2.49\text{m}$ ,  $5.68\text{m}$  and  $8.86\text{m}$  are depicted in Figures 8.37-4 to 8.37-6, respectively for the upwind- and upstream-difference schemes. Where available, experimental results extracted from Kumar and Cox (1983), are also presented.

Contour plots of u-velocity (Figures 8.37-7 and 8.37-8), v-velocity (Figures 8.37-9 and 8.37-10), temperature (Figures 8.37-11 and 8.37-12) and pressure (Figures 8.37-13 and 8.37-14) are presented for the upwind- and upstream-difference schemes, respectively.

Finally, the velocity vectors are presented in Figures 8.37-15 and 8.37-16 for the upwind- and upstream-difference schemes.

### 8.38 Discussion of results

The following discussion is relative to the UDS predictions, unless otherwise stated.

The u-velocity profiles. Figures 8.37-1 and 8.37-3 show that both the UDS and upstream schemes predicted similar results. This is not surprising, since the upstream scheme was not directly applied to the momentum equations but only the energy equation. Thus, the observed differences between the predictions of the UDS and upstream schemes are only due to the density differences caused by the temperature differences. This effect is stronger in the upper half of the enclosure at the  $x=5.81\text{m}$  plane (Figure 8.37-1), and in the lower half of the enclosure for the  $x=8.63\text{m}$  plane (Figure 8.37-2). The velocity profiles at the 'doorway',  $x=8.87\text{m}$  plane (Figure 8.37-3), are almost identical. This is mainly due to the fact that most of the flow there is horizontal, and so the scheme reverts to the UDS scheme over most of that plane. Both schemes lead to poor results at the  $5.81\text{m}$  plane (ie no stratified flow, as predicted by the experimental results) but this may be due to the viscosity value used (see relevant discussion in Markatos, Malin and Cox (1982)). It will be interesting in this context to apply the upstream scheme to the momentum equations as well. The maximum difference between the velocity result predicted by the two schemes is approximately 8%.

The temperature profiles. Figures 8.37-4 and 8.37-5 show a marked difference between the results, especially at the  $x=2.49\text{m}$  and  $x=8.86\text{m}$  planes in the upper half of the enclosure. The predictions with the UPSTREAM scheme are on average 10% to 12% better than those for the UDS. However, the 'soffit' temperature is poorly predicted by both schemes, where the UDS is again the worse of the two.

The other schemes used for the experimental compartment are not

presented since similar trends to those of the standard compartment, see sub-sections 6.32 to 6.36, high source test cases were evident.

- \* Preliminary comparisons with experiment tend to favour (within 10-12%) the LEDS and the upstream scheme.
  
- \* The QUDS, QUDSE, QUDSER and Raithby's skew schemes failed to converge for this test problem, despite the author's best efforts. This is true even for the cases where the schemes were introduced only in the energy equation and not in the momentum equations. It is true that, by inspecting coefficients of these schemes, a technique could have been devised to prevent the divergence of these schemes; for example, it could have been arranged that above a certain mesh Peclet number the QUDS reverted to the UDS. However, this would be a problem-dependent choice and generally is a strong desideratum, for practical applications.
  
- \* Among the schemes that converged for the UDS, HDS, LEDS and PDS there is no distinct advantage concerning computational time; all requiring between 10-11.5 secs per sweep on the Prime 750 minicomputer, for the grid used, and about the same total number of sweeps for a given accuracy. The upstream difference scheme required about 10% more CPU seconds per sweep compared to the UDS scheme CPU time; however, this increase is not too great since this scheme also requires fewer iterations to converge.

Inspection of the above results, as well as others not displayed here, resulted in the following principal findings:

- # The UDS, HDS, LEDS and PDS schemes predicted the expected trends of temperature variations. The CDS failed to converge for the strong heat source cases.
- # For low heat sources, there was an overall difference of about 10% among the temperature profiles predicted by the schemes. For strong heat sources the disagreement was even higher, at about 15%.
- # The highest degree of difference among the schemes was found at about 20% of the height of the room.
- # For low heat sources the vertical velocity profiles predicted by the various schemes were in agreement to within 2%, whereas the horizontal velocity profiles displayed a maximum level discrepancy of 5%. For high heat sources large differences were observed in the velocity profiles.

#### 8.4 Conclusions

The overall conclusions of the present study, to compare the predictions of the upstream-difference scheme with some of the generally used numerical schemes, has revealed that the scheme can predict better and accurate results without the added complexity of divergence. The

upstream scheme has been tested for both laminar and turbulent flows where 'false-diffusion' would have existed for the conventional, locally, one-dimensional, numerical schemes.

The upstream-difference scheme provides an alternative to the UDS/LEDS schemes, in that it is unconditionally stable, more accurate by about 10% for the cases considered, and only marginally (approximately 6% fewer steps) more expensive to run.

## 8.5 Closure

In this chapter the application of the upstream-difference scheme to various test cases has been presented, together with comparisons of other conventional and generally used numerical schemes and experimental results (where available).

## CHAPTER 9

### 9. CONCLUSIONS

The main points of importance that emerge from the previous chapters of this thesis are classified into two sub-sections. These two sub-sections are as follows:

- (a) one-dimensional study - conclusions; and,
- (b) two-dimensional study - conclusions.

This then leads to the classification of the overall points of importance in a much general context with regards to stability, accuracy, economy and applicability of the various numerical-schemes considered.

#### 9.1 One-Dimensional Study - Conclusions

Of the numerical schemes applied to the one-dimensional test cases, it is concluded that the higher-order schemes, in general, perform well, although care must be taken to ensure their stability. The accuracy of the higher-order schemes is much greater than low-order schemes when they converge because the truncation errors, from Taylor series analysis, are much smaller and not of the diffusive type. The low-order schemes on the other hand prove stable except that they suffer from larger errors which are diffusive in nature. It has also been shown that the first-order upwind-difference scheme proves more stable and accurate than the central-difference scheme which is second-order accurate.

This arises mainly due to the fact that some physical intuition has been incorporated within the formulation of the numerical scheme.

Therefore, the one-dimensional study serves the purpose of clarifying the misunderstanding present in the solution of the convection-diffusion equation with regards to truncation errors only, since no false-diffusion is present in one-dimension. Furthermore, it provides some guidelines for numerical analysts and practitioners as to which schemes are stable, accurate, economical and physically viable.

## 9.2 Two-Dimensional Study - Conclusions

The two-dimensional study was performed to clarify the errors present due to the nature of the locally one-dimensional treatment of the flow, together with the effect when the flow is skew to the grid lines. It is the 'local one-dimensional flow' assumptions that gives rise to 'false-diffusion', unlike the real one-dimensional flow problems where only truncation errors were the cause of inaccuracies. The study points, in general, towards the inadequacy of all the locally one-dimensional schemes available to-date for evaluating accurate and economical solutions with fairly coarse grids.

Extensions exist of the locally one-dimensional upwind-difference scheme, namely the skew upstream-difference scheme and the vector-upstream-difference scheme. These schemes take into account the grid-to-flow angle explicitly with the formulation of the numerical scheme influence coefficients. Although they are first-order accurate,

they have proved quite accurate and are extensively used. However, they are restricted to small grid-to-flow angles due to the non-bounded nature of the influence coefficients, which results in highly undesirable numerical oscillations.

To improve the numerical scheme it was considered in this work to formulate the influence coefficients along the lines of the skew-upstream-difference scheme, but with simultaneous satisfaction of all the conditions of stability, accuracy and possibly free from false-diffusion. This was achieved by considering inflows and outflows directly at the corners of the control-volume, thus ensuring positive influence coefficients. This results in the formulation of the upwind in streamline direction-differencing scheme (ie UPSTREAM), which accounts for all the above mentioned pitfalls which hinder the performance of the various available numerical-difference schemes. The upstream-difference scheme is a compromise between accuracy and stability. The reason for the compromise is that a stable scheme was achieved only by considering a scheme which is applied at the inflow and outflow at corners, although only first-order accurate, and the accuracy being achieved by careful and simple physical sense being incorporated within the formulation, ie the local flow direction dependence of the flow. Unfortunately, the new scheme (as well as every other existing 'skew' scheme) cannot be guaranteed to be conservative.

The results obtained by the use of the upstream-difference scheme show a marked improvement in various test cases considered during the study and it is in this direction that future research should be directed for fruitful results and major improvements.

### 9.3 Summary of Overall Conclusions and Findings

The important conclusions of the present study have helped to clarify the various advantages and disadvantages of locally one-dimensional and flow oriented schemes for the solution of multi-dimensional fluid-flow problems.

The important properties that a numerical scheme should satisfy have been discussed, these being conservation, boundedness and physical insight to the flow problems.

The boundedness property, a requirement for a diagonal dominant influence coefficient matrix, ensures numerical stability. Violation of this property is the main reason for the failure of the higher order and existing flow oriented schemes.

The conservation property, if satisfied leads to the boundedness property.

The relevance of the numerical scheme to the flow structure provides great improvements to the physical basis of the link between the upwind to that at the current location. This clearly leads to no downwind contributions to the evaluation of convected species.

The main contribution of the present work is firstly to clarify the problems of the available schemes. These are then utilised to formulate a new flow-direction upstream scheme, which is bounded and reduces 'false-diffusion'. The application and performance of the scheme has

been demonstrated by applying it to some classical test problems. The analysis of which revealed that the new scheme proved accurate and economical.

The study also examined the validity of the truncation errors within the process of false-diffusion which lead to a more precise and meaningful definition of 'false-diffusion'.

The specific findings concerning the performance of various finite-volume schemes, for different test cases are summarised below.

#### Locally one-dimensional schemes

The locally one-dimensional schemes all, in general, give rise to excessive errors for flows which are oblique to the grid lines. Some of these schemes fail because the restriction on the cell Peclet number is not adhered to and others give rise to plausible results.

In general, the lower-order numerical schemes prove well suited for all test cases where the flow is directed towards one or the other grid-line directions. The reason for this is that even for simple flows, the higher-order schemes have to be used with care due to the restriction on the cell Peclet number. Furthermore, the aim of reverting to higher-order schemes is to improve accuracy and also reduce false-diffusion errors; however, locally one-dimensional numerical schemes fail to reduce false-diffusion errors since no explicit information of the local velocity direction is utilised within the scheme.

Stable higher-order schemes, obtained by modifying the nature of the influence coefficients and source terms, prove more accurate than their original schemes. However, there is an order of magnitude increase in overall cost of computing solutions.

The view of the author is that when one wishes to use the locally one-dimensional schemes, it is best to use a low-order scheme, since with some selective grid refinements, plausible and cost-effective results are easily obtained, unlike with the high-order schemes where fine tuning of the convergence parameters has also to be considered.

#### Flow oriented schemes

The flow-oriented schemes, only a few of which exist, are an extension of the locally one-dimensional schemes, where the flow direction explicitly appears within the formulation of the influence coefficients. Once again, the simplest flow-oriented scheme, the skew scheme of Raithby (1976b) although only first-order accurate, provides a great improvement in numerical accuracy when it converges. However, convergence is not so easy when applied to complex problems. The downfall of the scheme is that it is not bounded and the conservative properties which must be satisfied by a numerical scheme for it to be able to predict accurate and economical solutions are not satisfied.

It is because of the instabilities, due to shortcomings in the influence coefficients, that it was found necessary to devise a special treatment to produce a bounded scheme. This leads to monotonic convergence and solutions which are virtually free from false-diffusion.

The practice devised was to consider inflows and outflows at 'corners' of the control-volumes. This stabilises the influence coefficients, since non-adjacent face contributions are felt by its neighbouring cell faces of the same control-volume. This leads to non-negative influence coefficients.

The above practice leads to a new numerical scheme termed as UPstream in STREAMline direction scheme, ie UPSTREAM scheme. The results obtained by the newly-formulated scheme provides the following important points:

- # the scheme is bounded and conservative;
- # it virtually eliminates false-diffusion;
- # it improves convergence and accuracy; and
- # it is economical and is comparable to the conventional upwind-difference scheme in terms of computational costs.

#### 9.4 Closure

This chapter presented the overall conclusions of the study performed. The conclusions of the study prove useful since the work was performed in two stages:

- # classification of all the schemes in terms of accuracy, economy and boundedness; and,
- # a new formulation to overcome some of the pitfalls of the available schemes to increase the accuracy, economy and

boundedness, ie the stability of the numerical scheme.

However, there are some shortcomings of the scheme which require further examination. These are outlined in the next chapter.

## CHAPTER 10

### 10. FURTHER RECOMMENDATIONS

#### Suggestions for Further Work

The available evidence indicates that the UPSTREAM scheme performs very well for problems where the flow is inclined to the grid-lines together with no other restriction, either on the source term or the fineness of the grid. However, since there are many problems of practical importance, it is worth pursuing and extending the scheme to three-dimensional problems with a possible extension to transient problems. This in the first instance can be aimed at being applied to the improvement of the convected scalar only, since, many test cases can be devised to check the formulation.

Regarding the application of the UPSTREAM scheme to the flow-field predictions, some areas require further investigation, these are as follows:

- # The weighting procedure, utilised to average the velocity at the 'cell-corner' in the momentum equation requires a set of rules to achieve this uniquely in all situations possible.
  
- # Furthermore, it is possible to utilise the one-dimensional exponential solution along with the 'corner-approach', instead of the first-order approximation, to improve the approximation further.

# The computation of the exponential functions in the previous step requires an economical procedure, since in general, exponential functions are time-consuming, ie expensive to evaluate. In the first instance a polynomial approximation can be utilised for the exponential function.

# The UPSTREAM scheme, in its present form, is non-conservative, when applied to the velocities, and further improvement is required to achieve this.

Finally, the improvements suggested above to further improve the UPSTREAM scheme would greatly benefit the computational fluid dynamics practitioners, since then a very versatile and highly accurate numerical scheme would be available to tackle multi-dimensional, multi-phase problems of real importance which with present day resources and numerical schemes is virtually impossible.

ALLEN D N DE G (1962)

'A Suggested Approach to Finite-Difference Representation of Differential Equations with an Application to Determine Temperature Distributions near Sliding Contact'. Q. J. Mech. Appl. 15, pp11-33.

ALLEN D N DE G & SOUTHWELL R V (1955)

'Relaxation Methods Applied to Determine the Motion in Two Dimensions of a Viscous Fluid Past a Fixed Cylinder'. Q. J. Mech. Appl. Math. 8, pp129.

ATIAS M, WOLFSHTEIN M & ISRAELI M (1977)

'Efficiency of Navier-Stokes Solvers'. AIAA J. 15, No. 2, pp263-266.

ATKINS D J, MASKELL S J & PATRICK M A (1980)

'Numerical Predictions of Separated Flows'. Int. J. Num. Meths. Eng. 15, pp129-144.

BACK L H & ROSCHKE E J (1972)

'Shear-Layer Flow Regimes and Wave Instabilities and Re-attachment Lengths Downstream of an Abrupt Circular Channel Expansion'. J. Appl. Mech. 39, Trans ASME Series 7, pp677.

BACK L H & ROSCHKE E J (1976)

'The Influence of Upstream Conditions on Re-attachment Lengths Downstream of an Abrupt Circular Expansion'. J. Biomechanics. 9, p481.

BARRETT K (1982)

'Super Upwinding - Elements of Doubt and Discrete Differences of Opinion on the Numerical Muddling of the Incomprehensible Defective Confusion Equation'. [Title inspired by B P Leonard]. In Numerical Modelling in Diffusion Convection [Ed. J Caldwell & A Moscardini], Pentech Press, London.

BHATTACHARYA T K & DATTA A B (1985)

'A Residual Method of Finite-Differencing for the Elliptic Transport Problem and Its Application to Cavity Flow'. Int. J. Num. Meth in Fluids. 5, pp71.

BLOWERS R M (1971)

'Some Theoretical Aspects of the Upwind Difference Method for the Numerical Solution of the Steady-State Navier-Stokes Equations in Two Dimensions'. CEGB Report No. RD/L/N143/71.

BOURCIER M & FRANCOIS C (1969)

'Integration Numeric de Equation de Navier Stokes'. Un Domaine Karre. Rech Aerosp. No. 131, pp23.

BOZMAN J D & DALTON C (1973)

'Numerical Study of Viscous Flow In a Cavity'. J. Comp. Phys. 12, pp348.

BRADSHAW P (1976) (EDITOR)

'Turbulence Topics in Applied Physics'. 12, Berlin, Springer-Verlag.

BRIGGS D G (1975)

'A Finite-Difference Scheme for the Incompressible Advection-Diffusion Equation'. Computer Meth. Appl. Mech. Eng. 6, pp233-241.

BURGGRAF O R (1966)

'Analytical and Numerical Studies of the Structure of Steady Separated Flows'. J. Fluid Mech. 24, pp113.

CARETTO L S, GOSMAN A D, PATANKAR S V, POTTER R & SPALDING D B (1972)

'Two Numerical Procedures for Three-Dimensional Recirculating Flows'. Proc. Int. Conf. on Num. Meth. in Fluid Dyn. Paris.

CASTRO I P (1978)

'The Numerical Prediction of Recirculating Flows'. Proc. of 1st Int. Conf. on Num. Meth. in Laminar and Turb Flow, Swansea, UK. Eds. Taylor, Morgan and Brebbia, Pentech Press.

CASTRO I P, CLIFFE K A & NORGETT M J (1982)

'Numerical Predictions of the Laminar Flow over a Normal Flat Plate'. Int. J. Num. Meths. Fluids. 2, p61-88.

CHIEN J C (1977)

'A General Finite-Difference Formulation with Application to Navier Stokes Equations'. Comput. Fluids. 5, pp15-31.

CHOW L C & TIEN C L (1978)

'An Examination of Four Differencing Schemes for Some Elliptic-Type Convection Equations'. Num. Heat Transfer. 1, pp87-100.

CONTE S D & DE BOOR C (1980)

'Elementary Numerical Analysis an Algorithmic Approach' (3rd Ed.). McGraw-Hill Kogakusha Limited.

COURANT R. ISAACSON E & REES M (1952)

'On the Solution of Non-Linear Hyperbolic Differential Equations by Finite-Differences'. Communications on Pure and Applied Mathematics. 5, p243.

DENHAM M K & PATRICK M A (1974)

'Laminar Flow over a Downstream Facing Step in a Two-Dimensional Flow Channel'. Trans. Inst. Chem. Eng. 52, pp361-367.

DENNIS S C R (1960)

'Finite-Differences Associated with Second-Order Differential Equations'. Quart. Jour. Mech and Appl. Math. XIII, Pt 4.

DENNIS S C R (1973)

'Numerical Solution of the Vorticity Transport Equation'. Lecture Notes in Physics. 19, pp120-129.

DENNIS S C R & CHANG GAU-ZU (1969)

'Numerical Integration of the Navier-Stokes Equations in Two Dimensions'. MRC Tech. Summary Report 859. Mathematics Research Centre, University of Wisconsin, Madison, Wisconsin.

DE VAHL DAVIS G & MALLINSON G D (1976)

'An Evaluation of Upwind and Central Difference Approximations by a Study of Recirculating Flow'. *Comp. Fluids*. 4, pp24-43.

FORSYTHE G E & WASON W (1960)

'Finite-Difference Methods for Partial-Differential Equations'. Wiley, New York.

FORTIN M, PEYRET R & TEMAM R (1971)

'Approximations by a Study of Recirculating Flows'. Lecture Note in Physics (Springer-Verlag, NY). 8, pp337.

GALLAGHER R H, ZIENKIEWICZ O C, ODEN J T, MORANDI CECCHI M & TAYLOR C (1978)

'Finite Element in Fluids'. 3, John Wiley & Sons, Chichester.

GLOWINSKI R (1982)

'A Review of Finite-Element Methods for Fluid-Flow Problems'. Proc. of int. Symp. on Refined Modelling of Flows. IAHR, Paris.

GOSMAN A D, PUN W M, RUNCHAL A K, SPALDING D B & WOLFSHTEIN M (1969)

'Heat and Mass Transfer in Recirculating Flows'. Academic Press, London and New York.

GREENSPAN D (1967)

'Numerical Studies of Two-Dimensional Steady-State Navier-Stokes Equations for Arbitrary Reynolds Number'. Report No. 9, University of Wisconsin, Dept of Computer Science.

GREENSPAN (1969)

'Numerical Studies of Prototype Cavity Flow Problems'. Computer J. 12, pp89.

GRESHO P M & LEE R L (1979)

'Don't suppress the wiggles - they're telling you something' - in Hughes T J R (ed.). Proc. of a Symp. on Finite Element Meth. for Convection Dominated Flows, pp37-61, ASME Winter Annu. Meet. New York.

GRIFFITHS D F (1977)

'On the Approximation of Convergence Problems in Fluid Dynamics'. Int. J. Num. Meths. Eng. p1477-1482.

GUPTA M M & MANOHAR R P (1979)

'Boundary Approximations and Accuracy'. J. Comp. Physics in Viscous Flow Computations. 31, pp265.

HAN T, HUMPHREY J A C & LAUNDER B E (1981)

'A Comparison of Hybrid and Quadratic-Upstream Differencing in High Reynolds Number Elliptic Flows'. *Comp. Meth. Appl. Mech. Eng.* 29, pp81-95.

HARLOW H & WELCH J E (1965)

'Numerical Calculation of Time-Dependent Viscous Incompressible Flow of Fluid with Free Surface'. *Physics of Fluid.* 8, pp2182.

HASSAN Y A, RICE J G & KIM J H (1983)

'A Stable-Mass-Flow-Weighted Two-Dimensional Skew Upwind Scheme'. *Num. Heat Transfer.* 6, pp395-408.

HEINRICH J C, HUYAKORN P S, ZIENKIEWICZ O C & MITCHELL A R (1977)

'An Upwind Finite-Element Scheme for Two-Dimensional Convective Transport Equation'. *Int. J. Num. Meth. Eng.* 11, pp131-143.

HINZE J O (1959)

'Turbulence. An Introduction to its Mechanism and Theory'. *McGraw-Hill Series in Mech. Eng.*

HOUSEHOLDER A S (1964)

'The Theory of Matrices in Numerical Analysis'. *Blaisdell, New York.*

HUGHES T J R & BROOKS A (1979)

'A Multi-Dimensional Upwind Scheme with No Crosswind Diffusion' - in Hughes T J R (ed.). Proc. of a Symp. on Finite-Element Methods for Convection Dominated Flows. pp19-35. ASME Winter Annu. Meet. New York.

HUGHES T J R, LIU W K & BROOKS A (1979)

'Finite-Element Analysis of Incompressible Viscous Flows by the Penalty Function Formulation'. J. Comp. Phys. 30, pp1-60.

HUNG P G, LAUNDER B E & LESCHZINER M A (1985)

'Discretisation of Non-Linear Convection Processes: A Broad Range Comparison of Four Schemes. Comp. Meths. Appl. Mech. Eng. 48, pp1.

ИЛИН А М (1969)

'Differencing Scheme for a Differential Equation with a Small Parameter Affecting the Highest Derivative. Steklov Math. Inst. of the Academy of Science of the USSR. pp590-602.

IRIBARNE A, FRANTISAK F, HUMMEL R L, & SMITH J W (1972)

'An Experimental Study of Instabilities and other Flow Properties of a Laminar Pipe Jet'. AIChE J. 18, No. 14, pp689.

KAWAGUTI M (1961)

'Numerical Solutions of the Navier-Stokes Equation for Flow in a Two-Dimensional Cavity'. J. Phys. Soc. Japan, 16, No. 11, p2307.

KELLOGG R B, SHUBIN G R & STEPHENS A B (1960)

'Uniqueness and the Cell Reynolds Number'. Siam J. Numer. Anal. 17, No. 6.

KUMAR S & COX G (1983)

'The Application of a Numerical Field Model of Smoke Movement to the Physical Scaling of Compartment Fires'. In Numerical Methods in Thermal Problems edited by Lewis, Johnson and Smith. p837. Pineridge Press.

LAUNDER B E & SPALDING D B (1972)

'Mathematical Models of Turbulence'. Academic Press, London and New York.

LE FEUVRE R F (1970)

'The Application of a Semi-Orthogonal Finite Integral Technique to Predict Inclined-Plane and Cylindrical Couett Flows'. Report Nos. EF/TN/A/33 and HTS/74/5, Imperial College, London.

LEONARD B P (1977)

'New-Flash: Upstream Parabolic Interpolation'. Proc. of 2nd GAMM Conf. on Numerical Methods in Fluid Mechanics, Koln, Germany p97.

LEONARD B P (1979)

'A Stable and Accurate Convective Modelling Procedure Based on Quadratic Upstream Interpolation'. Comp. Meths. Appl. Mech. Eng. 19 pp59-98.

LEONARD B P, LESCHZINER M A & MCQUIRK J (1978)

'Third-Order Finite-Difference Method for Steady Two-Dimensional Convection'. Num. Meth. in Laminar and Turbulent Flow. p807. University of Wales, Swansea, UK.

LESCHZINER M A (1977)

'On the Problem of Numerical Diffusion in Recirculating Flows'. Proc. of 2nd GAMM Conf. on Numerical Methods in Fluid Mechanics. Cologne. pp105-112.

LESCHZINER M A (1980)

'Practical Evaluation of Three Finite Difference Schemes for the Computations of Steady-State Recirculating Flows'. Comp. Meth. in Appl. Mech and Eng. 23. pp293-312.

LESCHZINER M A & RODI W (1981)

'Calculation of Annular and Twin Parallel Jets using Various Discretisation Schemes and Turbulence Model Variants'. ASME J. Fluids. Eng. 103. pp352-360.

LILLINGTON J N (1980)

'The Application of a Vector Upstream Differencing Scheme for the Calculation of Recirculating Flow in Rod Bundle Geometry'. Num. Meth. for Non-Linear Problems. Swansea, Wales.

LILLINGTON J N (1981)

'A Vector Upstream Differencing Scheme for Problems in Fluid Flow Involving Significant Source Terms in Steady-State Linear Systems'. Int. J. Num. Meth. Fluids, 1, pp3-16.

LILLINGTON J N & SHEPHERD I M (1978)

'Central Difference Approximations to the Heat Transport Equations'. Int. J. Num. Meth. Eng. 12, pp1697-1704.

MACAGNO E O & HUNG T K (1967)

'Computational and Experimental Study of a Captive Annular Eddy'. J. Fluid Mech. 28, p43.

MALIN M R, ROSTEN H I, SPALDING D B & TATCHELL D G (1985)

'Application of PHOENICS to Flow Around Ship's Hulls'. Second Int. Symp. on Ship Viscous Resistance. Editor Lars Larsson, SSPA Symposium.

MARKATOS N C (1974)

'Transport Phenomena Through Wavy Interfaces'. PhD Thesis, University of London.

MARKATOS N C (1978)

'Transient Flow and Heat Transfer of Liquid Sodium Coolant in the Outlet Plenum of Fast Nuclear Reactors'. Int J. Heat Mass Transfer, 21, 1565.

MARKATOS N C (1984)

'A New Conservative, Non-Diffusive and Unconditionally Stable Scheme'.

3.6.84 Private Communication.

MARKATOS N C, MALIN M R AND COX G (1982)

'Mathematical Modelling of Buoyancy Induced Smoke Flow in Enclosures'.

Int. J. Heat Mass Transfer. 25, 1, pp63.

MARKATOS N C & PERICLEOUS K A (1984)

'Laminar and Turbulent Natural Convection in an Enclosed Cavity'.

IJHMT, 27, No. 5, p755-772.

MILITZER J, NICOLL W B & ALPAY S A (1977)

'Some Observations on the Numerical Calculation of the Recirculation Region of Twin Parallel Symmetric Jet Flow'. Proc. of a Symp. on

Turbulent Shear Flows. Pennsylvania State Univ, USA, 18, p11.

NALLASWAMY M & KRISHNA PRASAD K (1977)

'On Cavity Flow at High Reynolds Numbers'. J. Fluid Mech. 79,

pp391-414.

PATEL M K (1985)

'Full Formulation of the Skew Scheme'. Internal Technical Report

TP/NUMOD/86/3 Thames Polytechnic (London).

PATEL M K & MARKATOS N C (1984)

'An Evaluation of Eight Discretisation Schemes for Two-Dimensional Laminar Fluid Problems (4 Test Cases)'. Internal Technical Report TP/NUMOD/85/4 Thames Polytechnic (London).

PATEL M K & MARKATOS N C (1985a)

'An Evaluation of Eight Discretisation Schemes for Two-Dimensional Mathematical Modelling of Buoyancy-Induced Smoke-Flow in Enclosures'. TP/NUMOD/85/4 Internal Technical Report, Thames Polytechnic (London).

PATEL M K & MARKATOS N C (1985b)

'On the Discretisation Schemes for Transport Equations'. Polymodel 8 Proceeding, Teeside Polytechnic, Middlesborough, UK.

PATEL M K & MARKATOS N C (1986a)

'An Evaluation of Eight Discretisation Schemes for Two-Dimensional Convection-Diffusion Equations'. Int. J. Num. Meth. Fluids. 6, pp124-154.

PATEL M K & MARKATOS N C (1986b)

'Evaluation of Ten Discretisation Schemes for Modelling Buoyancy-Induced Smoke-Flow in Enclosures'. To appear: Int. J. Num. Meth. Fluids.

PATEL M K, MARKATOS N C & CROSS M (1985a)

'A Critical Evaluation of Seven Discretisation Schemes for Convection-Diffusion Equations'. Int. J. Num. Meth. Fluids. 5, pp225-244.

PATEL M K, MARKATOS N C & CROSS M (1985b)

'Method of Reducing False-Diffusion Errors in Convection-Diffusion Problems'. Appl. Math. Modelling 1985, 9, pp302.

PATEL M K, CROSS M, MARKATOS N C & MACE A C (1986)

'An Evaluation of Eleven Discretisation Schemes for Predicting Elliptic Flow and Heat Transfer in Supersonic Jets'. IJHMT (to appear).

PAN F & ACRIVOIS R (1967)

'Steady Flow in Rectangular Cavities'. J. Fluid Mech. 28, pp643.

PATANKAR S V (1980)

'Numerical Heat Transfer and Fluid Flow'. Hemisphere, Washington DC.

PATANKAR S V (1975)

'Numerical Prediction of Three-Dimensional Flows, in Studies in Convection: Theory, Measurement and Applications'. Edited by B E Launder, 1, Academic Press, New York.

PATANKAR S V & SPALDING D B (1972)

'A Calculation Procedure for Heat, Mass and Momentum Transfer in Three-Dimensional Flows'. Int. J. Heat and Mass Transfer. 15, p1787.

POLLARD A (1980)

'Entrance and Diameter Effects on the Laminar Flow in Sudden Expansions'. In: Momentum and Heat Transfer Processes in Recirculating Flows, Launder and Humphrey (Ed.) ASME (HTD). 13, p21.

POLLARD A & SIU ALAN L W (1982)

'The Calculation of Some Laminar Flows Using Various Discretisation Schemes'. Comp. Meths. Appl. Mech and Eng. 35, p293.

PUN W M & SPALDING D B (1967)

'A Procedure for Predicting the Velocity and Temperature Distributions in a Confined, Steady, Turbulent, Gaseous, Diffusion Flame'. Report SF/TN/11, Imperial College Mech. Eng. Dept. London.

PUN W M & SPALDING D B (1976)

'A General Computer Program for Two-Dimensional Elliptic Flows'. HTS/76/2, Imperial College, London, UK.

RAITHBY G D (1976a)

'A Critical Evaluation of Upstream Differencing Applied to Problems involving Fluid Flow'. Comp. Meth. Appl. Mech. Eng. 9, pp75-103.

RAITHBY G D (1976b)

'Skew Upstream Differencing Schemes for Problems involving Fluid Flows'. Comp. Meth. Appl. Mech. Eng. 9, pp153.

RAITHBY G D & TORRANCE K E (1974)

'Upstream-Weighted Differencing Schemes and their Application to Elliptic Problems Involving Fluid-Flow'. Computers and Fluids. 2, pp191-206.

ROACH P J (1972)

'Computational Fluid Dynamics'. Hermosa Publishers, Albuquerque, NM.

ROACHE P (1975)

'The Lad, Nos and Split Nos Methods for the Steady-State Navier-Stokes Equations'. Comp. Fluids. 3, pp179.

ROACH P J (1976)

'Computational Fluid Dynamics'. Hermosa Publishers, Revised Edition, New Mexico.

ROACH P J & MUELLER T J (1970)

'Numerical Solutions of Laminar Separated Flows'. AIAA J. 8, No. 3, p530.

RUBIN S G & KHOSLA P K (1977)

'Polynomial Interpolation Methods for Viscous Flow Calculations'. J. Comp. Phys. 24, pp217.

RUNCHAL A K (1972)

'Convergence and Accuracy of Three Finite-Difference Schemes for Two-Dimensional Conduction and Convection Problems'. Int. J. Num. Meths. Eng. 4, p541.

RUNCHAL A K & WOLFSHTEIN M (1966)

'A Finite-Difference Procedure for the Integration of the Navier-Stokes Equations'. Report SF/TN/1 Imperial College, Mech. Eng. Dept. London.

RUNCHAL A K, SPALDING D B & WOLFSHTEIN M (1967)

'The Numerical Solution of the Elliptic Equations for Transport of Vorticity, Heat and Matter in Two-Dimensional Flows'. Report SF/TN/2 Imperial College, Mech. Eng. Dept. London.

SIMUNI L M (1961)

'The Numerical Solution of Some Problems in the Flow of a Viscous Fluid'. Inzheng Zhur. 4, No.3, p446.

SMITH G D (1969)

'Numerical Solution of Partial Differential Equations'. Oxford Univ Press, London.

SPALDING D B (1966)

'Notes on the Solution of the Navier-Stokes Equations for Steady Two-Dimensional Turbulent Flow by Finite-Difference Techniques'. Report SF/TN/5 Imperial College, Mech. Eng. Dept. London.

SPALDING D B (1972)

'A Novel Finite-Difference Formulation for Differential Expressions involving both First and Derivatives'. Int. J. Num. Meth. Eng. 4, p551.

SPALDING D B (1976)

'Basic Equations of Fluid Mechanics and Heat and Mass Transfer and Procedures for Their Solution'. Report No. HTS/76/6 Imperial College, Mech. Eng. Dept.

STUBLEY G D, RAITHBY G D & STRONG A B (1980)

'Proposal for a New Discrete Method based on an Assessment of Discretisation Errors'. Num. Heat. Tran. 3, p411.

THOM A (1933)

'The Flow Past Circular Cylinders at Low Speeds'. Proc. Roy. Soc. London, A141, p651.

THOM A & APLET C J (1961)

'Fluid Computation in Engineering and Physics'. D van Nostrand Co. London.

TUANN S Y & OLSON M D (1978)

'Review of Computing Methods for Recirculating Flows'. J. Comp. Phys. 29, pp1.

WOLFSHTEIN M (1967)

'Convection Processes in Turbulent Impinging Jets'. Report SF/R/2, Imperial College, Mech. Eng. Dept. London.

WOLFSHTEIN M (1968)

'Numerical Smearing In One-Sided Difference Approximations to the Equations of Non-Viscous Flows'. Report EF/TN/A/3 Imperial College, Mech. Eng. Dept. London.

ZIENKIEWICZ O C (1977)

'The Finite-Element Method'. 3rd Ed. McGraw-Hill, London.

ZUBER I (1972)

'A Mathematical Model of the Combustion Chamber'. Bechovice Monographs and Memoranda No. 12.

Truncation error	IV $\phi P$	III $\phi P$	II $\phi P$	IV $\phi P$	IV $\phi P$	IV $\phi P$	IV $\phi P$
Principal part	$\Delta x^3$	$\Delta x^2$	$\Delta x$	$\Delta x^3$	$\Delta x^3$	$(4x-3)\Delta x^3$	$\Delta x^3$
Scheme	CDS	CDS	UDS	LDS	LUDS	LSUDS	LEDS QUDS

TABLE 6.14.1: TRUNCATION ERRORS FOR THE DIFFERENCING SCHEMES  
FOR  $S(x)=0$

Test case	Peclet number $P=\rho u/\Gamma$	Range of mesh Peclet number	Number of nodes	Source term $S(x)$
1	$1-10^5$	$0.2-10^3$	5-100	0
2	"	"	"	50
3	"	"	"	x
4	"	"	"	-x
5	"	"	"	$x^2-x-1$
6	"	"	"	$-x^2+x-1$
7	"	"	"	$-x^2-x+1$
8	"	"	"	$x^2+x+1$

TABLE 6.15.1: ONE-DIMENSIONAL TEST CASES CONSIDERED

Test case	Exact	CDS	UDS	LDS	LUDS	LSUDS	LEDS	QUDS
1	0.0183	-0.3279	0.1997	-0.0753	0.1263	0.0183	0.0183	-0.1154
	0.0183	0.0000	0.1111	0.0161	0.0583	0.0183	0.0183	0.0102
	0.0183	0.0123	0.0625	0.0201	0.0298	0.0183	0.0183	0.0181
2	1.9725	2.4918	1.7004	2.1130	1.8105	1.972	1.972	2.1713
	1.9725	2.0000	1.8334	1.9758	1.9126	1.972	1.972	1.9845
	1.9725	1.9815	1.9063	1.9698	1.9552	1.972	1.972	1.9729
3	0.0358	-0.3009	0.2153	-0.0553	0.1408	0.0358	0.0379	-0.0921
	0.0358	0.0180	0.1278	0.0337	0.0747	0.0358	0.0364	0.0283
	0.0358	0.0300	0.0797	0.0375	0.0470	0.0358	0.0360	0.0357
4	0.0008	-0.3459	0.1842	-0.0954	0.1118	0.0008	0.0013	-0.1387
	0.0008	-0.0180	0.0944	-0.0014	0.0419	0.0008	0.0002	-0.0079
	0.0008	0.0053	0.0453	0.0027	0.0127	0.0008	0.0007	0.0005
5	-0.0283	-0.3953	0.1637	-0.1275	0.0859	-0.028	-0.028	-0.1707
	-0.0283	-0.0478	0.0699	-0.0306	0.0140	-0.028	-0.028	-0.0372
	-0.0283	-0.0346	0.0185	-0.0264	-0.0161	-0.028	-0.028	-0.0286
6	-0.0132	-0.3732	0.1758	-0.1107	0.0994	-0.013	-0.013	-0.1516
	-0.0132	-0.0322	0.0834	-0.0155	0.0284	-0.013	-0.013	-0.0214
	-0.0132	-0.0194	0.0328	-0.0114	-0.0012	-0.013	-0.013	-0.0134
7	0.0299	-0.3144	0.2048	-0.0633	0.1377	0.030	0.026	-0.1067
	0.0299	0.0118	0.1190	0.0278	0.0698	0.030	0.029	0.0213
	0.0299	0.0240	0.0721	0.0317	0.0414	0.030	0.030	0.0296
8	0.0849	-0.2285	0.2547	0.0001	0.1823	0.0848	0.0889	-0.0326
	0.0849	0.0682	0.1721	0.0829	0.1209	0.0849	0.0860	0.0781
	0.0849	0.0794	0.1266	0.0865	0.0953	0.0849	0.0852	0.0848

TABLE 6.16.1: TEST CASE RESULTS FOR  $P=20$ ,  $\chi=0.8$  AND  $N=5, 10, 20$

Scheme	Reynolds Number	N	I	N/Nu	T/Tu	T/N
ODS	50	166	1640	1.506	1.803	9.880
	100	194	1932	1.863	2.247	9.960
	150	194	1966	1.974	2.427	10.113
	200	206	2265	2.016	2.691	11.003
UDS	50	110	900	1.000	1.000	8.273
	100	104	860	1.000	1.000	8.259
	150	98	810	1.000	1.000	8.263
	200	102	842	1.000	1.000	8.255
HDS	50	106	866	0.964	0.952	8.170
	100	102	820	0.981	0.953	8.170
	150	98	980	1.000	0.963	7.959
	200	100	818	0.980	0.253	8.120
LEDS	50	108	924	0.982	1.015	8.336
	100	104	872	1.000	1.013	8.385
	150	100	818	1.020	1.010	8.180
	200	100	830	0.980	1.009	8.300
PDS	50	112	888	1.018	0.976	7.929
	100	108	844	1.038	0.981	7.813
	150	104	786	1.061	0.970	7.358
	200	106	820	1.039	0.974	7.736
QUDS	50	98	1180	0.891	1.296	12.041
	100	96	1110	0.923	1.290	11.563
	150	96	1044	0.980	1.280	10.873
	200	94	1056	0.922	1.239	11.353
QUDSE	50	94	1214	0.933	1.334	12.913
	100	92	1102	0.885	1.291	11.978
	150	92	1016	0.939	1.281	11.043
	200	92	1082	0.902	1.283	11.761
QUDSER	50	134	1958	1.400	2.141	12.649
	100	138	1886	1.519	2.183	11.937
	150	160	1784	1.633	2.202	11.130
	200	138	1832	1.549	2.200	11.722

TABLE 6.25.1.1: COMPUTATIONAL DETAILS TO OBTAIN A GIVEN ACCURACY  
USING VARIOUS SCHEMES

Scheme	Reynolds Number	$l_r/h$	$l_r/D$	$l_r/hRe$
CDS	50	3.95	1.97	0.079
	100	8.10	4.05	0.081
	150	12.51	6.25	0.083
	200	16.66	8.33	0.083
UDS	50	4.38	2.19	0.083
	100	8.59	4.29	0.086
	150	12.84	6.42	0.086
	200	17.29	8.63	0.086
HDS	50	4.52	2.26	0.090
	100	8.91	4.45	0.089
	150	13.33	6.67	0.089
	200	17.68	8.84	0.088
LEDS	50	4.52	2.26	0.090
	100	8.91	4.45	0.089
	150	13.32	6.66	0.089
	200	17.68	8.84	0.088
PDS	50	4.52	2.26	0.090
	100	8.90	4.45	0.089
	150	13.32	6.66	0.089
	200	17.67	8.84	0.0088
QUDS	50	4.46	2.23	0.089
	100	8.88	4.44	0.089
	150	13.26	6.63	0.088
	200	17.64	8.82	0.088
QUDSE	50	4.46	2.23	0.089
	100	8.86	4.43	0.089
	150	13.30	6.63	0.089
	200	17.64	8.82	0.088
QUDSER	50	4.46	2.22	0.089
	100	8.86	4.43	0.089
	150	13.30	6.65	0.089
	200	17.64	8.82	0.088

TABLE 6.25.1.2: COMPARISON OF RE-ATTACHMENT LENGTHS USING VARIOUS SCHEMES

Reynolds Number	$l_r/h$	$l_r/D$	$l_r/hRe$
50	4.41	2.2	0.0882
100	8.81	4.3	0.0881
150	13.22	6.5	0.0881
200	17.62	8.8	0.0881

TABLE 6.25.1.3: REFERENCE RE-ATTACHMENT LENGTHS USED FOR  
COMPARISON [POLLARD (1980b); MACAGNO (1963)]

Scheme	Re No.	N	T	N/Nu	T/Tu	T/N
CDS	100	126	24	1.518	2.000	0.191
	400	191	56	2.274	4.308	0.293
UDS	100	83	12	1	1	0.143
	400	84	13	1	1	0.155
HDS	100	79	11	0.952	0.917	0.139
	400	87	12	1.036	0.923	0.138
LEDS	100	90	15	1.084	1.250	0.167
	400	89	15	1.060	1.154	0.169
PDS	100	87	13	1.048	1.048	0.149
	400	88	14	1.048	1.077	0.159
QUDS	100	91	18	1.096	1.500	0.198
	400	101	19	1.202	1.462	0.188
QUDSE	100	295	96	3.554	8.000	0.325
	400	277	84	3.298	6.462	0.303
QUDSER	100	185	48	2.229	4.003	0.259
	400	200	43	2.381	3.308	0.215

TABLE 6.25.2.1: COMPUTATIONAL DETAILS TO OBTAIN ACCURACY USING  
VARIOUS SCHEMES FOR RE=100 AND 400

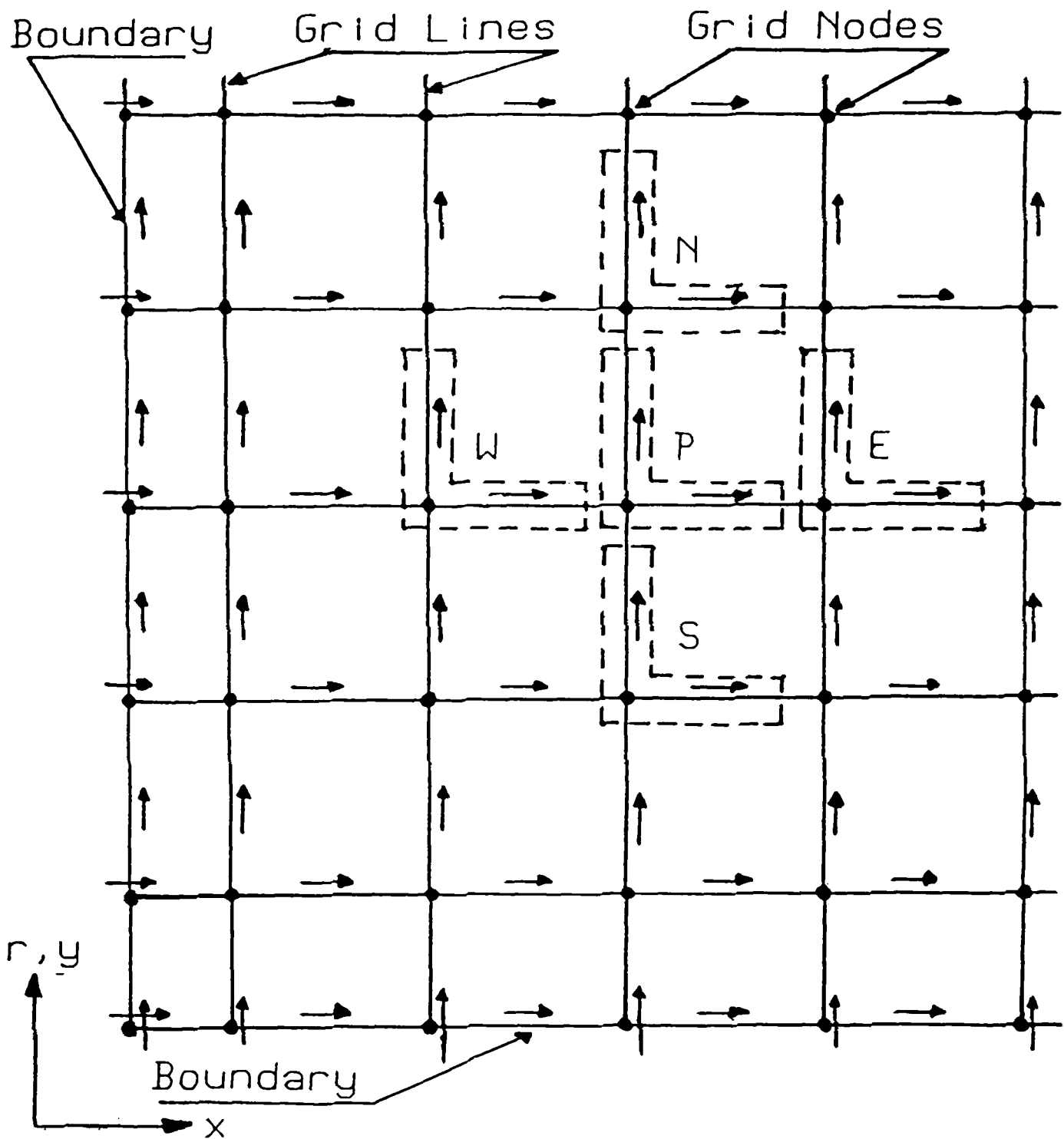
SOLUTIONS

GRID NODE	Y DIST	UDS	HDS	LEDS	PDS	QUDS	QUDSER	RDS	SKEW	EXACT
1	5.56E-2	17.8	17.8	17.8	17.8	7.17	7.69	19.4	10	10
2	1.67E-1	37.3	37.3	37.3	37.3	4.11	2.52	41.9	10	10
3	2.78E-1	66.6	66.3	66.6	66.6	20	2.56	74.3	10	10
4	3.89E-1	101	101	101	101	67	50.3	111	10	10
5	5.00E-1	135	135	135	135	135	135	146	260	260
6	6.11E-1	166	166	166	166	201	220	176	260	260
7	7.22E-1	191	191	191	191	245	271	201	260	260
8	8.33E-1	212	212	212	212	266	283	219	260	260
9	9.44E-1	227	227	227	227	266	269	233	260	260
10	1.00E-0	227	227	227	227	266	269	233	260	260

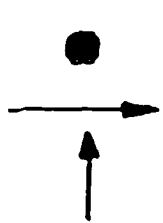
ERRORS

GRID NODE	Y DIST	UDS	HDS	LEDS	PDS	QUDS	QUDSER	RDS	SKEW	EXACT
1	5.56E-2	78	78	78	78	-28	-23	94	0	0
2	1.67E-1	273	273	273	273	-59	125	319	0	0
3	2.78E-1	566	566	566	566	100	74	643	0	0
4	3.89E-1	910	910	910	910	570	403	1010	0	0
5	5.00E-1	-48	-48	-48	-48	-48	-48	-44	0	0
6	6.11E-1	-36	-36	-36	-36	-22	-15	-32	0	0
7	7.22E-1	-26	-26	-26	-26	-6	4	-22	0	0
8	8.33E-1	-18	-18	-18	-18	2	9	-16	0	0
9	9.44E-1	-12	-12	-12	-12	2	3	-10	0	0
10	1.00E-0	-12	-12	-12	-12	2	3	-10	0	0
<u>%RMS</u>		351	351	351	351	185	136	393	0	0

TABLE 6.45.1: COMPARISON BETWEEN VARIOUS SCHEMES FOR FLOW AT 45°  
TO THE  $\Gamma=10^{-10}$ , X-STATION=0.5



SYMBOL

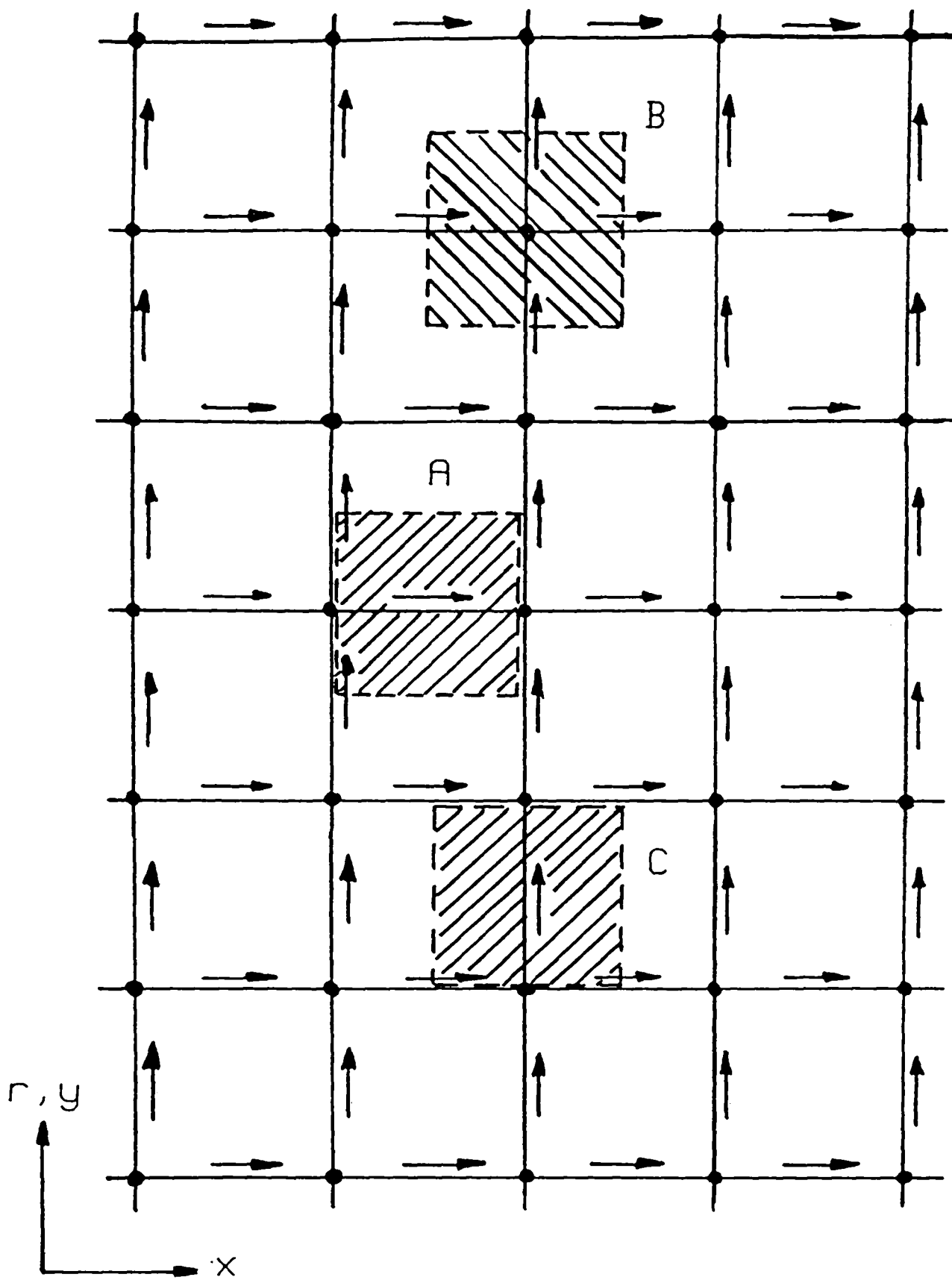


VARIABLE

$\phi, P$   
 $u$ -velocity  
 $v$ -velocity

FIGURE  
2.32-1

FINITE-DIFFERENCE GRID AND  
VARIABLE LOCATIONS



SYMBOL

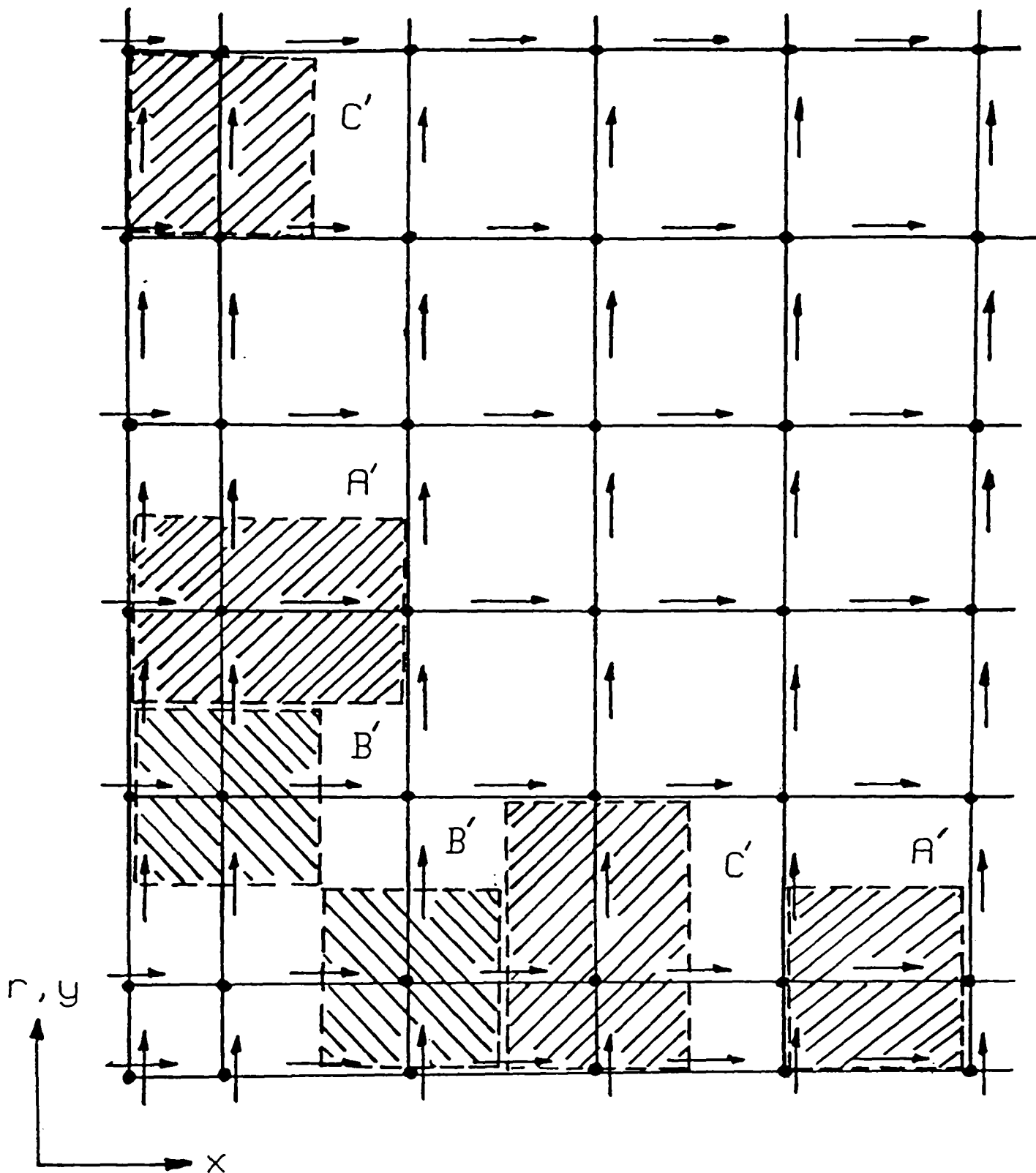
CONTROL-VOLUME

A  
B  
C

u-velocity  
 $\phi$ -general variable  
 v-velocity

FIGURE  
2.33-1

GENERAL CONTROL VOLUMES



SYMBOL

CONTROL-VOLUME

A'  
B'  
C'

u-velocity  
 $\phi$ -general variable  
 v-velocity

FIGURE  
2.33-2

WALL CONTROL VOLUMES

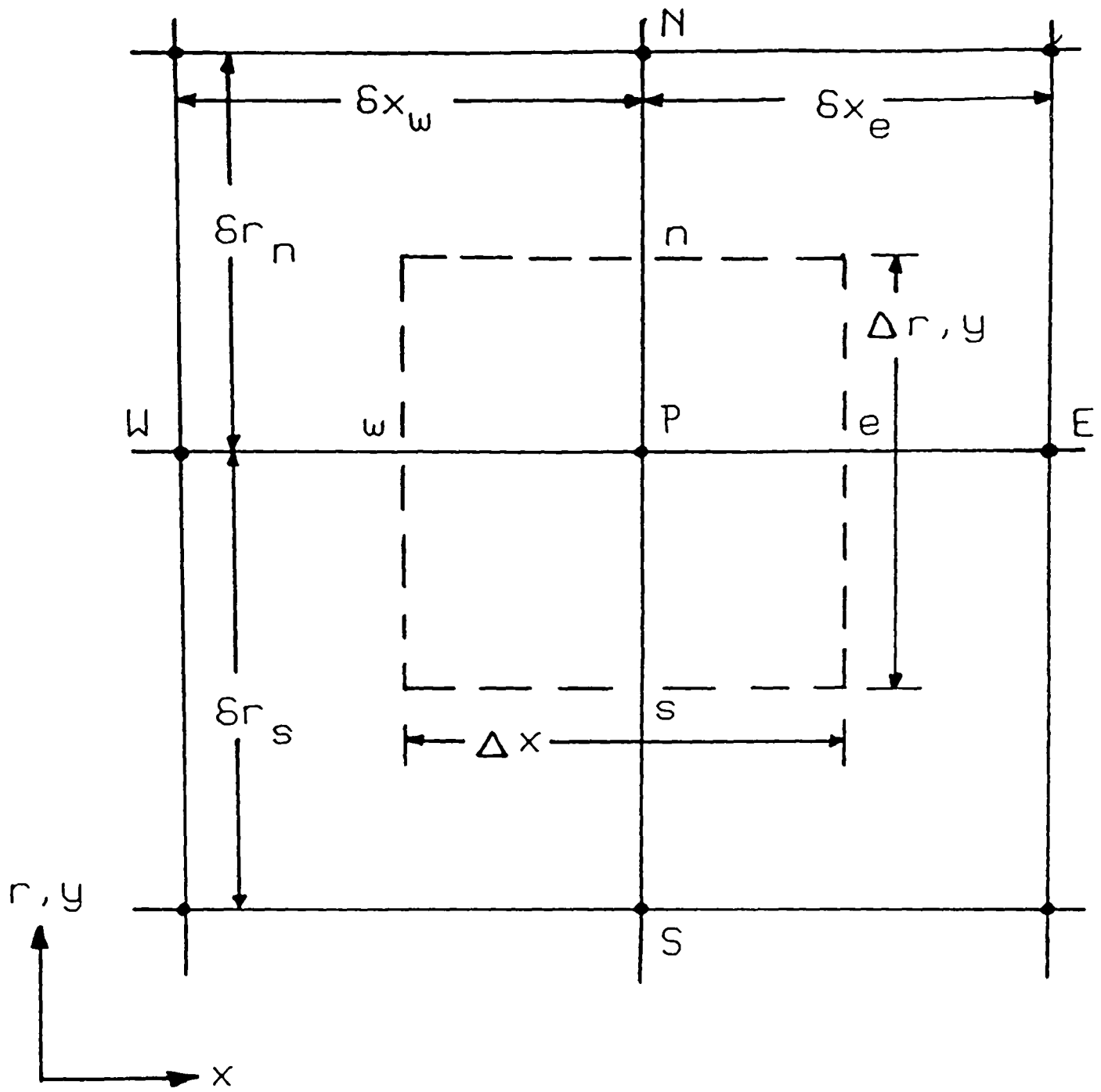


FIGURE  
2.4-1

CONTROL-VOLUMES AND NOTATION FOR  
FINITE-DIFFERENCE EQUATION

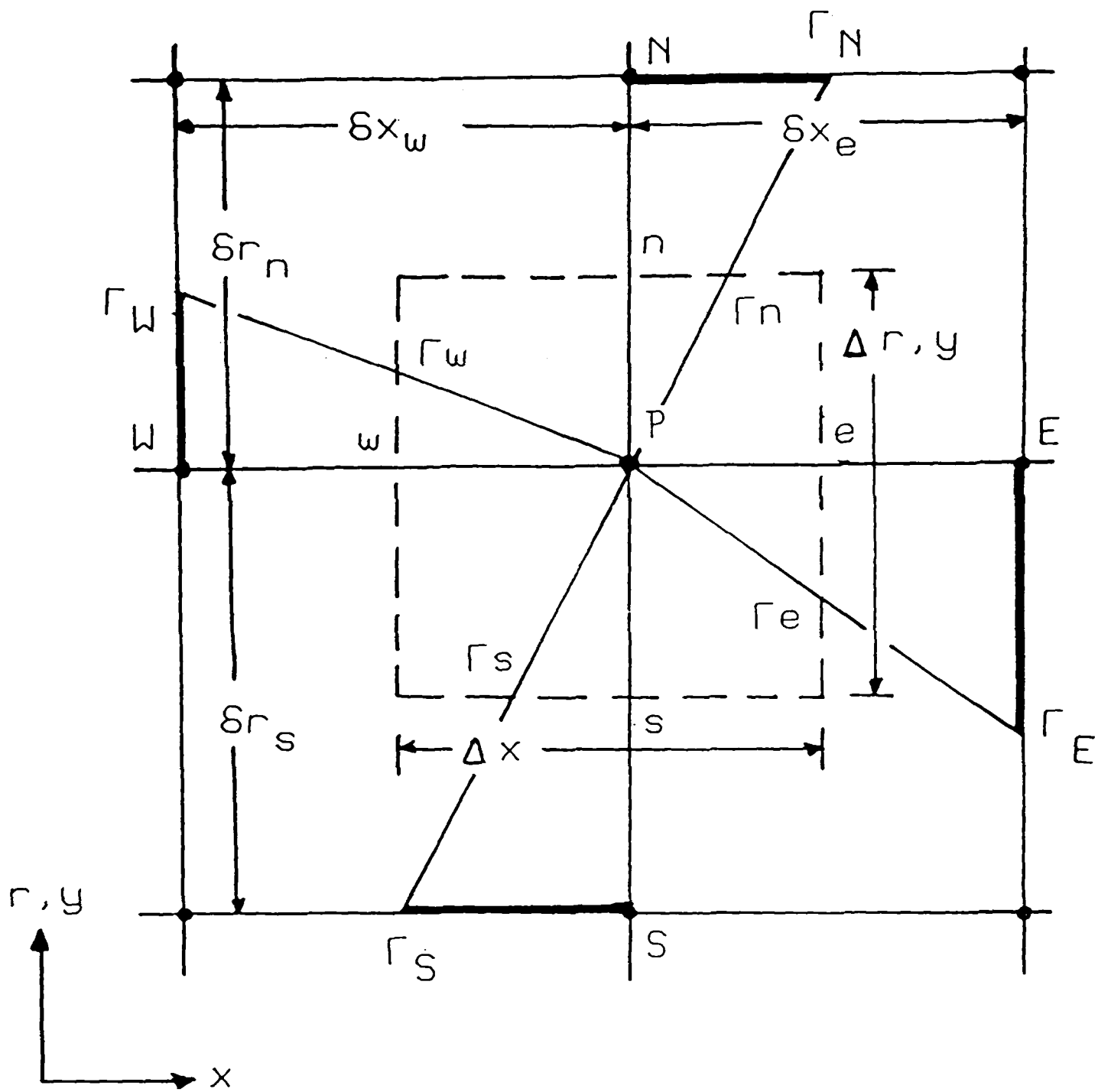


FIGURE  
4.11-1

CONTROL-VOLUME FOR DIFFUSION TERM  
APPROXIMATION (5-STAR CLUSTER)

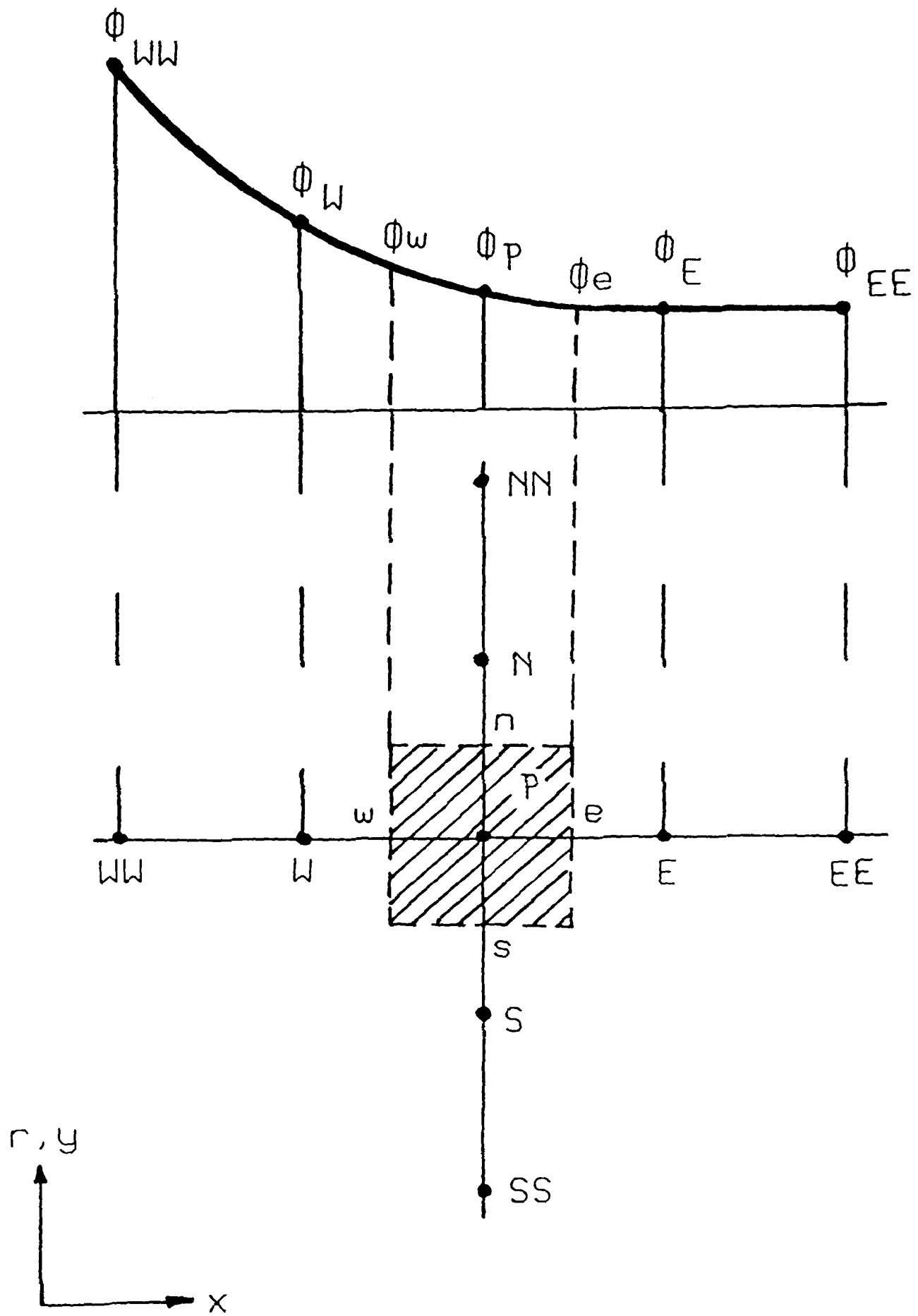


FIGURE  
4.12.9-1

QUADRATIC UPSTREAM-DIFFERENCE SCHEME  
INTERFACIAL VALUES AND NINE-POINT STARS

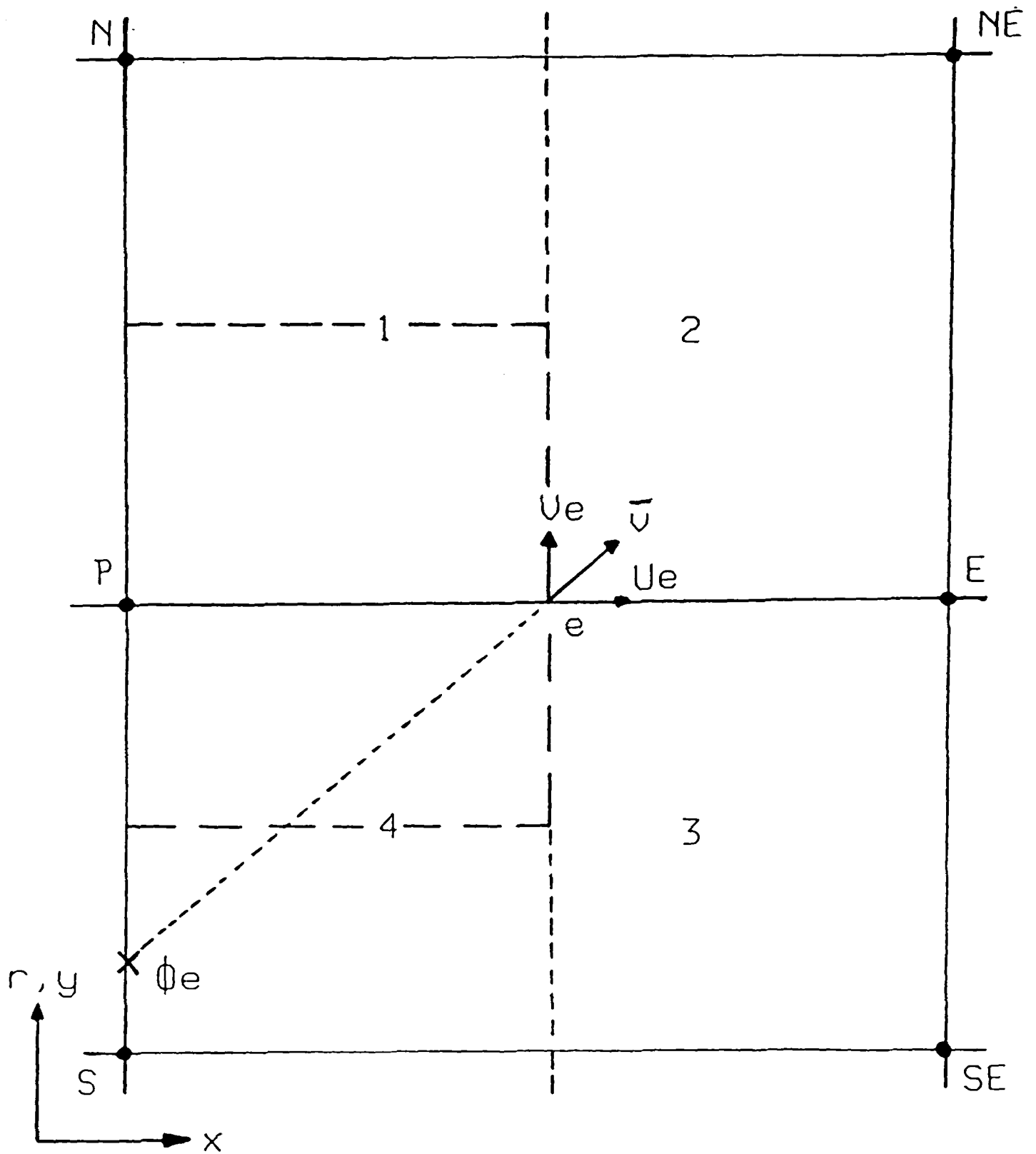


FIGURE  
4. 12. 13-1

INTERPOLATION REGION FOR THE SKEW-  
DIFFERENCE SCHEME

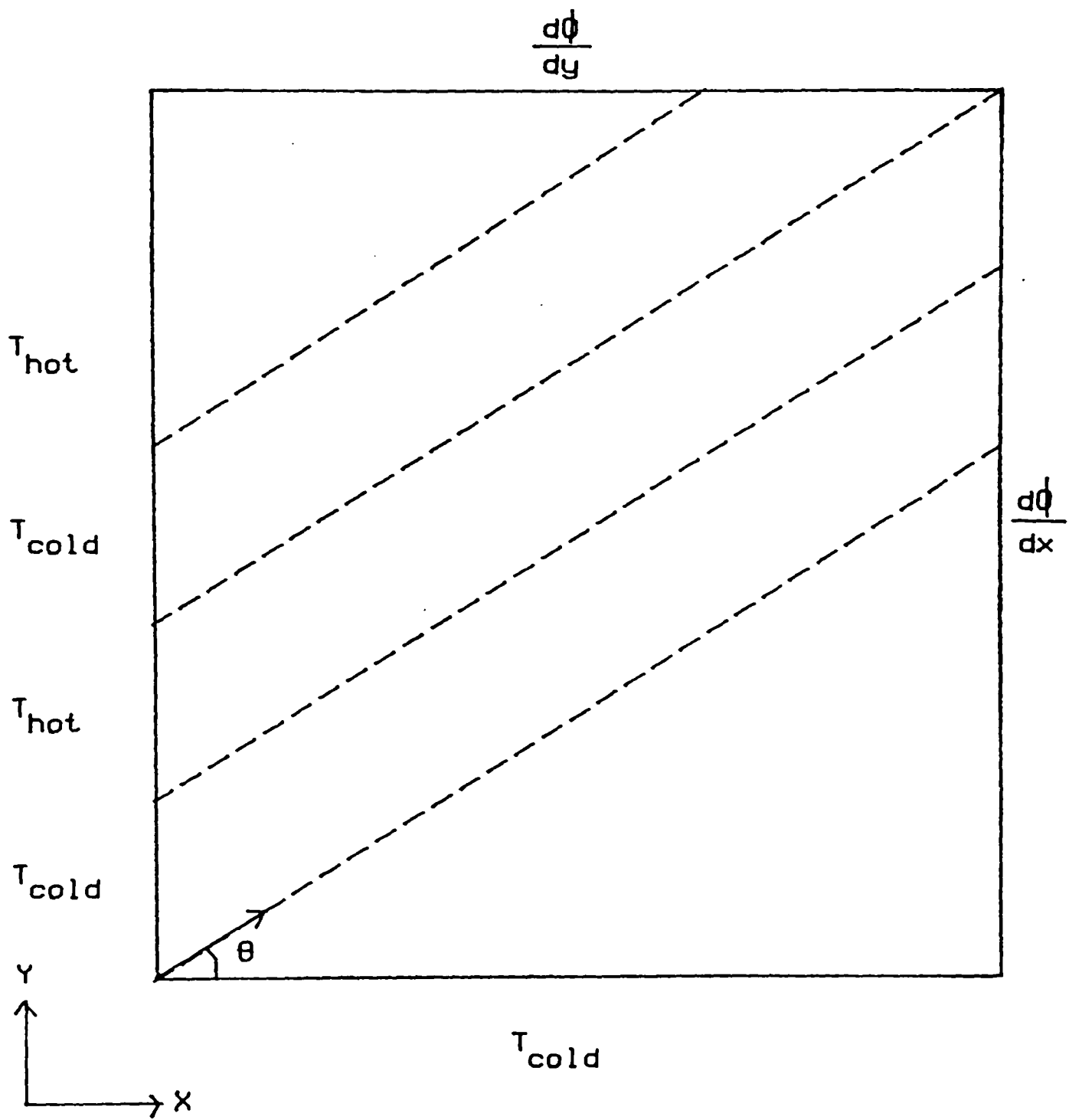


FIGURE  
5.3-1

SITUATION WITH FLOW AT  $\theta$ -DEGREES  
TO THE GRID-LINES

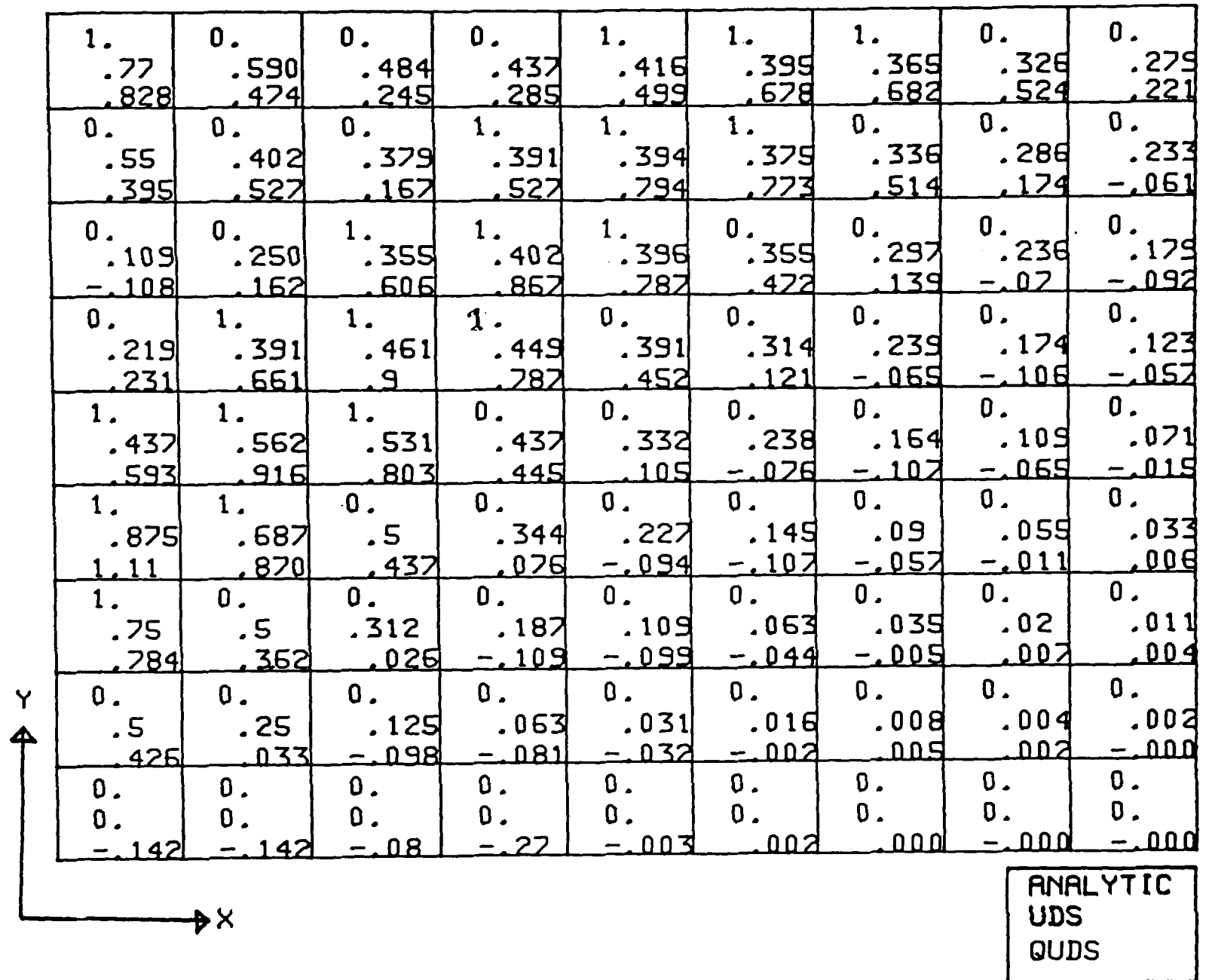


FIGURE  
5.3-2

SITUATION WITH FLOW AT 45 DEGREES TO THE GRID-  
LINES WITH ANALYTIC, UDS AND QUDS RESULTS

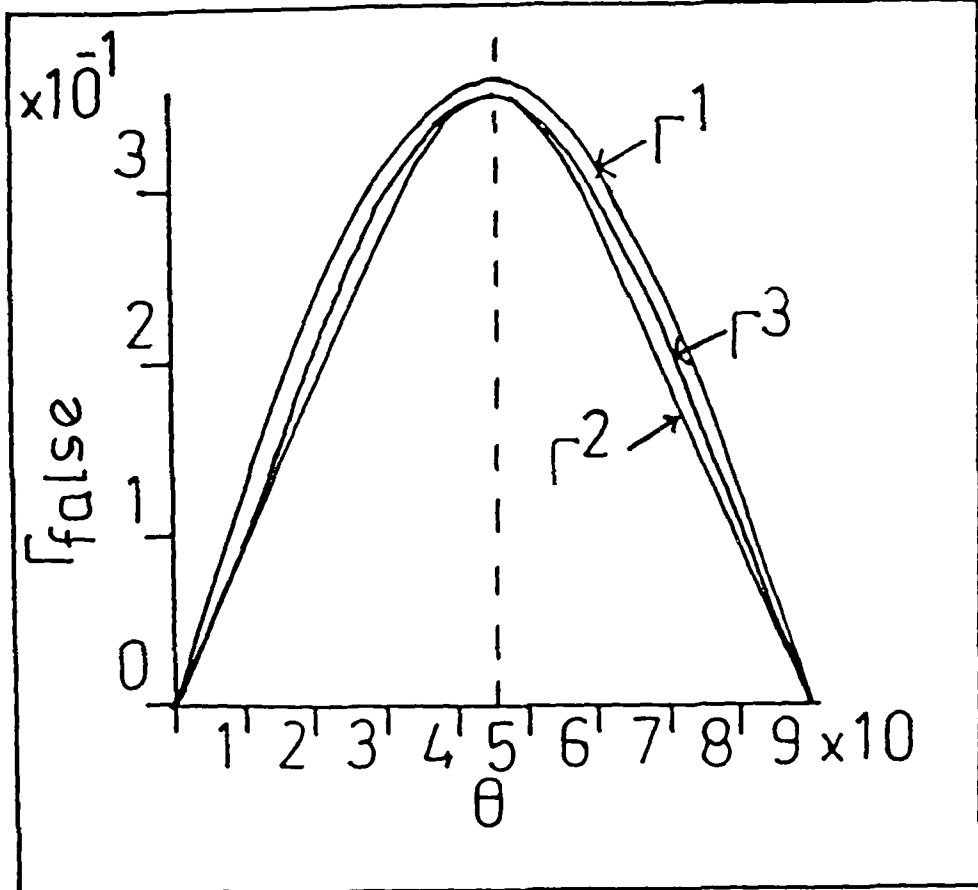


FIGURE  
5.3-3

FALSE-DIFFUSION COEFFICIENTS PREDICTED BY  
EXPRESSIONS 5.3-1a, 1b AND 1c

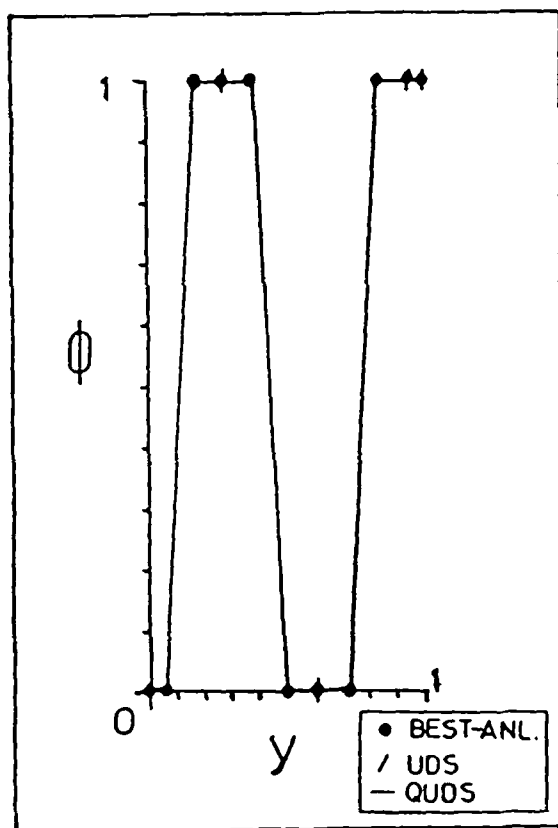


FIGURE  
5.3-4

PREDICTED AND BEST ANALYTIC SOLUTION  
FOR  $\theta=45$  DEGREES AT  $IX=1$

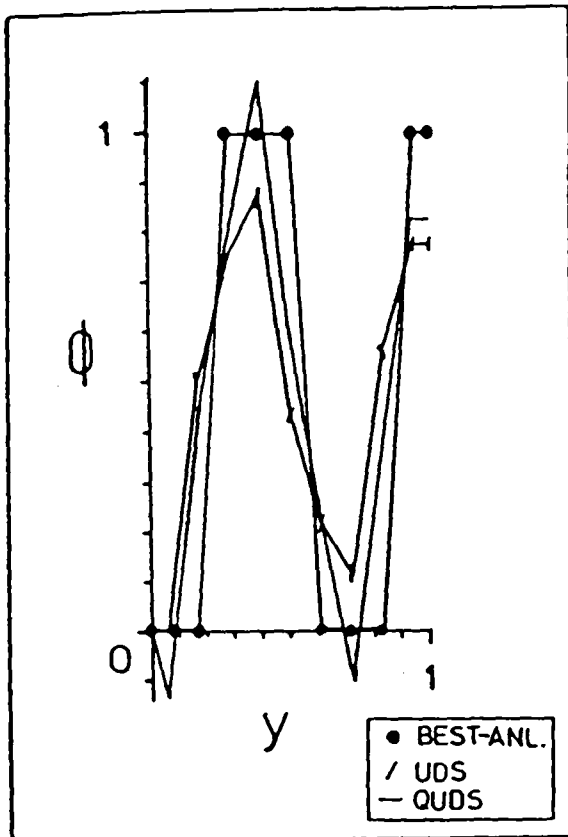


FIGURE  
5.3-5

PREDICTED AND BEST ANALYTIC SOLUTION  
FOR  $\theta=45$  DEGREES AT IX=2

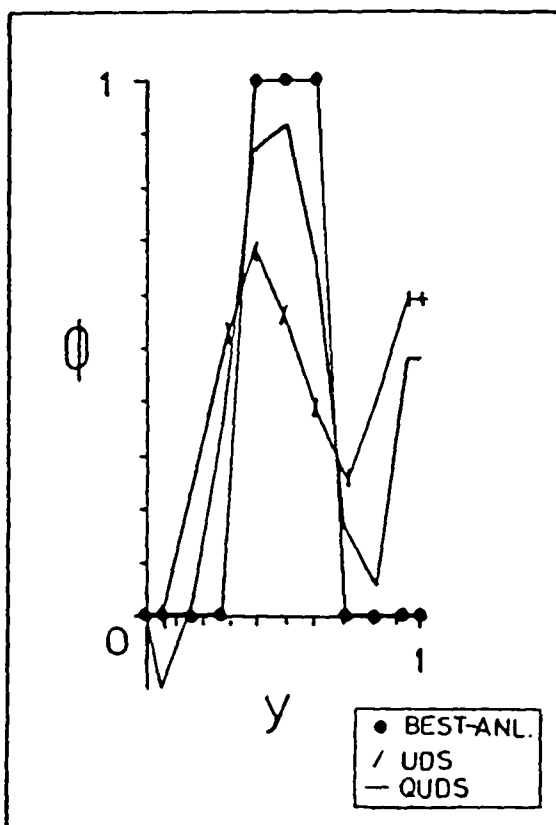


FIGURE  
5.3-6

PREDICTED AND BEST ANALYTIC SOLUTION  
FOR  $\theta=45$  DEGREES AT IX=3

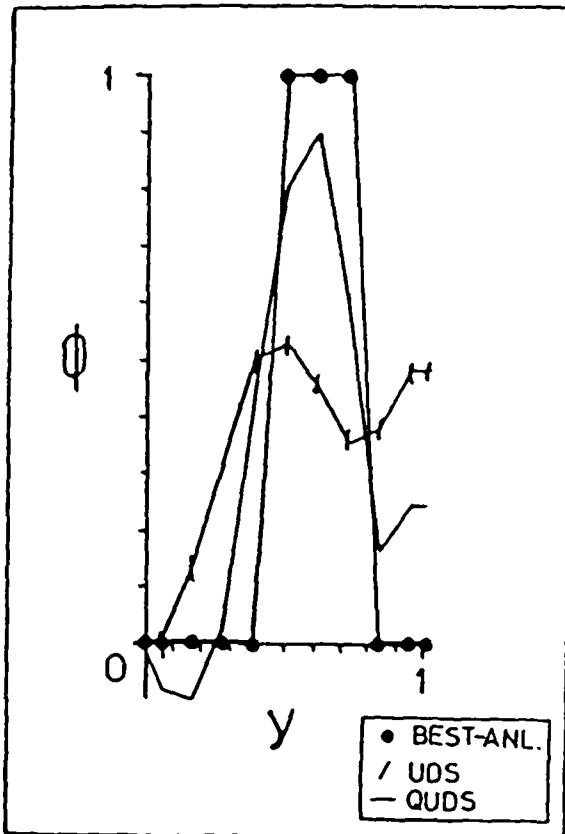


FIGURE  
5.3-7

PREDICTED AND BEST ANALYTIC SOLUTION  
FOR  $\theta=45$  DEGREES AT IX=4

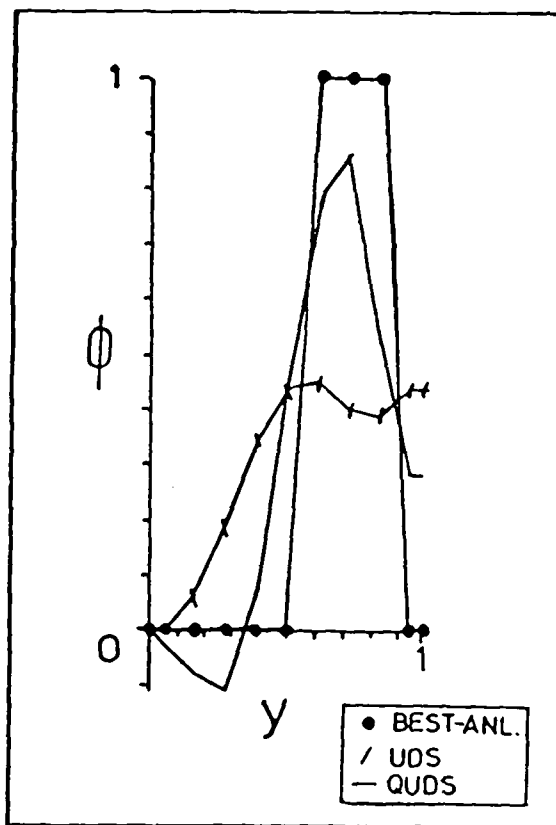


FIGURE  
5.3-8

PREDICTED AND BEST ANALYTIC SOLUTION  
FOR  $\theta=45$  DEGREES AT IX=5

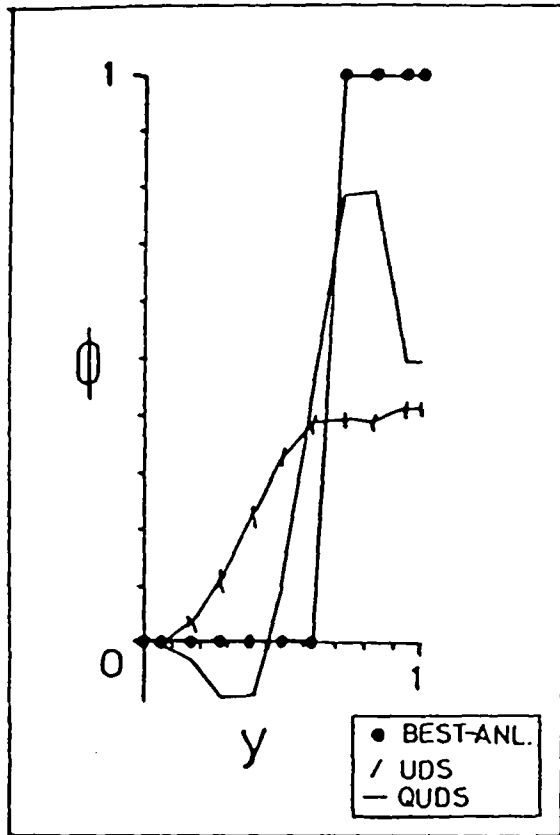


FIGURE  
5.3-9

PREDICTED AND BEST ANALYTIC SOLUTION  
FOR  $\theta=45$  DEGREES AT IX=6

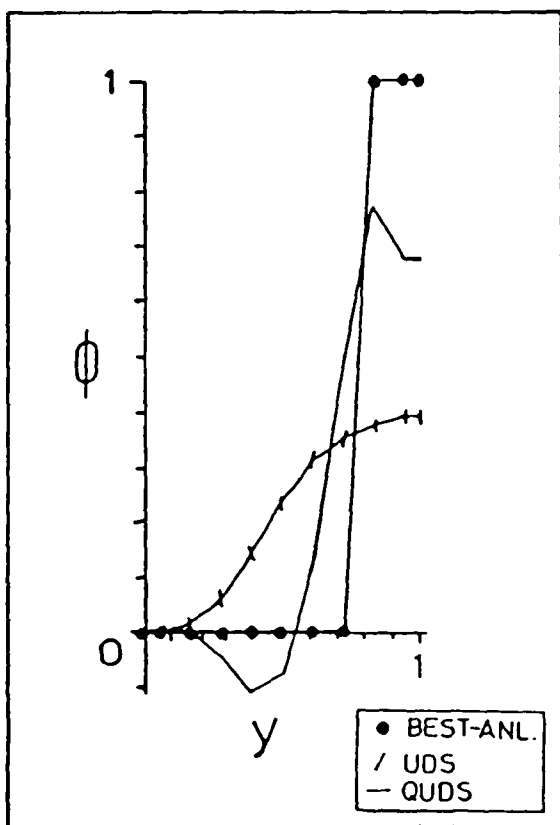


FIGURE  
5.3-10

PREDICTED AND BEST ANALYTIC SOLUTION  
FOR  $\theta=45$  DEGREES AT IX=7

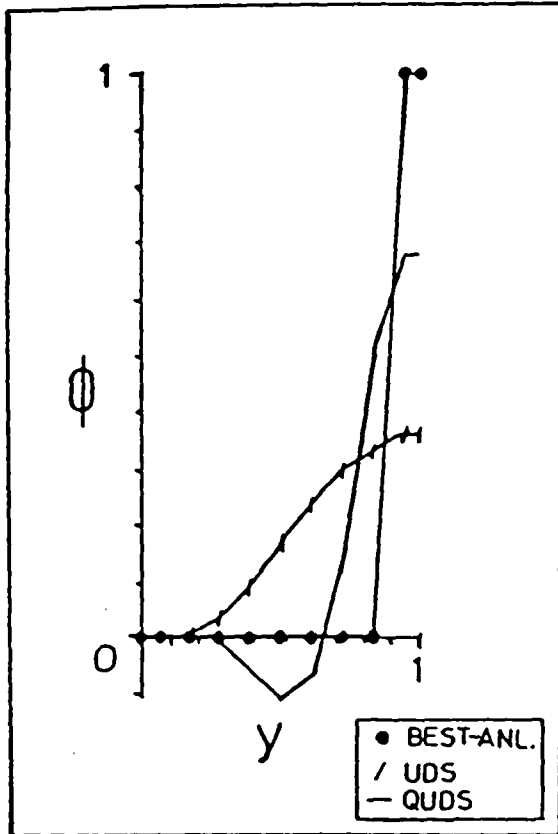


FIGURE  
5.3-11

PREDICTED AND BEST ANALYTIC SOLUTION  
FOR  $\theta=45$  DEGREES AT  $IX=8$

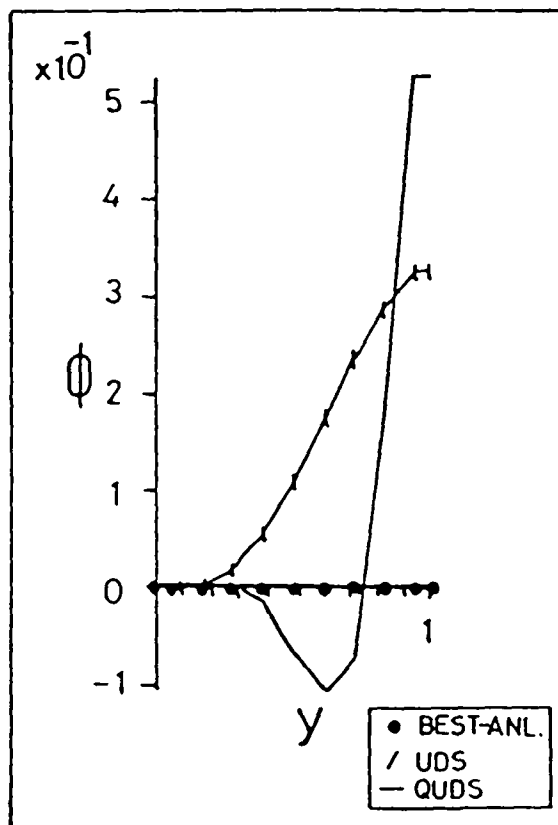


FIGURE  
5.3-12

PREDICTED AND BEST ANALYTIC SOLUTION  
FOR  $\theta=45$  DEGREES AT  $IX=9$

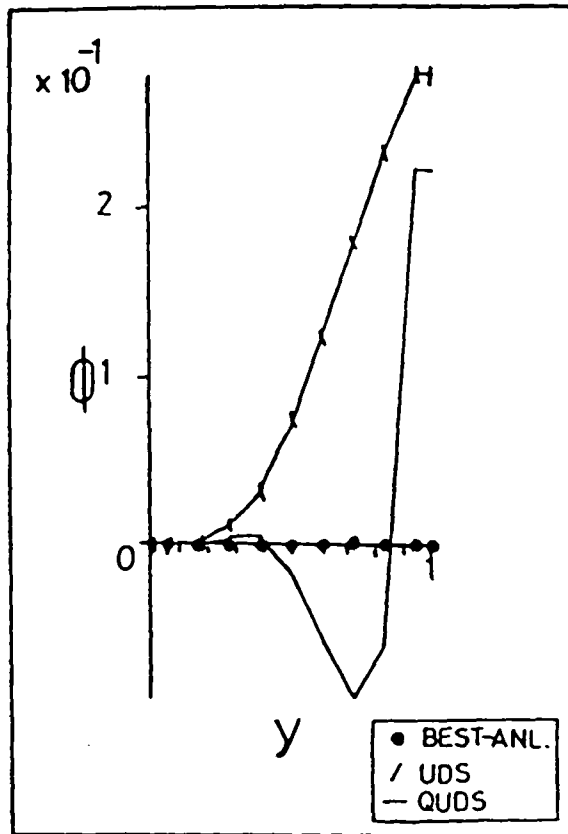


FIGURE  
5.3-13

PREDICTED AND BEST ANALYTIC SOLUTION  
FOR  $\theta=45$  DEGREES AT  $IX=10$

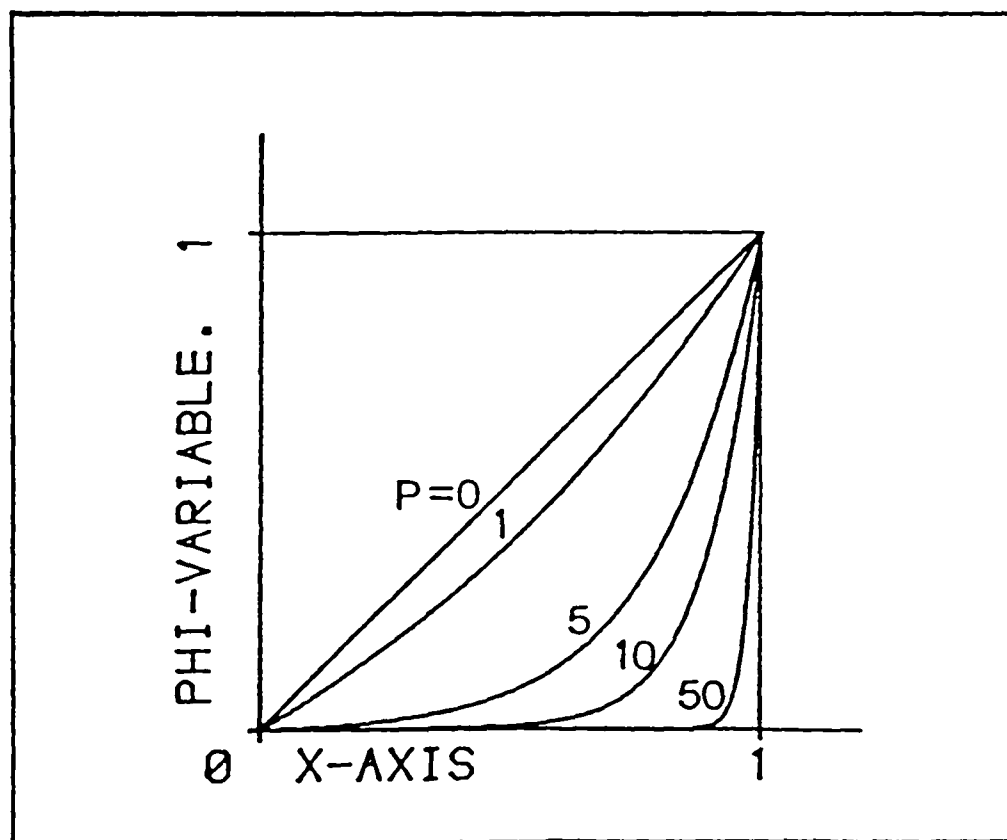


FIGURE  
6.16-1

ANALYTIC SOLUTION OF THE ONE-DIMENSIONAL,  
ZERO SOURCE PROBLEM FOR  $P=0, 1, 5, 10$  AND  $50$

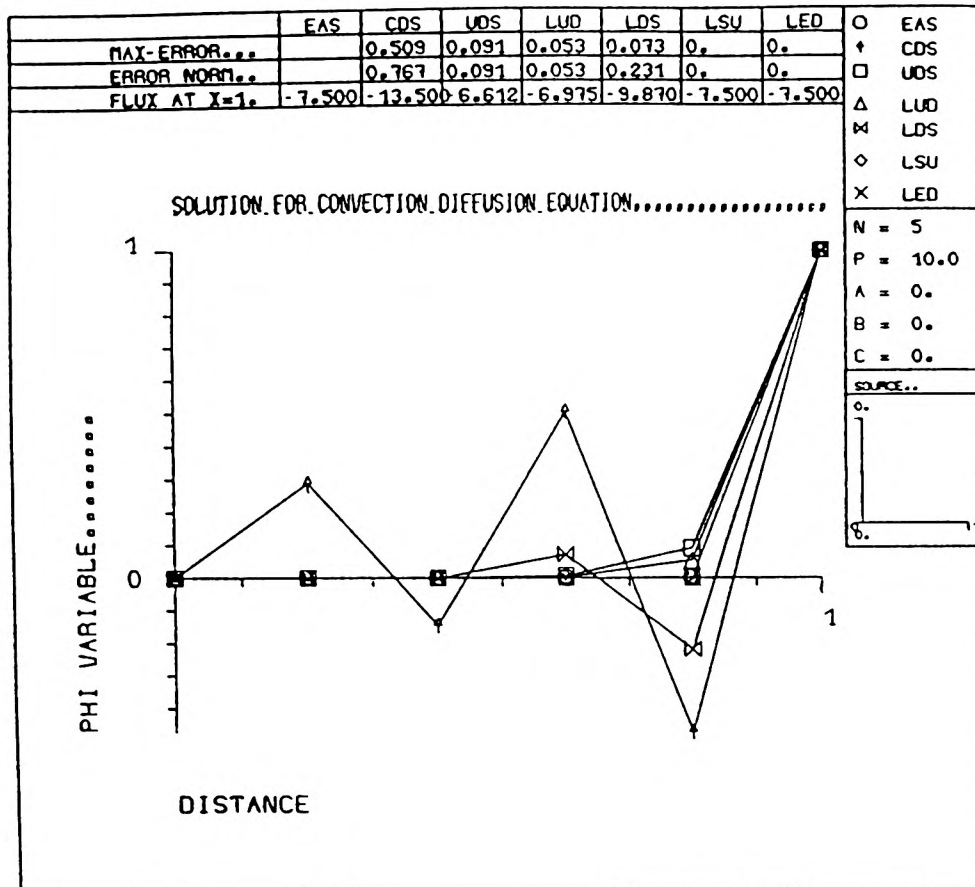


FIGURE  
6.16-2

NUMERICAL SOLUTION FOR ZERO SOURCE

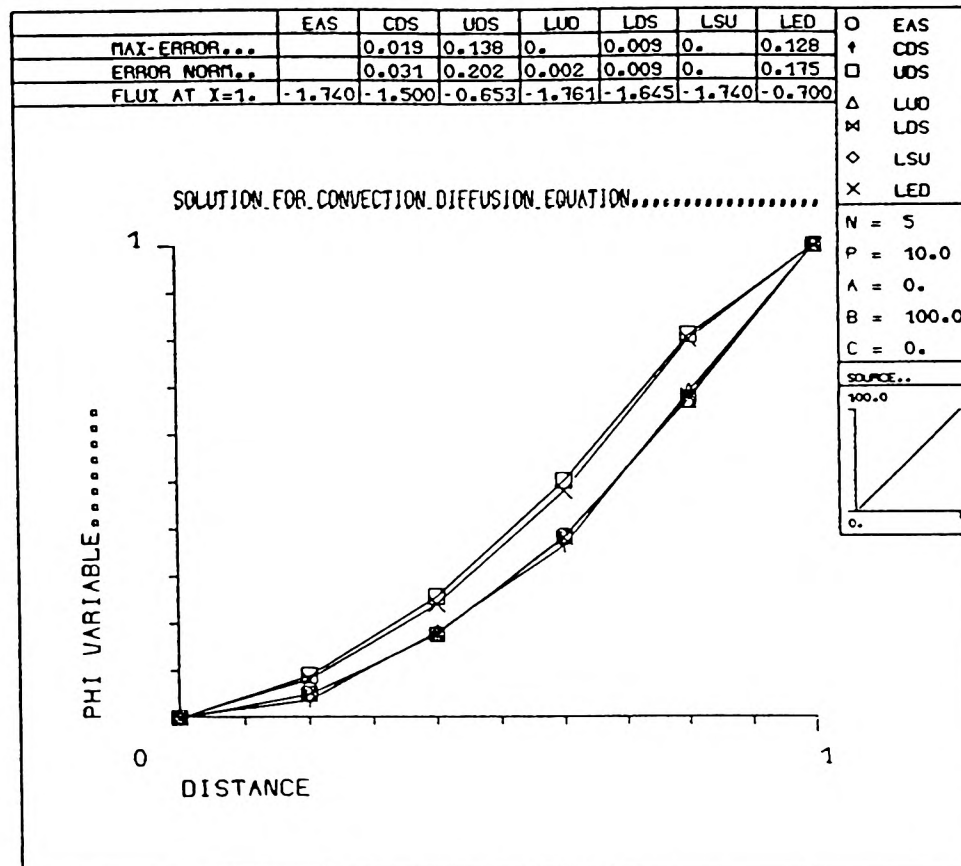


FIGURE  
6.16-3

NUMERICAL SOLUTION FOR LINEAR, POSITIVE  
GRADIENT, SOURCE

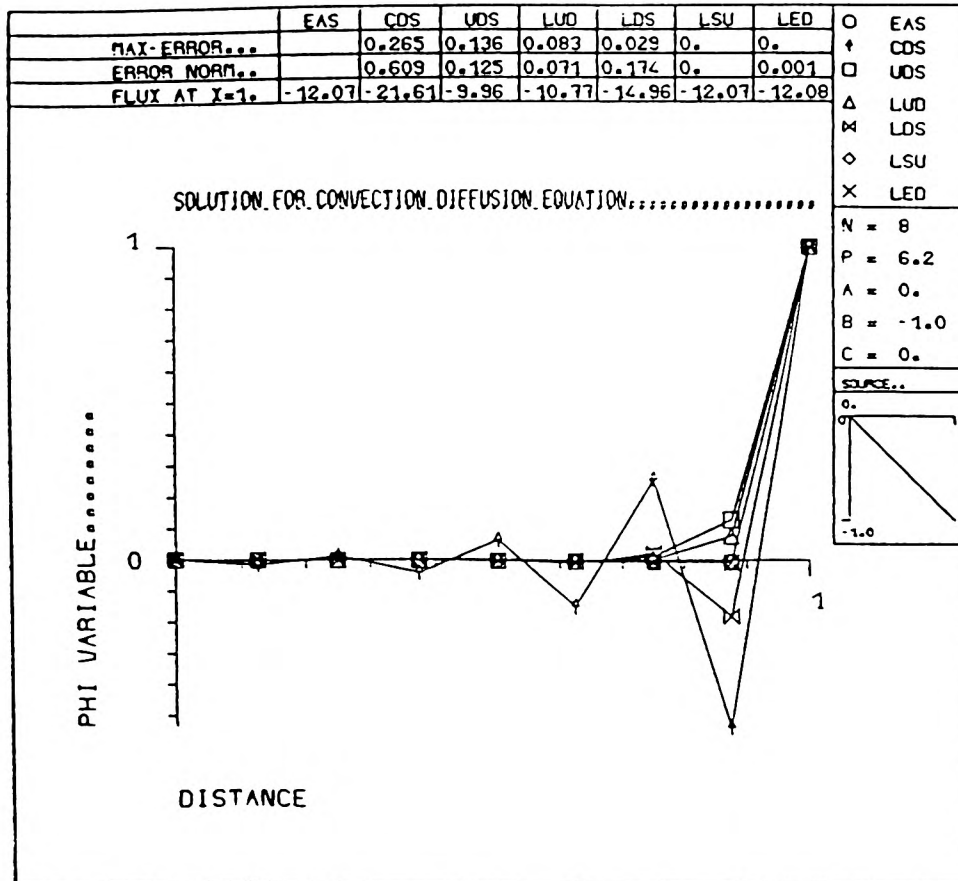


FIGURE  
6. 16-4

NUMERICAL SOLUTION FOR LINEAR, NEGATIVE  
GRADIENT, SOURCE

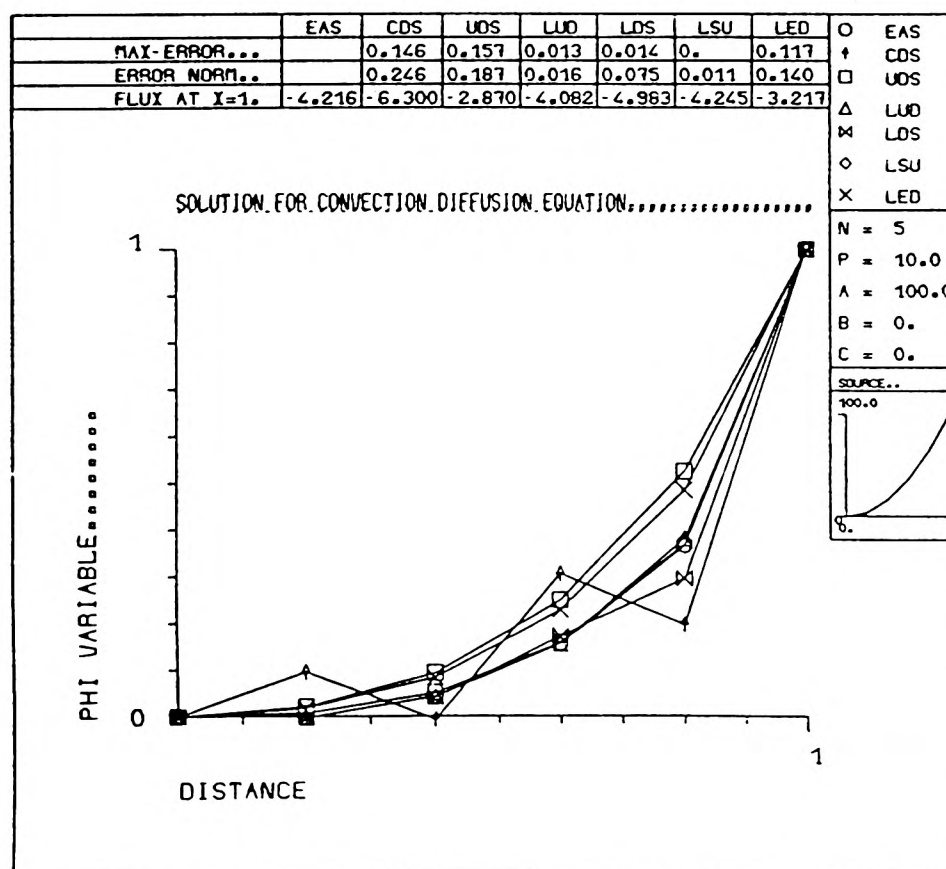


FIGURE  
6. 16-5

NUMERICAL SOLUTION FOR QUADRATIC,  
POSITIVE GRADIENT, SOURCE

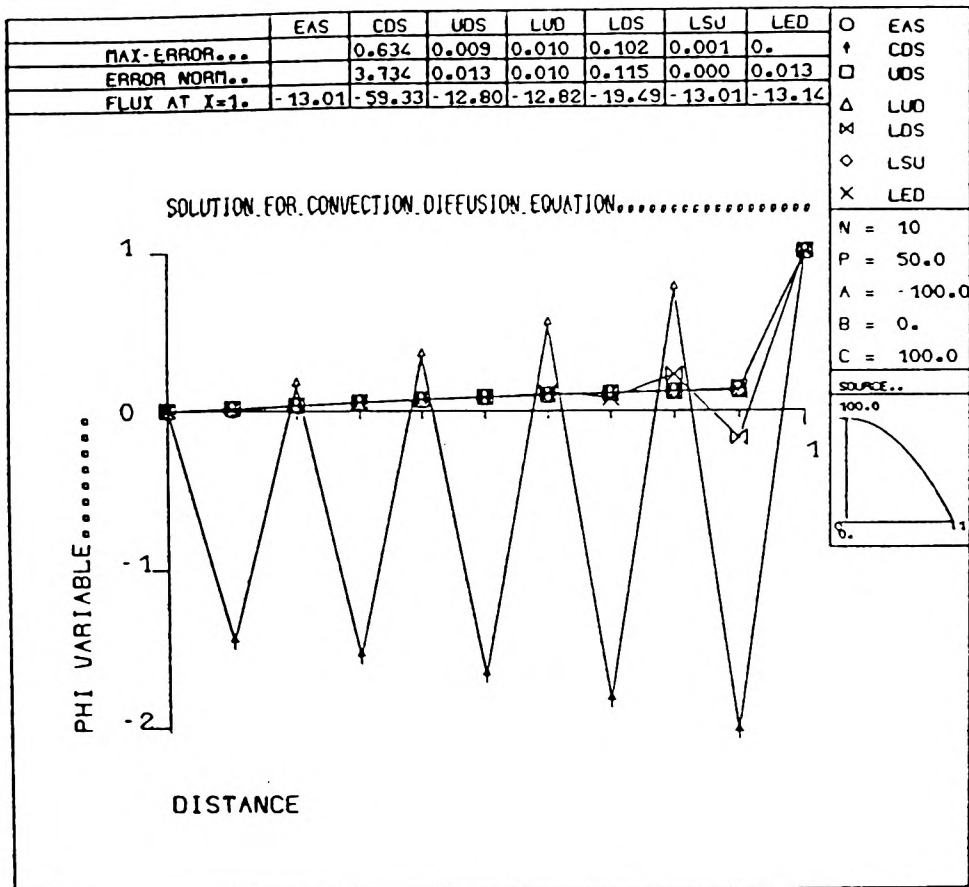


FIGURE  
6.16-6

NUMERICAL SOLUTION FOR QUADRATIC,  
NEGATIVE GRADIENT, SOURCE

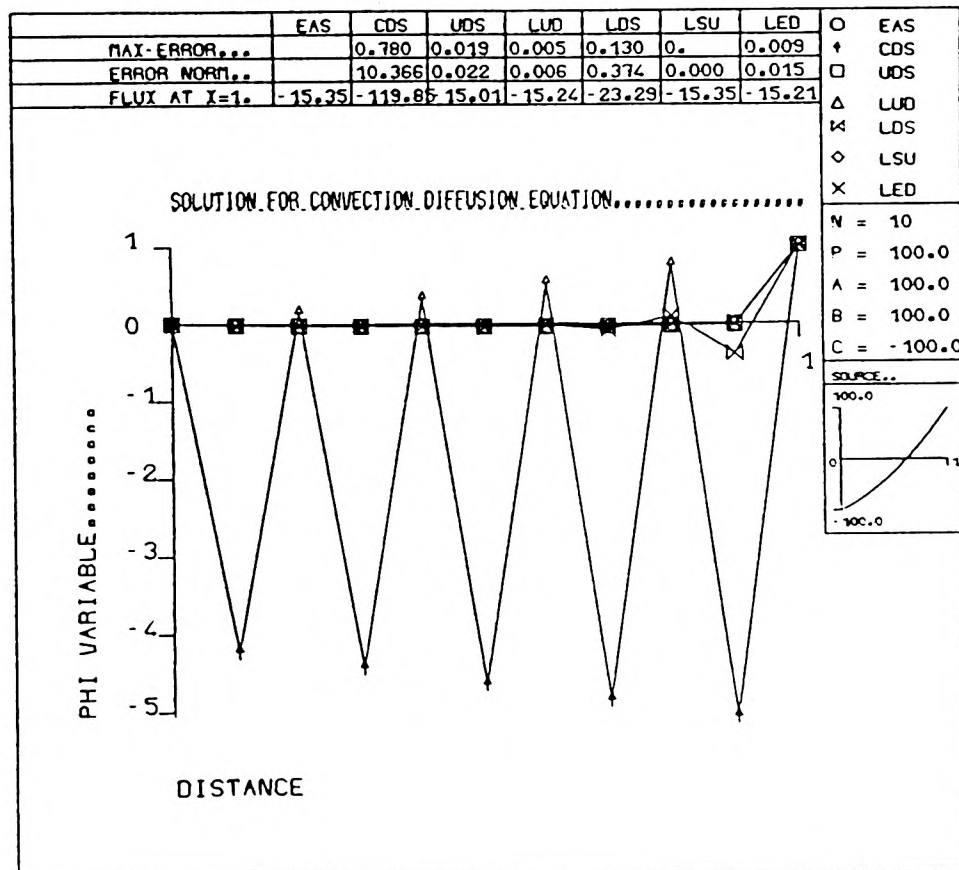


FIGURE  
6.16-7

NUMERICAL SOLUTION FOR LARGE SOURCES,  
DETAILS ON GRAPH

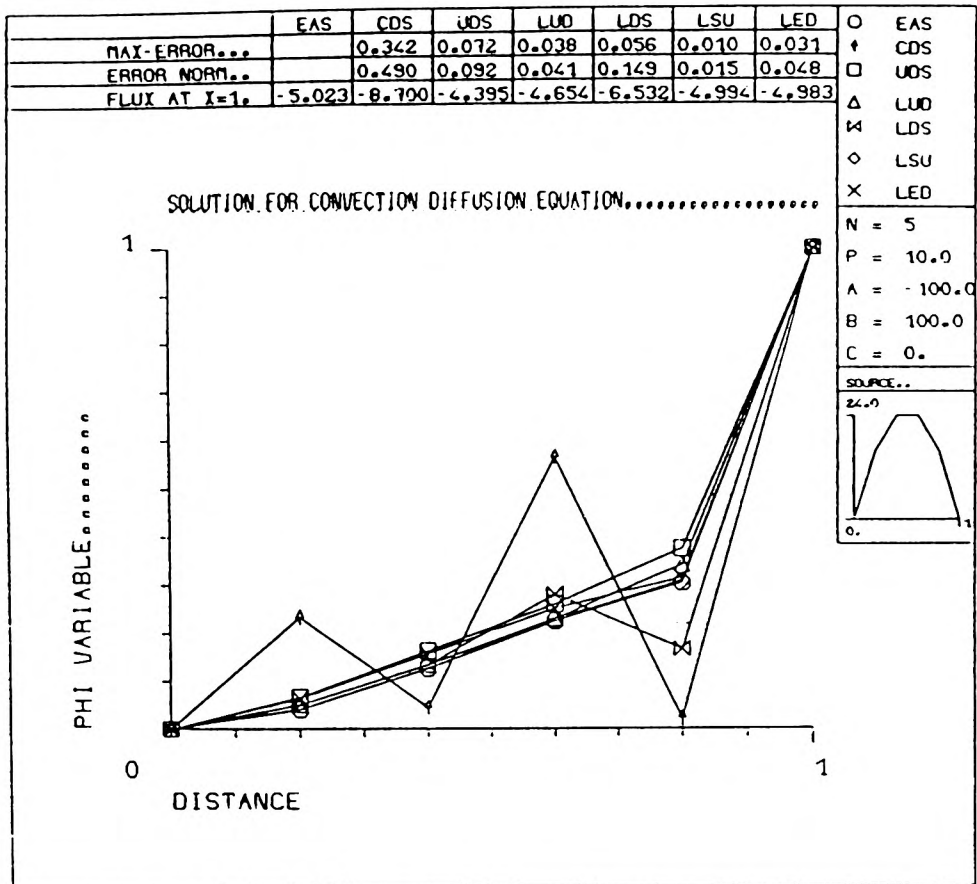


FIGURE  
6.16-8

NUMERICAL SOLUTION FOR LARGE SOURCES.  
DETAILS ON GRAPH

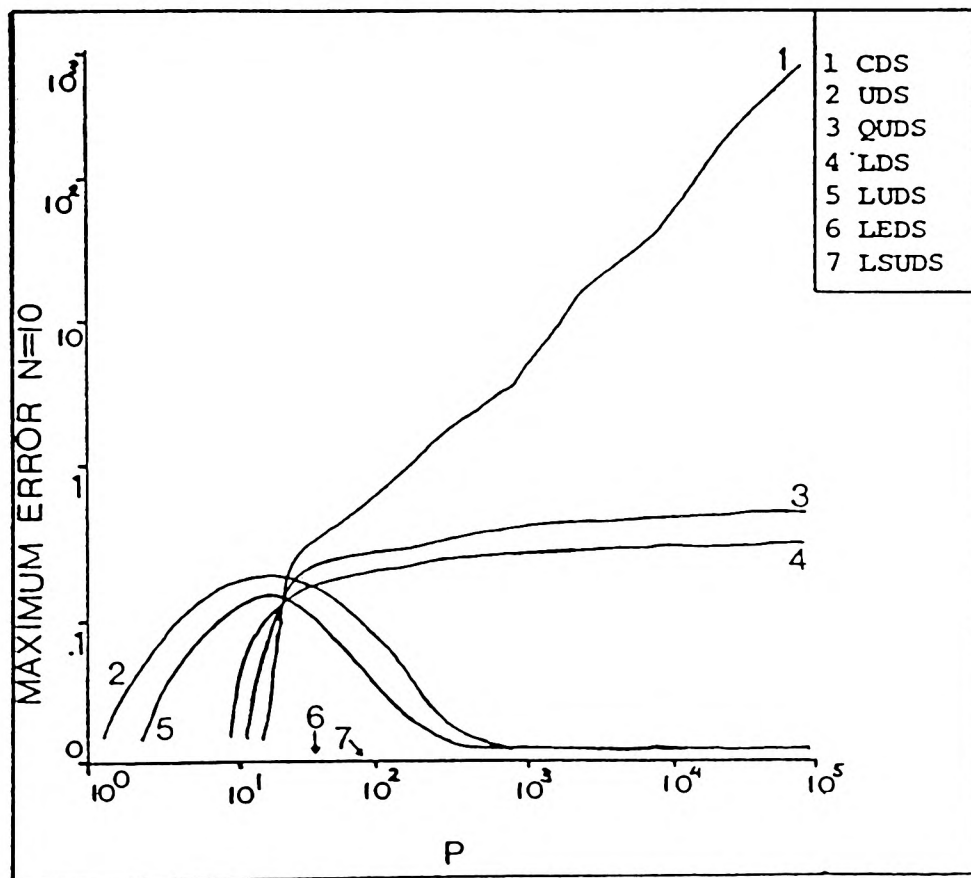


FIGURE  
6.16-9

PLOT OF MAXIMUM ERROR VERSUS  
PECLET NUMBER OF  $N=10$

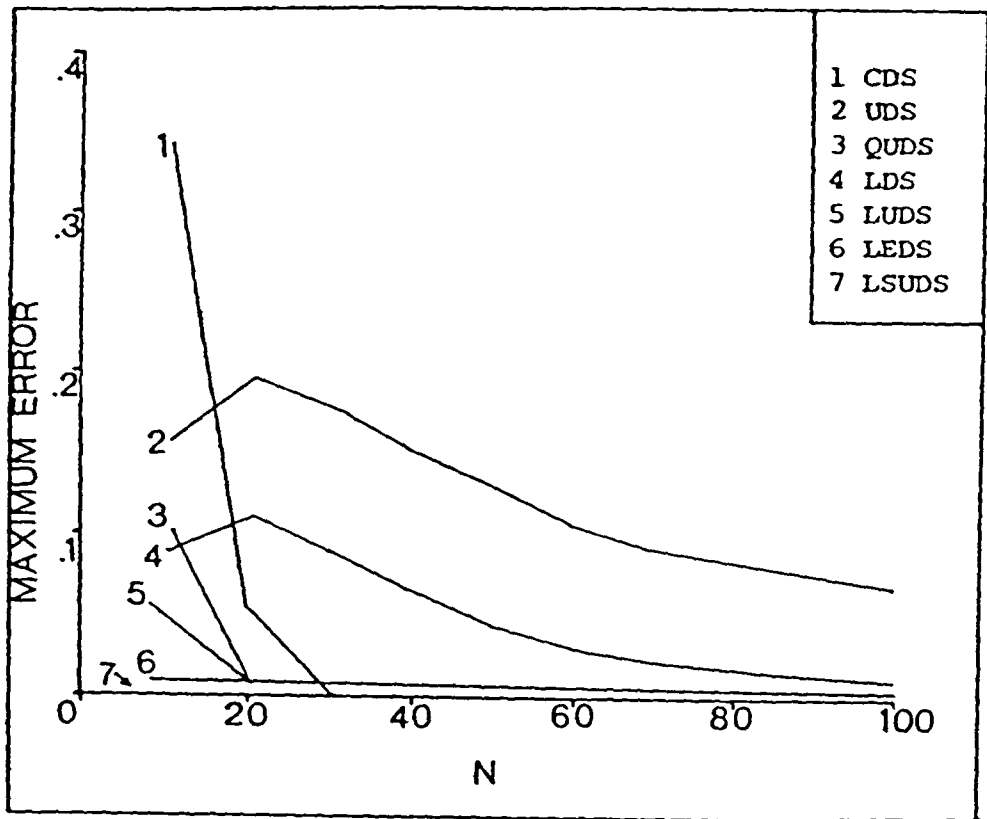


FIGURE 6.16-10

PLOT OF MAXIMUM ERROR VERSUS NUMBER OF NODES FOR  $S(X) = -X^2 + X + 1$

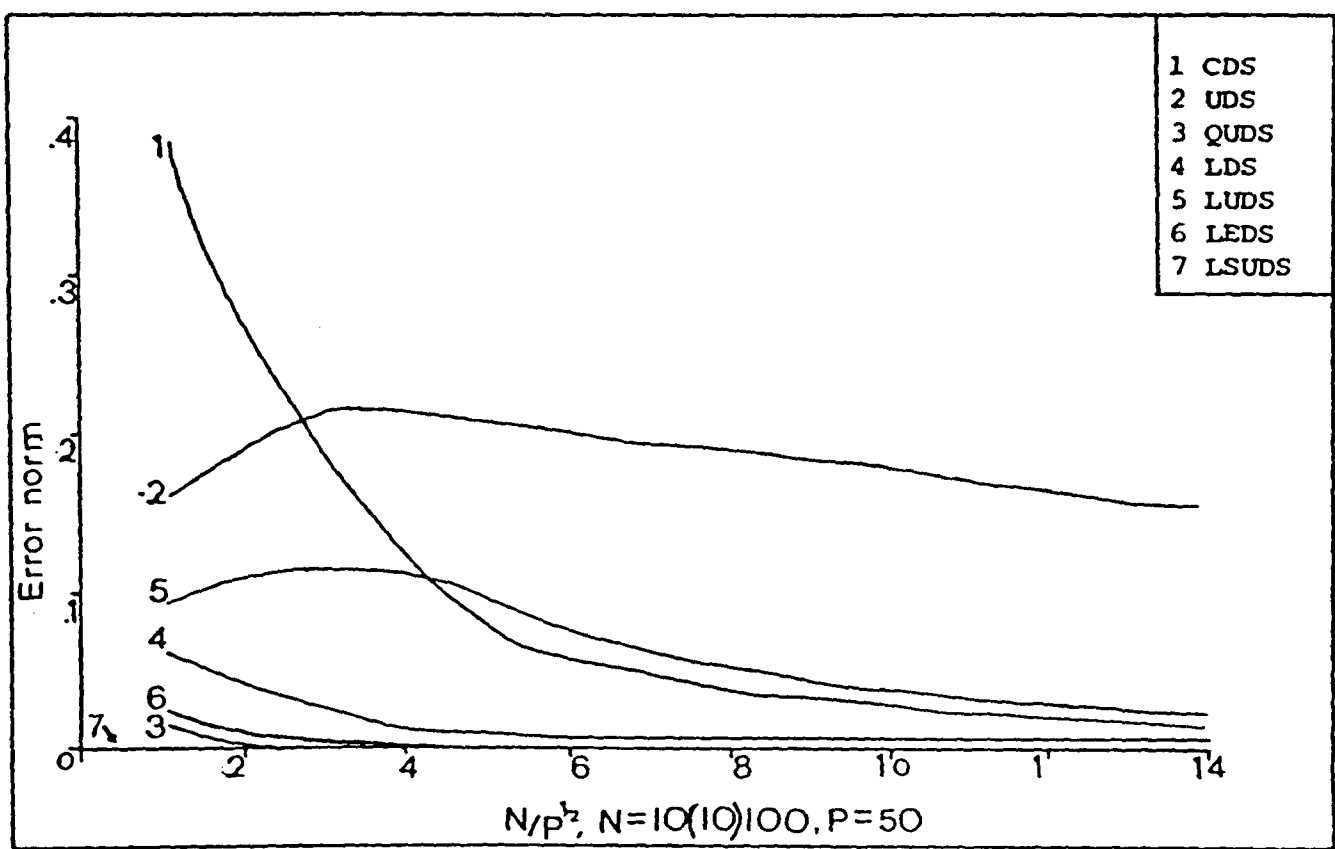


FIGURE 6.16-11

PLOT OF ERROR NORM VERSUS  $N/P^{1/2}$  FOR  $P=50$  AND  $N$  RANGING FROM 1 TO 100 IN STEPS OF 10

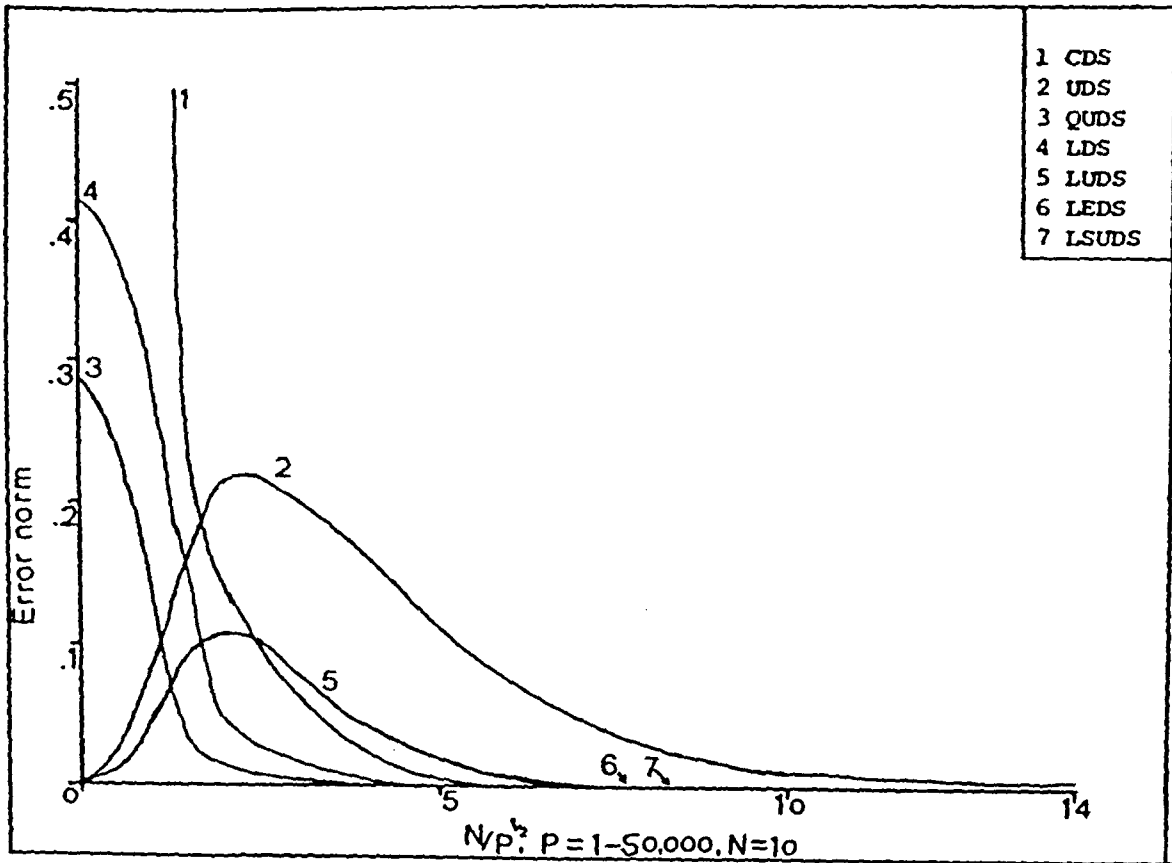


FIGURE  
6.16-12

PLOT OF ERROR NORM VERSUS  $N/P^{1/2}$  FOR  
 $N=10$  AND  $P$  RANGING FROM 1 TO 50,000

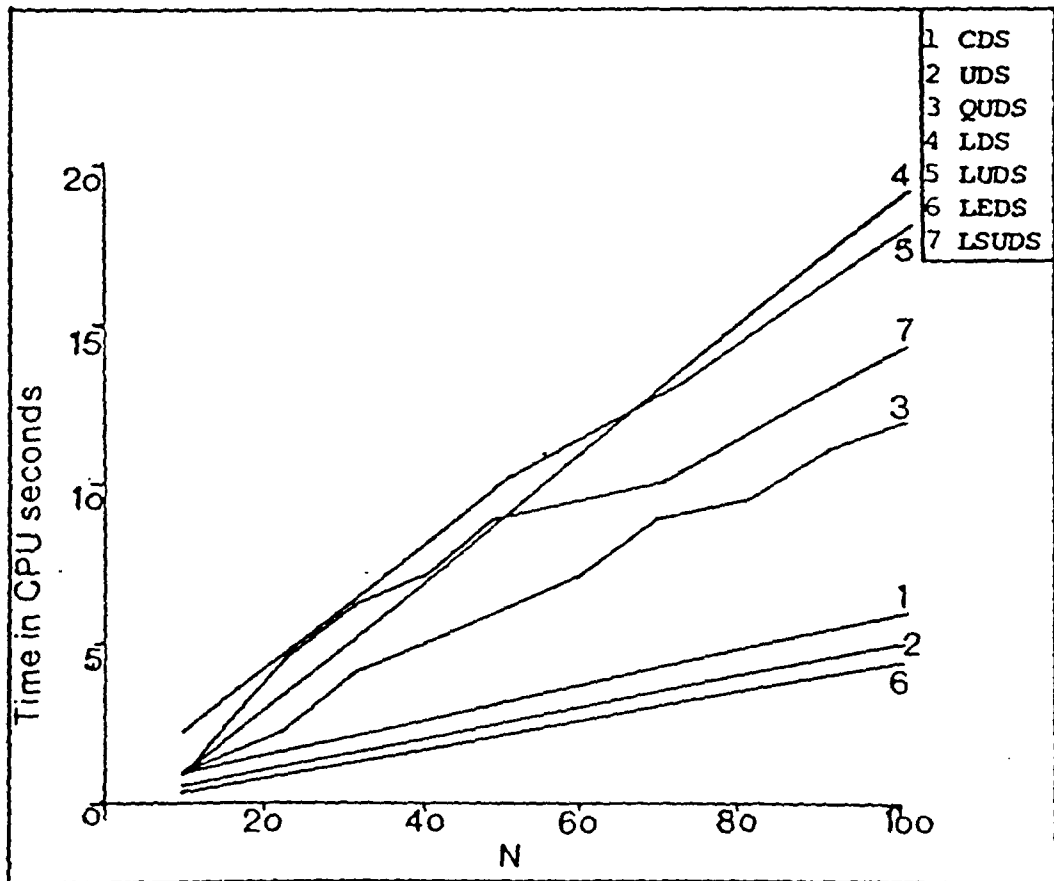
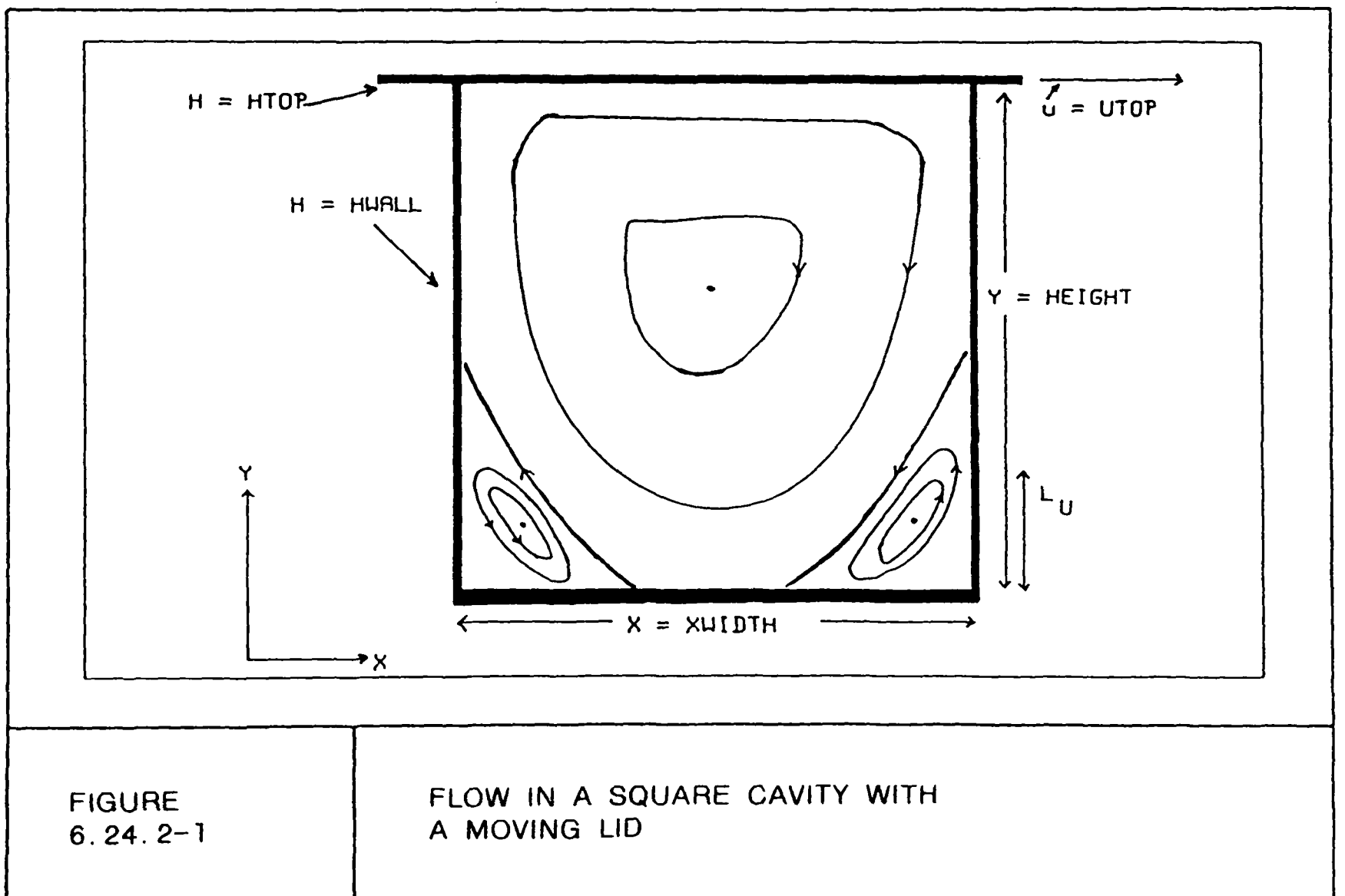
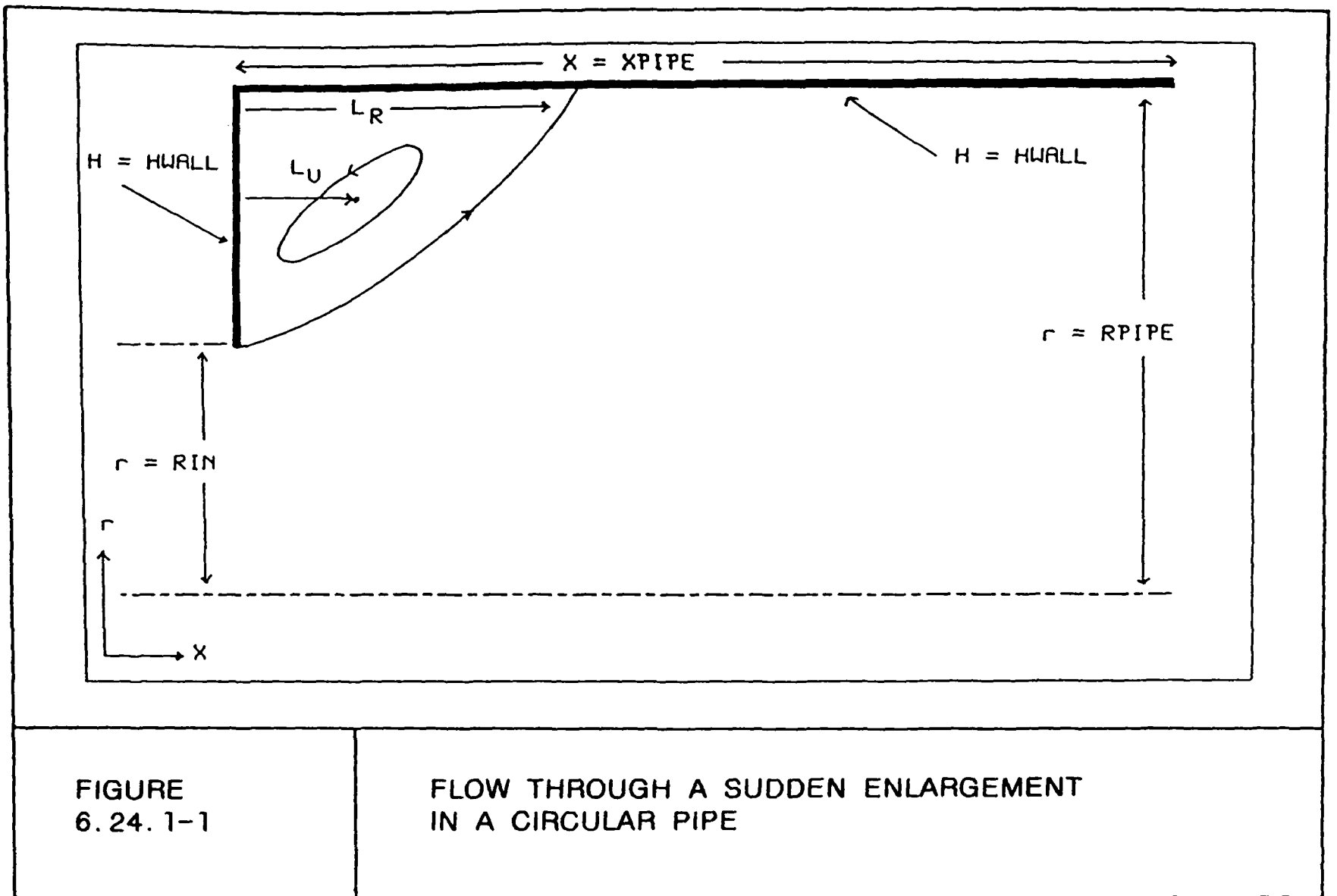


FIGURE  
6.16-13

PLOT OF CPU SECONDS VERSUS NUMBER  
OF NODES FOR  $S(X)=-X$



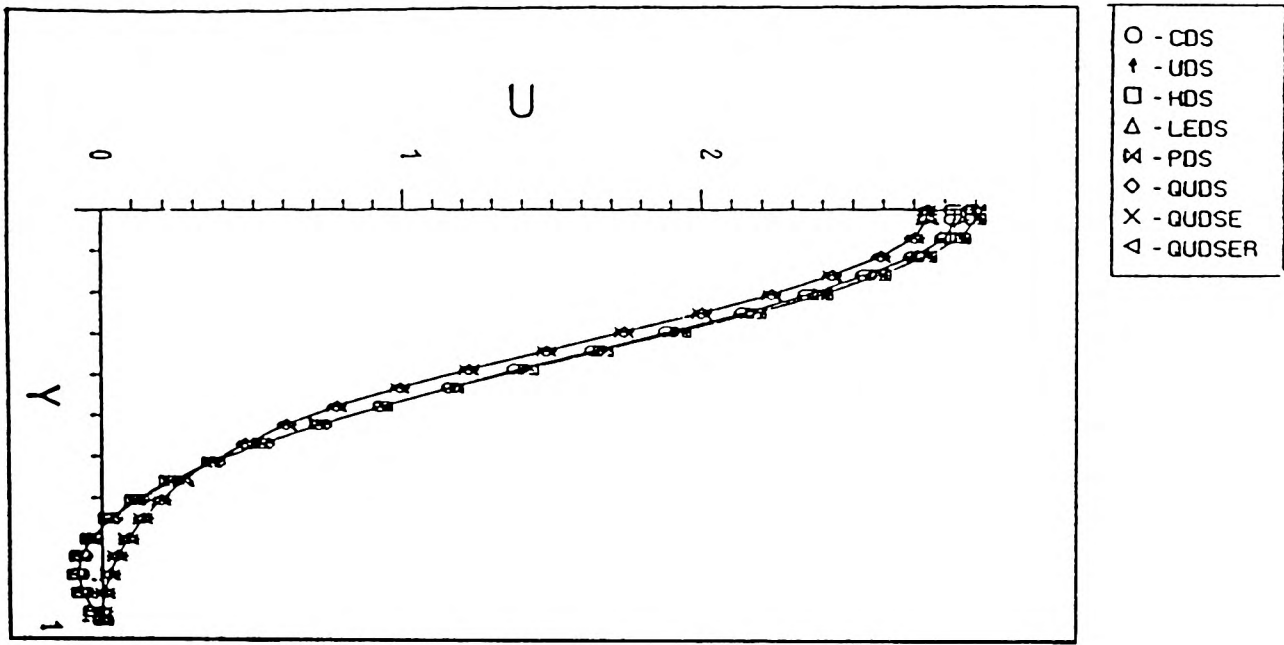


FIGURE  
6.25.1-1

AXIAL VELOCITY PROFILE AT X CENTRELINE  
FOR VARIOUS SCHEMES, AT  $Re=200$

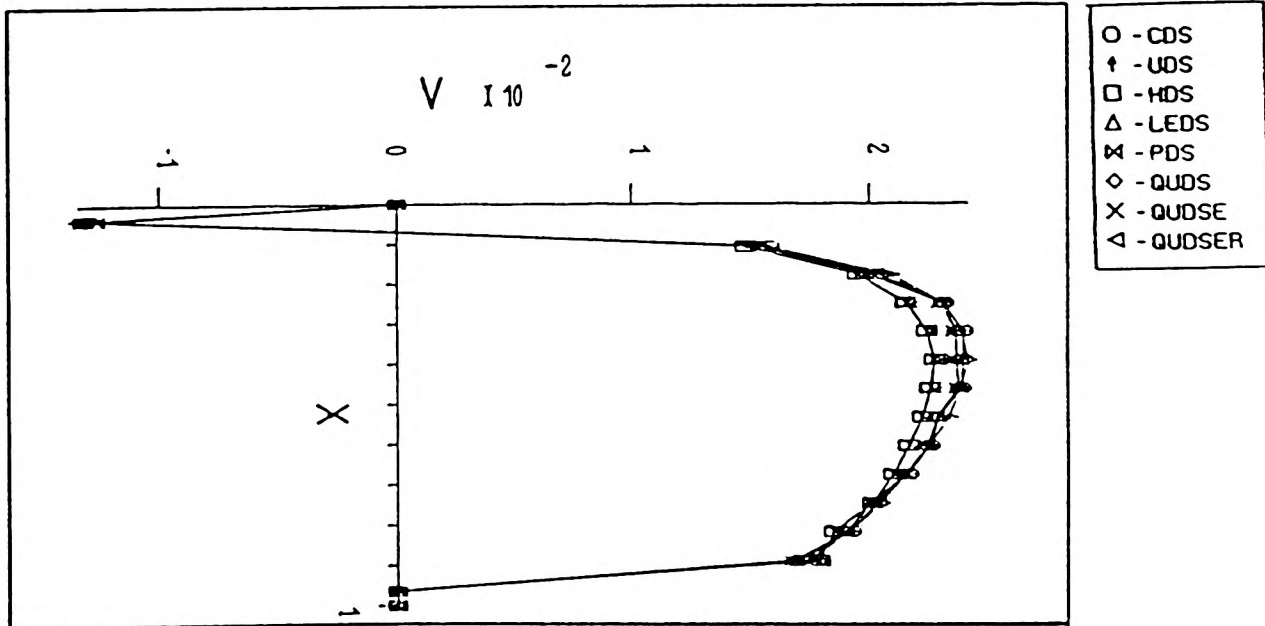


FIGURE  
6.25.1-2

RADIAL VELOCITY PROFILE AT Y CENTRELINE  
FOR VARIOUS SCHEMES, AT  $Re=200$

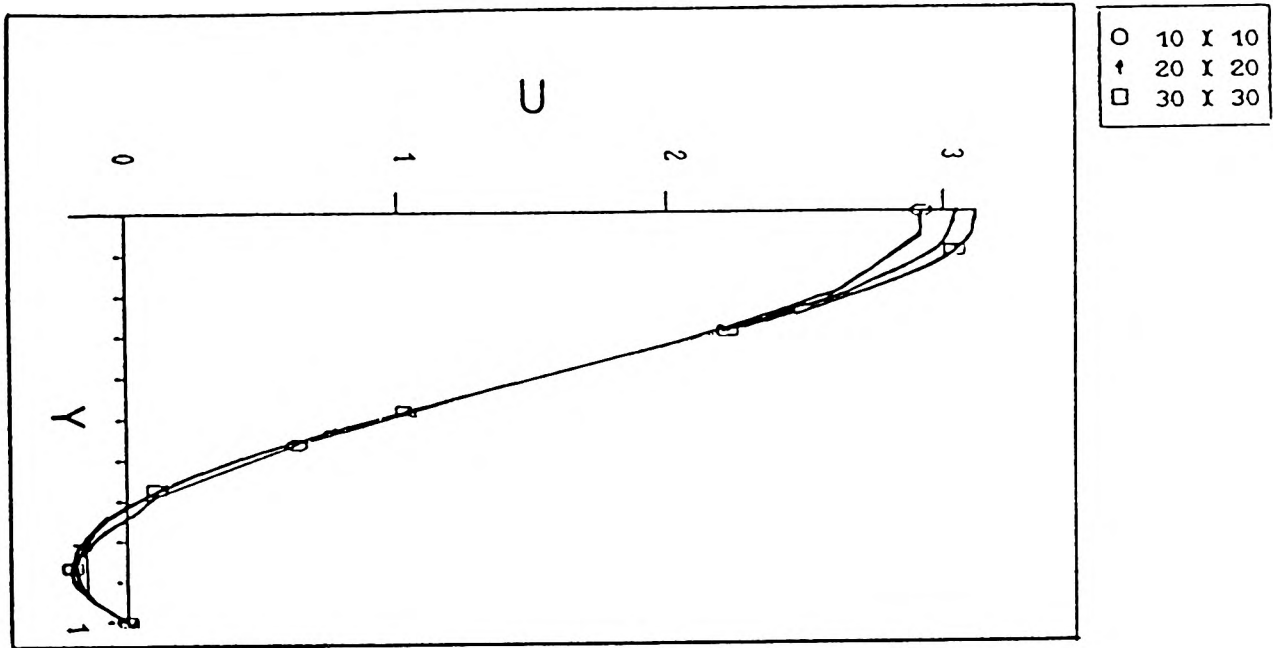


FIGURE  
6.25.1-3

AXIAL VELOCITY, GRID REFINEMENT STUDIES  
FOR CDS FOR  $Re=200$

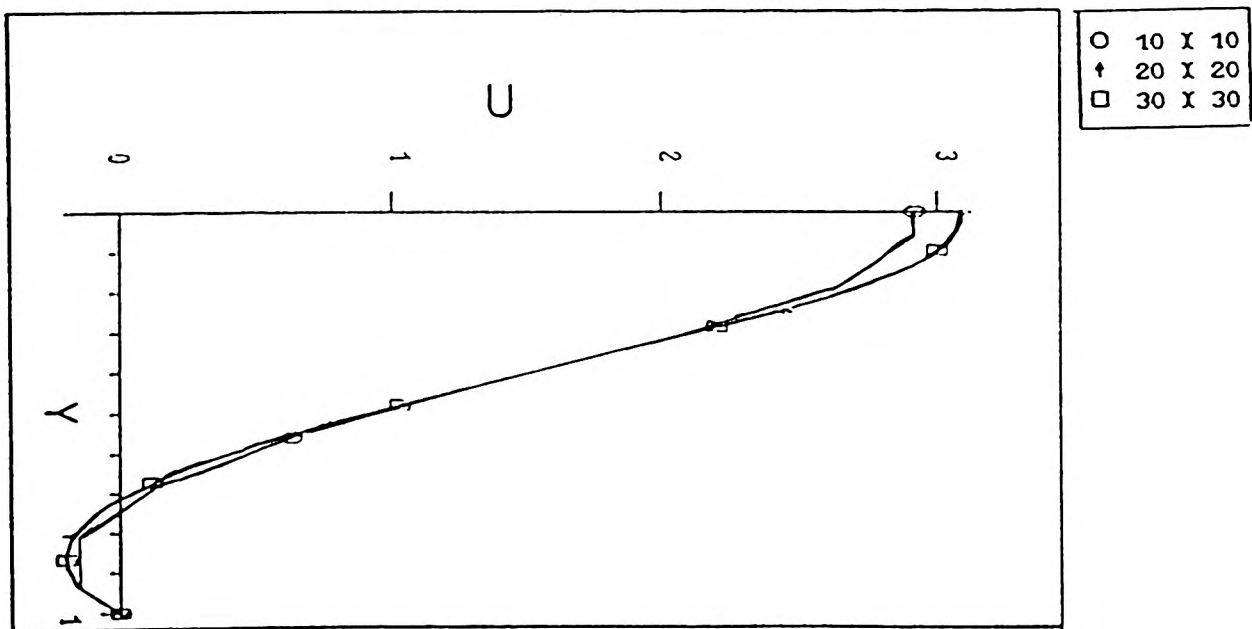


FIGURE  
6.25.1-4

AXIAL VELOCITY, GRID-REFINEMENT STUDIES  
FOR QUDS FOR  $Re=200$

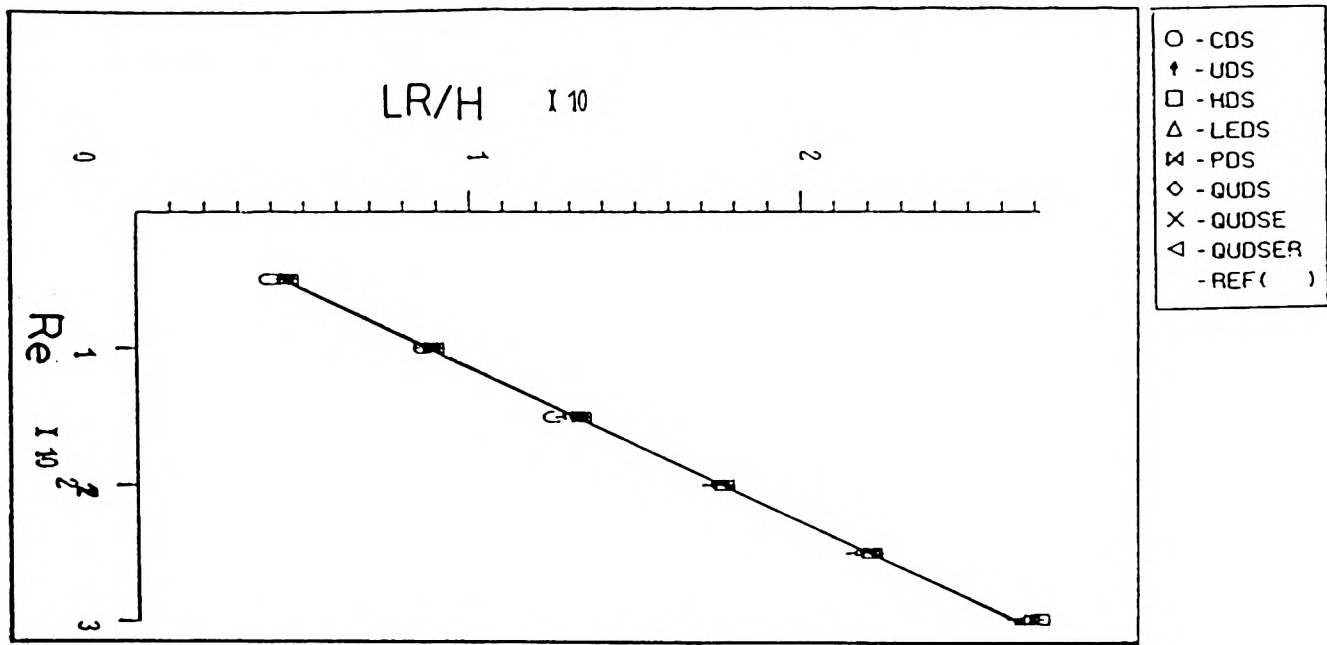


FIGURE  
6.25.1-5

PLOT OF RE-ATTACHMENT VARIATION WITH  
REYNOLDS NUMBER ( $l_r/h$  vs  $Re$ )

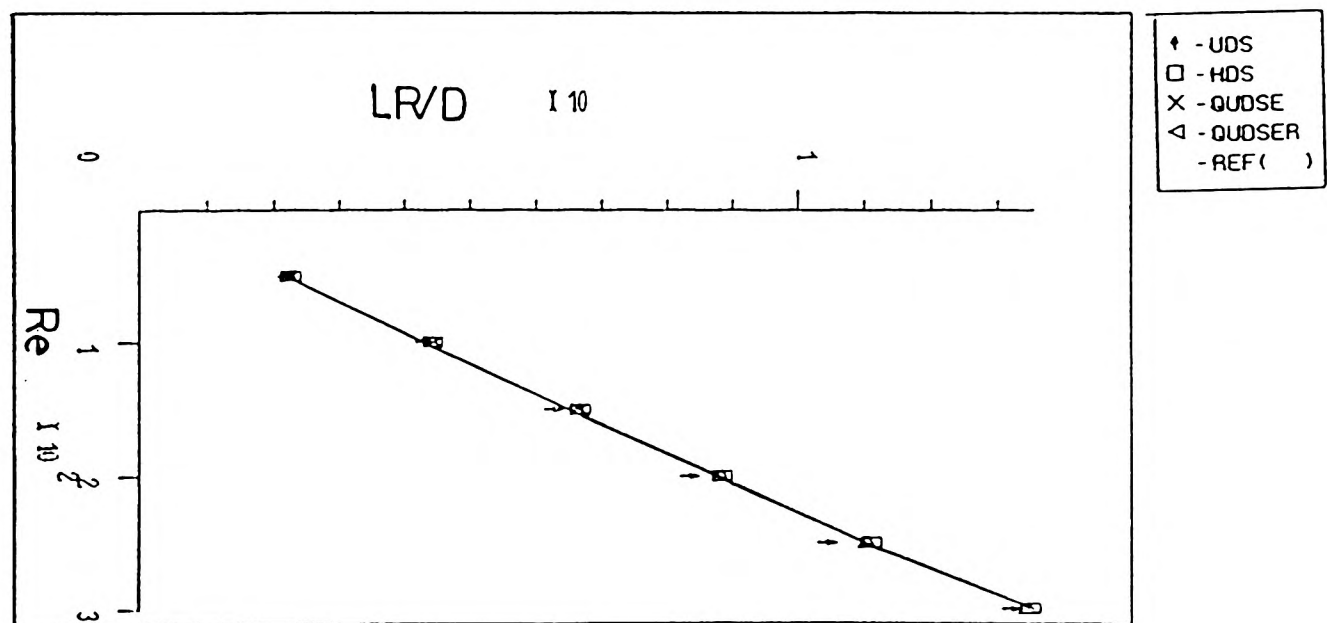


FIGURE  
6.25.1-6

PLOT OF RE-ATTACHMENT VARIATION WITH  
REYNOLDS NUMBER ( $l_r/d$  vs  $Re$ )

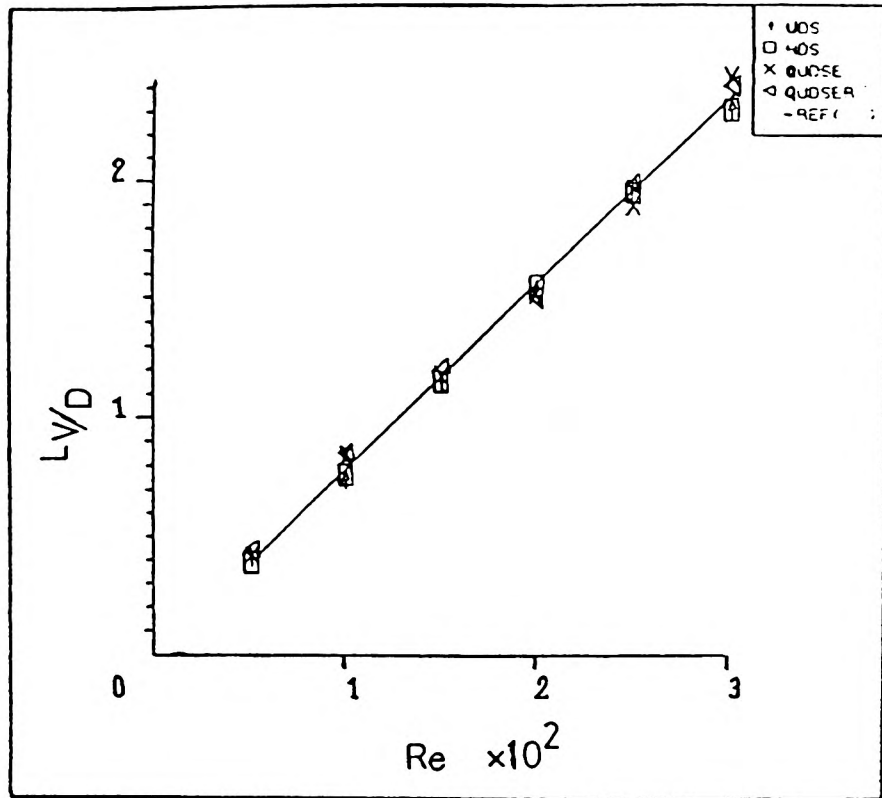


FIGURE  
6.25.1-7

CHARACTERISTICS OF RECIRCULATION CENTRE  
VARIATION WITH REYNOLDS NUMBER ( $L_v/D$  vs  $Re$ )

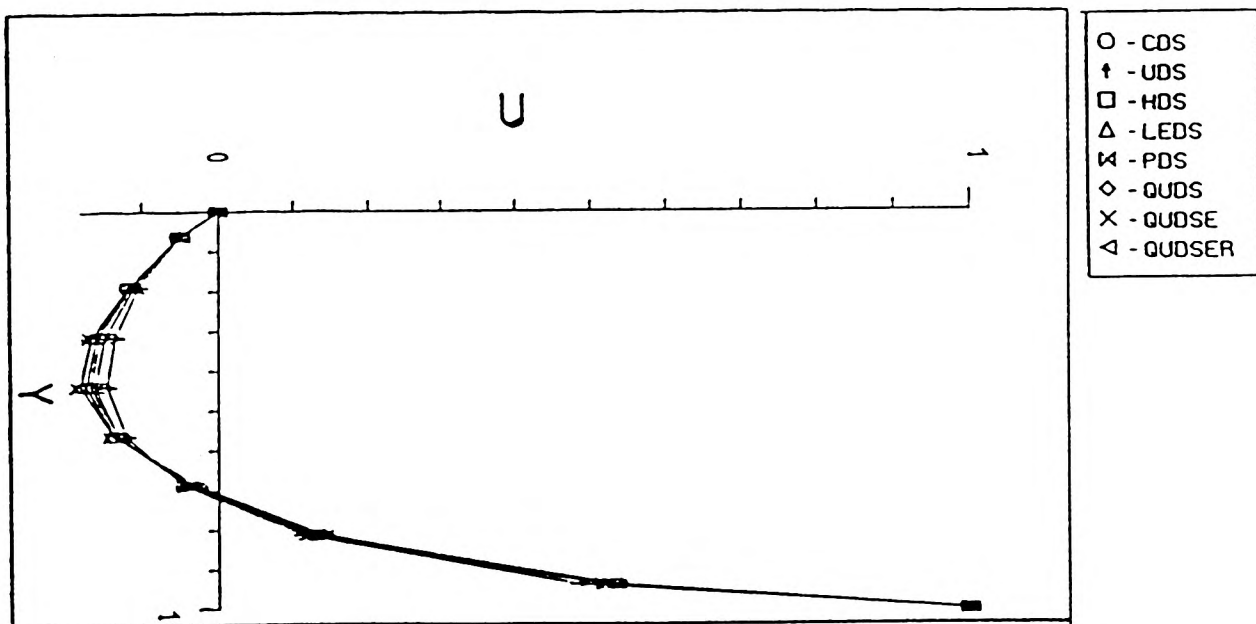


FIGURE  
6.25.2-1

AXIAL VELOCITY PROFILE AT X-CENTRELINE,  
FOR VARIOUS SCHEMES, FOR  $Re=100$

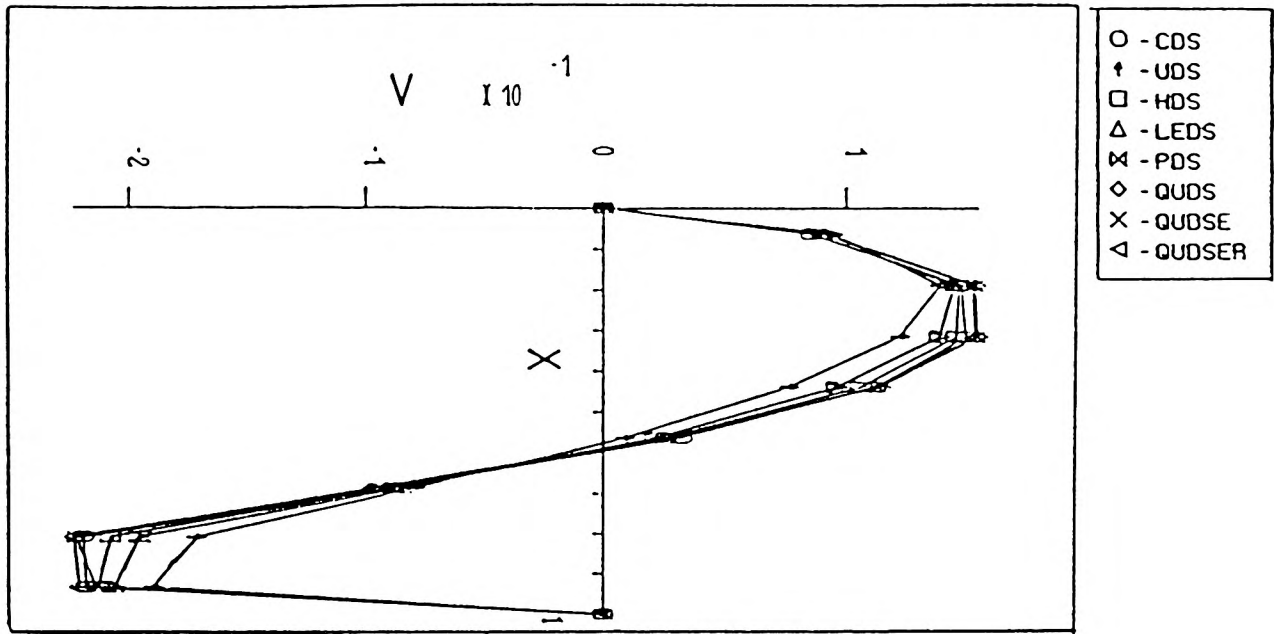


FIGURE  
6.25.2-2

RADIAL-VELOCITY PROFILE AT X-CENTRELINE,  
FOR VARIOUS SCHEMES, FOR  $Re=100$

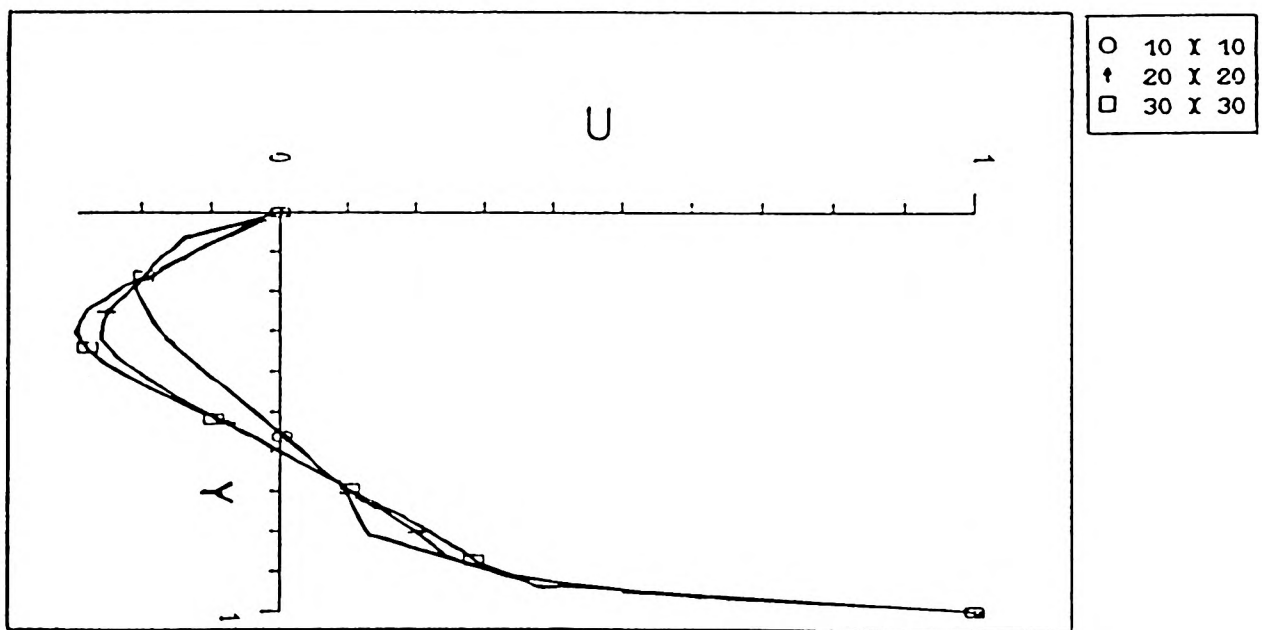


FIGURE  
6.25.2-3

AXIAL-VELOCITY, GRID REFINEMENT STUDIES  
FOR CDS, FOR  $Re=400$

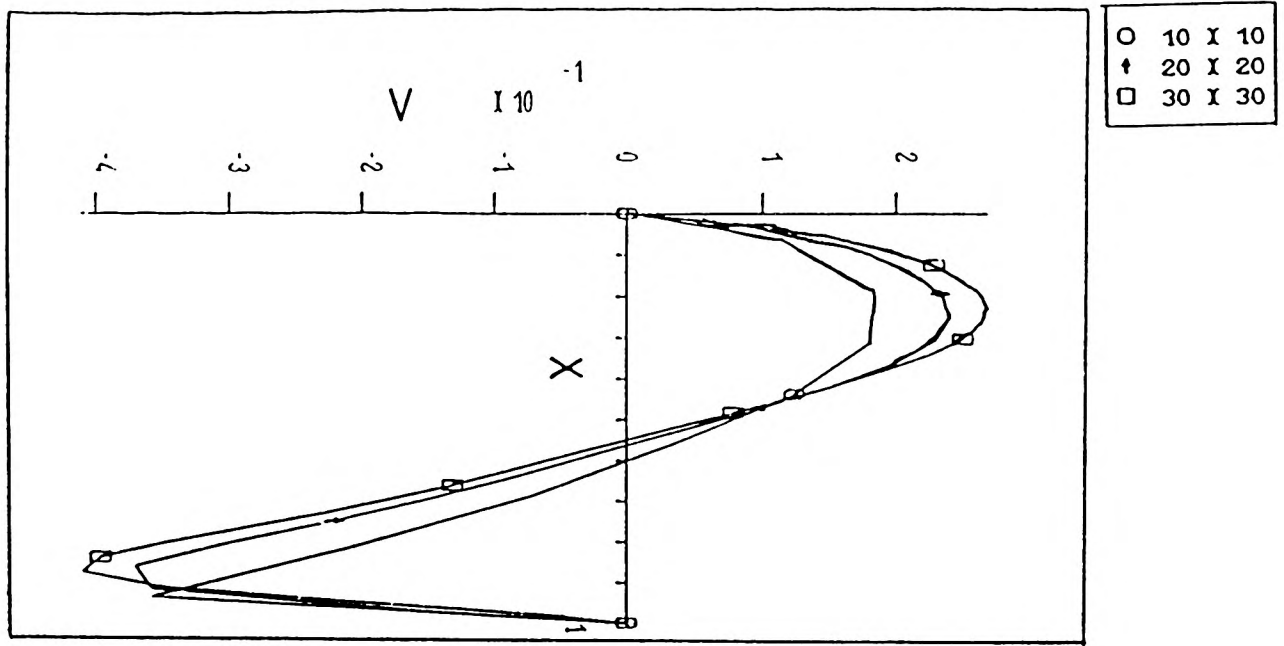


FIGURE  
6.25.2-4

RADIAL VELOCITY, GRID REFINEMENT STUDIES  
FOR CDS, FOR  $Re=400$

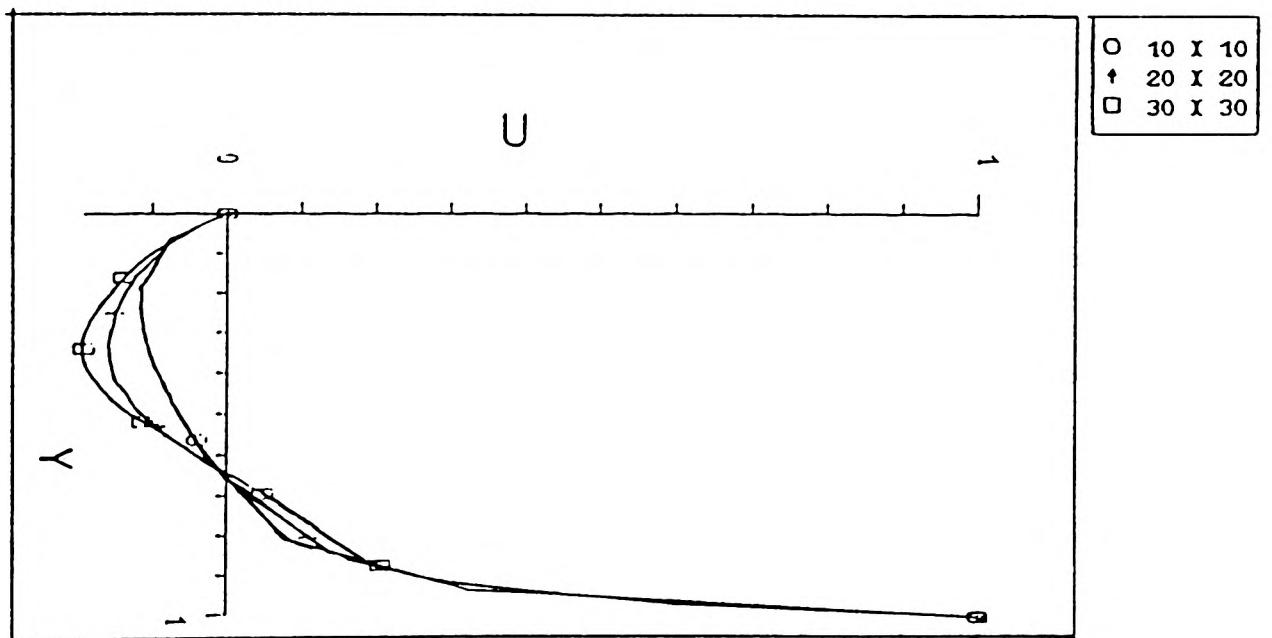


FIGURE  
6.25.2-5

AXIAL VELOCITY, GRID REFINEMENT STUDIES  
FOR UDS, FOR  $Re=400$

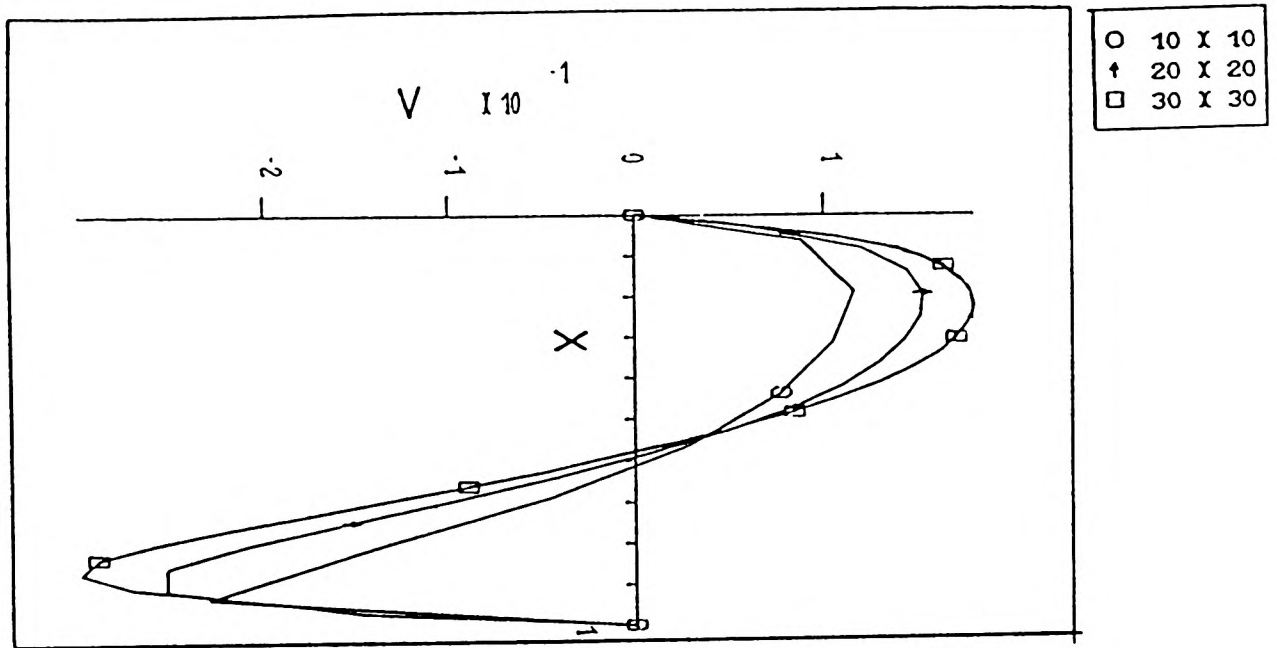


FIGURE  
6.25.2-6

RADIAL VELOCITY, GRID REFINEMENT STUDIES  
FOR UDS, FOR  $Re=400$

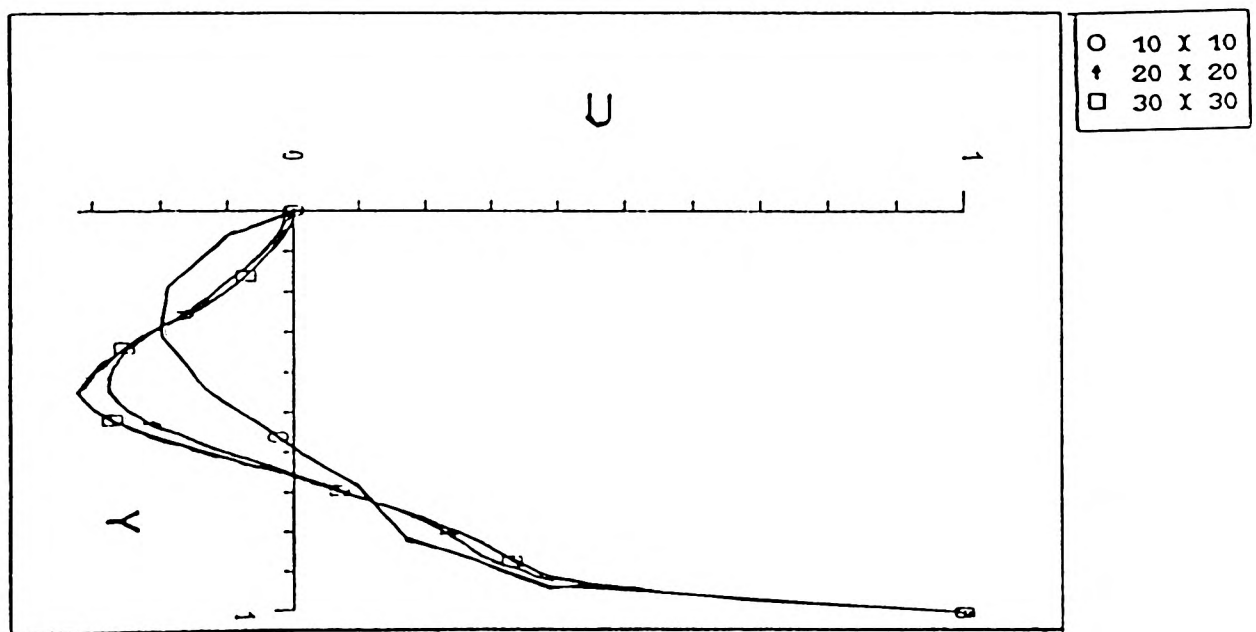


FIGURE  
6.25.2-7

AXIAL VELOCITY, GRID REFINEMENT STUDIES  
FOR QUS, FOR  $Re=400$

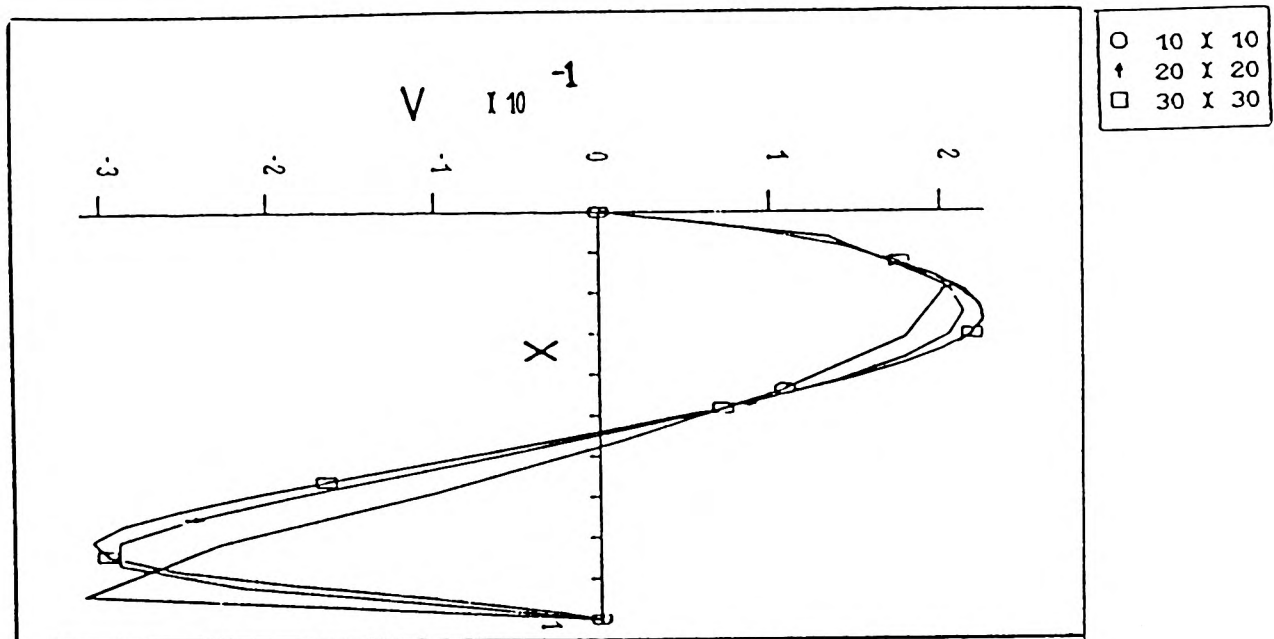


FIGURE  
6.25.2-8

RADIAL VELOCITY, GRID REFINEMENT STUDIES  
FOR QUDS, FOR  $Re=400$

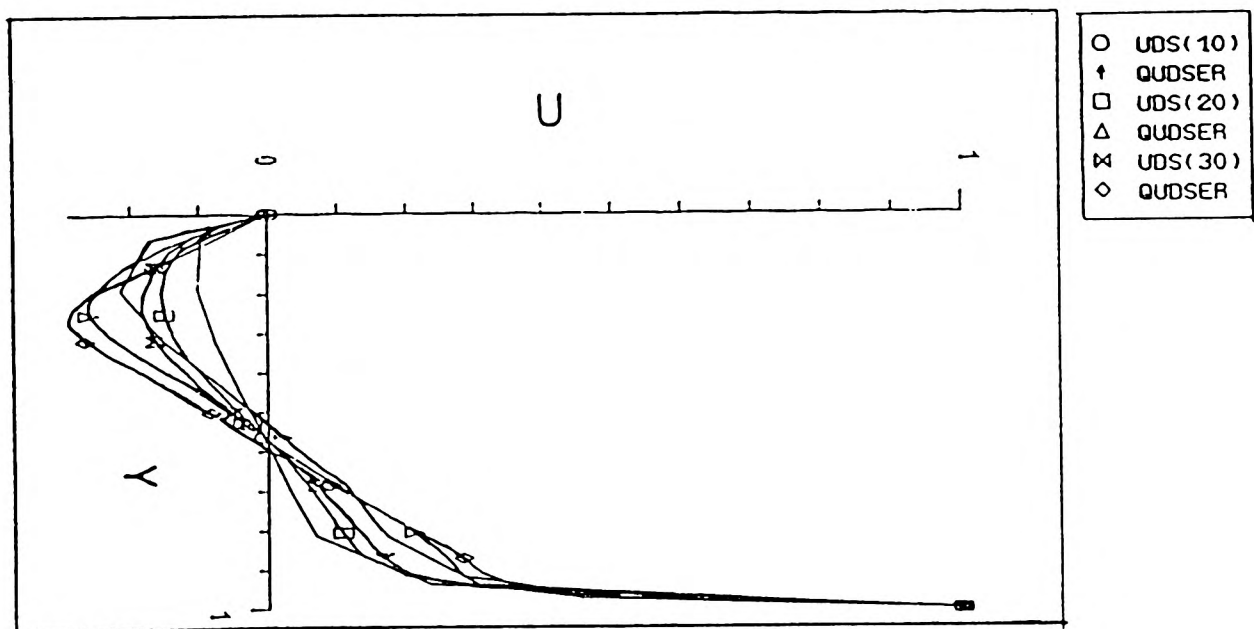


FIGURE  
6.25.2-9

AXIAL VELOCITY, GRID REFINEMENT STUDIES  
FOR UDS/QUDSER, FOR  $Re=1000$

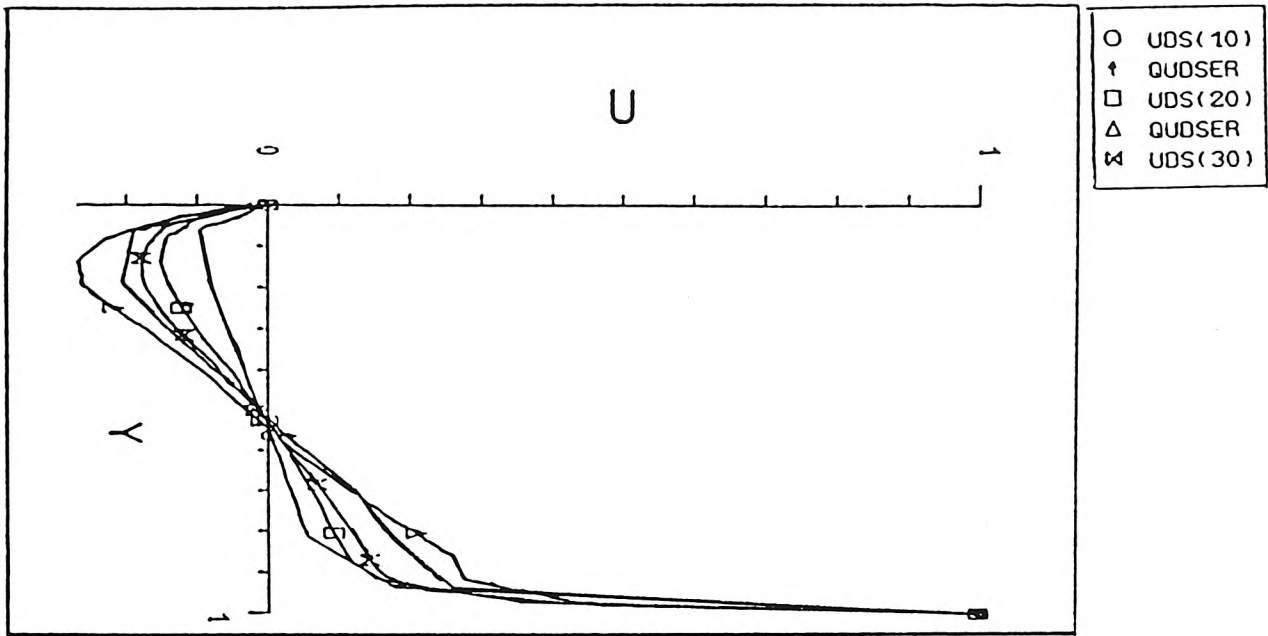


FIGURE  
6.25.2-10

AXIAL VELOCITY, GRID REFINEMENT STUDIES  
FOR UDS/QUDSER, FOR  $Re=2000$

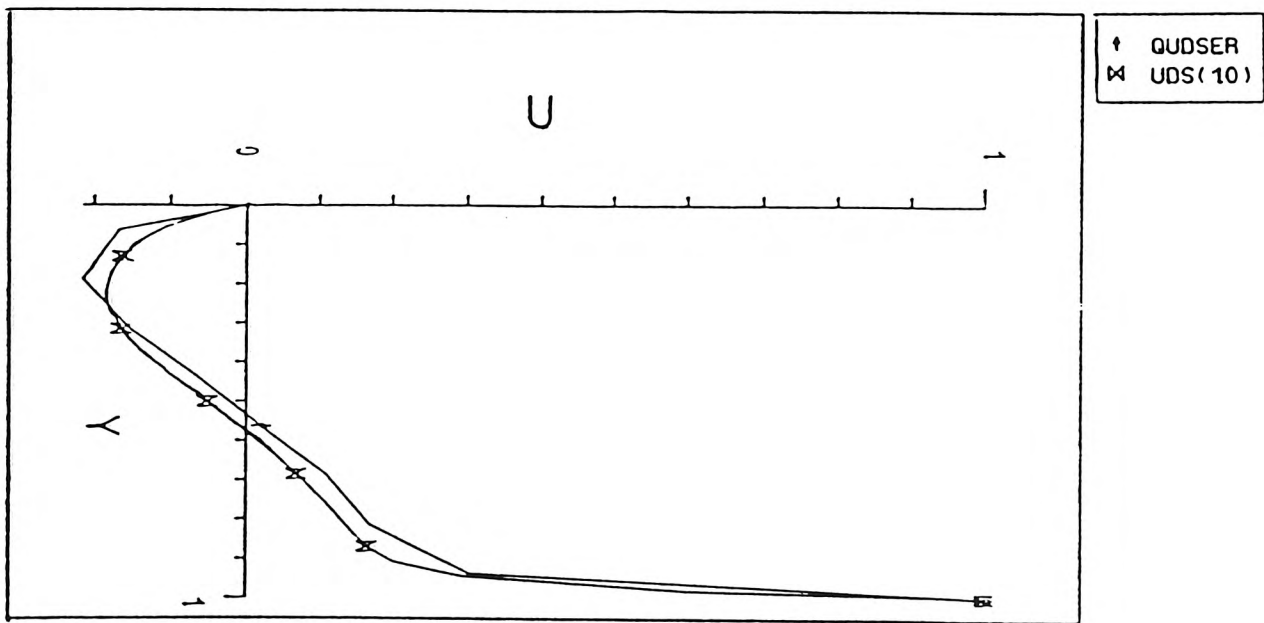


FIGURE  
6.25.2-11

AXIAL VELOCITY, GRID DEPENDENT STUDIES,  
FOR UDS/QUDSER, FOR  $Re=1000$

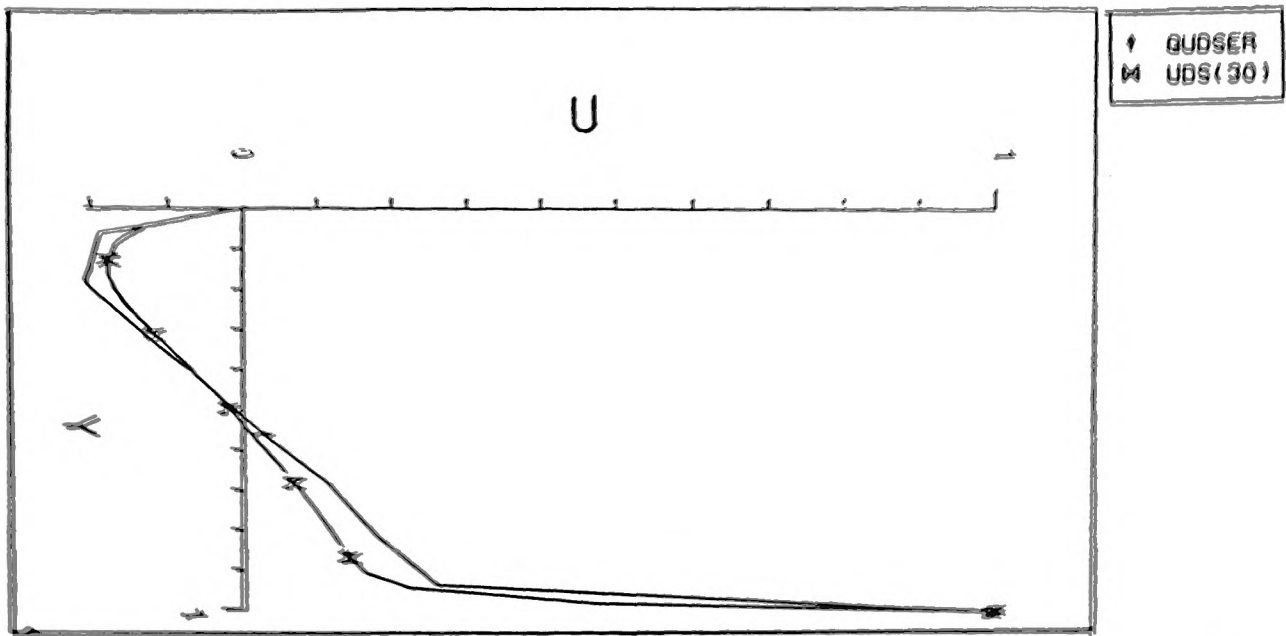


FIGURE  
6.25.2-12

AXIAL VELOCITY, GRID DEPENDENT STUDIES,  
FOR UDS/QUDSER, FOR  $Re=2000$

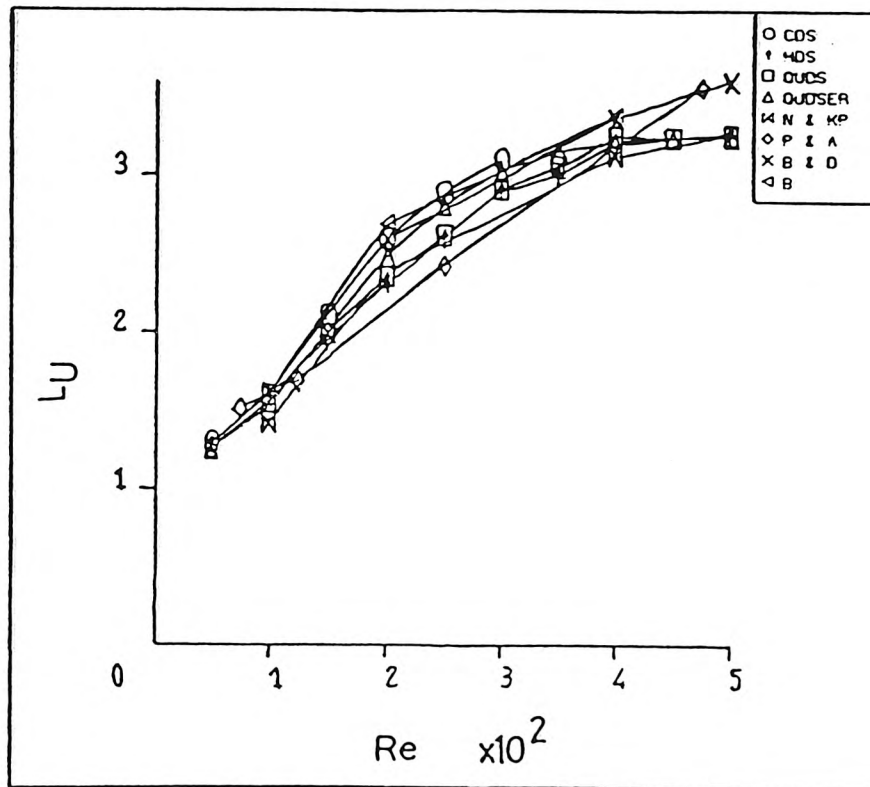


FIGURE  
6.25.2-13

COMPARISON OF VARIOUS UPSTREAM VORTEX  
HEIGHTS AGAINST REYNOLDS NUMBER ( $L_U$  vs  $Re$ )

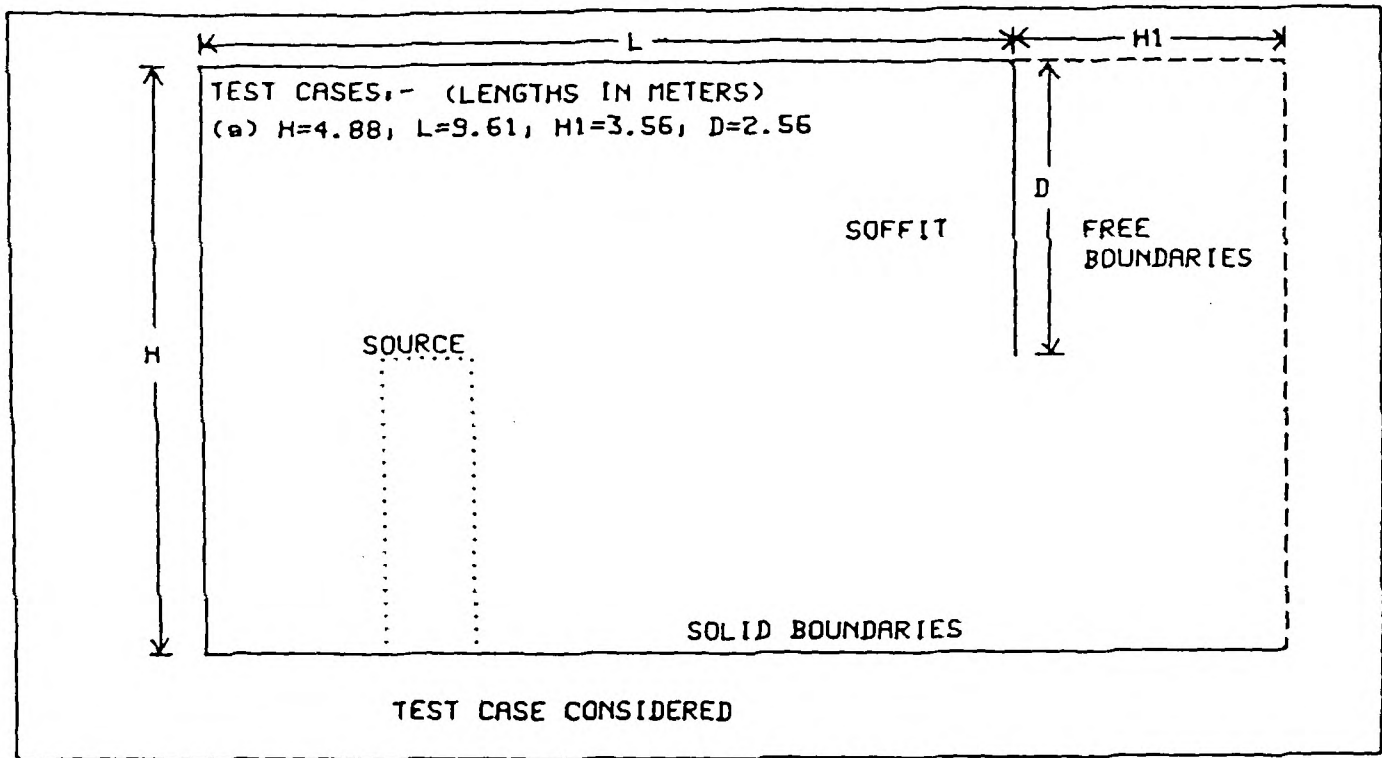


FIGURE  
6.33-1

TEST CASE CONSIDERED

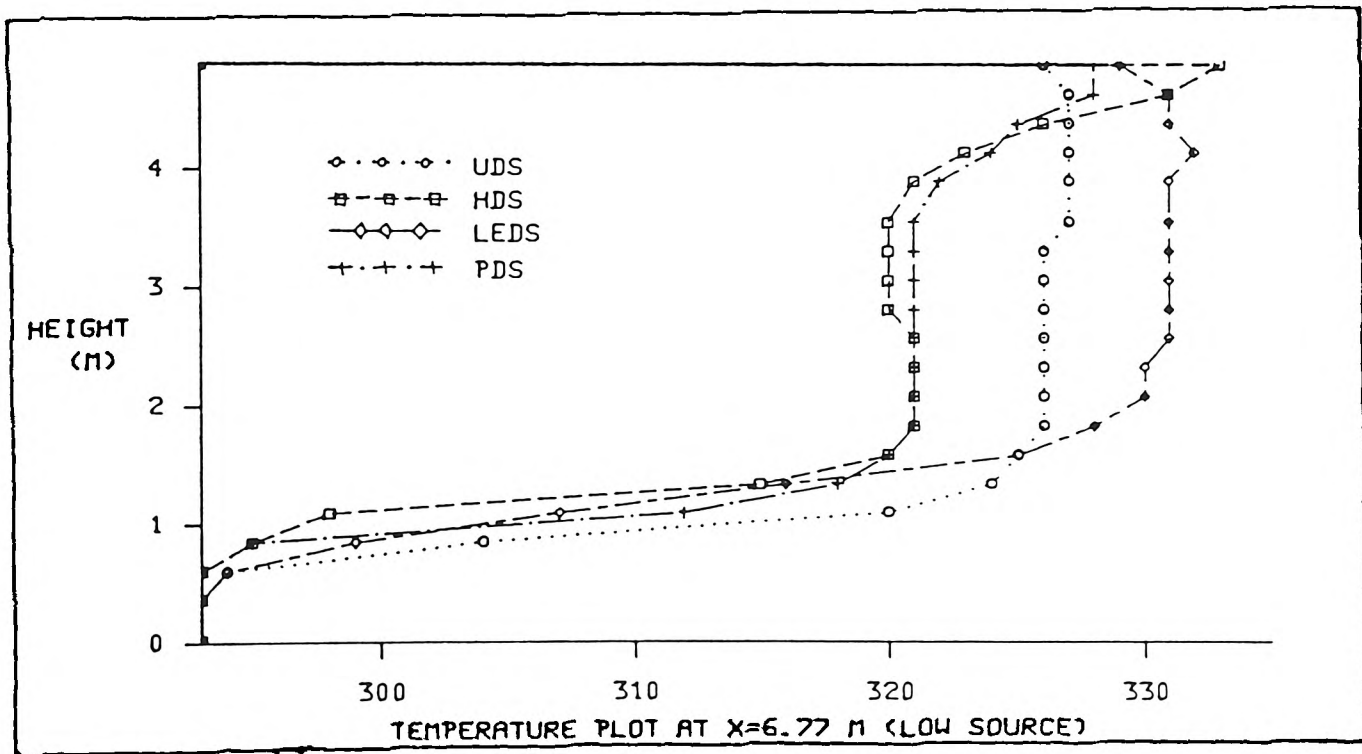


FIGURE  
6.34-1

TEMPERATURE VARIATION AT  
 $x=6.77$ m (LOW SOURCE)

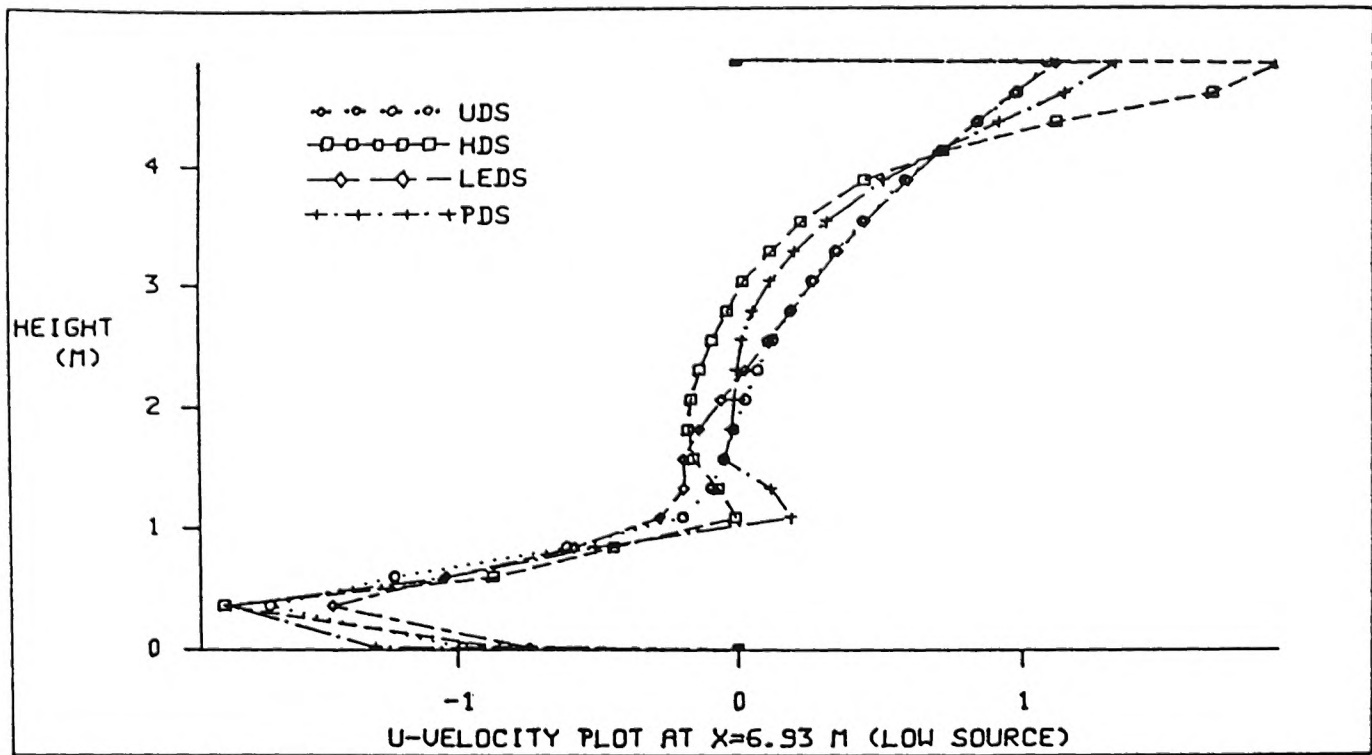


FIGURE  
6.34-2

U-VELOCITY VARIATION AT  
x=6.93m (LOW SOURCE)

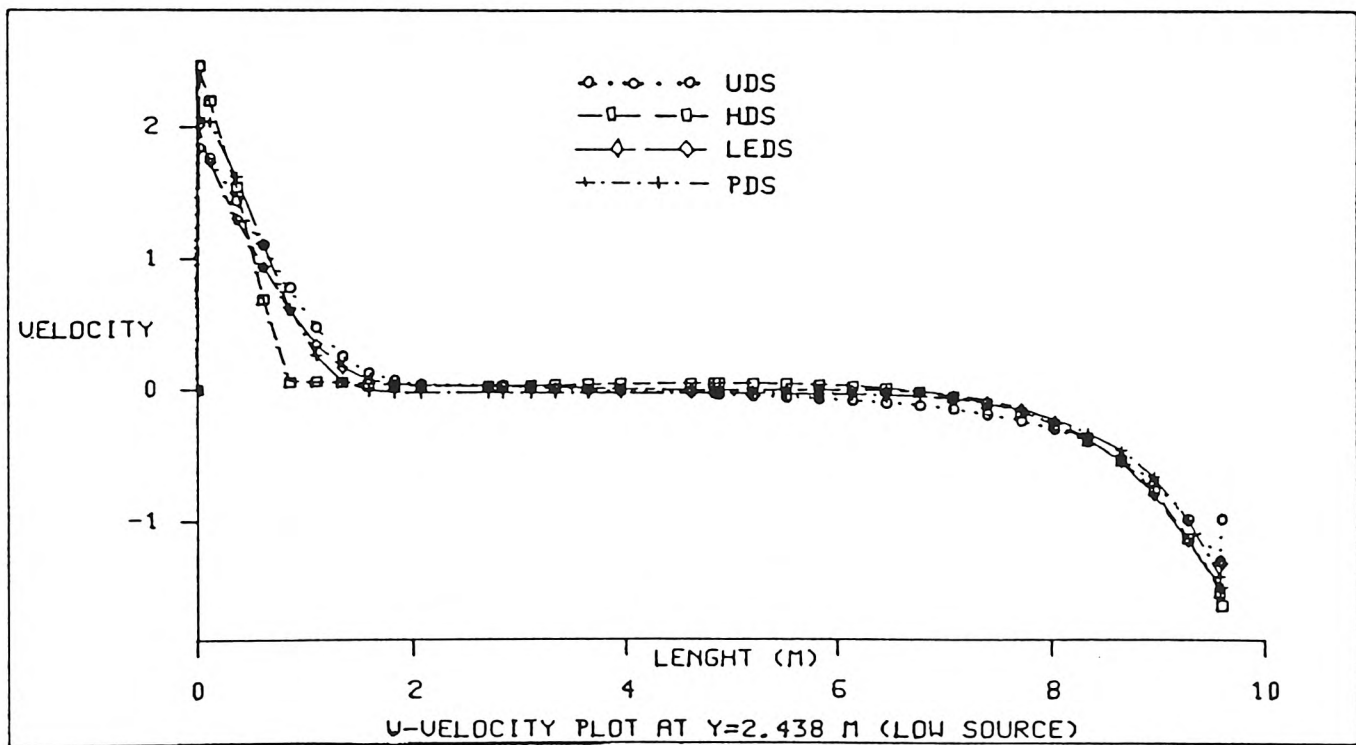


FIGURE  
6.34-3

V-VELOCITY LOCATION AT  
y=2.438m (LOW SOURCE)

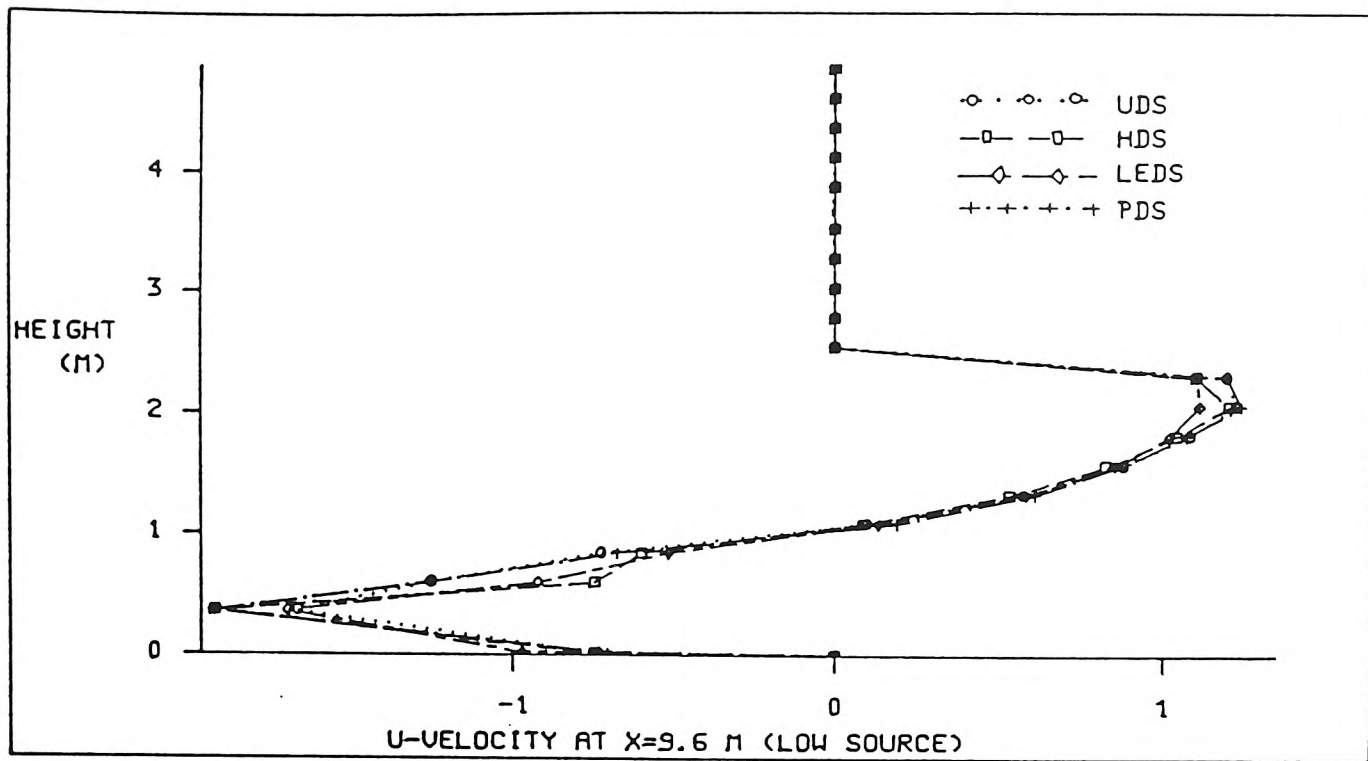


FIGURE  
6.34-4

U-VELOCITY VARIATION AT  
x=9.6m (LOW SOURCE)

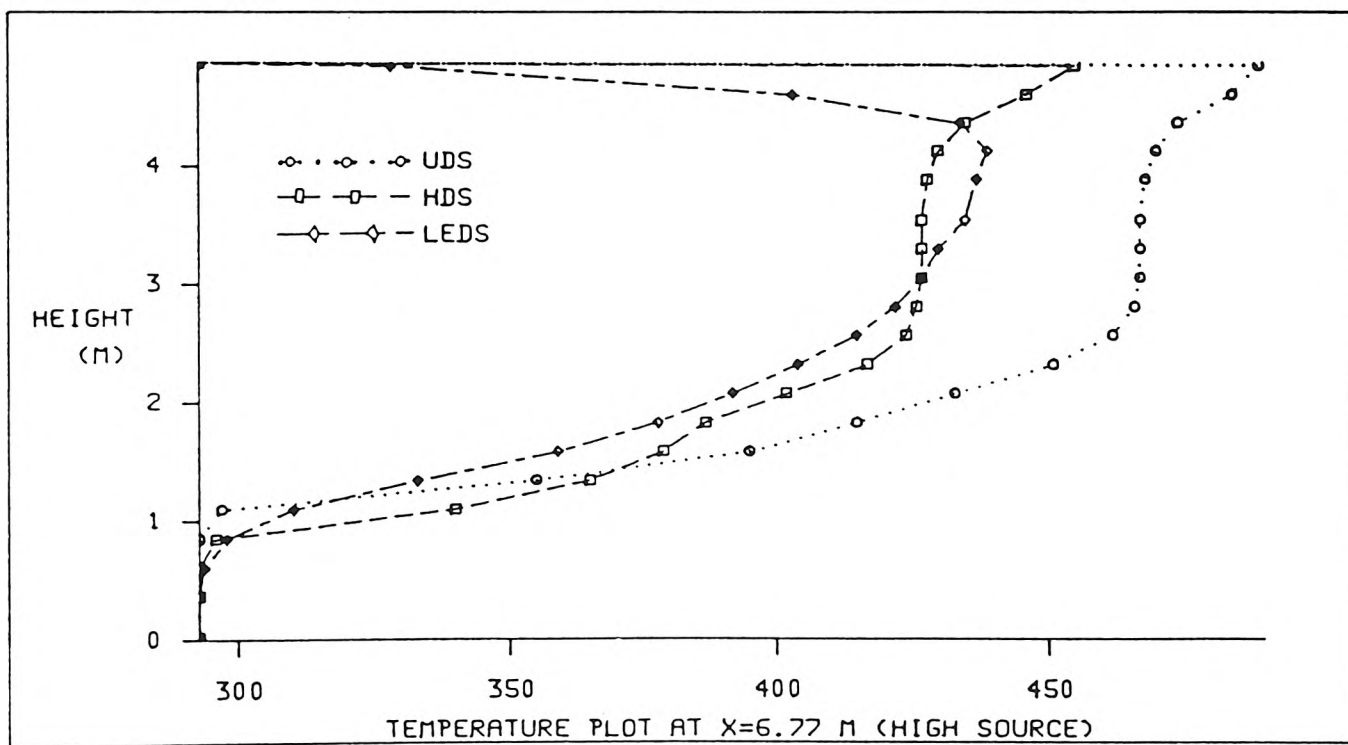


FIGURE  
6.34-5

TEMPERATURE VARIATION AT  
x=6.77m (HIGH SOURCE)

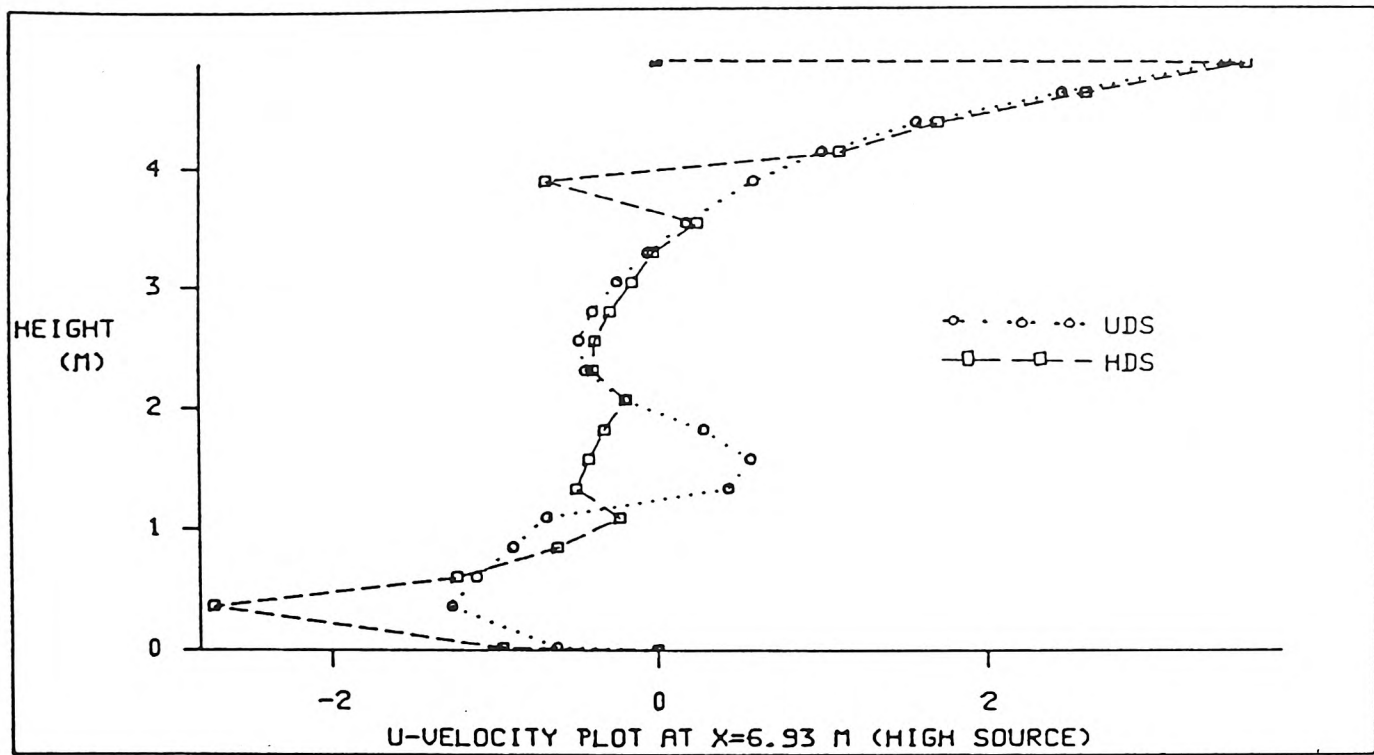


FIGURE  
6.34-6

U-VELOCITY VARIATION AT  
x=6.93m (HIGH SOURCE)

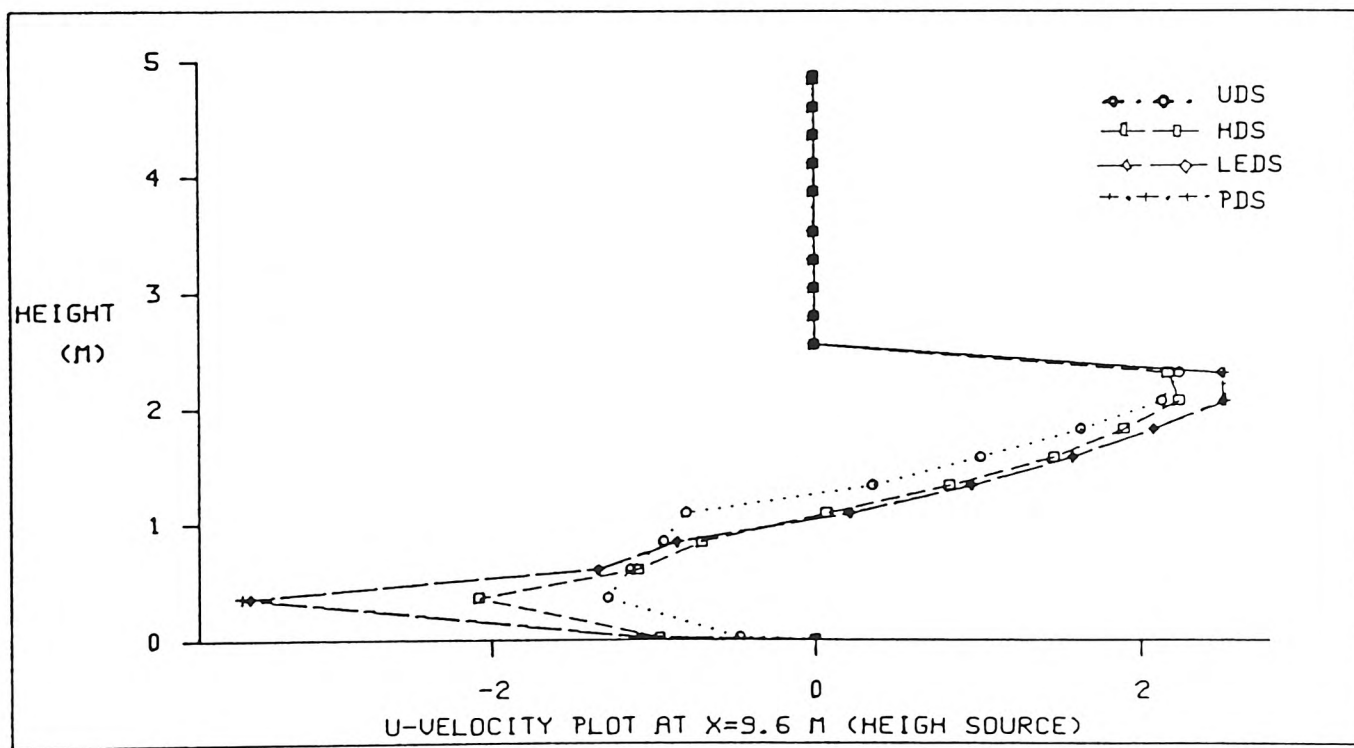


FIGURE  
6.34-7

U-VELOCITY VARIATION AT  
x=9.6m (HIGH SOURCE)

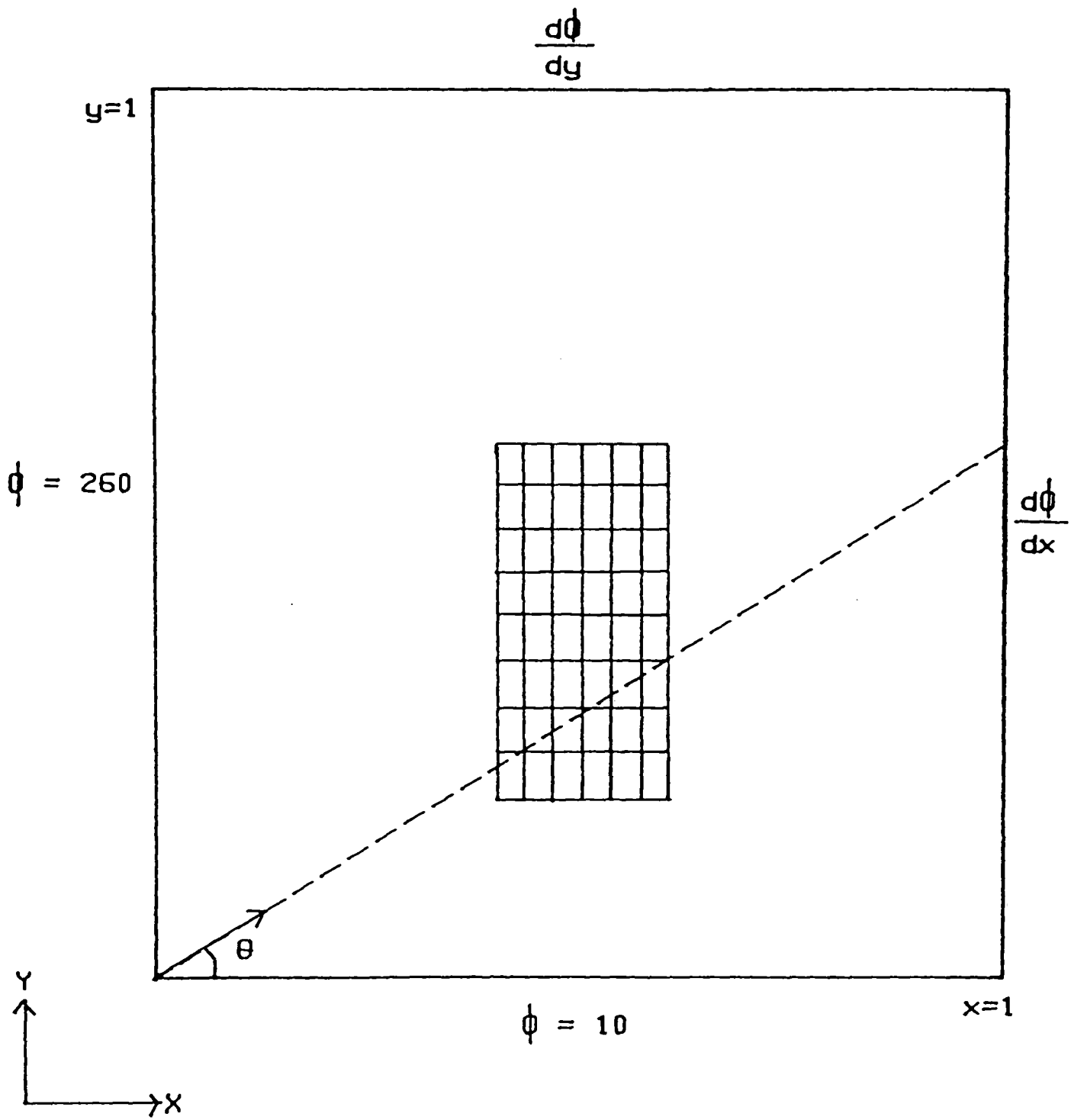


FIGURE  
6.44-1

SCALAR TRANSPORT TEST PROBLEM

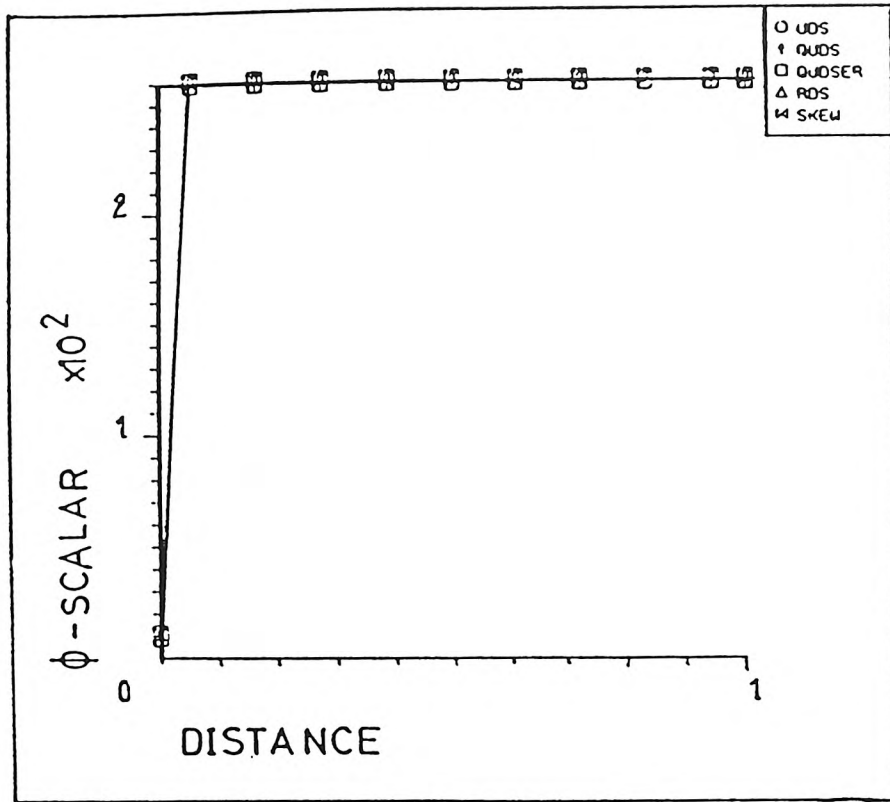


FIGURE  
6.45-1

$\phi$ -PROFILES FOR  $\theta=0$  DEGREES AT  
 $x=0.5$  (11 x 11)

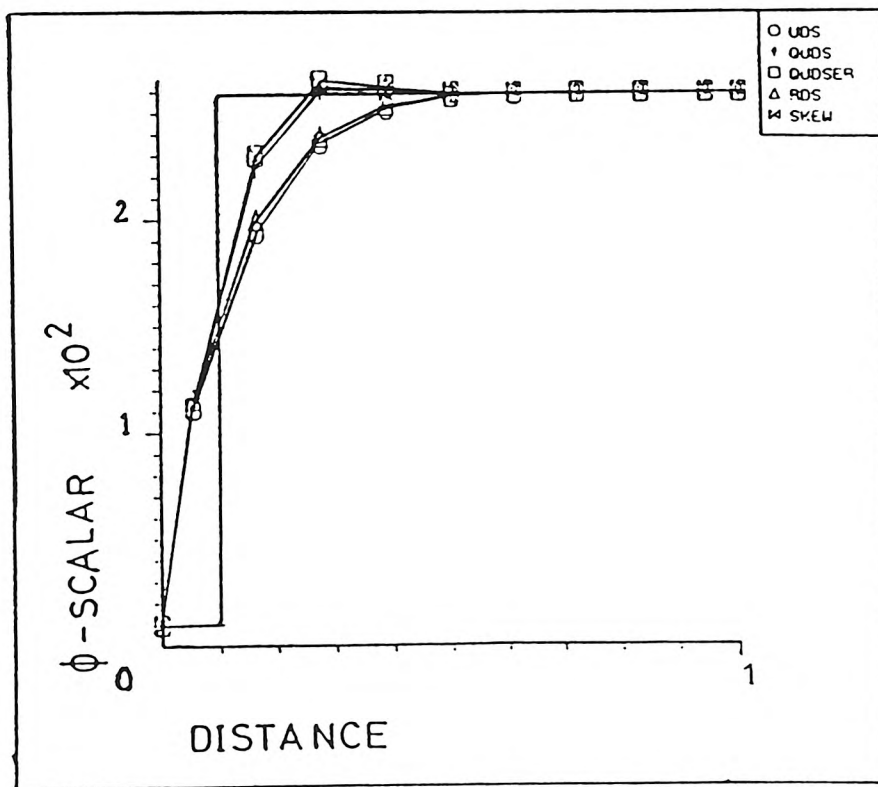


FIGURE  
6.45-2

$\phi$ -PROFILES FOR  $\theta=11.3$  DEGREES AT  
 $x=0.5$  (11 x 11)

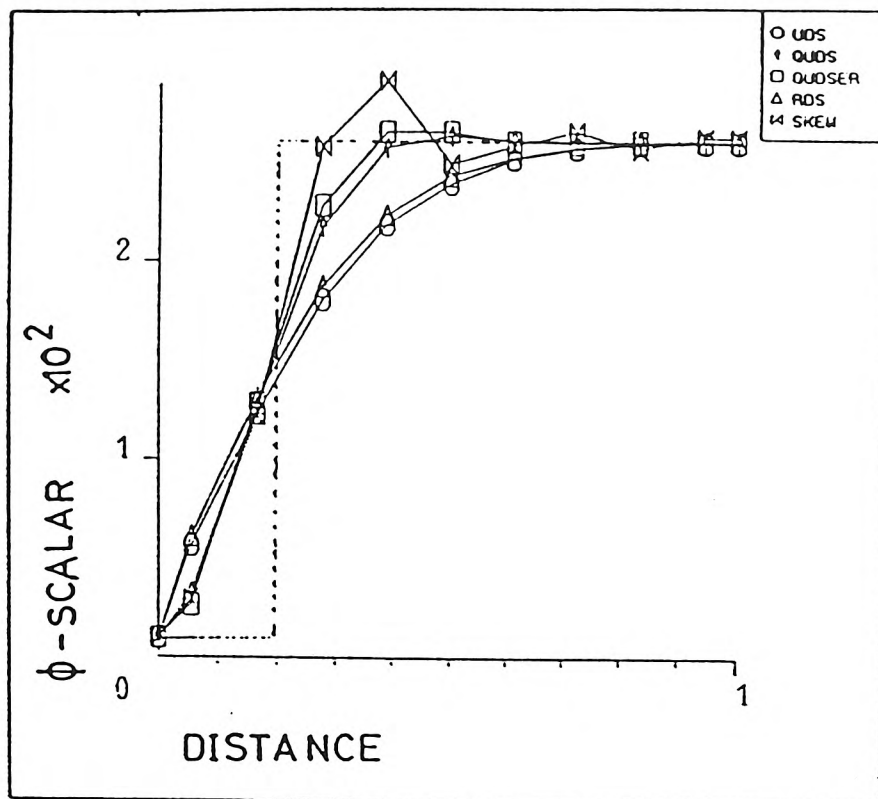


FIGURE  
6.45-3

$\phi$ -PROFILES FOR  $\theta=21.8$  DEGREES AT  
 $x=0.5$  (11 x 11)

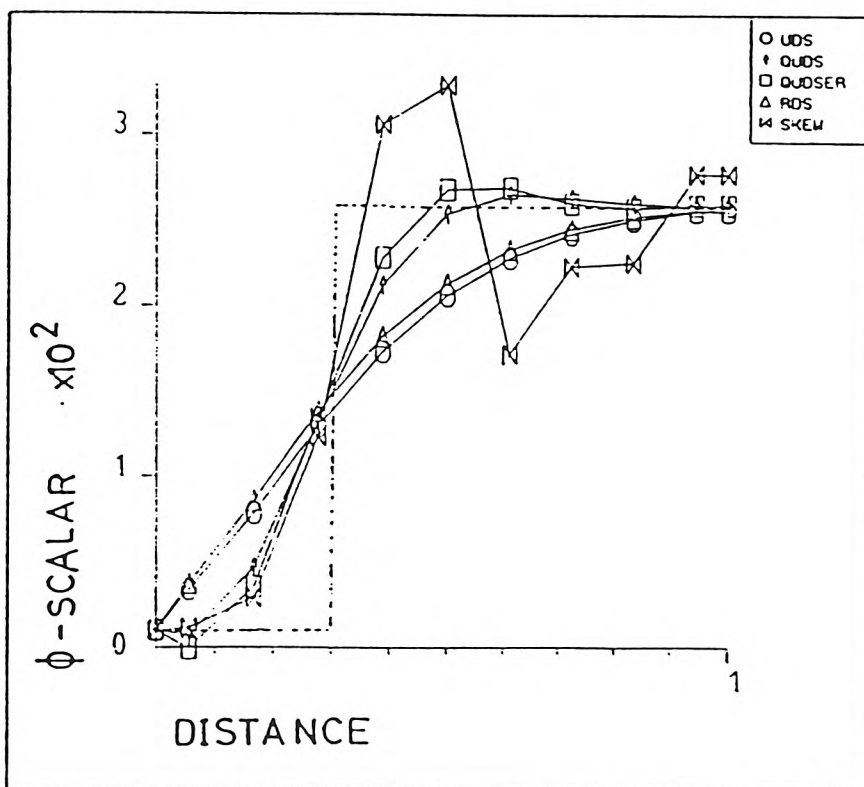


FIGURE  
6.45-4

$\phi$ -PROFILES FOR  $\theta=31$  DEGREES AT  
 $x=0.5$  (11 x 11)

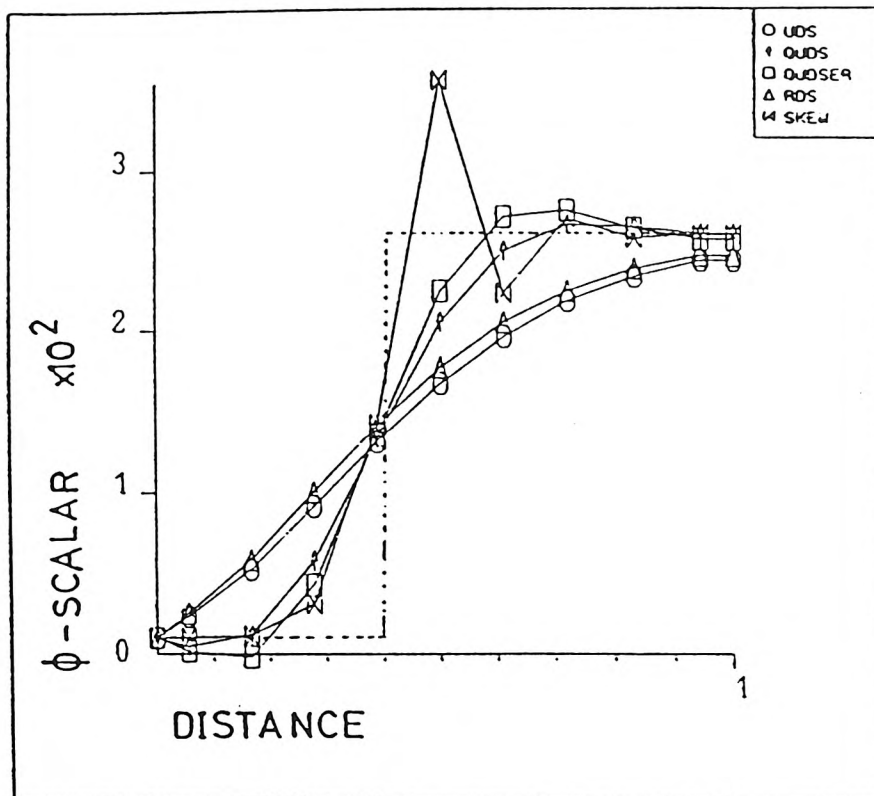


FIGURE  
6.45-5

$\phi$ -PROFILES FOR  $\theta=38.7$  DEGREES AT  
 $x=0.5$  (11 x 11)

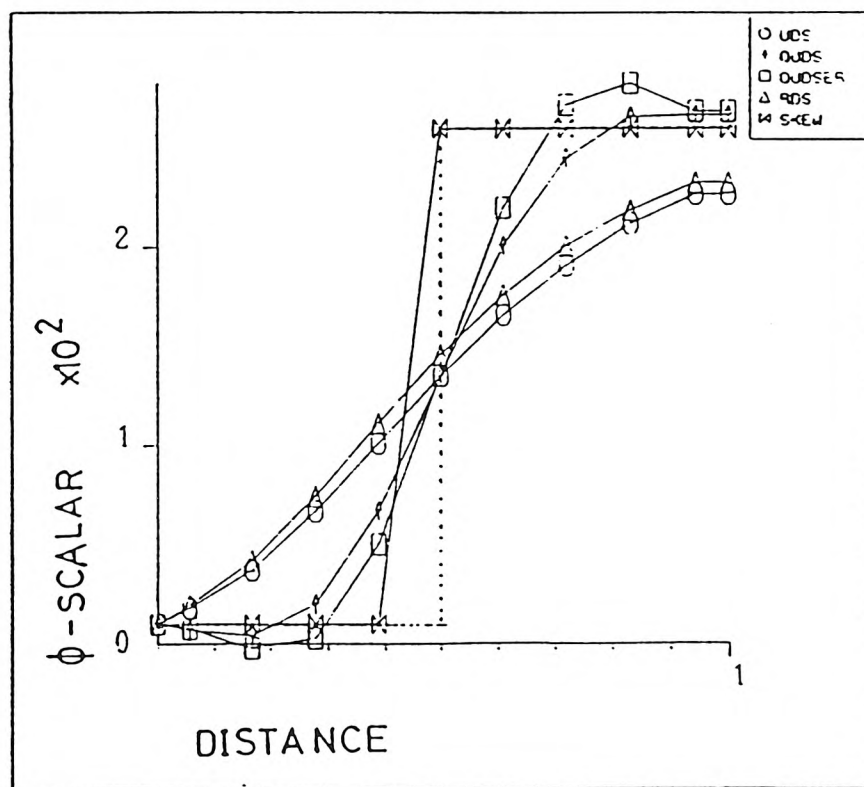


FIGURE  
6.45-6

$\phi$ -PROFILES FOR  $\theta=45$  DEGREES AT  
 $x=0.5$  (11 x 11)

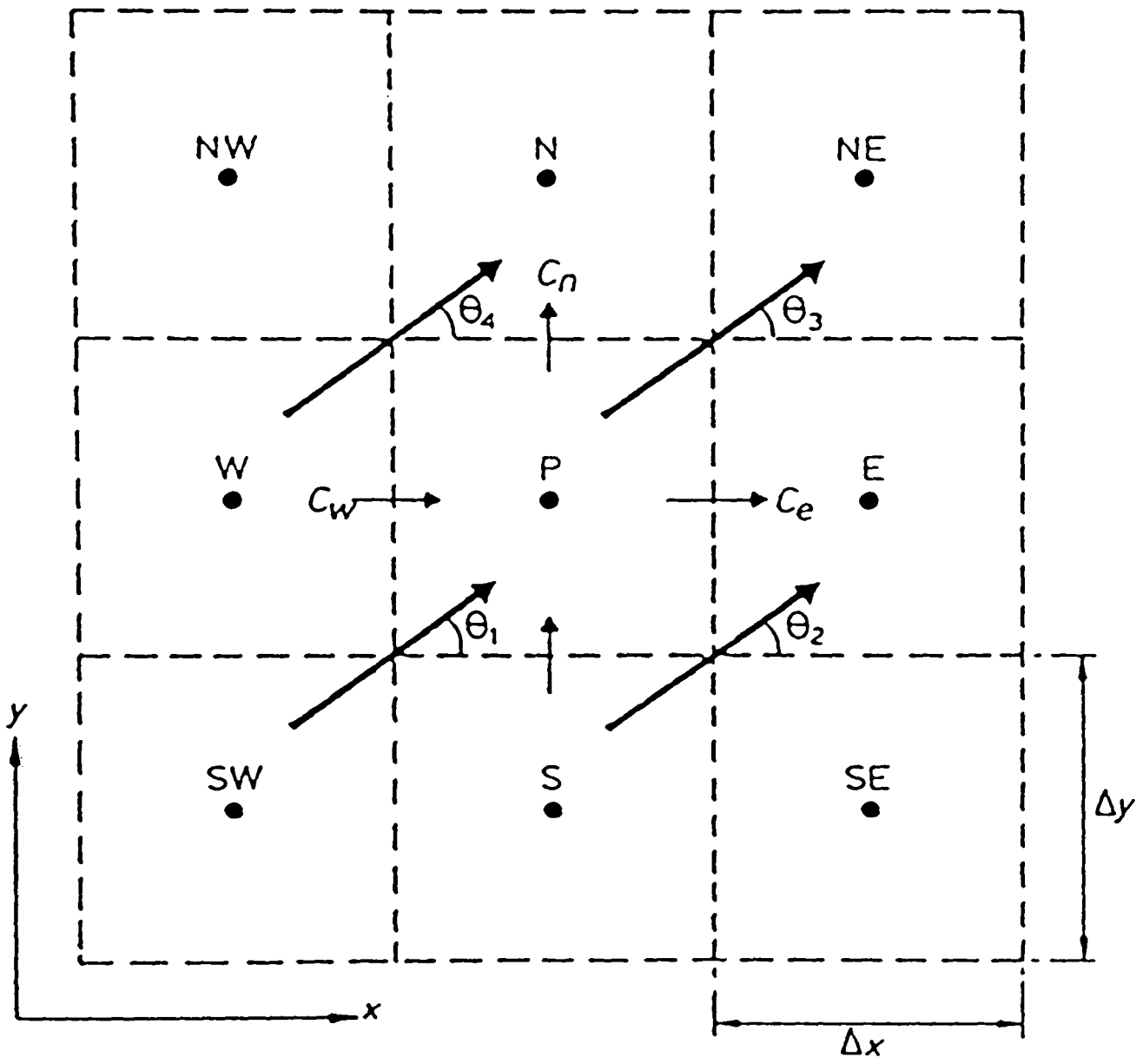


FIGURE  
7.13-1

SEGMENT OF CALCULATION FOR  
THE UPSTREAM SCHEME

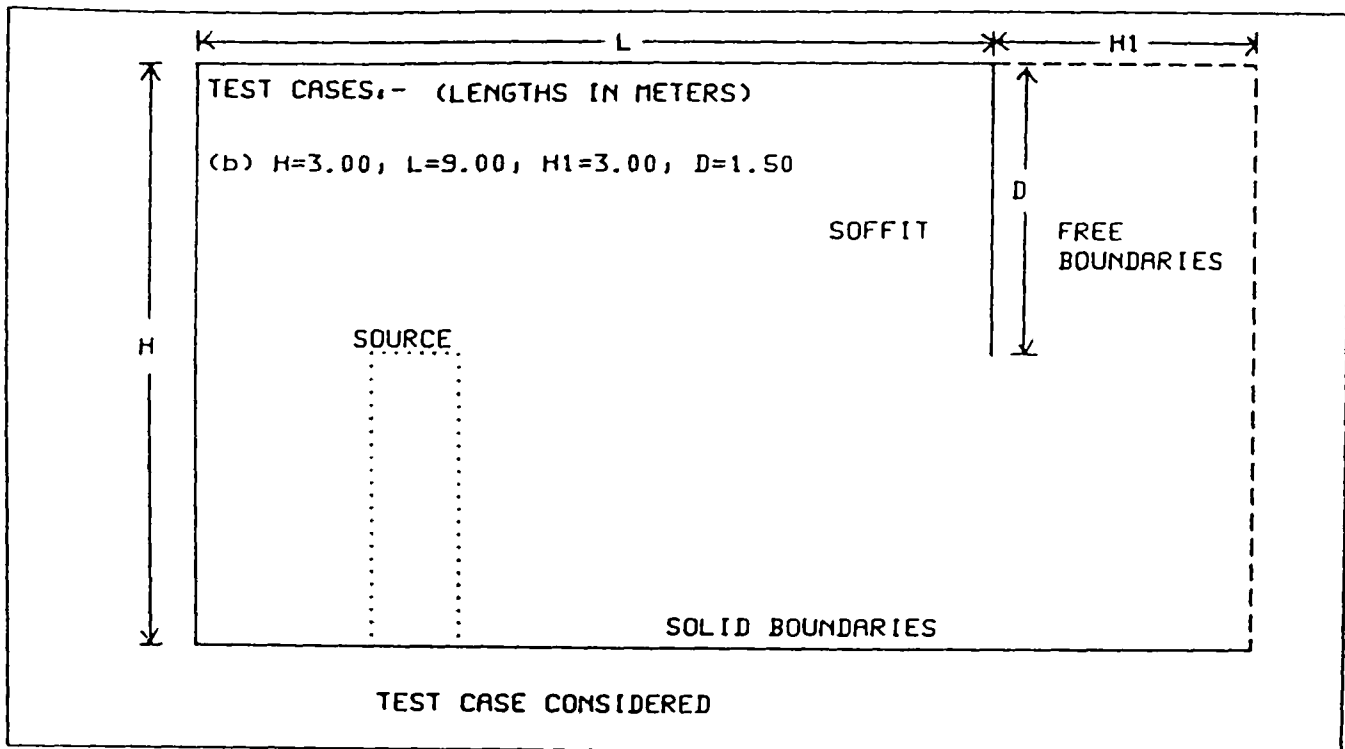


FIGURE  
8.2-1

TEST CASE CONSIDERED

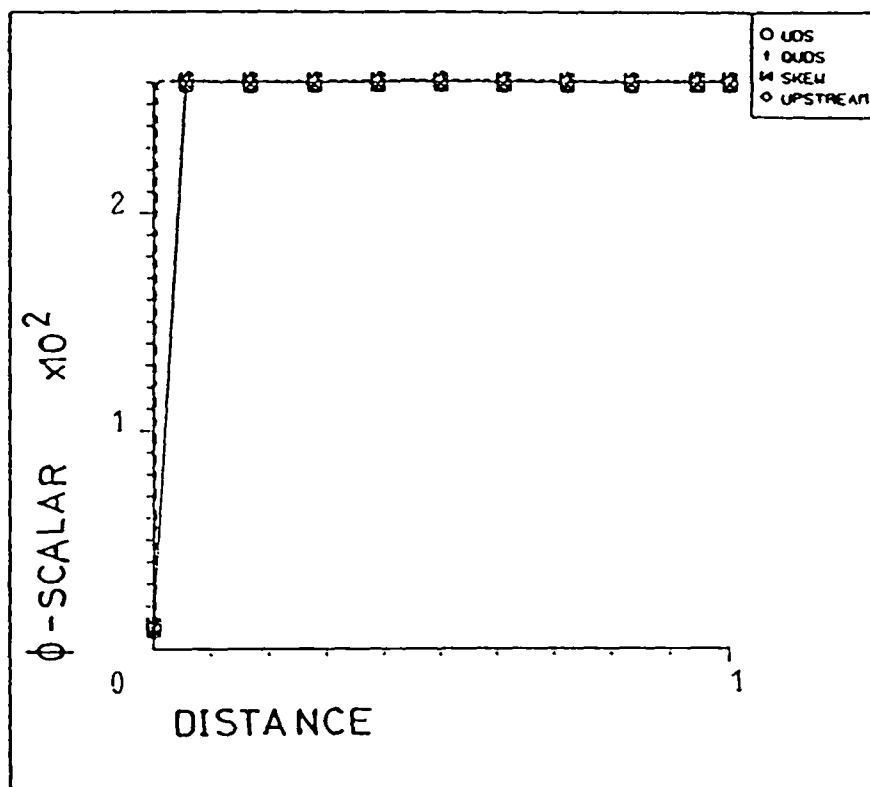


FIGURE  
8.31-1

$\phi$ -PROFILES FOR  $\theta=0$  DEGREES AT  
 $x=0.5$  (11 x 11)

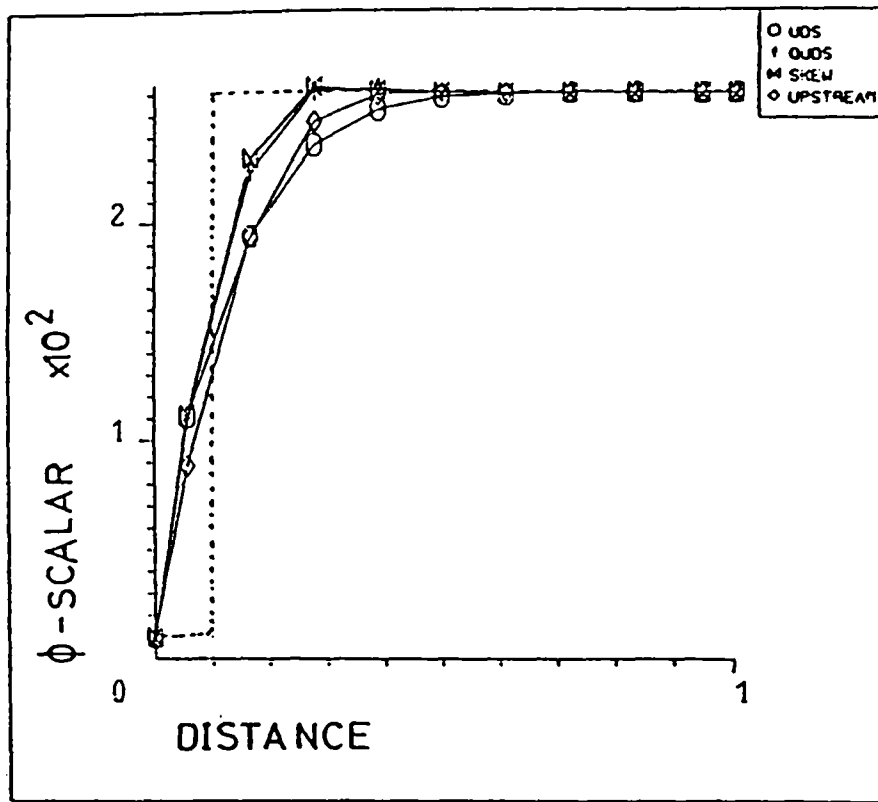


FIGURE  
8.31-2

$\phi$ -PROFILES FOR  $\theta = 11.3$  DEGREES  
(11 x 11)

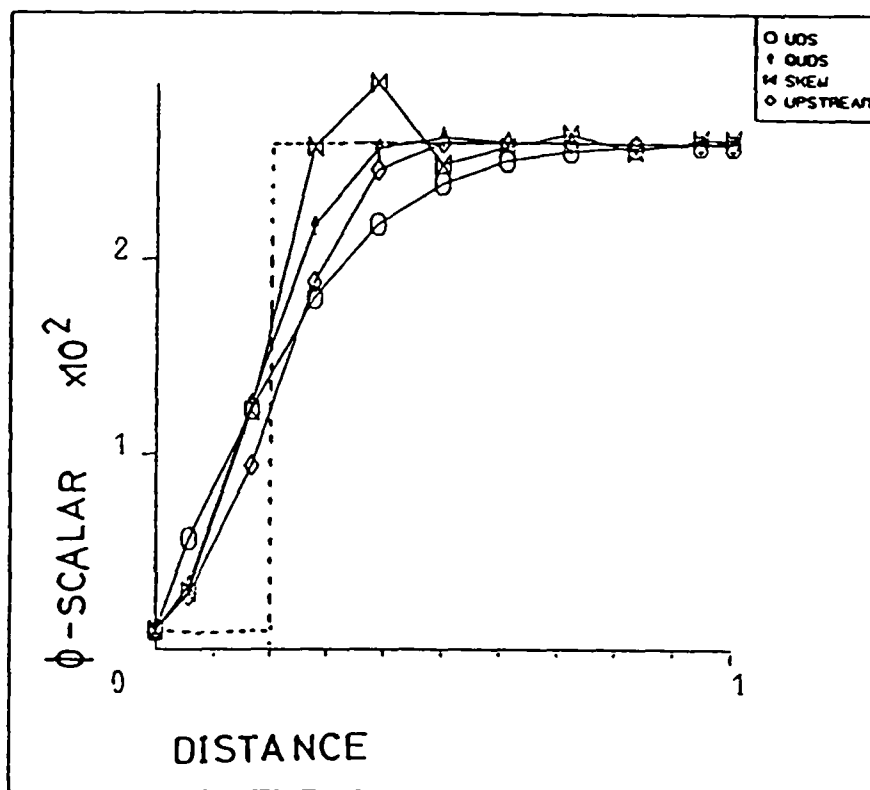


FIGURE  
8.31-3

$\phi$ -PROFILES FOR  $\theta = 21.8$  DEGREES  
(11 x 11)

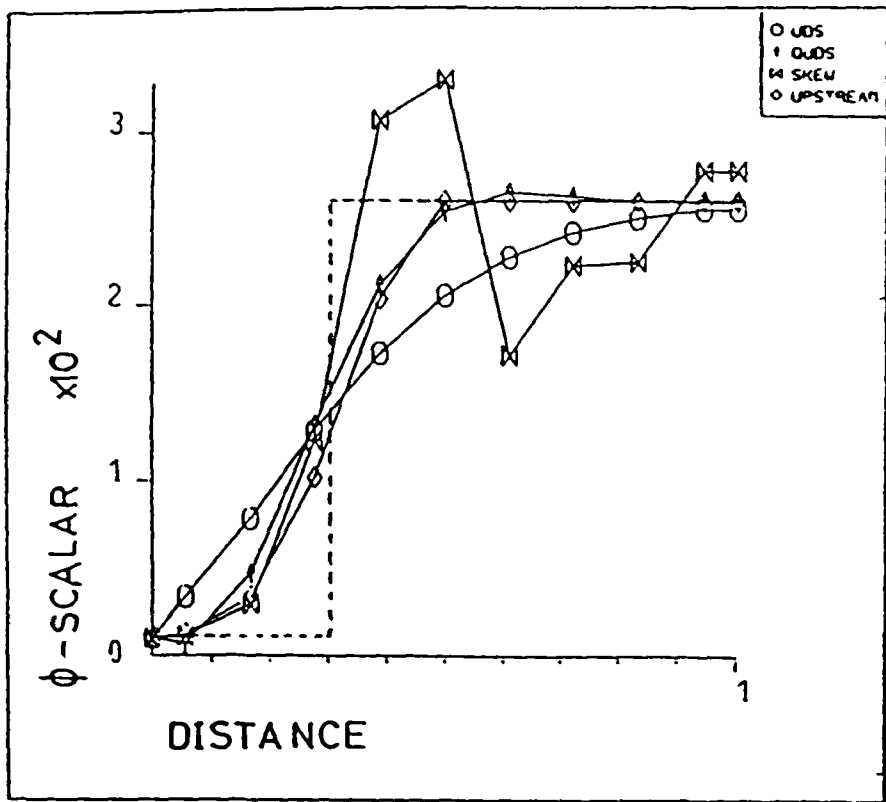


FIGURE  
8.31-4

$\phi$ -PROFILES FOR  $\theta=31$  DEGREES  
(11 x 11)

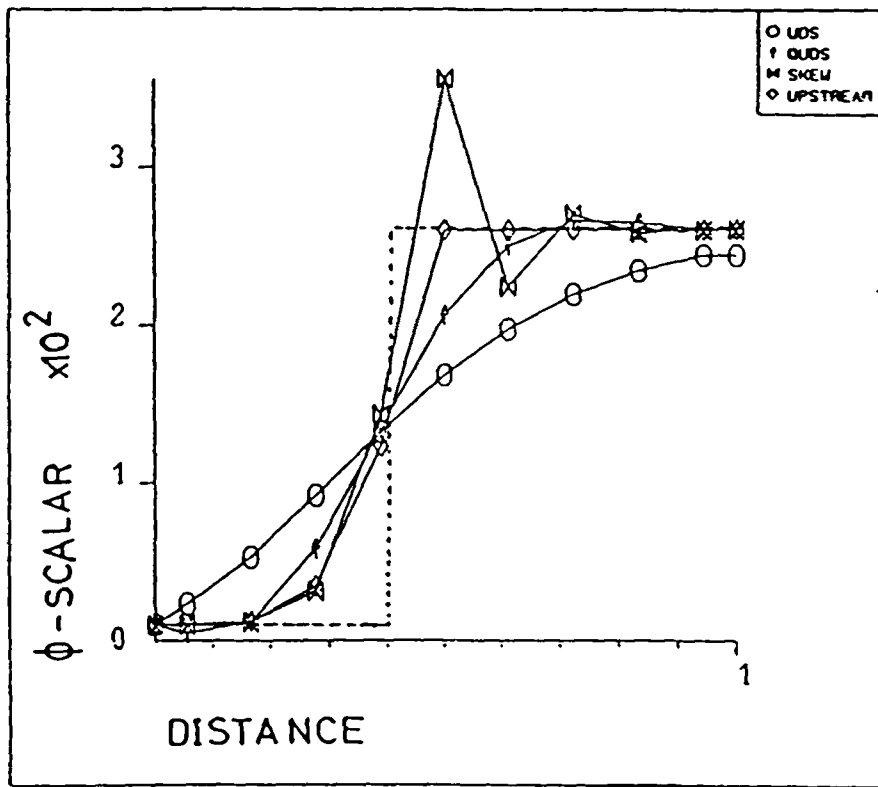


FIGURE  
8.31-5

$\phi$ -PROFILES FOR  $\theta=38.7$  DEGREES  
(11 x 11)

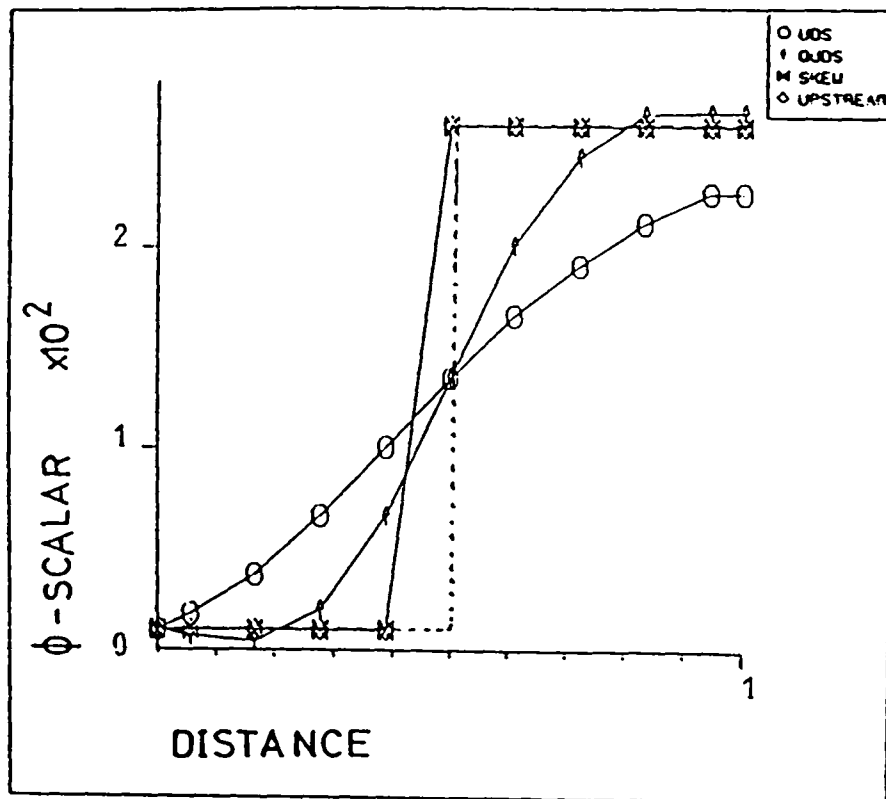


FIGURE  
8.31-6

$\phi$ -PROFILES FOR  $\theta=45$  DEGREES AT  
 $x=0.5$  (11 x 11)

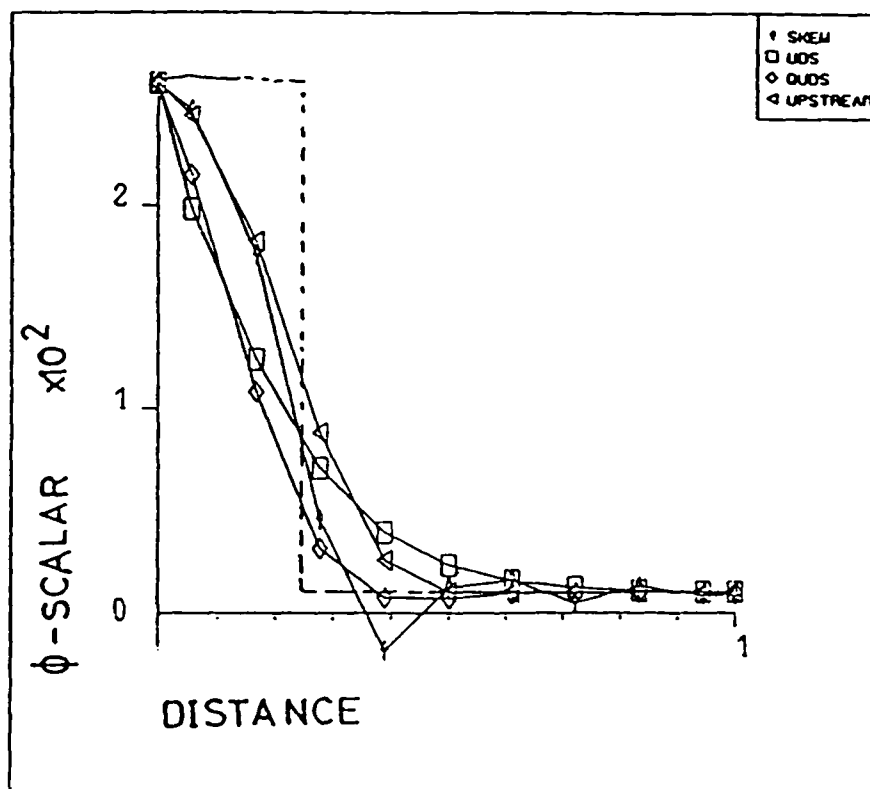


FIGURE  
8.31-7

$\phi$ -PROFILES FOR  $\theta=67.5$  DEGREES AT  
 $y=0.4$  (11 x 11)

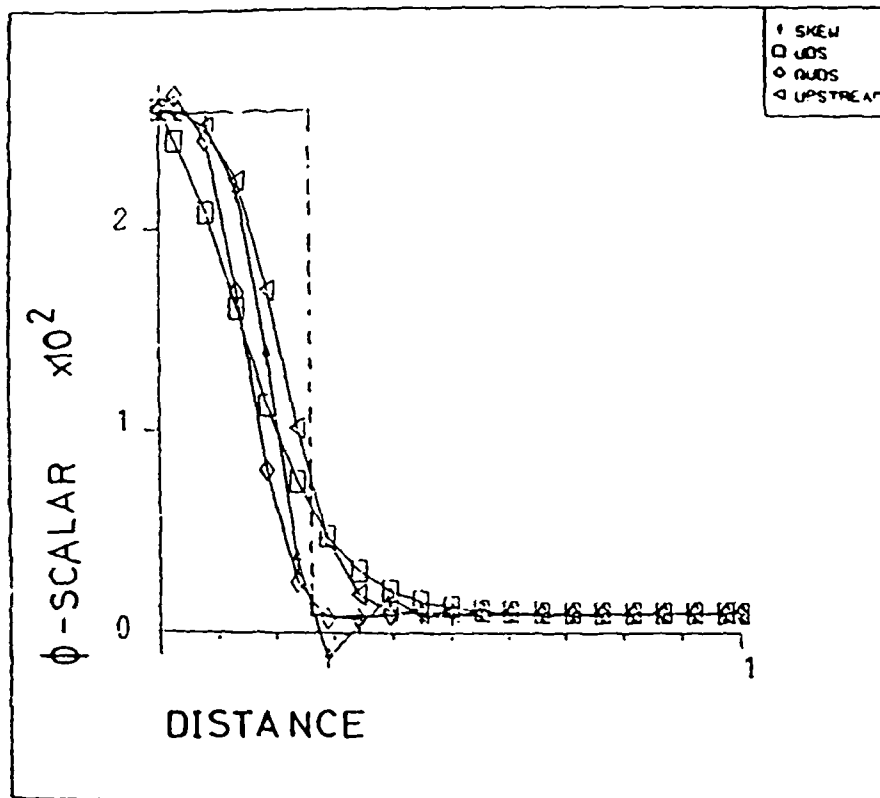


FIGURE  
8.31-8

$\phi$ -PROFILES FOR  $\theta=67.5$  DEGREES AT  
 $y=0.4$  (21 x 21)

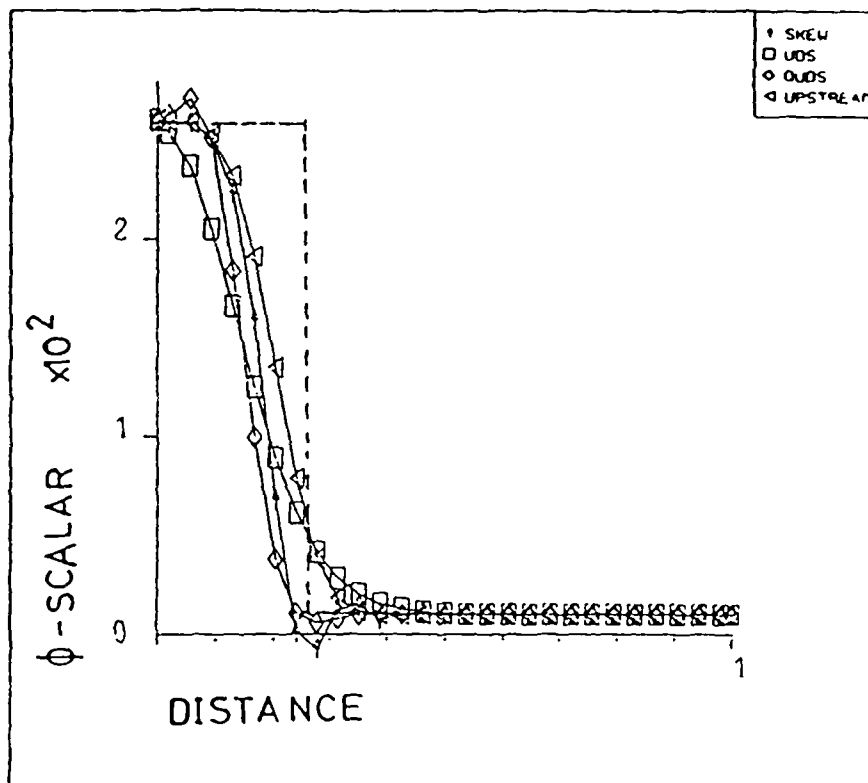


FIGURE  
8.31-9

$\phi$ -PROFILES FOR  $\theta=67.5$  DEGREES AT  
 $y=0.4$  (31 x 31)

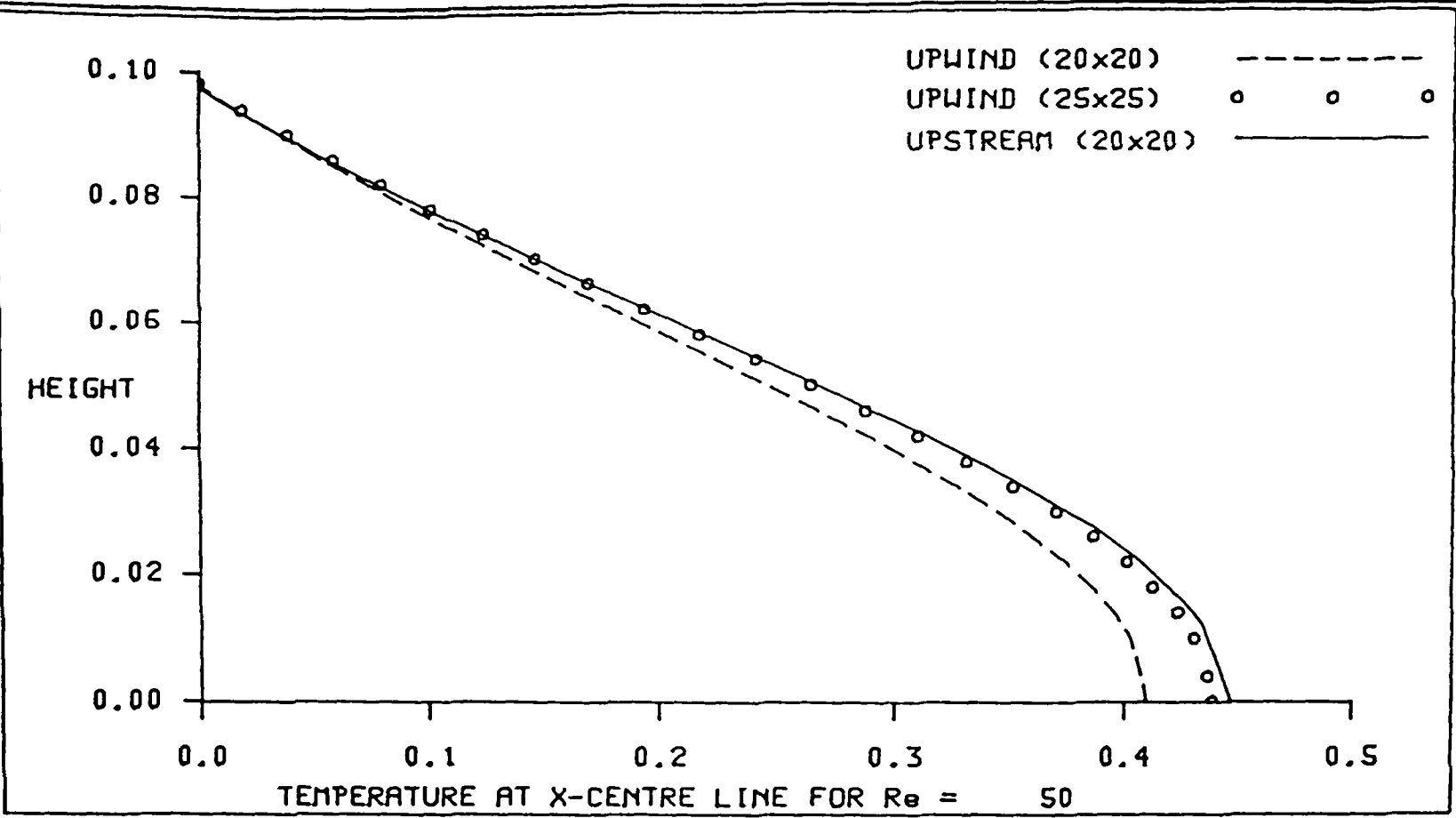


FIGURE  
8.33-1

TEMPERATURE VARIATION AT X-CENTRELINE  
FOR  $Re=50$

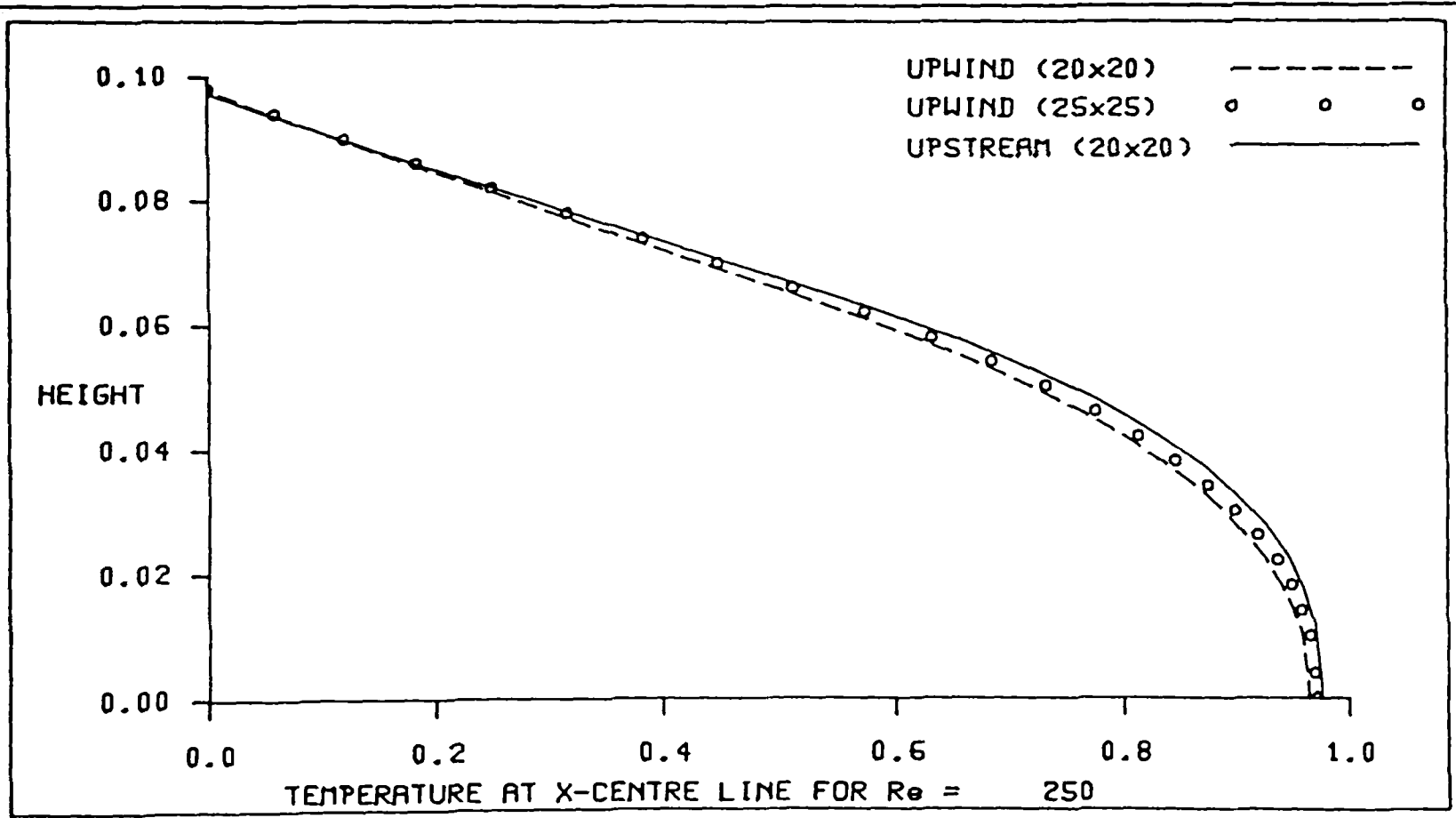


FIGURE  
8.33-2

TEMPERATURE VARIATION AT X-CENTRELINE  
FOR  $Re=250$

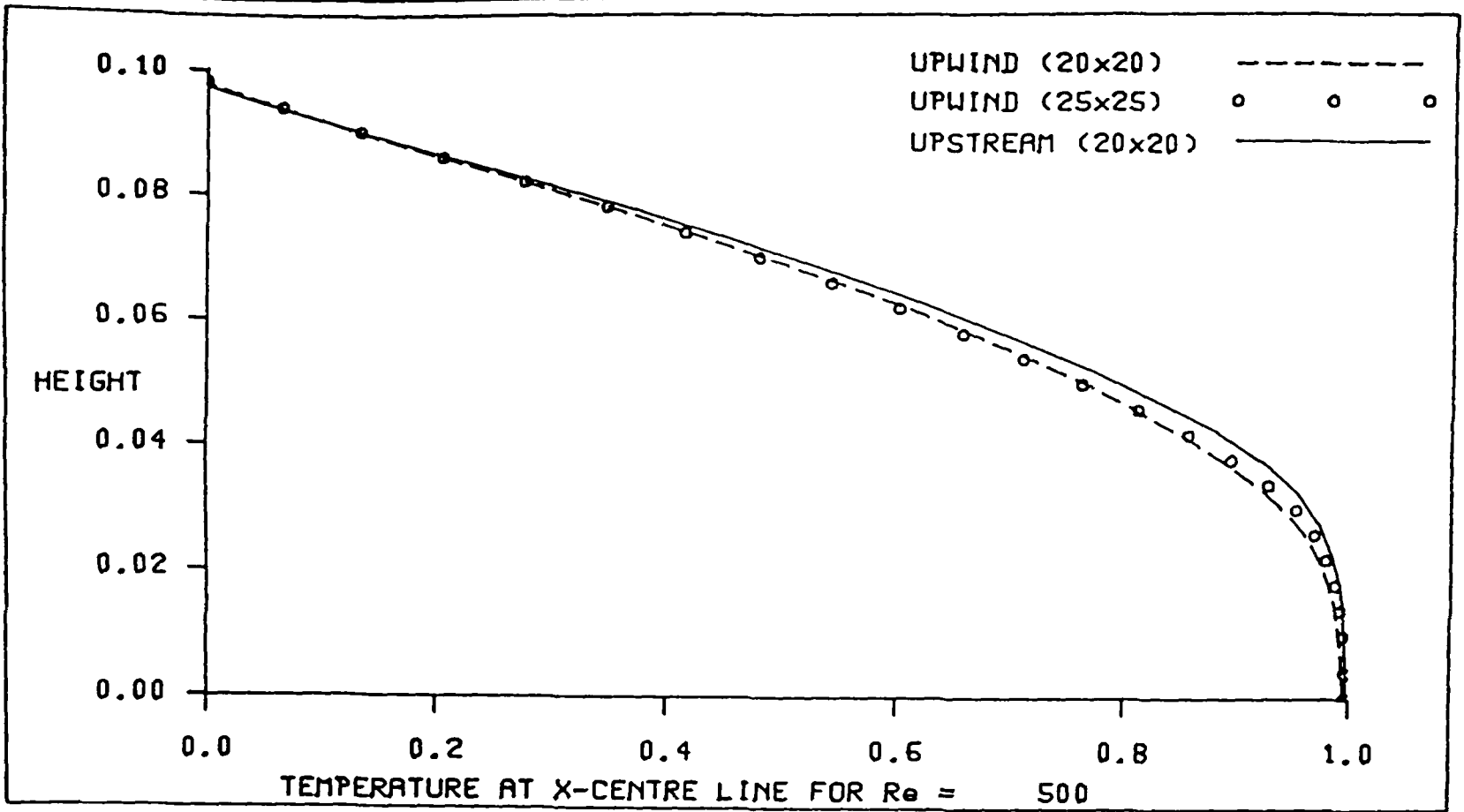


FIGURE  
8.33-3

TEMPERATURE VARIATION AT X-CENTRELINE  
FOR  $Re=500$

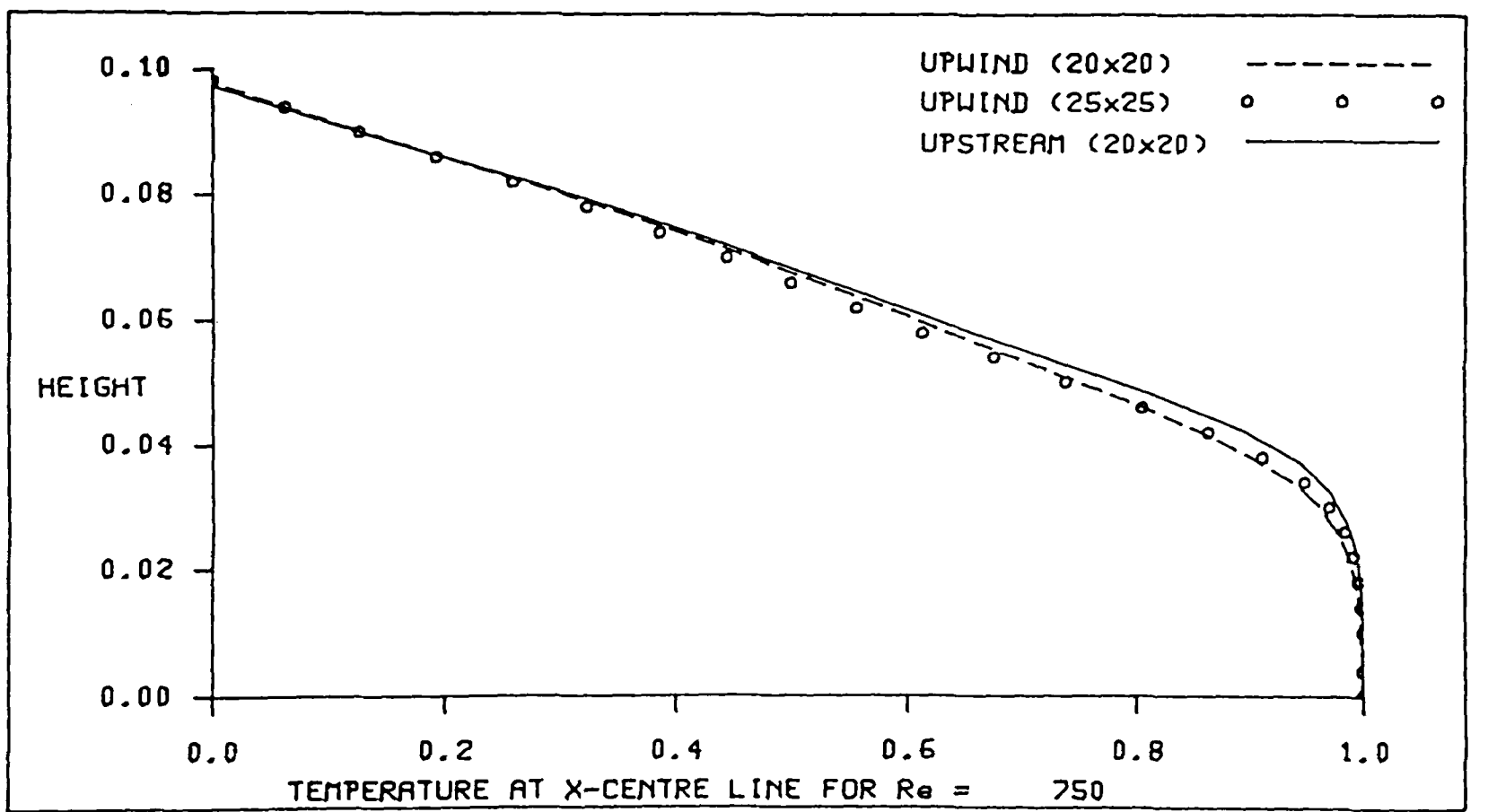


FIGURE  
8.33-4

TEMPERATURE VARIATION AT X-CENTRELINE  
FOR  $Re=750$

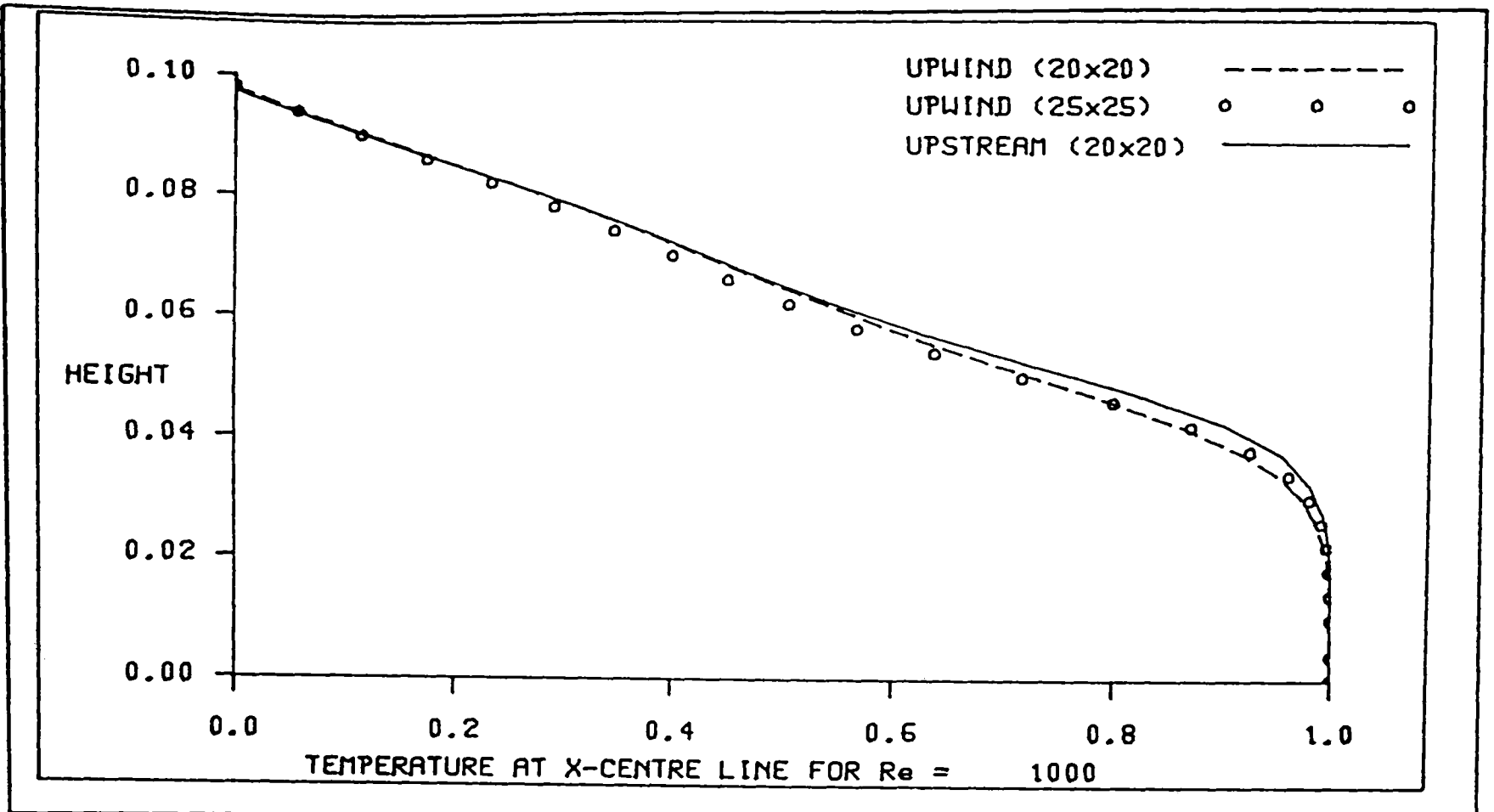


FIGURE  
8.33-5

TEMPERATURE VARIATION AT X-CENTRELINE  
FOR  $Re=1000$

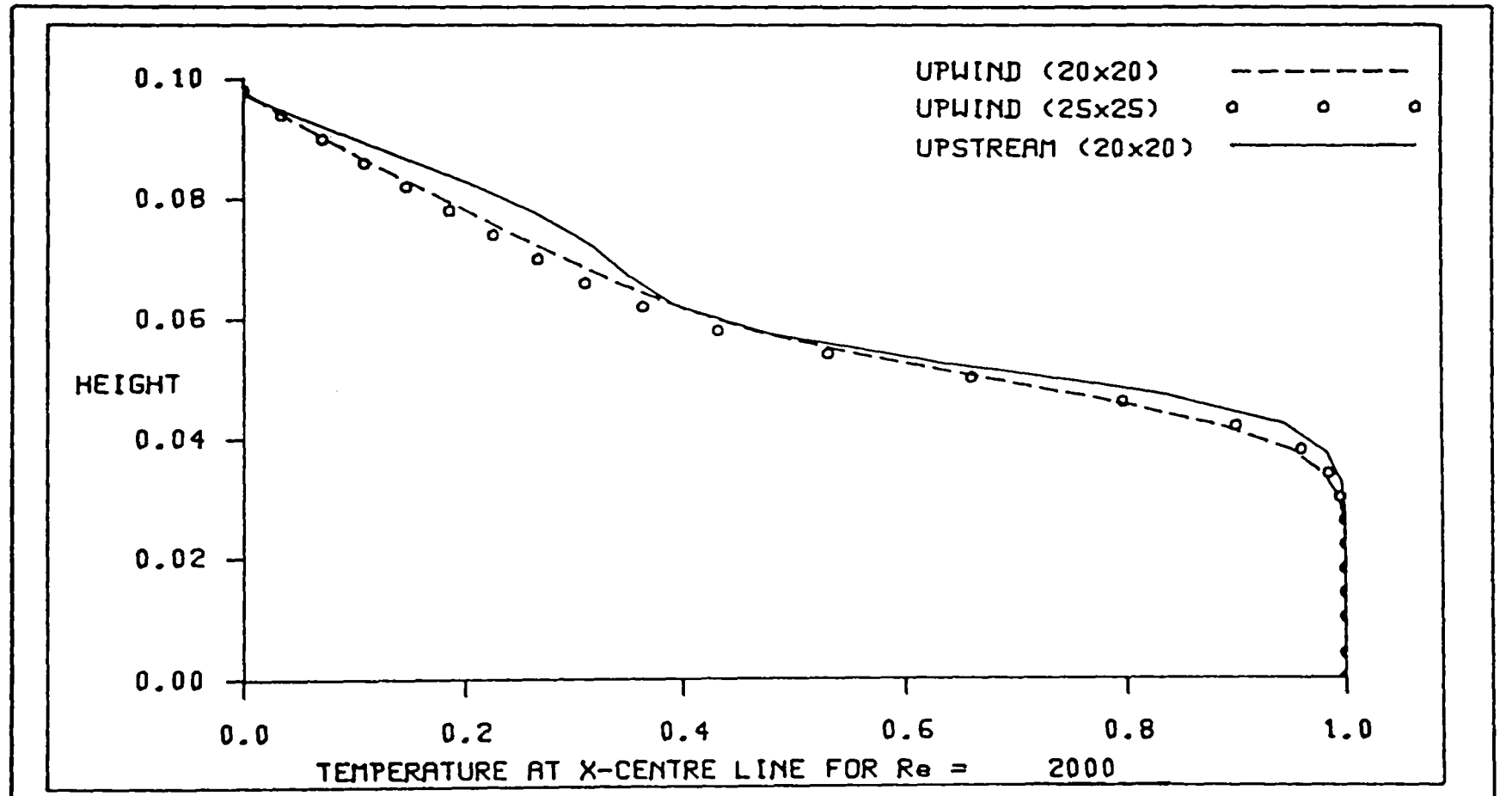


FIGURE  
8.33-6

TEMPERATURE VARIATION AT X-CENTRELINE  
FOR  $Re=2000$

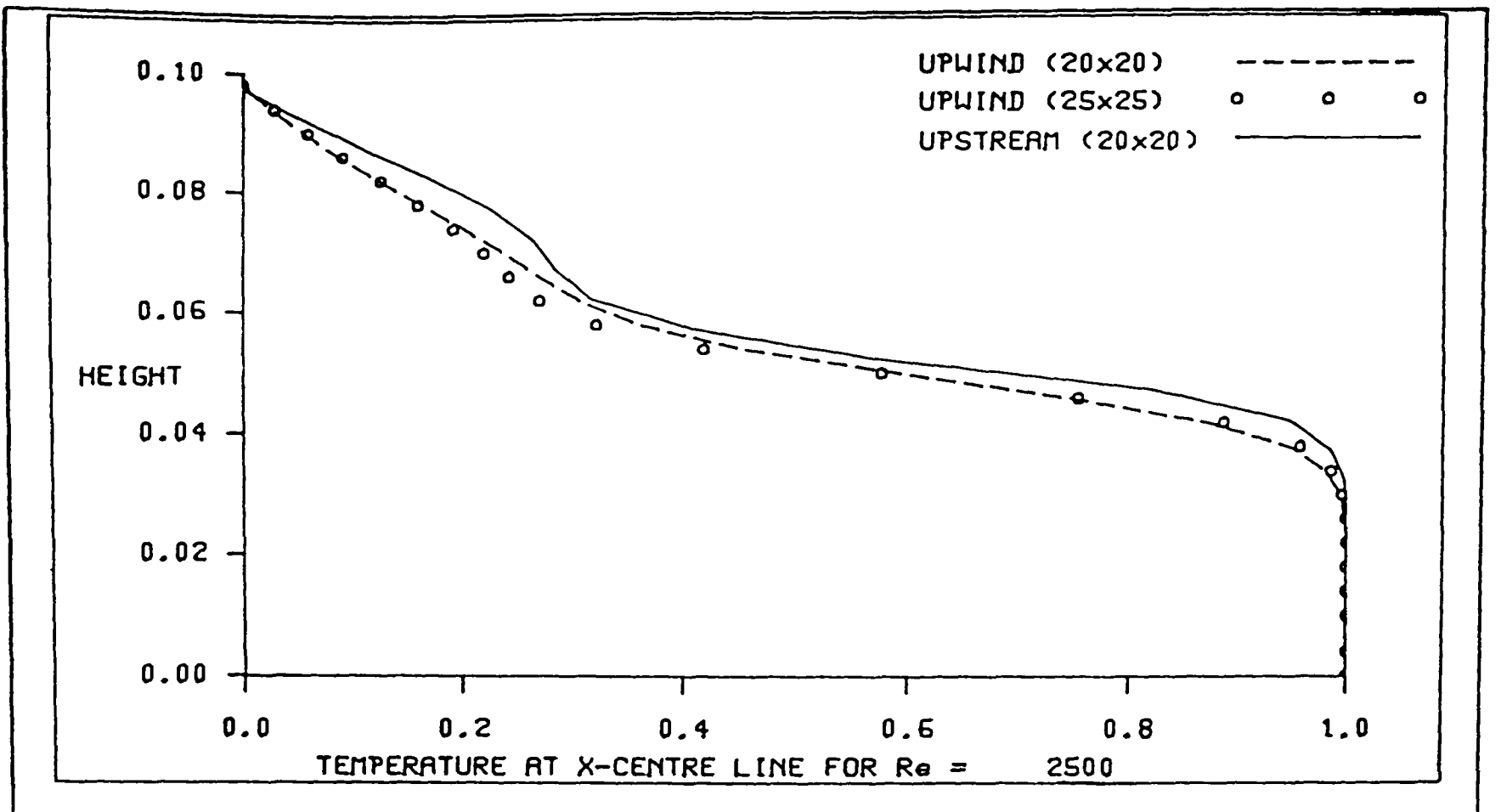


FIGURE  
8.33-7

TEMPERATURE VARIATION AT X-CENTRELINE  
FOR  $Re=2500$

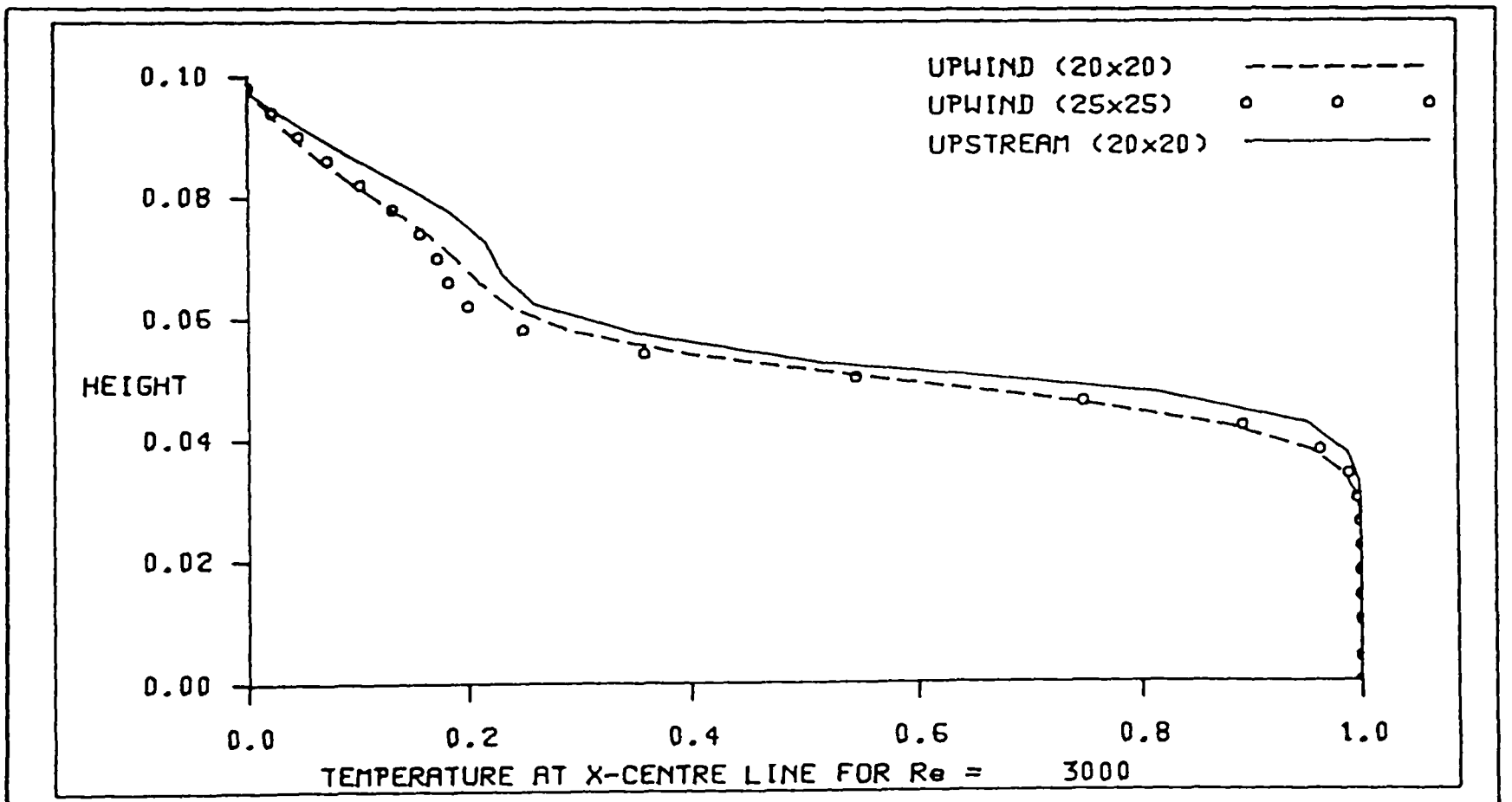


FIGURE  
8.33-8

TEMPERATURE VARIATION AT X-CENTRELINE  
FOR  $Re=3000$

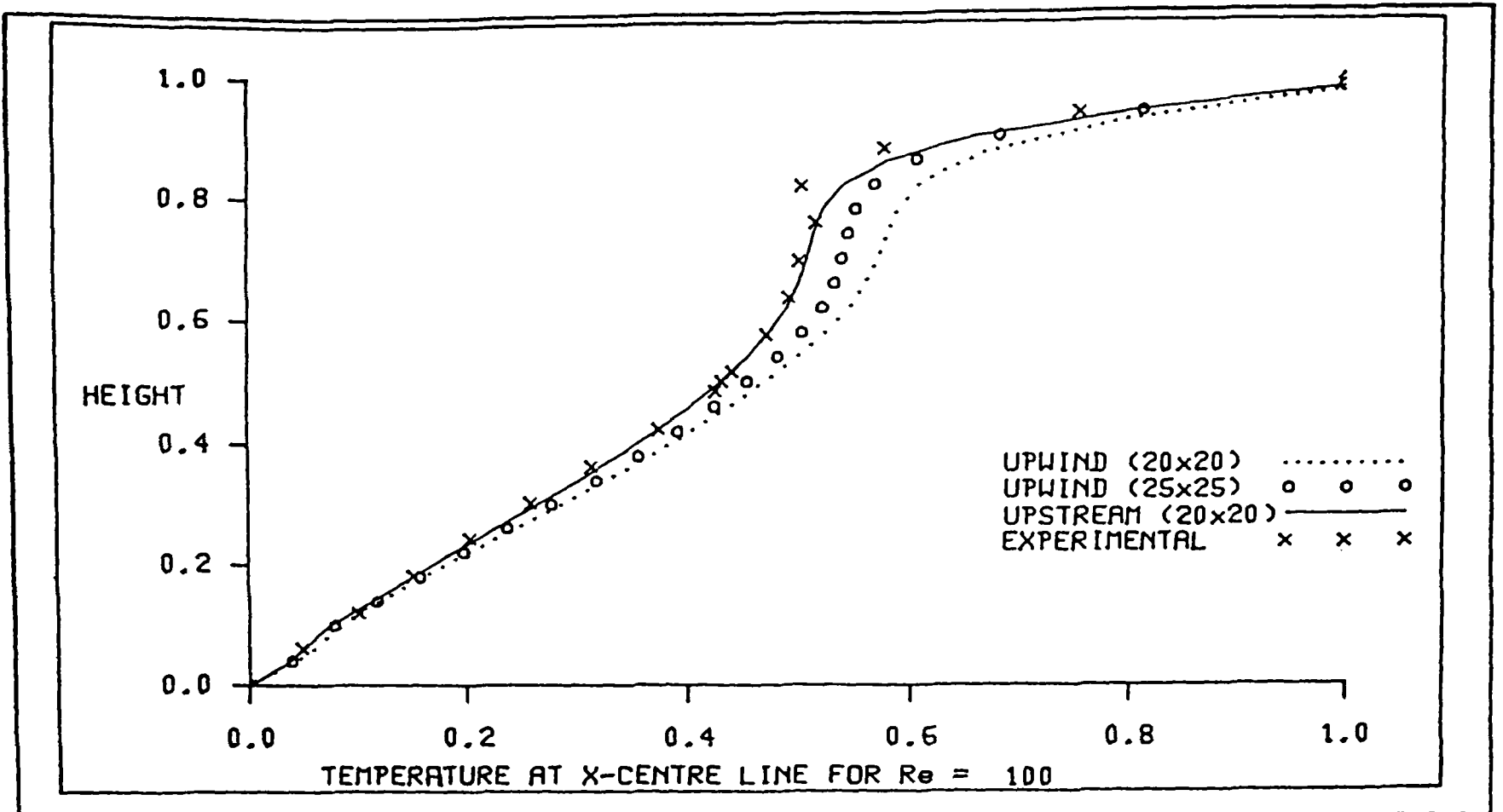


FIGURE  
8.35-1

TEMPERATURE VARIATION AT X-CENTRELINE  
FOR  $Re=100$

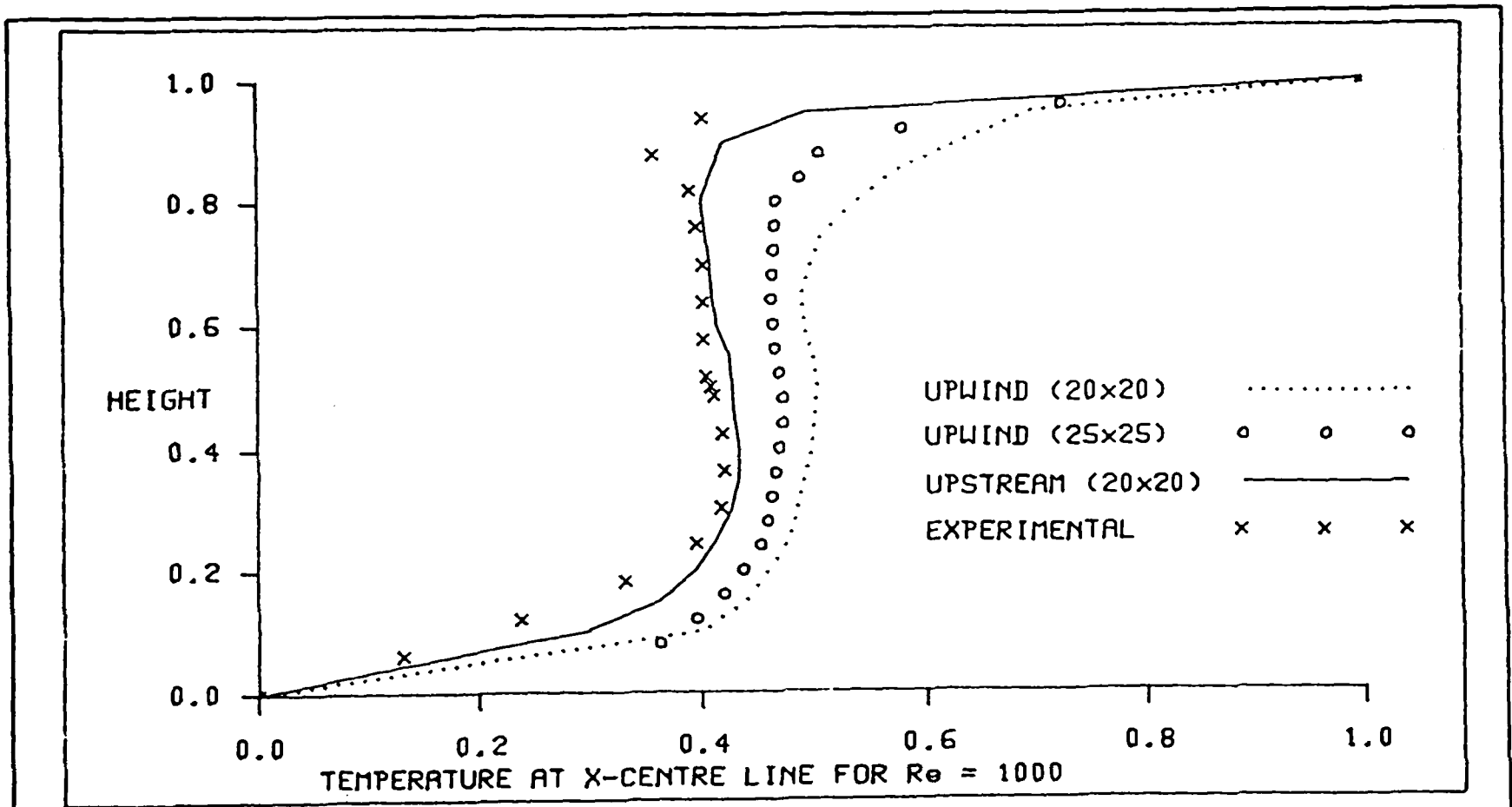


FIGURE  
8.35-2

TEMPERATURE VARIATION AT X-CENTRELINE  
FOR  $Re=1000$

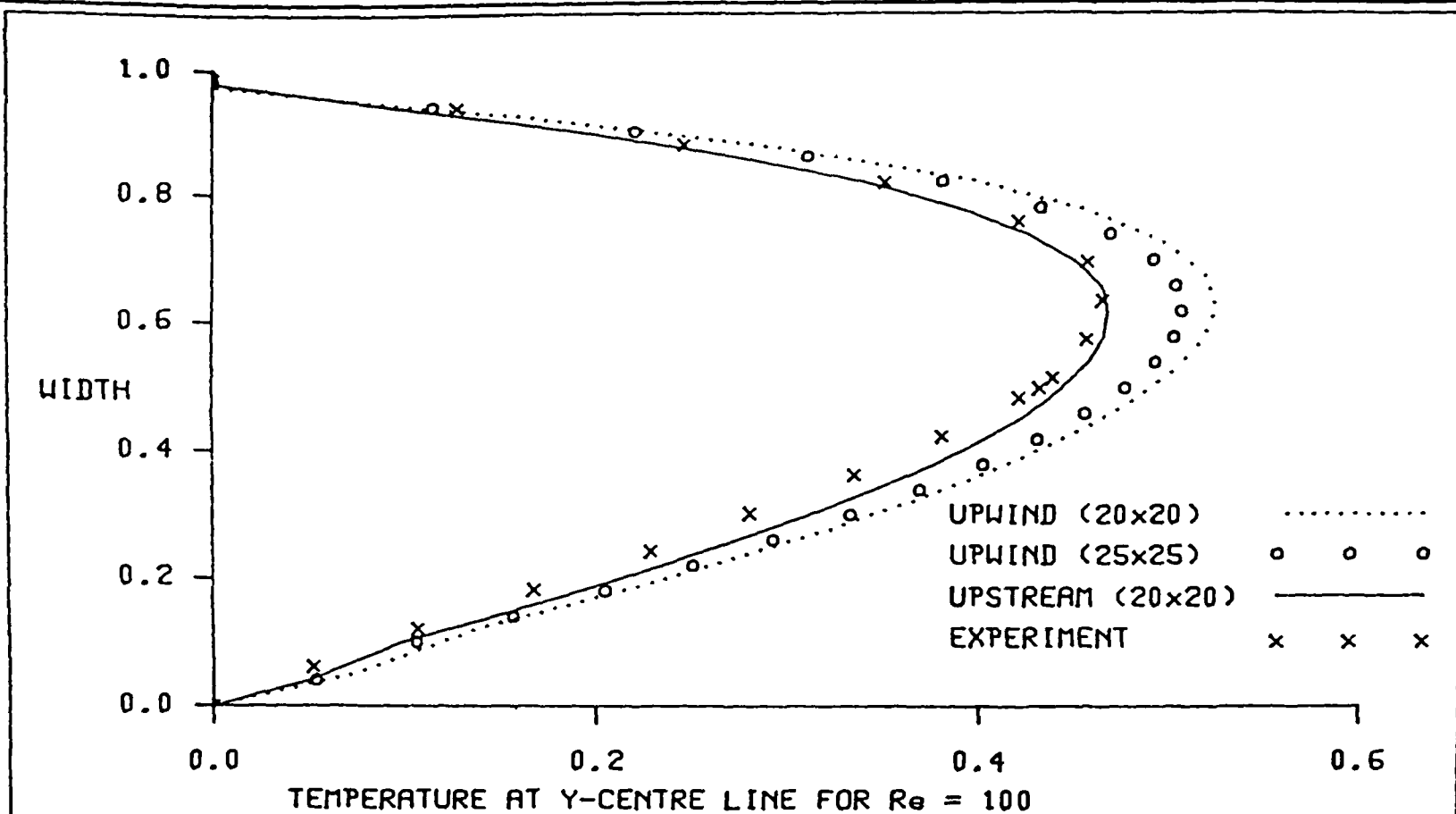


FIGURE  
8.35-3

TEMPERATURE VARIATION AT X-CENTRELINE  
FOR  $Re=100$

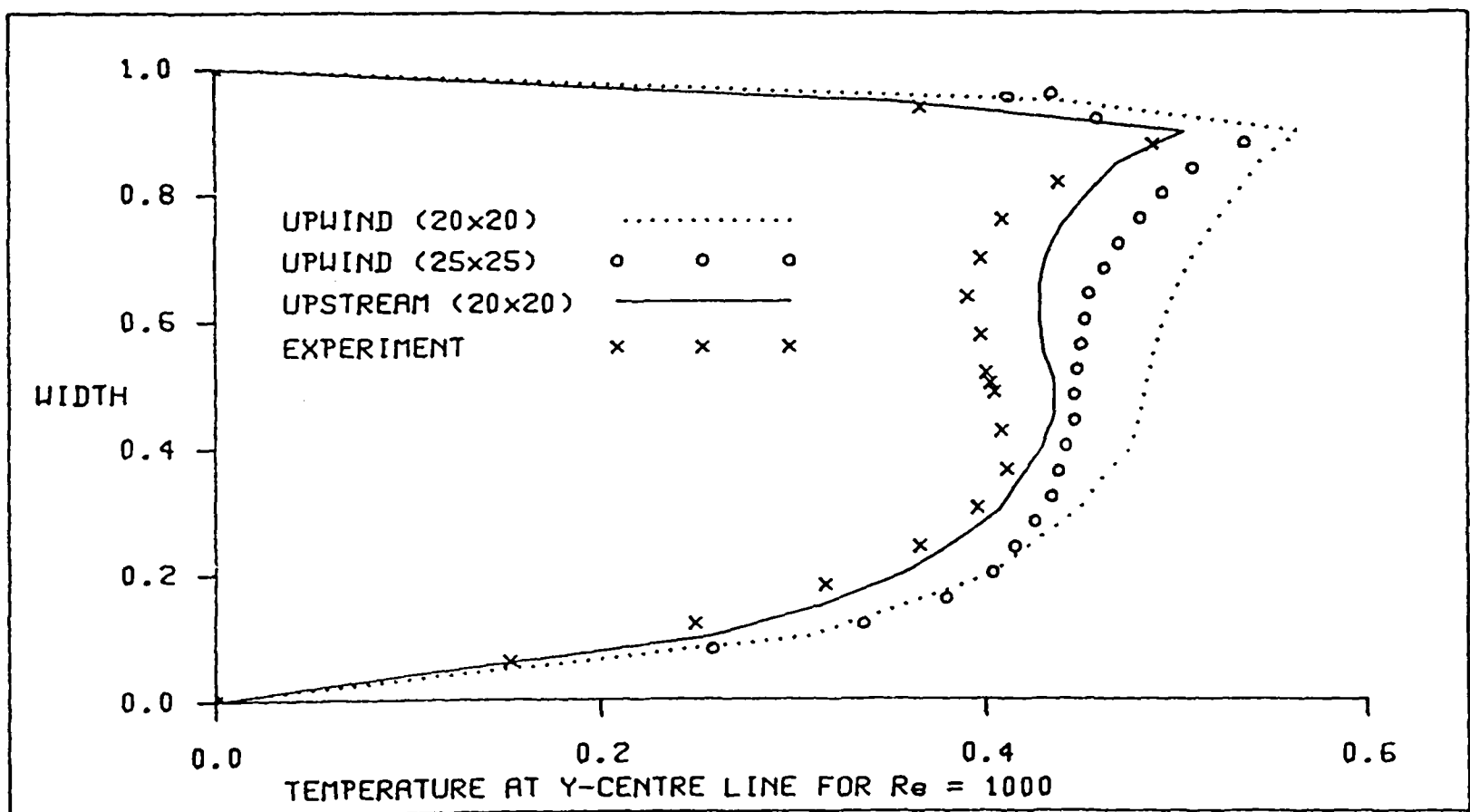


FIGURE  
8.35-4

TEMPERATURE VARIATION AT X-CENTRELINE  
FOR  $Re=1000$

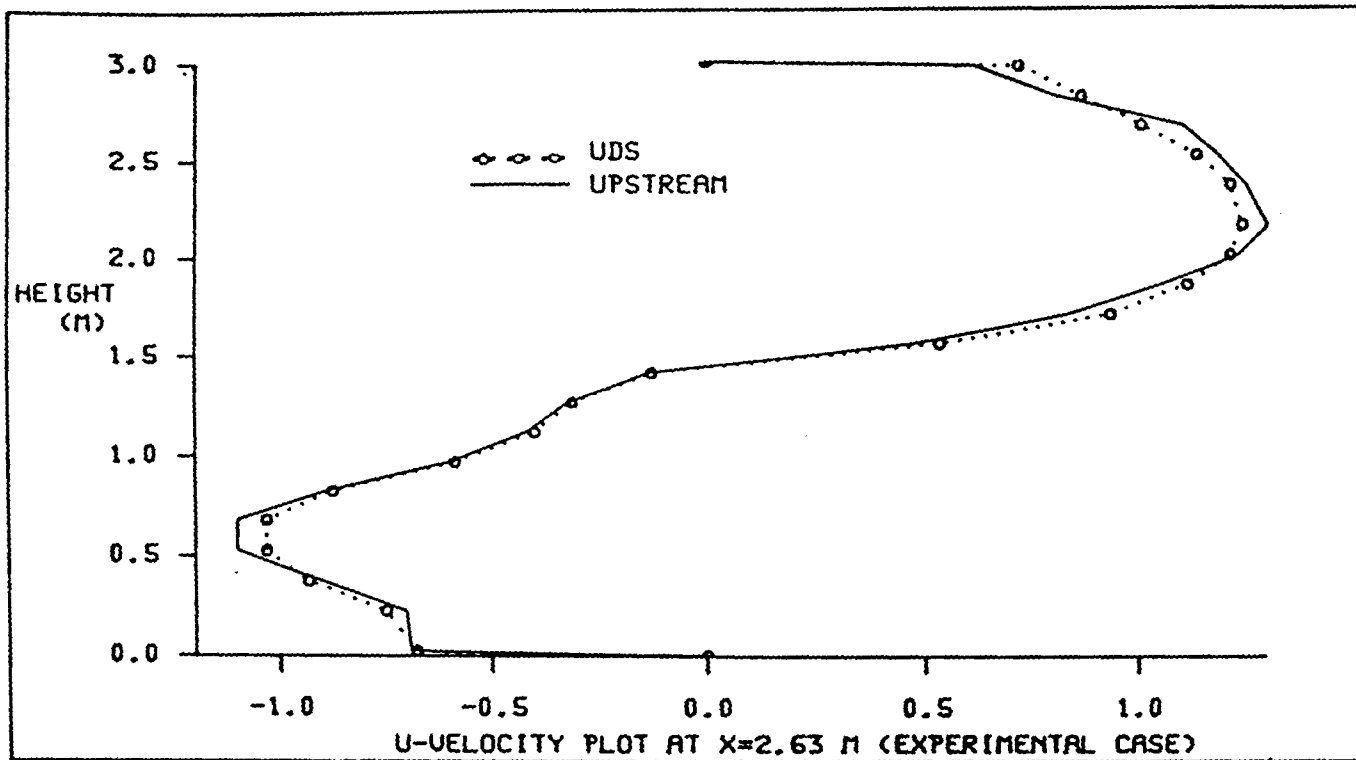


FIGURE  
8.37-1

U-VELOCITY VARIATION AT  $x=2.63\text{m}$   
(EXPERIMENTAL CASE)

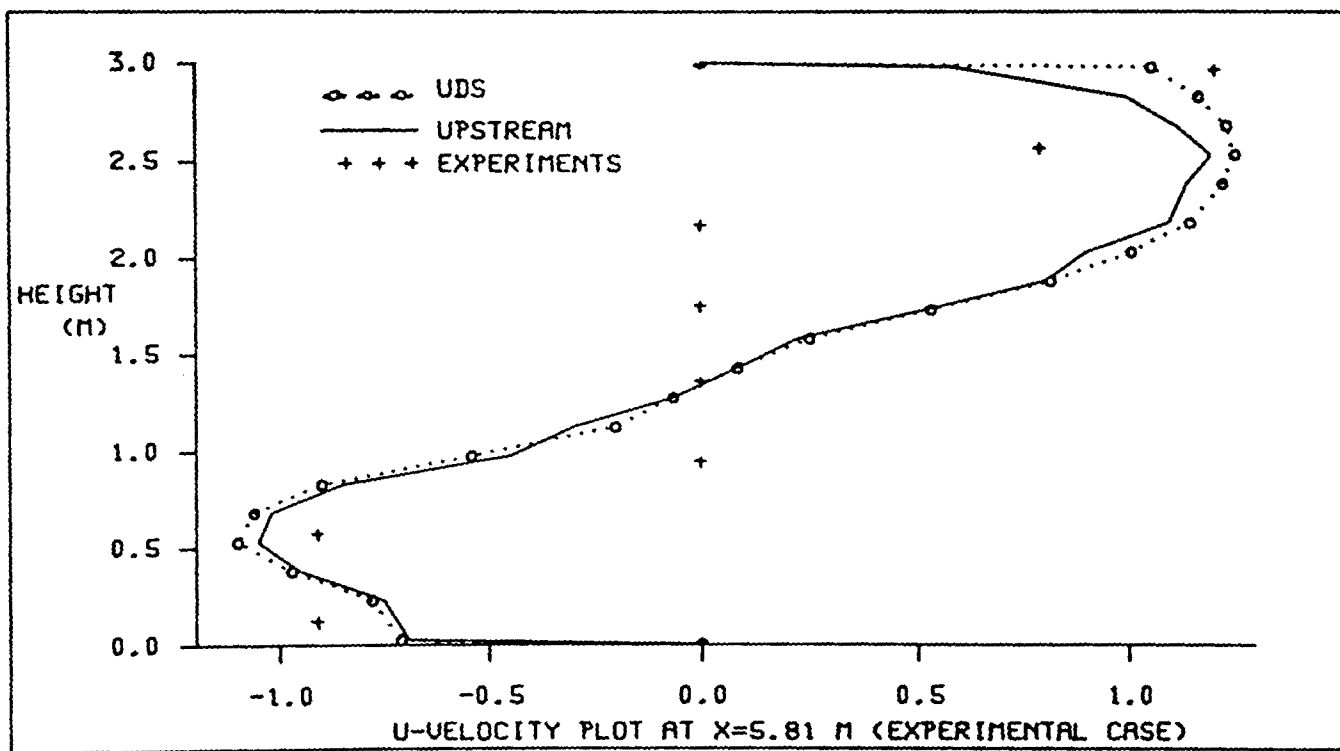


FIGURE  
8.37-2

U-VELOCITY VARIATION AT  $x=5.81\text{m}$   
(EXPERIMENTAL CASE)

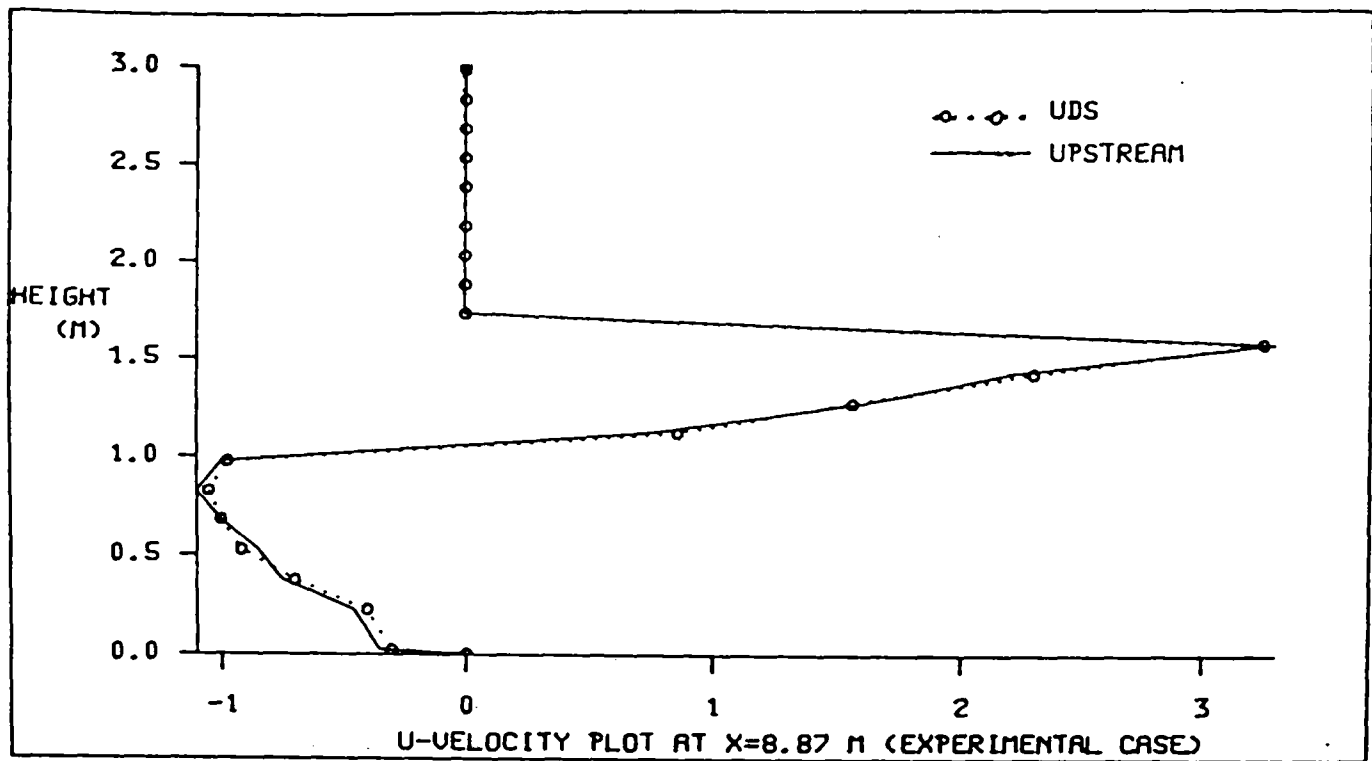


FIGURE 8.37-3

U-VELOCITY VARIATION AT x=8.87m (EXPERIMENTAL CASE)

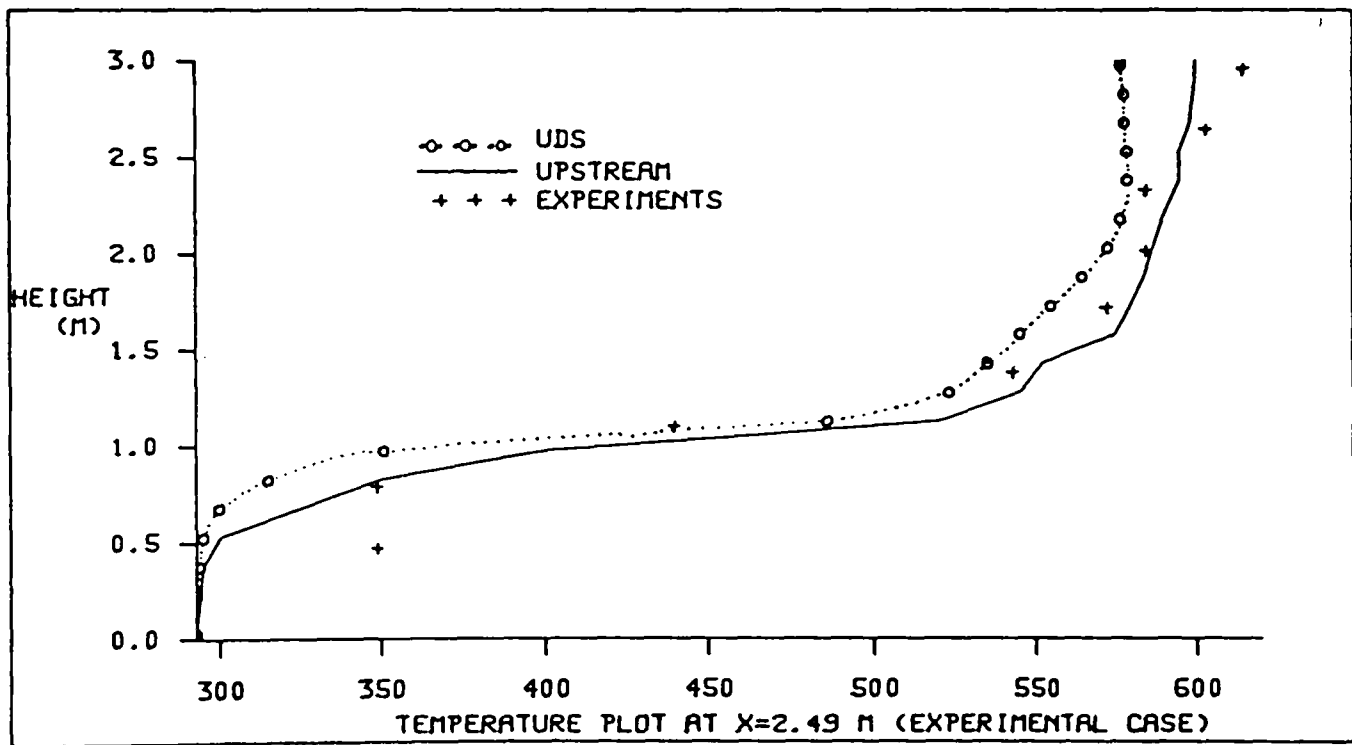


FIGURE 8.37-4

TEMPERATURE VARIATION AT x=2.49m (EXPERIMENTAL CASE)

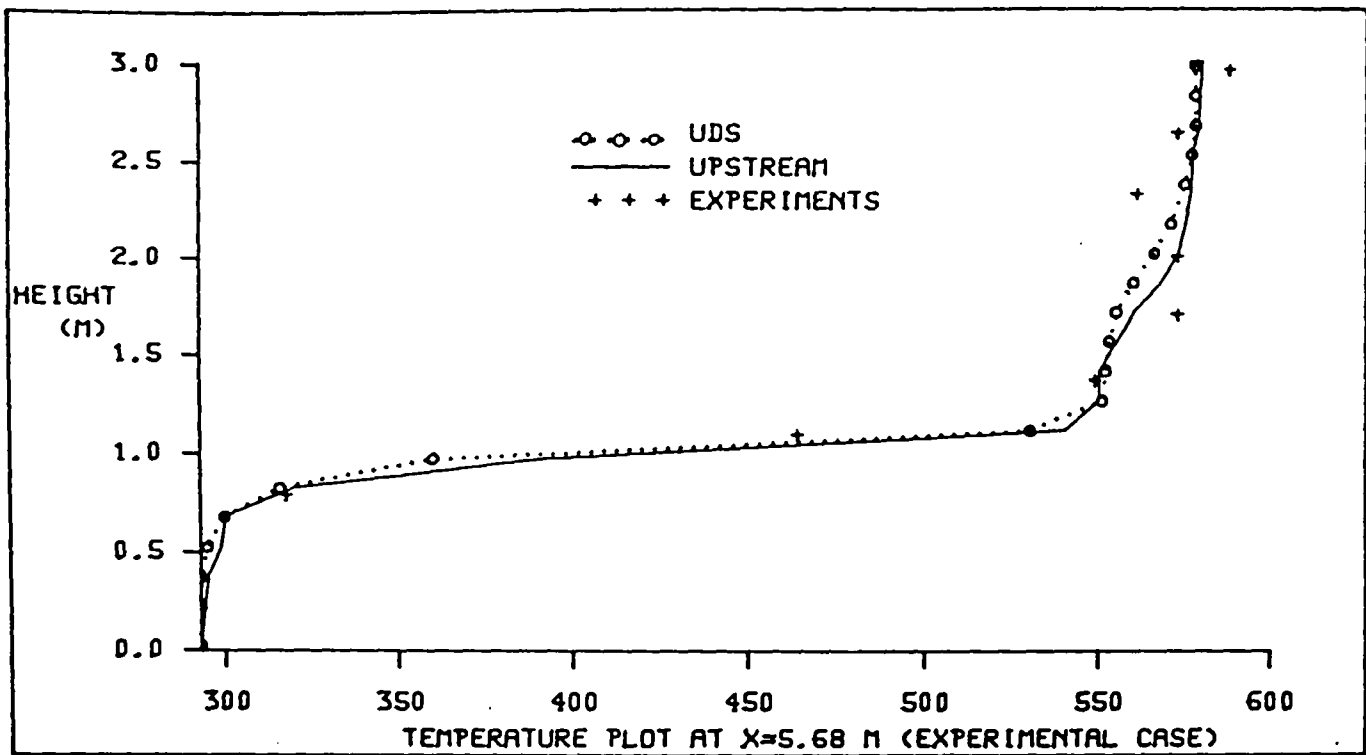


FIGURE 8.37-5

TEMPERATURE VARIATION AT x=5.68m (EXPERIMENTAL CASE)

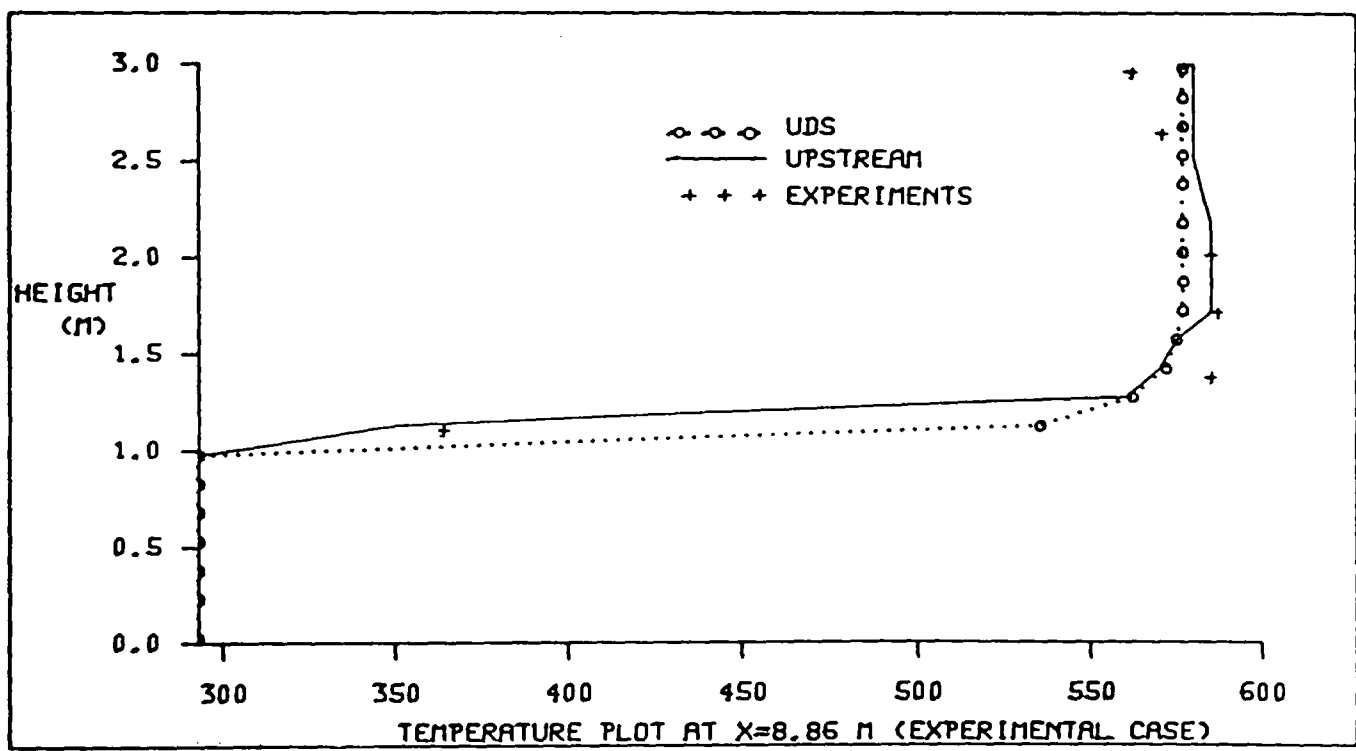


FIGURE 8.37-6

TEMPERATURE VARIATION AT x=8.86m (EXPERIMENTAL CASE)

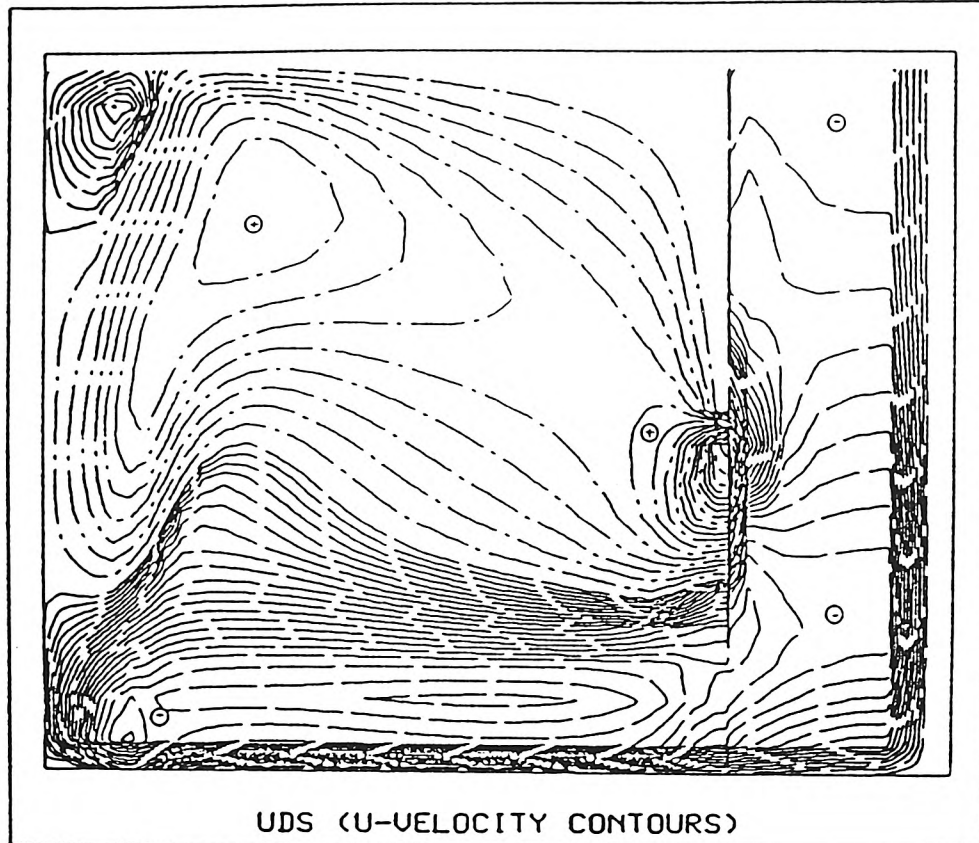


FIGURE  
8.37-7

U-VELOCITY CONTOURS FOR UDS

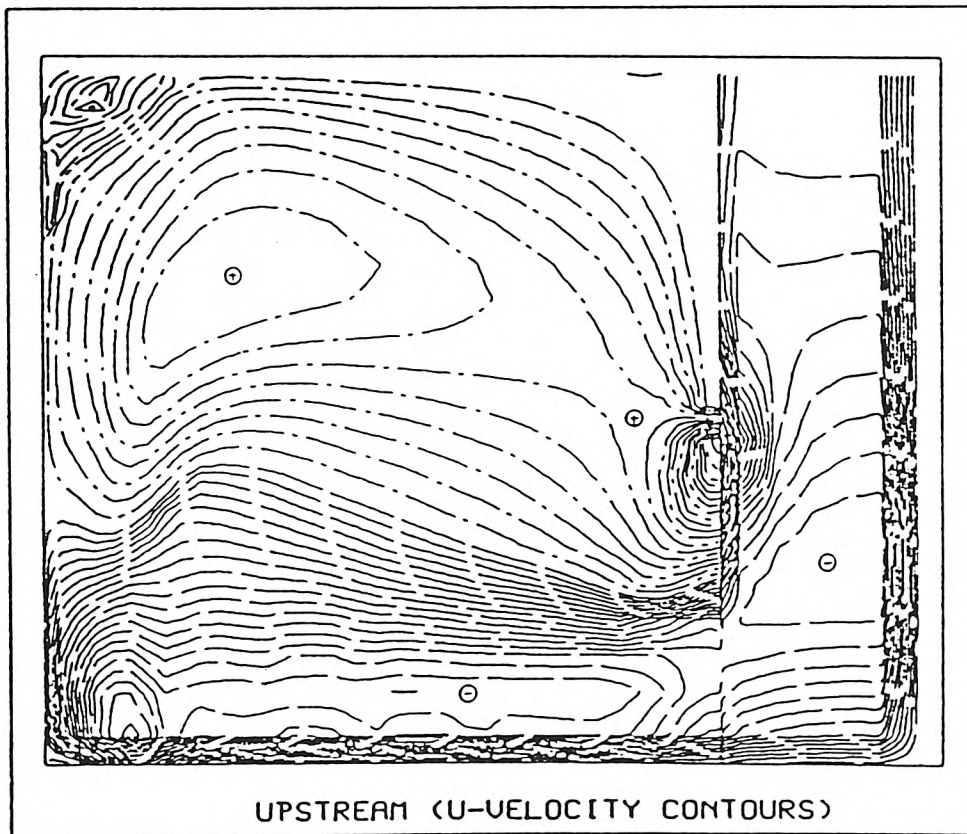


FIGURE  
8.37-8

U-VELOCITY CONTOURS FOR UPSTREAM

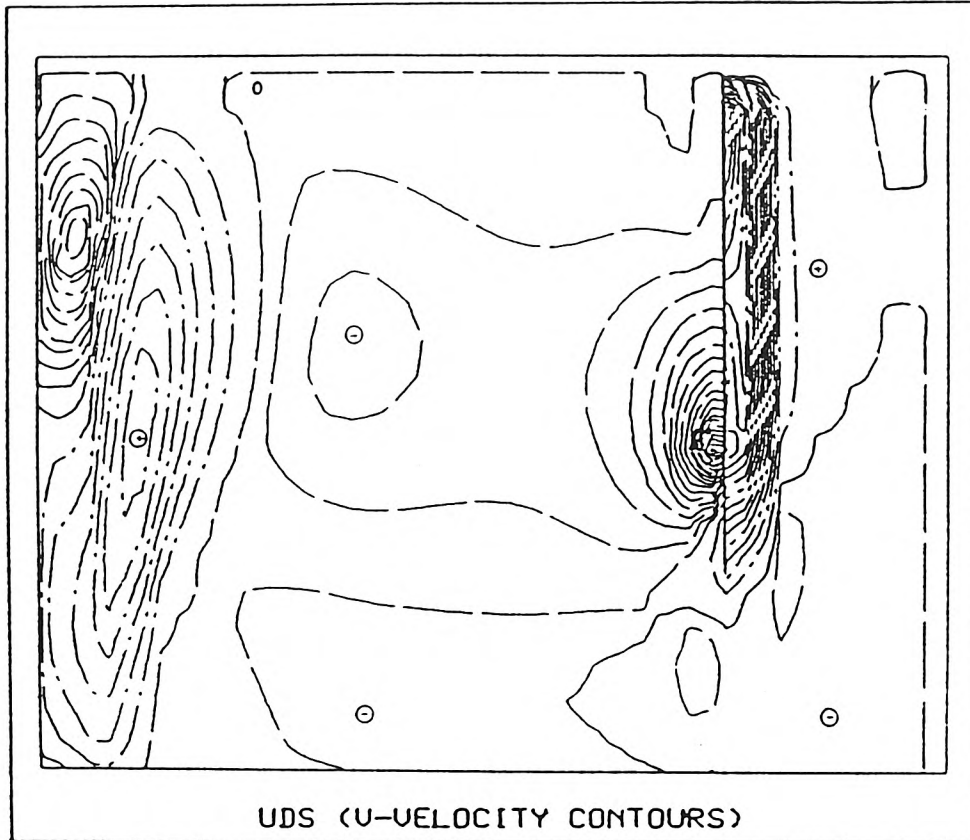


FIGURE  
8.37-9

V-VELOCITY CONTOURS FOR UDS

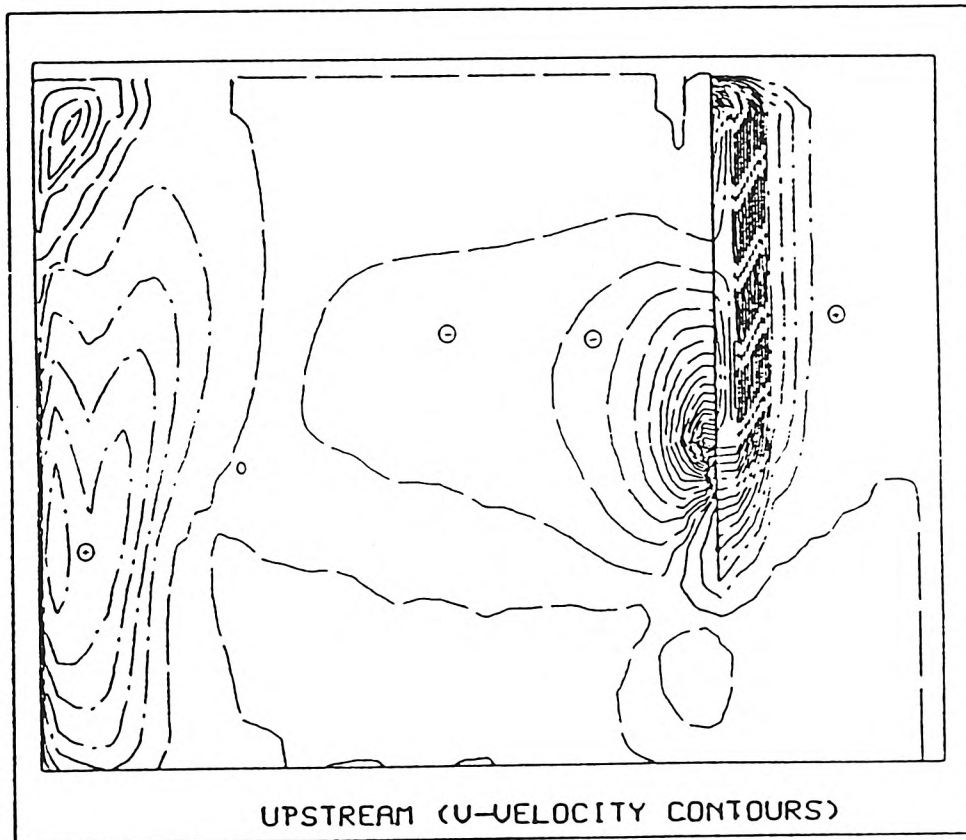


FIGURE  
8.37-10

V-VELOCITY FOR UPSTREAM

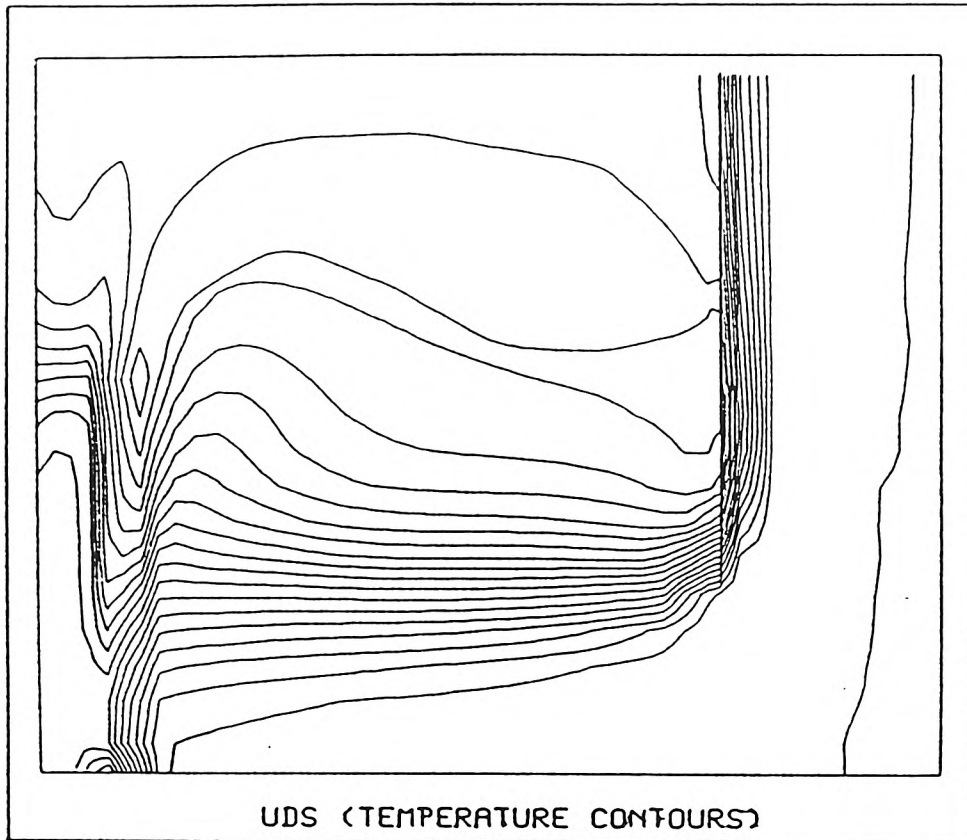


FIGURE  
8.37-11

TEMPERATURE CONTOURS FOR UDS

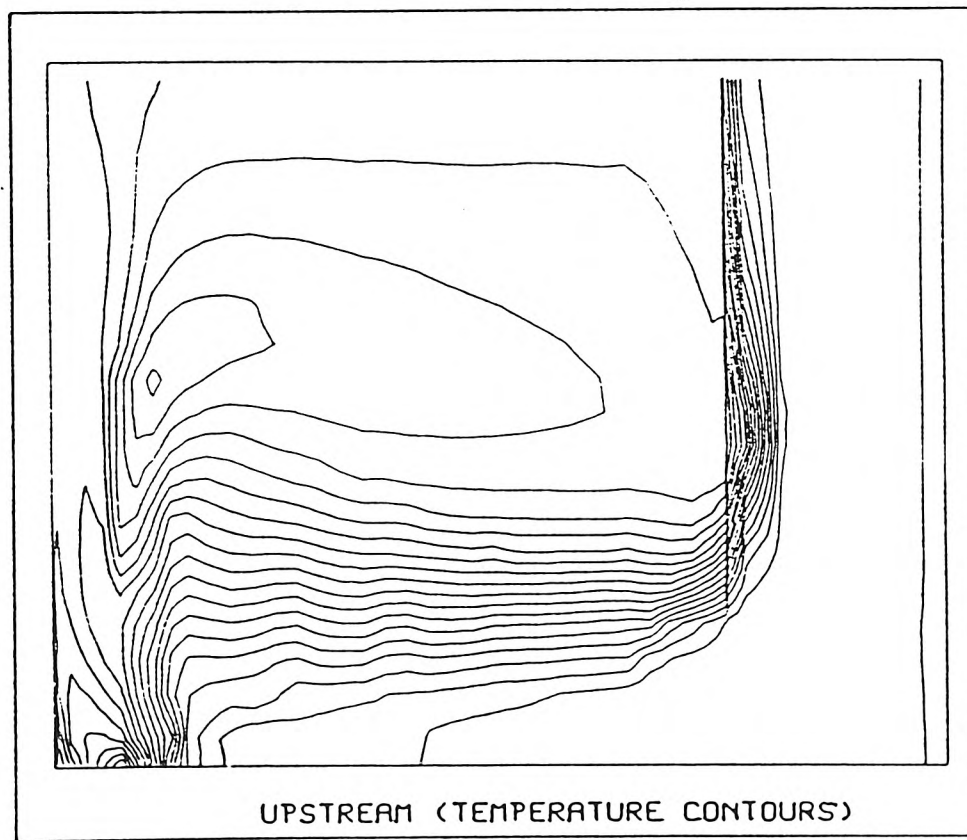


FIGURE  
8.37-12

TEMPERATURE CONTOURS FOR UPSTREAM

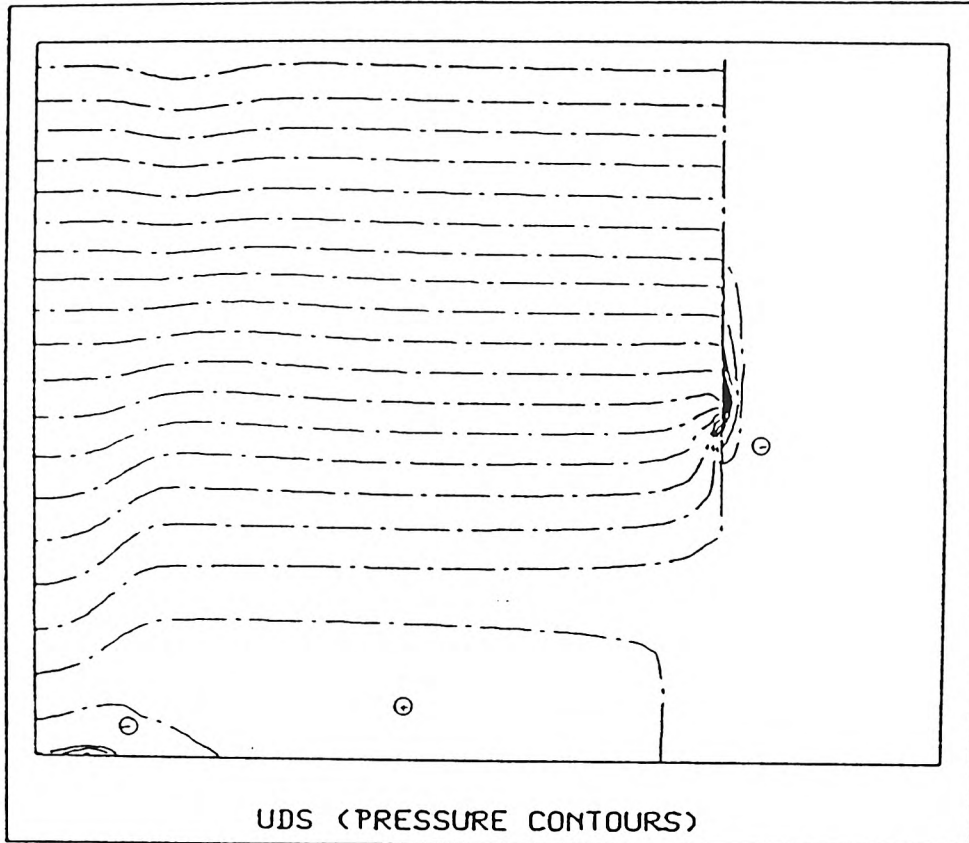


FIGURE  
8.37-13

PRESSURE CONTOURS FOR UDS

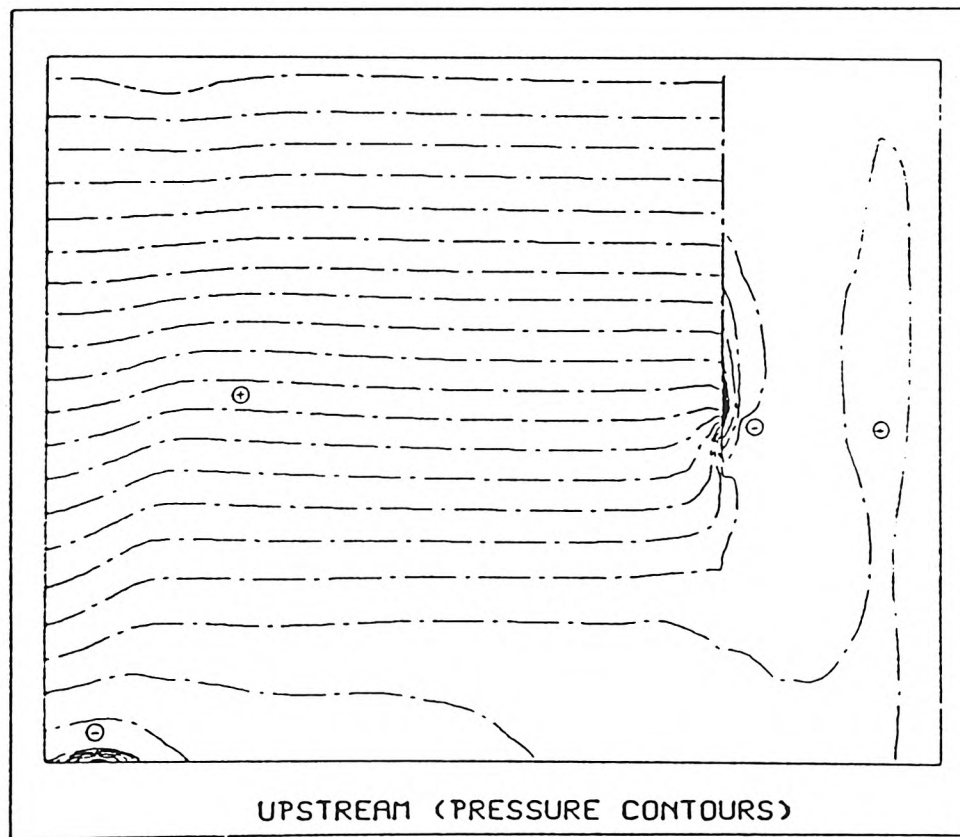


FIGURE  
8.37-14

PRESSURE CONTOURS FOR UPSTREAM

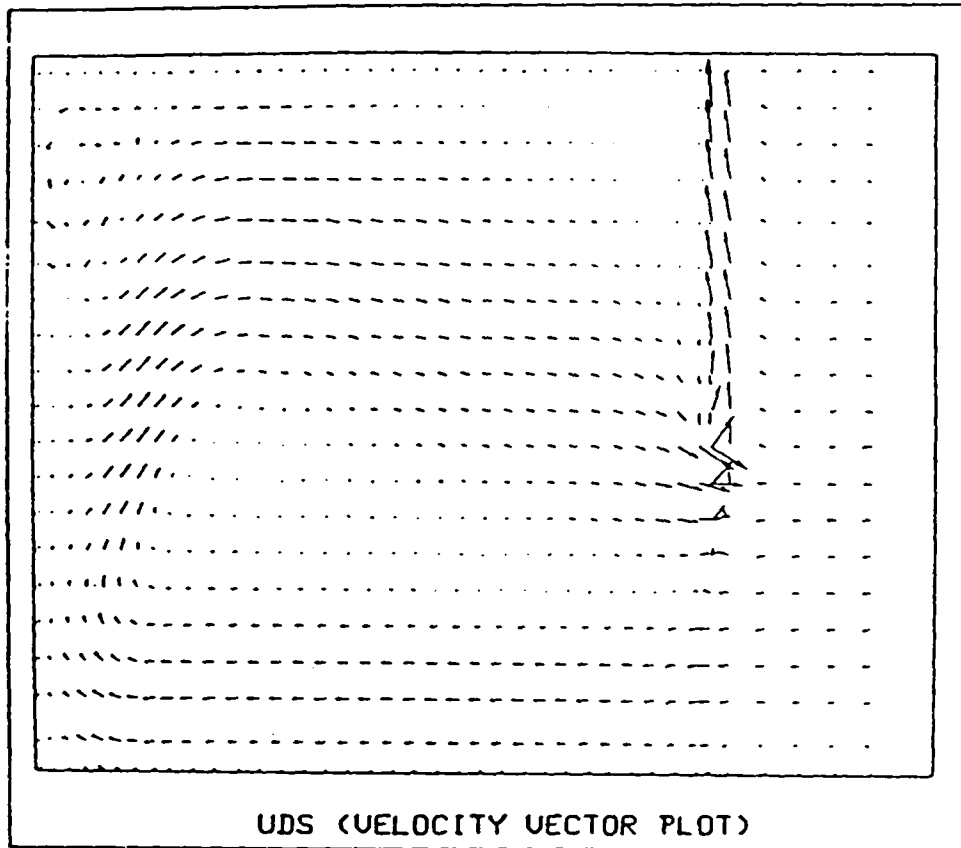


FIGURE  
8.37-15

VELOCITY VECTORS FOR UDS

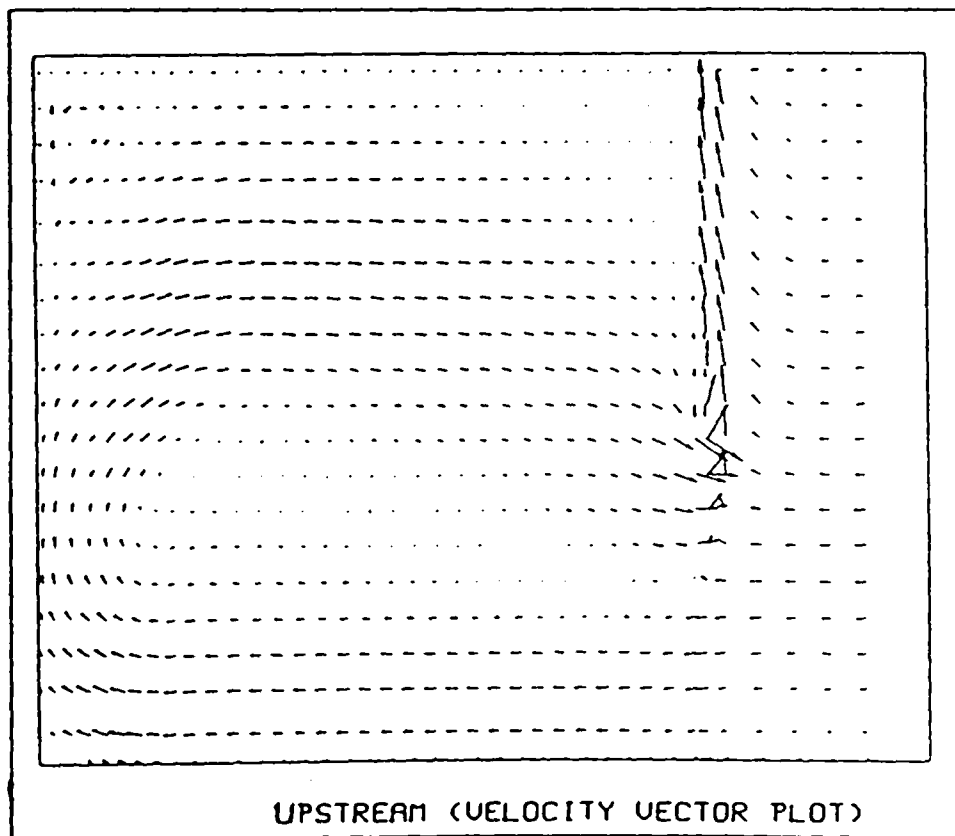


FIGURE  
8.37-16

VELOCITY VECTOR FOR UPSTREAM

## APPENDIX A2.1

### The Time-Averaged Conservation Equations

The equations are given in tensor notation.

#### The continuity equation

$$\frac{\partial}{\partial t} (\bar{\rho}) + \frac{\partial}{\partial x_j} (\bar{\rho} u_j) - S_\rho = 0 \quad (\text{A2.1-1}).$$

#### The momentum equation

$$\frac{\partial}{\partial t} (\bar{\rho} u_i) = \frac{\partial}{\partial x_j} (\bar{\rho} u_j u_i - (\mu + \mu_t) \frac{\partial u_i}{\partial x_j}) = S_{u_i} = 0 \quad (\text{A2.1-2});$$

where  $(-)$  denotes the time-averaged values.

#### Scalar equation

$$\frac{\partial}{\partial t} (\bar{\rho} \phi) + \frac{\partial}{\partial x_j} (\bar{\rho} u_j \phi - (\frac{\mu}{\sigma_\phi} + \frac{\mu_t}{\sigma_{\phi,t}}) \frac{\partial \phi}{\partial x_j}) - S_\phi = 0 \quad (\text{A2.1-3});$$

where  $S_\phi$  is the source/sink for the time-averaged quantities.

## APPENDIX A3.1

### The Tri-diagonal Matrix Algorithm (TDMA)

The TDMA, [(Householder (1964))], is applied at a given constant x-line for the general equation of the form:

$$A_p \phi_p = A_N \phi_N + A_S \phi_S + S \quad (\text{A3.1-1a});$$

which for clarity, is rewritten as:

$$D_i \phi_i = A_i \phi_{i+1} + B_i \phi_{i-1} + C_i \quad (\text{A3.1-1b}).$$

Here,  $i$  denotes a location along the y-line and the coefficients are evaluated directly from equation (A.3.1-1a). The  $\phi$ -values are then obtained as follows. Suppose that:

$$\bar{\phi}_i = \bar{A}_i \phi_{i+1} + \bar{B}_i \quad (\text{A.3.1-1c});$$

where,

$$\bar{A}_i = A_i / (D_i - B_i \bar{A}_{i-1}) \quad (\text{A.3.1-1d});$$

and

$$\bar{B}_i = (C_i + \bar{B}_{i-1} B_i) / (D_i - B_i \bar{A}_{i-1}) \quad (\text{A.3.1-1e});$$

are clearly recurrence relationships.

The values of  $A_1$  and  $B_1$  are prescribed as follows:

$$\bar{A}_1=0 \quad ; \quad \bar{B}_1 = \phi_1 \quad \text{(A.3.1-1f)}.$$

Starting at the high- $i$  end of the system, a backwards substitution is applied to obtain the values of  $\phi$  on the  $x$ -line.

## APPENDIX A4.1

### Locally-Exact-Difference Scheme (details)

Integrating equation:

$$\frac{\partial}{\partial x_i} (\rho u_i \phi) = \frac{\partial}{\partial x_i} \left( \Gamma \frac{\partial \phi}{\partial x_i} \right) + S \quad (\text{A4.1-1a});$$

twice gives:

$$\phi = \frac{F}{u} + C_1 e^{u/\Gamma x} \quad (\text{A4.1-1b});$$

assuming that  $F$  and  $u$  are constant between two adjacent 'nodal' values. Then by evaluating  $\phi$  in (A4.1-1b) for the west face, between  $i$  and  $i-1$ , and eliminating the constant of integration  $C_1$ , we get:

$$\frac{\phi_i - \phi_{i-1}}{\phi_i - \phi_{i-1}} = \frac{\exp(u_w/\Gamma_w(x-x_i)) - 1}{\exp(u_w/\Gamma_w(x_i-x_{i-1})) - 1} \quad (\text{A4.1-1c});$$

where the flux at the west face,  $J_w$ , has the form:

$$J_w = \frac{u_w(\phi_{i-1} - \phi_i) \exp(-u_w/\Gamma_w \Delta x)}{(1 - \exp(u_w/\Gamma_w \Delta x))} \quad (\text{A4.1-1d});$$

and similarly  $J_e$  has the form:

$$J_e = \frac{u_e(\phi_{i-1} - \phi_i) \exp(u_e/\Gamma_e \Delta x)}{(1 - \exp(u_e/\Gamma_e \Delta x))} \quad (\text{A4.1-1e}).$$

Equations (A4.1-1d) and (A4.1-1e) can be written in a simpler form by

introducing two new functions, these being:

$$g_p(\xi) = \frac{\xi}{\exp(\xi)-1}$$

and

(A4.1-1f);

$$g_m(\xi) = \frac{-\xi}{\exp(\xi)-1}$$

thus giving:

$$J_w = \Gamma_w(g_m(u_w\Delta x/\Gamma_w)\phi_{i-1} - g_p(u_w\Delta x/\Gamma_w)\phi_i)/\Delta x \quad (\text{A4.1-1g});$$

and

$$J_e = \Gamma_e(g_m(u_e\Delta x/\Gamma_e)\phi_i - g_p(u_e\Delta x/\Gamma_e)\phi_{i+1})/\Delta x \quad (\text{A4.1-1h}).$$

Finally, the finite-difference form for equation (A4.1-1a) using the locally-exact-difference scheme, is:

$$J_e - J_w = S^* \quad (\text{A4.1-1l}).$$

APPENDIX A4.2

Consider equation (4.12.8-1) together with (4.11.1-1) which gives the Leonard-superupwind-difference scheme for  $u > 0$  and  $P = u/\Gamma$ :

$$\begin{aligned} & \frac{P}{6\Delta x} \lambda (2\phi_{i+1} + 3\phi_i - 6\phi_{i-1} + \phi_{i-2}) + (1-\lambda)(11\phi_i - 18\phi_{i-1} + 9\phi_{i-2} - 2\phi_{i-3}) \\ & - \frac{1}{h^2} (\phi_{i-1} - 2\phi_i + \phi_{i+1}) = L(\phi_i), \quad i \in [3, N-1] \end{aligned} \quad (A4.2-1a);$$

together with

$$\phi_0(0) = 0 \quad ; \quad \phi_N(1) = 1.$$

Substituting:

$$\phi = \frac{\exp(Px_i) - 1}{\exp(P) - 1} \quad (A4.2-1b);$$

In (A4.2-1a) and simplifying we have:

$$\lambda = \frac{6 - (6 + 11P)_e \exp(-P_e) + 7P_e \exp(-2P_e) - 2P_e \exp(-3P_e) - \beta}{2P_e (1 - \exp(-P_e))^3} \quad (A4.2-1c);$$

where:

$$\beta = \frac{\Delta x^4}{2} \exp(-P_e) + 2P_e \Delta x^4 \exp(-P_e) - 3P_e \frac{\Delta x^4}{2} \exp(-P_e) \quad (A4.2-1d);$$

which, when neglected, is the error in the numerical

Leonard-superupwind difference scheme; even then  $\beta \ll 1$ , so it would be wise to neglect such terms as the scheme is already rather involved. Similar expressions for  $\lambda$  and  $\beta$  can be obtained for  $u < 0$ .

Modifications at the boundary need the introduction of two further weighting parameters,  $\gamma$  and  $\mu$ . Once again consider the case  $u > 0$  and use the finite-difference representation, for  $i=1$ :

$$\frac{P}{2h} (\phi_2 - \phi_0 + \mu(\phi_3 - 3\phi_2 + 3\phi_1 - \phi_0)) - \frac{1}{h^2}(\phi_0 - 2\phi_1 + \phi_2) = L_1(\phi_1) \quad (\text{A4.2-1e});$$

which when substituted by equation (A4.2-1b), yields:

$$\mu = \frac{\exp(-P_e)(1 - \exp(P_e)) - P_e(1 + \exp(-P_e))/2}{(P_e(1 - \exp(-P_e)))^2/2} \quad (\text{A4.2-1f}).$$

Similarly, at the 'nodal' point  $i=2$ , we use an expression of the form of equation (A4.2-1e), which yields:

$$\gamma = \frac{(1 - \exp(-P_e)) - P_e(1 + \exp(-P_e))/2}{P_e(1 - \exp(-P_e))^2/2} \quad (\text{A4.2-1g}).$$

Similar expressions for the case  $u < 0$  can be obtained.

## APPENDIX A6.1

### Quadratic Upstream Difference Scheme Formulation for Non-Uniform Grid

Expressing the  $\phi$  value of the east face of the control volume, using a quadratic profile, yields in a compact form, the expression:

$$\phi_e = \frac{\phi_E + \phi_P}{2} - Q_i \quad (\text{A6.1-1a});$$

where

$$\begin{aligned} Q_i &= a_i \left[ \left( \frac{\phi_E}{2} + a_i \phi_W \right) / (1 + 2a_i) - \frac{\phi_P}{2} \right] \text{ for } \rho_i U_i \geq 0 \\ &= b_i \left[ \left( \frac{\phi_P}{2} + b_i \phi_{EE} \right) / (1 + 2b_i) - \frac{\phi_E}{2} \right] \text{ for } \rho_i U_i < 0 \end{aligned} \quad (\text{A6.1-1b});$$

and

$$a_i = \frac{DXG(iX+1)}{2DXG(iX)} \quad ; \quad b_i = \frac{DXG(iX+1)}{2DXG(iX+2)} \quad (\text{A6.1-1c});$$

where DXG is the internodal distance (see Table A6.1.1).

After further manipulation, for  $\rho_i U_i \geq 0$  and  $\rho_i U_i < 0$ , equation (A6.1-1a) can be rewritten as follows:

$$\begin{aligned} \phi_e &= \phi_P \left( \frac{1}{2} + \frac{1}{4} \frac{DXG(iX+1)}{DXG(iX)} \right) \\ &+ \phi_W \left( \frac{\frac{1}{2} DXG(iX+1) + \frac{1}{4} \frac{DXG(iX+1)^2}{DXG(iX)}}{DXG(iX+1) + DXG(iX)} - \frac{1}{2} \frac{DXG(iX+1)}{DXG(iX)} \right) \end{aligned}$$

$$+ \phi_E \left( \frac{1}{2} - \frac{1}{4} \frac{DXG(IX+1)}{[DXG(IX) + DXG(IX+1)]} \right) \text{ for } \rho_L U_L \geq 0 \quad (\text{A6.1-1d});$$

and

$$\begin{aligned} \phi_\theta &= \phi_P \left( \frac{1}{2} - \frac{1}{4} \frac{DXG(IX+1)}{[DXG(IX+2) + DXG(IX+1)]} \right) \\ &+ \phi_E \left( \frac{1}{2} - \frac{1}{4} \frac{DXG(IX+1)}{DXG(IX+2)} \right) \\ &- \phi_{EE} \left( - \frac{1}{4} \frac{[DXG(IX+1)]}{DXG(IX+2)[DXG(IX+2) + DXG(IX+1)]} \right) \text{ for } \rho_L U_L < 0 \end{aligned} \quad (\text{A6.1-1e}).$$

Similarly, expressions for the other control-volume cell-faces are obtained and a flux balance is performed, i.e.:

$$(\rho u \phi)_e - (\rho u \phi)_w + (\rho v \phi)_n - (\rho v \phi)_s = 0 \quad (\text{A6.1-1f}).$$

Expressing two further parameters, namely:

$$\begin{aligned} M_i^+ &= 1 \quad \text{for } F_L = \rho_L U_L \geq 0 \\ &= 0 \quad \text{otherwise} \end{aligned} \quad (\text{A6.1-1g});$$

and

$$\begin{aligned} M_i^- &= 1 \quad \text{for } F_L = \rho_L U_L < 0 \\ &= 0 \quad \text{otherwise} \end{aligned} \quad (\text{A6.1-1h});$$

and substituting expressions of the form represented by equations (A6.1-1d) and (A6.1-1e), yields an expression of the form:

$$(B_p - S_p)\phi_p - \Sigma B_{nb}\phi_{nb} + S_e \quad (A6.1-1l);$$

where the  $B_s$  and  $S_s$  are given by:

$$\begin{aligned} B_\beta^+ &= M_\beta^+ (D_\beta - (\frac{1}{2} - \frac{1}{4} (\frac{\alpha_1}{\alpha_1 + \alpha_0})) C_\beta) \\ &- M_\beta^- (D_\beta - (\frac{1}{2} - \frac{1}{4} (\frac{\alpha_1}{\alpha_2})) C_\beta - \frac{1}{4} (\frac{\alpha_0^2}{\alpha_1(\alpha_1 + \alpha)}) C_\gamma) \end{aligned}$$

for  $(\alpha, \beta, \gamma) \in (IX, E, w)$   
and  $\in (IY, N, s)$  (A6.1-1j);

$$\begin{aligned} B_\beta^+ &= M_b^+ (D_\beta + (\frac{1}{2} + \frac{1}{4} \frac{\alpha_0}{\alpha_1^-}) C_\beta + \frac{1}{4} (\frac{\alpha_1^2}{\alpha_0(\alpha_0 + \alpha_1)}) C_\gamma) \\ &+ M_\beta^- (D_\beta + (\frac{1}{2} - \frac{1}{4} (\frac{\alpha_0}{\alpha_1 + \alpha_0})) C_\beta) \end{aligned}$$

for  $(\alpha, \beta, \gamma) \in (IX, W, e)$   
and  $\in (IY, S, n)$  (A6.1-1k);

$$\begin{aligned} S_C &= -\frac{1}{4} M_w^+ \phi_{ww} Z_w - \frac{1}{4} M_s^+ \phi_{ss} Z_s \\ &+ \frac{1}{4} M_e^+ \phi_{ee} Z_e + \frac{1}{4} M_n^- \phi_{nn} Z_n \end{aligned}$$

(A6.1-1l).

where

$$Z_\beta = \frac{\alpha_0^2}{\alpha_1^-(\alpha_1^- + \alpha_0)} \quad ; \quad Z_\beta = \frac{\alpha_1^2}{\alpha_2(\alpha_2 + \alpha_1)}$$

for  $(\beta, \alpha) \in (W, IX)$

for  $(\beta, \alpha) \in (e, IX)$

and  $\in (S, IY)$

and  $\in (n, IY);$

$$S_p = \frac{1}{4} M_e^+ Z_e + M_n^+ Z_n$$

$$- \frac{1}{4} M_w^- Z_w - M_s^- Z_s$$

(A6.1-1m);

where  $Z_\beta$  are as given above and the notation for  $\alpha$  is given in Table A6-1.1).

$\alpha$	IX	IY
$\alpha_0$	DXG(IX)	DYG(IY)
$\alpha_1$	DXG(IX+1)	DYG(IY+1)
$\alpha_2$	DXG(IX+2)	DYG(IY+2)
$\alpha_{1^-}$	DXG(IX-1)	DYG(IY-1)

DXG  $\cong$  distance between two nodal points in the X-direction      DYG  $\cong$  distance between two nodal points in the Y-direction

TABLE A6. 1. 1



